Université de Montréal

Techniques de catalyse et de flux continu pour faciliter la fermeture de molécules cycliques tendues

par Éric Lévesque

Département de chimie
Faculté des arts et des sciences

Thèse présentée à la Faculté des études supérieures et postdoctorales en vue de l'obtention du grade de *philosophiae doctor* (Ph. D.) en chimie

Août 2016

© Éric Lévesque, 2016

Résumé

Cette thèse décrit l'exploration de techniques de catalyse et de flux continu pour faciliter la fermeture de molécules cycliques tendues.

En premier lieu, un catalyseur de palladium permet de fermer un hétérocycle aromatique tendu, la structure benzo[*a*]imidazo[2,1,5-*c,d*]indolizine.[16] La tension de cycle contribue à donner au système π hautement délocalisé de ces molécules des propriétés photophysiques intéressantes, différentes de celles de leurs analogues non tendus.[21,33] Il a été démontré que leur longueur d'onde d'émission maximale peut être modulée de manière prévisible en modifiant les groupes fonctionnels conjugués au système aromatique. Le potentiel d'application en biochimie de ces fluorophores à déplacement de Stokes élevé a été exploré en étiquetant deux protéines en milieu biocompatible.

En second lieu, une version catalytique de la cycloaddition de Simmons-Smith a été optimisée. Dans cette transformation, une quantité catalytique d'un sel de zinc permet de former un carbénoïde hautement réactif à partir d'un composé aryldiazométhane. Ce carbénoïde peut réagir avec une grande variété d'alcènes pour former les arylcyclopropanes correspondants. Un catalyseur modifié permet même à la réaction d'avoir lieu en présence d'alcools primaires.

Enfin, la manipulation des composés aryldiazométhanes utilisés dans la cyclopropanation décrite ci-haut peut s'avérer risquée vu la toxicité et l'instabilité de ces composés. Pour minimiser ces risques, une méthode pour générer et purifier ces réactifs en flux continu a été développée. De cette manière, le composé dangereux est consommé à mesure qu'il est généré, dans un système fermé. Un large éventail d'aryldiazométhanes peut être produit en solution dans un solvant non-coordinant. La compatibilité de ces solutions avec des systèmes catalytiques requérant des réactifs propres et secs a été démontrée.

Mots-clés : Fluorescence, Hammett, Déplacement de Stokes, Étiquetage; Zinc, Carbénoïde, Cyclopropane, Diazo; Flux continu, Hydrazone, Purification.

Abstract

This thesis describes the exploration of catalysis and continuous flow techniques towards the formation of strained cyclic molecules.

First, a palladium catalyst enables the ring closure of a strained aromatic heterocycle, the benzo[*a*]imidazo[2,1,5-*c,d*]indolizine.[16] Ring strain gives these molecule's highly delocalized π system interesting photophysical properties that differ from those of unstrained analogs.[21,33] Their emissive properties can be predictably modulated by modifying functional groups conjugated to the aromatic core. These high Stokes-shift fluorophores' application potential in biochemistry was explored by the biocatalyzed labelling of two proteins in biocompatible media.

Second, a catalytic version of the Simmons-Smith cycloaddition was optimized. In this transformation, a catalytic amount of zinc salt allows the formation of a highly reactive carbenoid from an aryldiazomethane precursor. This intermediate can then react with a variety of alkenes, forming the corresponding arylcyclopropanes. A modified catalyst even enables the reaction to proceed in the presence of a primary alcohol group.

Finally, the handling of the aryldiazomethane precursors used in the above reaction can be hazardous due to these compound's instability and toxicity. To minimise these risks, a method to synthesise and purify these reagents in continuous flow was developed. This way, the dangerous chemical is consumed as it is generated, in a closed system. A large array of aryldiazomethane solutions in a non-coordinating solvent can be produced. These solutions' compatibility with sensitive catalytic systems requiring clean and dry reagents was demonstrated.

Keywords : Fluorescence, Hammett, Stokes shift, Labelling; Zinc, Carbenoid, Cyclopropane, Diazo; Continuous flow, Hydrazone, Purification.

Table des matières

Liste des tableaux

Liste des figures

Liste des sigles

α-LA : *Alpha*-Lactalbumine

λ_{ex} : Longueur d'onde d'un maxima d'excitation

λ_{em} : Longueur d'onde d'un maxima d'émission

Φ : Rendement quantique

ε : Absorptivité molaire

ADD : 1,1'-(AzoDicarbonyl)Dipipéridine

AL : Acide de Lewis

APCI : Atmospheric Pressure Chemical Ionization

BINOL : BINaphtOL

BL : Base de Lewis

BODIPY : *BOron-DIPYrromethane*.

CAM : *Cerium Ammonium Nitrate*

CGCC : *Center for Green Chemistry and Catalysis* (CCVC : Centre de Chimie Verte et Catalyse)

CMD : Concerted Metallation-Deprotonation

CREATE : Collaborative REsearch And Training Experience program

DBA : DiBenzylidèneAcétone

DBU : 1,8-DiazaBicycloUndéc-7-ène

DCM ou CH_2Cl_2: Dichlorométhane

DIPEA : DiIsoPropylÉthylAmine

DMA : DiMethylAcetamide

DMF : DiMethylFormamide

DFT : *Density Functional Theory* (Théorie des fonctionnelles de la densité)

DSSC : *Dye Sensitized Solar Cell* (cellules à pigment photosensible)

EDA : *Ethyl DiazoAcetate* (diazoacétate d'éthyle)

EDTA : ÉthylèneDiamine TétraAcétate

ESI : *ElectroSpray Ionisation*

FQRNT : Fonds de Recherche du Québec – Nature et Technologies

FRET : *Förster Resonance Energy Transfer* (Transfert d'énergie par résonance de type Förster)

FTIR : *Fourier Transform InfraRed*

GB1 : *Immunoglobulin-binding domain B1 of streptococcal protein G*

GEA : Groupe ÉlectroAttracteur

GED : Groupe ÉlectroDonneur

GFP : *Green Fluorescent Protein*

GP : *Groupe Partant*

HBTU : *2-(*1H-*Benzotriazol-1-yl)-1,1,3,3-TetramethylUronium hexafluorophosphate*

HOMO : *Highest Occupied Molecular Orbital*

HRMS : *High Resolution Mass Spectrometry*

KIE : *Kinetic Isotope Effect*

LUMO : *Lowest Unoccupied Molecular Orbital*

MOM *:* MéthOxyMéthyl

MTG : *Microbial TransGlutaminase*

Ni-NTA : Nickel-NitriloTetraAcetic acid

NSERC : *Natural Sciences and Engineering Research Council (of Canada)*

OLED : *Organic Light-Emitting Diode*

OMF/FMO : Orbitales Moléculaires Frontières/*Frontier Molecular Orbitals*

PROTEO : *Quebec network for research on PROTEin Function, Engineering, and ApplicatiOns*

PTFE :PolyTétraFluoroÉthylène

RMN/NMR : Résonance magnétique nucléaire/*Nuclear magnetic resonance*

RPECV : Répulsion des Paires Électroniques de la Couche de Valence

SDS-PAGE : *Sodium DodecylSulfate PolyAcrylamide Gel Electroporesis.*

SMBR/LRMS : Spectrométrie de Masse à Basse Résolution/*Low Resolution Mass Spectrometry*

STED : *STimulated Emission Depletion*

TBS : Tri-*tert*-Butyl Silyle

TD-DFT : *Time Dependent Density Functional Theory*

THF : TétraHydroFurane

TLC : *Thin Layer Chromatography* (CCM : Chromatographie sur Couche Mince)

TMG : Tetraméthylguanidine

UV : Ultraviolet

VWR : *Van Waters Rogers*, compagnie de fournitures de laboratoire

WWW : *World Wide Web*

Liste des abréviations

Ac : Acétate

Bn : Benzyl

Bz : Benzoyl

Et : Éthyl

*i*Pr : *iso*-Propyl

Me : Méthyl

Mes : Mésityl, 2,4,6-Triméthylphényl

*n*Pr : normalPropyl (linéaire)

Phen : 1,8-Phénanthroline

Piv : Pivaloyl

Pyr: Pyridine

*t*Bu: *tert*-Butyl

Tf : Triflate, Trifluorométhylsulfonyl

Trip : 2,4,6-Triisopropylphenyl

Ts : Tosyl, 4-TolylSulfonyle

À tous les grandes et grands scientifiques qui ont consacré leurs vies à l'avancée des connaissances de l'Humanité.

We really are standing on the shoulders of giants.

Remerciements

Je tiens à remercier en premier lieu ma copine Karelle, qui a su supporter mes humeurs instables comme un diazo et toutes ces soirées seule à l'appartement alors que je sacrais devant une machine ou un montage à la lumière du crépuscule. Merci à mes parents Francine et François ainsi qu'à mes grands-parents Cy et Françoise, pour avoir cru en moi depuis ma décision soudaine et résolue d'étudier la chimie. Merci à mes amis, de l'université et d'ailleurs, qui étaient là pour me rappeler de sortir du labo et de venir prendre une bière ou dix.

En second lieu, merci à André pour ses conseils rares mais utiles, pour m'avoir donné carte blanche sur le choix de mes projets et pour m'avoir permis d'aller présenter à toutes ces conférences (Pacifichem, deux ACS, deux CSC, QOMSBOC, CCVC, GRUM, ISCHA-3). Merci à Barbara pour accomplir avec talent et application toutes les tâches que les scientifiques détestent faire, dont entretenir la précieuse machine à café. Merci aux présents et anciens membres du groupe pour avoir rendu l'atmosphère de travail agréable et divertissante. Un clin d'œil en particulier à Guillaume B., Vincent, Nicolas, Guillaume P., Sam, Sophie, Jean Baptiste, Morgane, Emmanuelle, Chandra, Saher, Maxime, Jakob, Pascal, Léa, Cyril, Sébastien, William, Sylvain et Daniela. Merci à mes stagiaires Charline, Simon L. et Simon V., parce que deux têtes et deux paires de mains valent toujours mieux qu'une, surtout avec des collaborateurs motivés.

En troisième lieu, merci à tous les étudiants auxquels j'ai enseigné pendant mes démonstrations de laboratoires et mes répétitions. J'espère avoir réussi l'exploit colossal et gratifiant de vous transmettre de nouvelles connaissances.

En quatrième lieu, merci à tout le personnel de soutien de l'université de Montréal. Merci aux analystes du centre de Masse d'avoir ionisé mes librairies mal identifiées. Merci aux employés de l'atelier mécanique d'avoir toujours les bons conseils et les bons outils. Merci au personnel RMN d'entretenir ces merveilleuses machines pour tous ces « organiciens qui ne comprennent rien à la RMN ». Merci à Vanessa Kairouz de m'avoir laissé pomper des produits explosifs dans des machines dispendieuses.

Enfin, merci aux organismes subventionnaires (CRSNG, FQRNT, FESP de l'U de M., CCVC) qui nous rappellent que l'on vit dans un monde ou un jeune curieux peut être logé et nourri

par l'État simplement pour jouer aux LEGO® avec des atomes et créer des arc-en-ciel fluorescents au nom de l'idéal vague et grandiose du savoir humain.

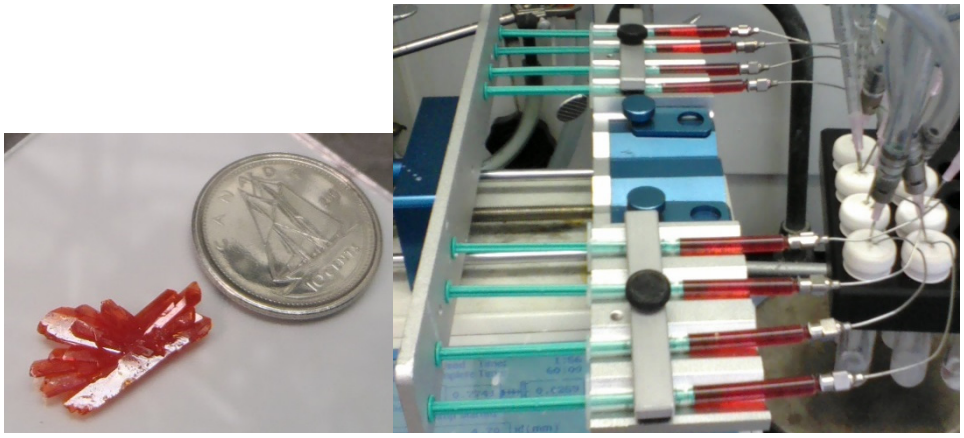

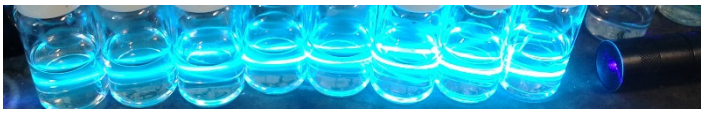

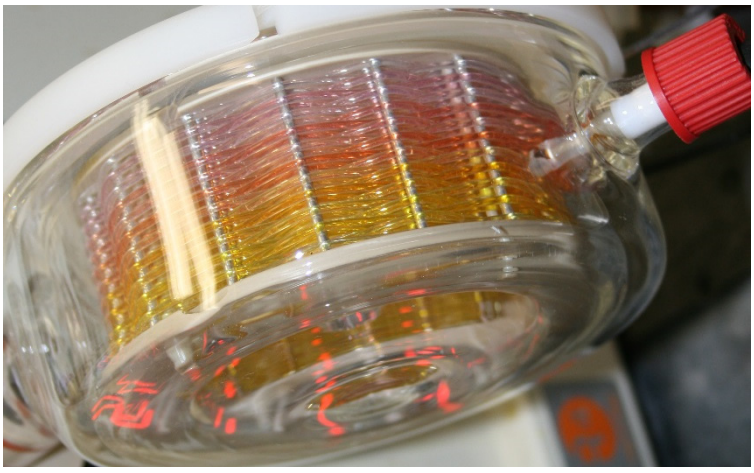

1.Introduction

Les carbocycles tendus sont des espèces chimiques fascinantes. Quand la valeur des angles entre les liaisons chimiques est plus petite que celle dictée par le RPECV (« Répulsion des Paires Électroniques de la Couche de Valence » (en anglais, VSEPR : Valence Shell Electron Pair Repulsion)),[1] la répulsion entre les électrons des liaisons endocycliques est surélevée. Une molécule cyclique tendue possède donc de l'énergie potentielle chimique, qui peut généralement être relâchée par le simple bris d'un lien σ. Un parallèle macroscopique peut être fait avec un ressort étiré, qui emmagasine l'énergie utilisée pour modifier sa longueur sous forme d'énergie potentielle mécanique. Les cycles tendus ont aussi tendance à être très rigides, étant donné que les changements conformationnels impliquent souvent la réduction temporaire des angles de liaisons et des angles dièdres. Leurs propriétés électroniques sont aussi différentes de celles de leurs analogues non tendus, les orbitales moléculaires occupées se déformant pour s'éloigner les unes des autres.

La connotation inconfortable du paragraphe précédent invoque la question : comment fait-on pour convaincre les atomes de carbone de former les liaisons qui les coincent dans de telles structures? Étant des espèces (relativement) hautes en énergie, le postulat de Hammond prédit que l'état de transition menant à leur formation aura une géométrie encore plus énergétique. Il existe plusieurs stratégies pour atteindre ce type d'état de transition. Une d'entre elles consiste à créer un réactif tellement haut en énergie que la formation d'un cycle tendu correspond à une descente dans un puits thermodynamique. Dans le cas des synthèses de cyclopropanes, le plus petit carbocycle, les carbènes et les carbénoïdes sont des exemples de telles espèces chimiques.

Étant donné l'énergie chimique élevée associée à ce type d'intermédiaires, les conditions de réaction permettant leur formation sont souvent drastiques, réduisant la chimiosélectivité et la compatibilité avec des molécules fragiles. L'utilisation de catalyseurs permet de contourner ce genre de problème. En effet, en permettant à la réaction de « passer par un autre chemin, » un catalyseur arrive à former les espèces énergétiquement élevées désirées en évitant les états de transitions difficiles d'accès qui leur sont associés.

Les composés diazo sont d'excellents précurseurs aux carbènes et carbénoïdes, permettant leur formation en conditions douces. Le coût énergétique de la formation de telles espèces est balancé par la relâche d'une molécule de diazote gazeux préalablement « piégée » dans la structure

chimique du composé diazo. L'énergie potentielle chimique élevée associée à cette possibilité de relâche de gaz entropiquement favorisée rend la plupart des composés diazo toxiques et explosifs, décourageant leur manipulation par des méthodes conventionnelles, surtout à large échelle. La chimie en flux continu permet de faciliter et de sécuriser la manipulation de ce genre d'intermédiaires en éliminant le besoin de les accumuler et en limitant les risques d'exposition.

2.Synthèse et caractérisation d'une série de fluorophores à émission ajustable et à haut déplacement de Stokes.

2.1.Généralités sur la fluorescence

Le phénomène de fluorescence est observé quand une substance émet de la radiation électromagnétique après avoir absorbé de la lumière incidente d'énergie plus élevée. La fluorescence est caractérisée empiriquement par un arrêt rapide de l'émission si la lumière incidente est interrompue, en contraste avec la phosphorescence, un phénomène connexe avec un temps de demi-vie beaucoup plus élevé.[2]

2.1.1.Diagramme de Franck-Condon[3]

Figure 1. Diagramme de Franck-Condon[3] représentant des niveaux d'énergie électroniques et vibrationnels

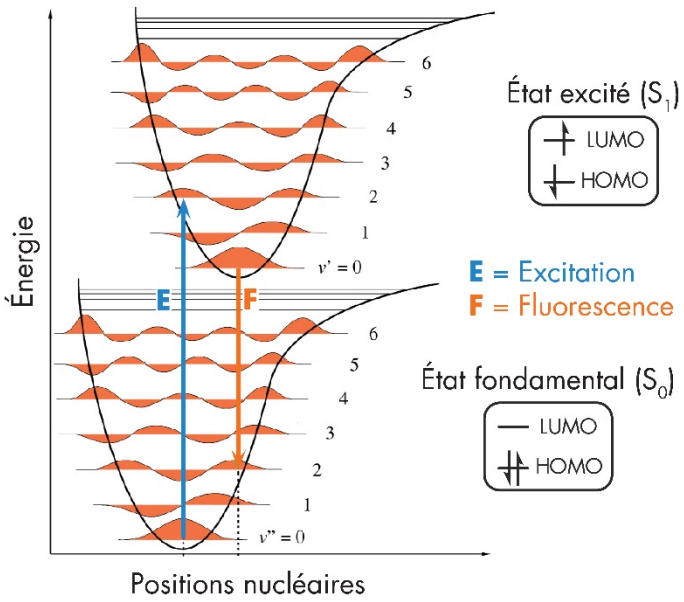

Le phénomène physico-chimique sous-jacent à la fluorescence est décrit dans la **Figure 1**. Supposons un système dans son état fondamental, aux plus bas niveaux électroniques et vibrationnels. Si un photon de la longueur d'onde appropriée interagit avec un tel système et lui transfère son énergie, il subit une transition vers un état électronique excité. Dans le cas ci-haut, le premier état excité singulet ou « S1 » correspond à la transition d'un électron vers la plus basse

orbitale moléculaire inoccupée (LUMO). Comme la géométrie fondamentale de cet état S1 diffère de celle de l'état S0, le système se retrouve aussi à un niveau vibrationnel excité. Le surplus d'énergie vibrationnelle est rapidement dissipé sous forme de chaleur car les relaxations vibrationnelles sont plus rapides que les relaxations électroniques. Le système est alors dans son état vibrationnel fondamental pour le niveau électronique S1. Si le retour au niveau S0 est concomitant à l'émission d'un photon, la fluorescence est observée. Cette transition peut aussi s'effectuer de manière non-radiative. De manière analogue à l'excitation, le système électroniquement relaxé n'a pas la géométrie fondamentale du niveau S0. Il dissipe ce surplus d'énergie à son environnement sous forme de vibrations (chaleur) et revient à l'état fondamental vibrationnel et électronique, complétant le cycle.[2]

La phosphorescence (absente de la **Figure 1**) implique la transition d'un état électronique excité singulet vers un état triplet « T1 ». Comme la transition électronique entre T1 et S0 peut être très lente vu qu'elle est interdite par la symétrie des orbitales, les systèmes phosphorescents sont caractérisés par un long temps de demi-vie. Ils peuvent continuer d'émettre des photons plusieurs heures après l'extinction de la lumière incidente.

2.1.2.Mesure de la fluorescence

Figure 2. Schéma simplifié du fonctionnement d'un fluorimètre

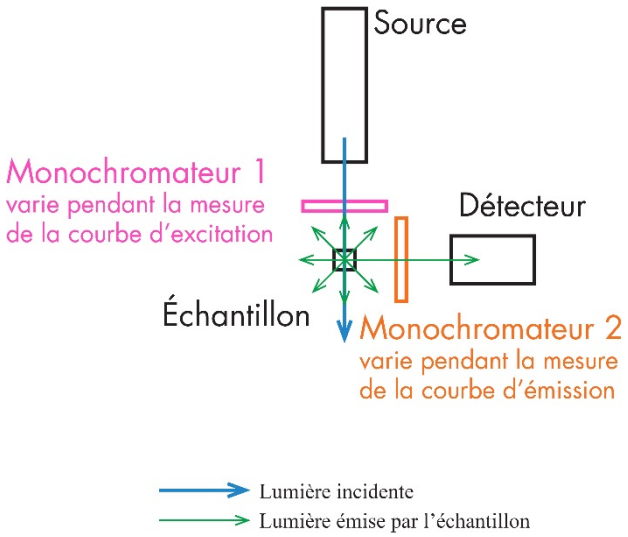

L'appareil permettant de mesurer la fluorescence se nomme un fluorimètre (**Figure 2**). Pour photoexciter l'échantillon, il utilise un faisceau de lumière à large spectre (UV/visible). La longueur

d'onde de la lumière incidente est sélectionnée à l'aide d'un ou plusieurs monochromateurs, typiquement à réseau (monochromateur 1 ci-haut). L'échantillon, s'il est fluorescent à la longueur d'onde choisie, émet des photons dans toutes les directions, mélangés aux photons provenant de la diffusion de la lumière incidente. Le monochromateur 2 permet de sélectionner la partie de la lumière émise qui sera détectée.

Figure 3. Graphique d'excitation-émission typique

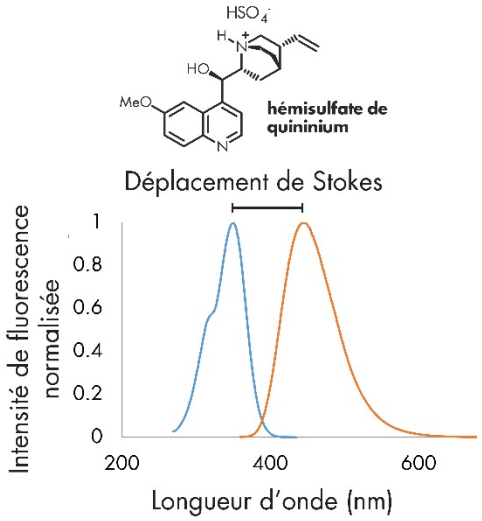

La mesure la plus commune acquise par un fluorimètre est le graphique d'excitation-émission. Pour l'obtenir, il faut en premier lieu déterminer une longueur d'onde à laquelle l'échantillon émet de la lumière et y fixer le monochromateur du détecteur (monochromateur 2 dans la **Figure 2**). Puis, le monochromateur de la source (monochromateur 1 dans la **Figure 2**) balaie une étendue de longueurs d'onde prédéterminée. La courbe d'excitation (en bleu dans la **Figure 3**) ainsi obtenue indique quelles longueurs d'onde sont les plus efficaces à provoquer la fluorescence de l'échantillon. Ensuite, le monochromateur de la source est fixé à un des maxima de la courbe d'excitation et le monochromateur du détecteur balaie les longueurs d'ondes en aval (énergétiquement parlant), générant la courbe d'émission. La position des maxima de ces courbes et leurs intégrations contiennent plusieurs informations sur les propriétés photophysiques de l'échantillon.

2.1.3.Caractéristiques désirables pour un fluorophore

Les propriétés optimales recherchées dans un fluorophores dépendent de l'application désirée. La stabilité chimique et thermique, la solubilité et la possibilité de former des liens covalents avec d'autres molécules de manière opérationnellement simple sont un avantage dans la plupart des cas. Pour certains domaines surtout liés à la microbiologie et la biochimie, l'affinité avec certaines molécules et le coefficient de partition entre les milieux polaires et apolaires ont un impact sur le potentiel d'application.

Du côté des propriétés photophysiques, celles ayant le plus d'impact sur les applications sont les maxima d'excitation (λ_{ex}) et d'émission (λ_{em}), le déplacement de Stokes et la brillance, qui combine le rendement quantique (Φ) et l'absorptivité molaire (ε).[4]

2.1.3.1.Maxima d'excitation et d'émission et déplacement de Stokes

Les maxima d'excitation et d'émission idéaux dépendent de la nature des émetteurs, des détecteurs et du milieu utilisés. Un λ_{ex} qui correspond à une des harmoniques de l'émission d'une source laser commerciale est nécessaire si une intensité lumineuse incidente élevée doit être utilisée. Alternativement, la capacité d'un fluorophore à être excité par une source à large spectre, caractérisée par des bandes d'excitation larges et plusieurs maxima peut aussi être désirable. Le λ_{em} doit, quant à lui, correspondre à de la lumière facile à détecter, peu absorbée par le milieu et qui n'interfère pas avec d'autres sources lumineuses présentes. Comme ces contraintes varient beaucoup en fonction de l'application, la possibilité de moduler et de prédire cette propriété en fonction de la structure du fluorophore est prisée.

Le déplacement de Stokes est tout simplement la différence entre les maxima d'excitation et d'émission (**Figure 4**). Il correspond à la quantité d'énergie non radiative dissipée par le système à chaque cycle de fluorescence.

Figure 4. Équation du déplacement de Stokes

$$Déplacement\ de\ Stokes = \lambda_{em} - \lambda_{ex}$$

Un fluorophore avec un déplacement de Stokes élevé réduit les risques d'autodésactivation ainsi que l'interférence entre la lumière émise et la lumière incidente diffusée. De plus, il peut être

combiné avec des fluorophore à déplacements de Stokes plus courts dans le même échantillon, permettant d'exciter plusieurs analytes avec la même lumière tout en détectant leurs émissions séparément. [5]

2.1.3.2.Rendement quantique

Le rendement quantique est souvent mentionné lorsque les fluorophores sont comparés entre eux. Il est défini par la fraction des photons absorbés qui mène à l'émission d'un photon.

Figure 5. Formule théorique du rendement quantique

$$\Phi = \frac{Photons_{émis}}{Photons_{absorbés}}$$

Il existe plusieurs manières de déterminer expérimentalement le rendement quantique. La méthode utilisée dans le projet ci-dessous consiste à obtenir le rendement quantique d'un inconnu en comparant l'intégration de son pic d'émission avec celle d'un standard au rendement quantique connu[6] (**Figure 6**). L'hémisulfate de quinine a été utilisé comme standard. Le ratio des intégrations est corrigé par l'inverse du ratio des absorbances pour tenir compte de la quantité différente de photons absorbés. Le ratio des carrés des indices de réfraction est multiplié pour tenir compte de l'erreur introduite par l'utilisation de solvants différents. Comme il est essentiel que l'intensité de la lumière incidente soit identique pour les deux mesures, ces dernières doivent être effectuées dans l'intervalle le plus court possible (la constante K de l'équation (2) est recalculée à chaque séance de mesures).

Figure 6. Détermination expérimentale du rendement quantique

$$(1)\quad \frac{\Phi_{échantillon}}{\Phi_{quinine}} = \frac{intégration_{échantillon}}{intégration_{quinine}} \cdot \frac{abs_{\lambda_{ex}\,quinine}}{abs_{\lambda_{ex}\,échantillon}} \cdot \frac{n_{solvant\ échantillon}^{\ 2}}{n_{solvant\ quinine}^{\ 2}}$$

$$(2)\quad \Phi_{échantillon} = \frac{K \cdot intégration_{échantillon} \cdot n_{solvant\ échantillon}^{\ 2}}{abs_{\lambda_{ex}\,échantillon}}$$

où

$$K = \frac{\Phi_{quinine} \cdot abs_{\lambda_{ex}\,quinine}}{intégration_{quinine} \cdot n_{solvant\ quinine}^{\ 2}}$$

2.1.3.3.Absorptivité molaire

Figure 7. Équation de Beer-Lambert liant la mesure de l'absorbance au coefficient d'extinction molaire

$$\varepsilon = \frac{abs_{\lambda_{ex}}}{[échantillon]}$$

Il est nécessaire de mesurer l'absorbance des fluorophores aux longueurs d'onde d'excitation pour obtenir le rendement quantique. Cette mesure est effectuée avec un spectrophotomètre. L'absorbance de la solution, divisée par sa concentration, permet de déterminer le coefficient d'absorptivité molaire (ε), parfois appelé coefficient d'extinction molaire. ε quantifie l'efficacité d'une mole de fluorophore à absorber des photons à une longueur d'onde spécifique.

2.1.3.4.Brillance

Figure 8. Équation de la brillance

$$Brilliance = \Phi_F \cdot \varepsilon$$

La brillance est une mesure qui permet de comparer l'efficacité photophysique des fluorophores. Le produit du rendement quantique et du coefficient d'absorptivité molaire donne en effet une valeur qui tient compte de toutes les étapes par lesquelles un photon incident est transformé en photon émis.[2] Le rendement quantique seul est insuffisant car un fluorophore fictif peut avoir un rendement quantique parfait ($\Phi = 1$) tout en étant inefficace à absorber les photons incidents (ε peu élevé). Ce fluorophore aura besoin d'une haute intensité de lumière incidente pour émettre un signal mesurable et sera donc peu utile. Inversement, un fluorophore avec un rendement quantique inférieur mais qui absorbe efficacement la lumière à son maximum d'excitation peut avoir une brillance plus élevée. Il aura donc besoin d'une lumière incidente moins intense pour générer un signal satisfaisant.

2.1.3.5.Photostabilité

La photostabilité est une autre propriété qui est essentielle à l'applicabilité des fluorophores. Elle représente la quantité moyenne de cycles excitation/émission qu'une molécule peut effectuer avant de subir un changement chimique qui l'empêche de fluorescer. Comme la vitesse de cette

dégradation varie selon de nombreux facteurs, la photostabilité est habituellement rapportée sous forme d'une comparaison avec la cinétique de dégradation d'un fluorophore connu exposé aux mêmes conditions. L'utilisation d'une source à spectre large permet d'exciter tous les fluorophores testés avec une intensité similaire (exemple à la page - 174 - (**Figure 75**)).

2.1.3.6.Exemples

Les valeurs des propriétés décrites ci-dessus pour quelques fluorophores commerciaux couramment utilisés sont présentées ci-dessous. La comparaison entre la **dansyl amide** et le **Cy3** démontre bien la relation entre le rendement quantique et la brillance. Même si son rendement quantique est bas, le **Cy3** a un coefficient d'extinction nettement supérieur qui lui permet d'émettre plus de lumière pour une intensité donnée de lumière incidente.

Tableau I. Propriétés photophysiques de fluorophores commerciaux couramment utilisés

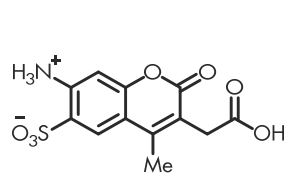

AlexaFluor 350

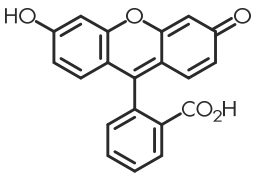

Fluorescéine

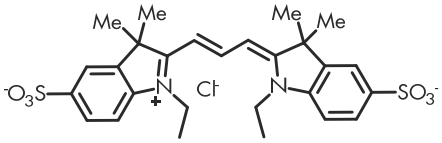

Cy3

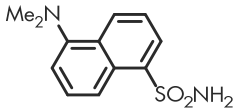

Dansyl amide

Composé	λ_{ex} (nm)	λ_{em} (nm)	Déplacement de Stokes (nm)	ε ($kL*mol^{-1}cm^{-1}$)	Φ_F[a]	Brilliance ($kL*mol^{-1}cm^{-1}$)
Alexafluor 350[7]	340	458	100	19	0.55	10.5
Fluorescéine[8]	494	521	18	90	0.92	83
Dansyl Amide[9]	335	516	181	4.2	0.37	1.6
Cy3[10]	560	575	15	150	0.09	13.5

2.2. Exemple d'une librairie de fluorophores modulables

Étant donné que les maxima d'excitation et d'émission optimaux pour un fluorophore dépendent de l'application visée, la possibilité de moduler ces propriétés par des changements structurels est désirable. En 2008, le groupe de Park a rapporté une librairie de fluorophores structurellement modulables, les 1,2-dihydropyrrolo[3,4-*b*]indolizin-3-one, nommés Séoulfluors.[11]

2.2.1. Synthèse des Séoulfluors

Figure 9. Synthèse des hétérocycles 1,2-dihydropyrrolo[3,4-*b*]indolizin-3-one

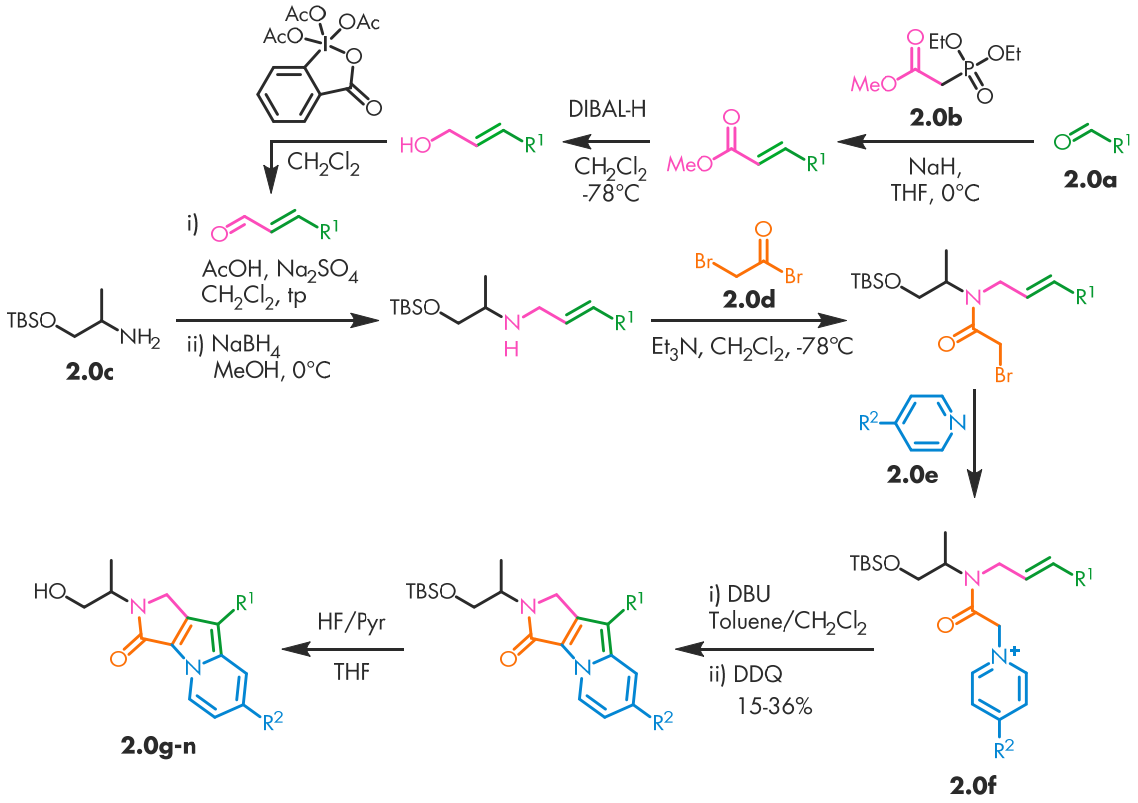

Les Séoulfluors sont synthétisés via une séquence linéaire de 8 étapes à partir d'un aldéhyde **2.0a**, d'un acétylphosphonate **2.0b**, de 2-amino-1-propanol (alaninol, **2.0c**), de bromure de bromoacétyle **2.0d** et d'une pyridine **2.0e** (**Figure 9**). L'aldéhyde et la pyridine peuvent porter des substituants variés, ce qui a permis la synthèse de nombreux fluorophores par une approche combinatoire. L'étape clé de cette séquence est celle où le cœur fluorescent est créé. Il s'agit d'une cycloaddition [3+2] intramoléculaire entre le dipôle 1,3 généré par la déprotonation d'un α-pyridinium amide (**2.0f**) et un alcène. Le produit est ensuite oxydativement aromatisé par traitement

au DDQ. Malheureusement, cette étape ne procède qu'avec un rendement modeste. Après le clivage du groupe protecteur TBS, l'alcool primaire peut être utilisé comme levier synthétique pour introduire des groupements réactifs de conjugaison. Ces groupements permettent d'étiqueter une molécule cible avec un fluorophore par formation d'un lien covalent.

2.2.2.Modélisation des orbitales moléculaires frontières

Figure 10. Représentation des orbitales moléculaires frontières de la structure 1,2-dihydropyrrolo[3,4-*b*]indolizin-3-one (image tirée de *ref. 11a*)

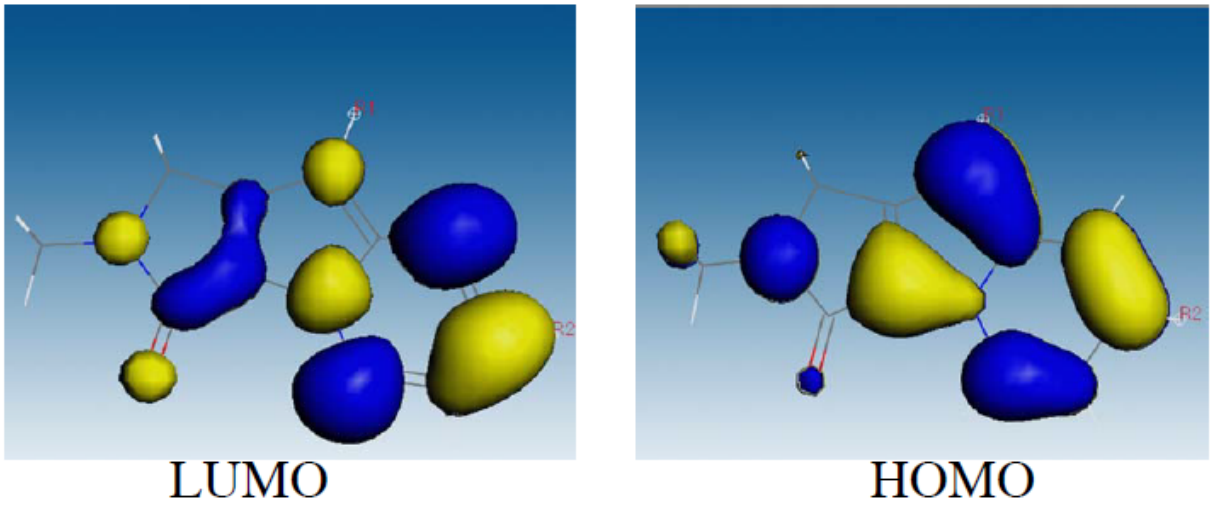

Les auteurs ont utilisé une méthode computationnelle pour rationaliser la relation entre les maxima d'émission observés et la substitution autour du cœur (*core*) fluorescent. Les résultats de leur modélisation des orbitales moléculaires frontières à l'état fondamental sont présentés dans la **Figure 10**. Si la densité de probabilité à la position R^2 ne semble pas changer significativement entre la HOMO et la LUMO, le lobe à la position R^1 est beaucoup plus petit sur la LUMO. Cette situation ouvre la porte à une stratégie permettant de moduler la différence d'énergie entre ces deux orbitales, qui est directement reliée aux propriétés émissives.

Figure 11. Stratégies de modulation des propriétés émissives

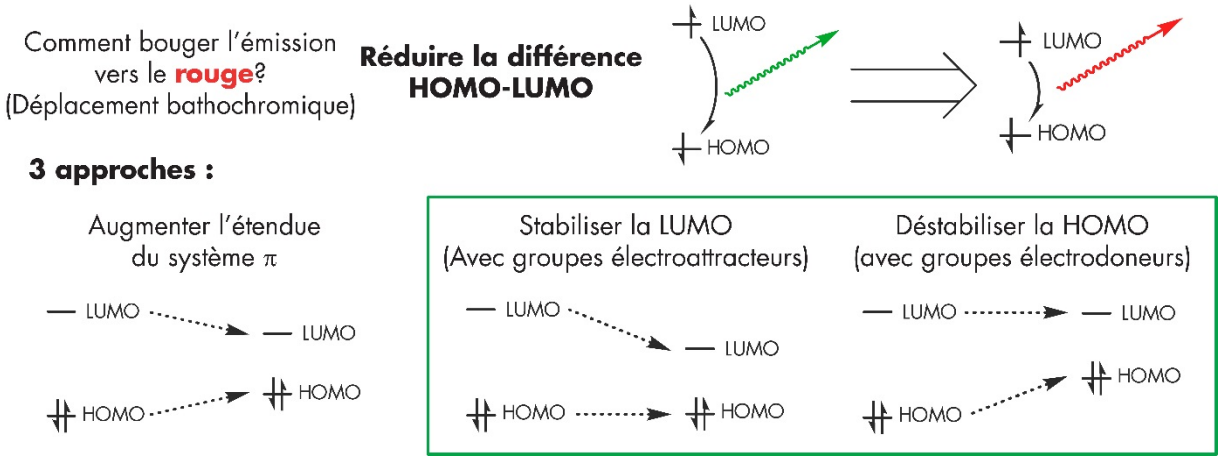

En effet, pour déplacer la longueur d'onde de la lumière émise vers le rouge, par exemple, il faut réduire l'écart énergétique entre les orbitales moléculaires frontières, ce qui a pour effet de réduire l'écart entre les états électroniques S0 et S1. Il existe trois approches générales pour réduire cet écart. Une approche fréquemment utilisée est d'augmenter l'étendue du système délocalisé à l'origine de la fluorescence.[12] Cette approche requiert habituellement plusieurs étapes de synthèse. Une alternative qui devient possible quand une position possède une densité électronique très différente entre la HOMO et la LUMO consiste à altérer le niveau d'énergie d'une orbitale frontière sans trop affecter l'autre. Dans le cas des Séoulfluors, un groupement électrodonneur en position R^1 déstabilise la HOMO plus que la LUMO car la probabilité de présence électronique y est plus grande. Cette modification réduit l'écart énergétique entre les OMF (Orbitales Moléculaires Frontières), causant un déplacement bathochromique du maximum d'émission. Une modification de substituant stablisant la LUMO est une autre manière d'observer ce phénomène.

2.2.3.Propriétés photophysiques des Séoulfluors

Tableau II. Propriétés photophysiques des Séoulfluors

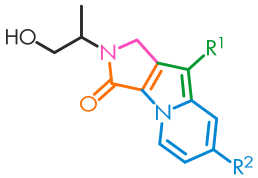

2.0g-n

Composé	R^1	R^2	λ_{ex} (nm)	λ_{em} (nm)	Déplacement de Stokes (nm)	ε ($kL*mol^{-1}cm^{-1}$)	Φ_F [a]	Brilliance ($kL*mol^{-1}cm^{-1}$)
2.0g	Me	Ac	396	471	75	5.6	0.82	4.6
2.0h	Ph	Ac	403	507	104	12	0.74	8.8
2.0i	2-$MeOC_6H_4$	Ac	404	508	104	16	0.71	11
2.0j	2-Thiophene	Ac	349	540	191	11	0.35	3.7
2.0k	4-NMe_2-C_6H_4	Ac	440	613	173	9.6	0.15	1.4
2.0l	2-$MeOC_6H_4$	H	320	461	141	17	0.37	6.2
2.0m	2-$MeOC_6H_4$	Ph	381	489	108	12	0.55	6.7
2.0n	2-$MeOC_6H_4$	CN	391	493	102	10	0.69	7.1

Le déplacement bathochromique de l'émission en fonction de l'effet électroattracteur des substituants R^1 décrit ci-haut est clairement visible pour les composés **2.0h**, **2.0j** et **2.0k** (**Tableau II**). Les effets reliés aux propriétés électroniques du substituant à la position R^2 sont beaucoup moins bien définis. Pareillement, la différence de densité électronique entre la HOMO et la LUMO est peu prononcée, rendant la prédiction de ces effets difficile.

2.3.Du sous-produit à la librairie

Comme pour un bon nombre de découvertes dans l'histoire de la chimie, ce projet a débuté par un résultat inattendu. Alors qu'il tentait d'effectuer un simple couplage de Suzuki-Miyaura[13], G. Pelletier , Ph. D. a remarqué un produit indésiré de couleur jaune très vive. Sous un tube fluorescent émettant des UVA (365 nm), le produit brillait d'une lumière bleue. Des analyses SMBR et RMN de routine ont permis d'élucider la nouvelle structure. Cet hétérocycle n'ayant pas encore été rapporté dans la littérature, plusieurs analogues ont été synthétisés par L. Constantineau-Forget, M. Sc. dans le but d'explorer les limites de la méthode synthétique. La plupart des produits émettaient toujours une lumière bleue sous l'irradiation UV. C'est autour de ce moment que je me suis joint à ce projet, avec en tête le désir de comprendre l'origine de la fluorescence de ces molécules, pour ultimement arriver à établir un lien entre leur structure chimique et leurs propriétés émissives.

2.3.1.Activation d'amides par l'anhydride trifluorométhanesulfonique

2.3.1.1.Mécanisme général

Parmi les différents groupements carbonyl neutres, l'amide est souvent décrit comme un des moins réactifs.[14] En effet, la forte conjugaison entre la liaison π et le doublet de l'azote rend l'amide très peu attrayant pour une espèce nucléophile. Par contre, vu la forte densité électronique centrée sur l'atome d'oxygène, la tendance de réactivité des carbonyles est inversée face à un électrophile, avec l'amide en tête de liste. Si l'électrophile utilisé peut convertir l'oxygène en groupe partant, un imidate activé tel que **2.0o** est formé. L'atome de carbone sp^2 du carbonyl initial devient alors un très bon électrophile. Il peut subir une réaction de type addition-élimination (ou élimination-addition *via* l'intermédiaire nitrilium **2.0p**) avec des nucléophiles variés. En bref, cette technique arrive à inverser la réactivité des amides face aux nucléophiles, leur permettant de réagir chimiosélectivement même en présence d'un aldéhyde.[15]

Figure 12. Mécanisme de l'activation d'amides avec l'anhydride trifluorométhanesulfonique en milieu basique

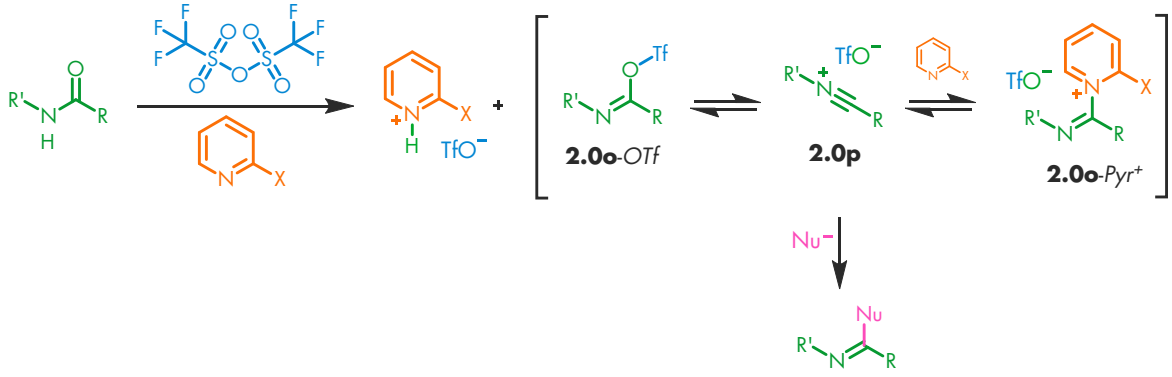

2.3.1.2. Cyclisation d'amidopyridines: synthèse d'imidazopyridines

Ce type de réaction impliquant une espèce électrophile hautement réactive est encore plus efficace lorsque le nucléophile fait partie de la même molécule. En effet, si un azote nucléophile comme celui d'un cycle pyridine se trouve à 4 atomes de distance du carbonyl de l'amide, une cyclisation *5-endo-trig* (*5-endo-dig* si l'intermédiaire nitrilium est impliqué) se produit rapidement après la formation de **2.0o**. Une simple déprotonation permet ensuite l'aromatisation, formant une imidazopyridine stable (**Figure 13**, **2.6'**).[16]

Figure 13. Cyclisation-déshydratation d'amidopyridine

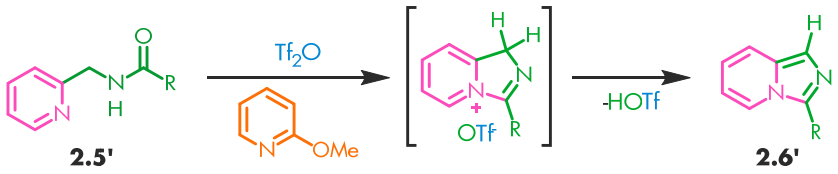

2.3.2.Arylation C-H intramoléculaire catalysée par le palladium, une découverte fortuite

Figure 14. Un couplage au rendement décevant?

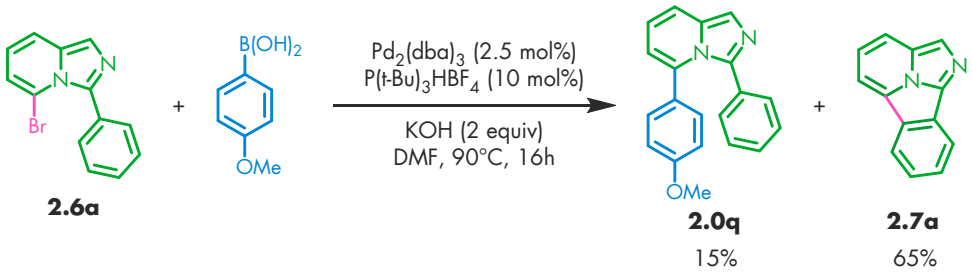

L'exemple ci-dessus décrit une des rares instances où un expérimentateur est satisfait d'un couplage de Suzuki-Miyaura dont le rendement n'excède pas 20%. Il apparaît que le complexe de palladium(II) formé par l'addition oxydante dans le lien carbone-brome réagit plus vite avec le cycle aromatique adjacent (intramoléculaire) qu'avec l'acide boronique (intermoléculaire), formant un palladacycle à 6 membres. Ensuite l'élimination réductrice expulse le palladium, l'augmentation de la tension de cycle étant compensée par la décompression stérique entre les ligands encombrés et le substrat aromatique (voir **Figure 20**, page - 26 -). Cette nouvelle structure hétérocyclique et fluorescente piqua notre intérêt et motiva l'optimisation rapide de la cyclisation au palladium, puis des techniques permettant de comprendre et de fonctionnaliser ce « cœur » aromatique.

2.4.Structures similaires connues

Même si nous avions une structure précédemment inconnue sous la main, les données rapportées sur des molécules similaires sont un bon point de départ et une base de comparaison pour établir les avantages et inconvénients de notre voie synthétique. De plus, la plupart des hétérocycles similaires sont aussi fluorescents, ce qui facilite la mise en perspective des propriétés photophysiques des benzo[*a*]imidazo[2,1,5-*c*,*d*]indolizines.

2.4.1.Benzo[*a*]imidazo[5,1,2-*cd*]indolizines via une cycloaddition [8+2]

Figure 15. Synthèse de Benzo[*a*]imidazo[5,1,2-*cd*]indolizines par cycloaddition-aromatisation oxydative avec un benzyne.

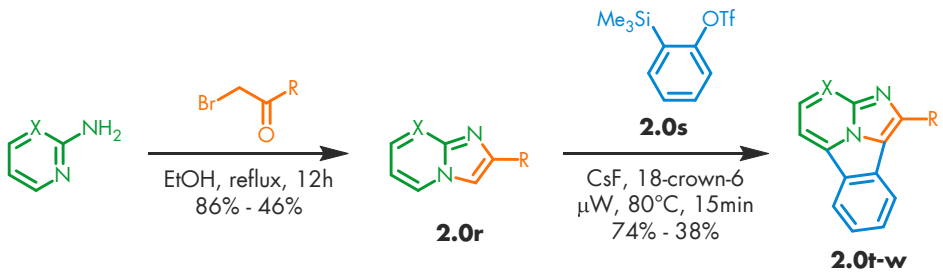

Le groupe de Cossio a rapporté la synthèse d'un hétérocycle benzo[*a*]imidazo[5,1,2-*cd*]indolizine (**2.0t-w**) qui diffère seulement par l'orientation du cycle imidazole fusionné.[17] La synthèse, très expéditive, a comme étape clé une cycloaddition [8+2] entre une imidazo[1,2-*a*]pyridine **2.0r** et un intermédiaire benzyne généré *in situ*, suivie d'une aromatisation oxydative (**Figure 15**). Le rendement de cette étape dépend fortement de la nature de la substitution sur l'imidazopyridine. Le mécanisme de cette réaction a été étudié et modélisé en détail.

Vu la complexité de la synthèse des trifluorométhanesulfonates de 2-triméthylsilylphényle (**2.0s**) substitués, la principale position facilement modifiable est celle du carbone exocyclique sur l'imidazole (**2.0t-w**, groupement R). L'effet de cette substitution sur la fluorescence est résumé dans le **Tableau III**. Le 4-nitro phényl est le seul substituant avec un effet notable, entraînant un déplacement bathochromique de l'émission et une augmentation marquée du déplacement de Stokes.

Tableau III. Propriétés photophysiques des benzo[*a*]imidazo[5,1,2-*cd*]indolizines

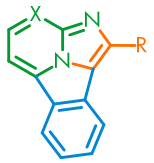

2.0t-w

Composé	R	λ_{ex} (nm)	λ_{em} (nm)	Déplacement de Stokes (nm)	ε (kL*mol^{-1}cm^{-1})	Φ_F[a]	Brilliance (kL*mol^{-1}cm^{-1})[31]
2.0t	CO_2Et	408	419	11	-	0.09	-
2.0u	4-$MeOC_6H_4$	419	428	9	-	0.37	-
2.0v	4-FC_6H_4	418	425	7	-	0.38	-
2.0w	4-$NO_2C_6H_4$	419	589	170	-	0.10	-

2.4.2.Imidazo[5,1,2-*de*]naphtho[1,8-*ab*]quinolizine par oxydation directe

Figure 16. Synthèse de la structure imidazo[5,1,2-*de*]naphtho[1,8-*ab*]quinolizine.

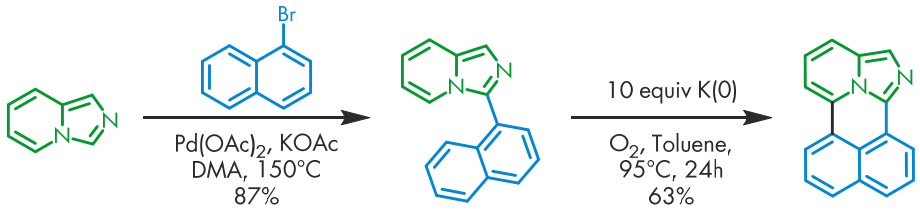

2.0x **2.0y**

Une autre manière, plus drastique, de générer un système conjugué cyclique étendu contenant une imidazo[1,5-*a*]pyridine implique une cyclisation directe oxydative en présence de potassium métallique.[18,19] Étonnamment, le composé **2.0x** est très peu fluorescent, avec un rendement quantique de seulement 0.005 (ou 0.5%). Le coefficient d'absorptivité molaire n'est pas rapporté. Le composé **2.0y** est, quant à lui, fluorescent dans la lumière violette-bleue, comme la plupart des 1-arylimidazo[1,5-*a*]pyridines.

Tableau IV. Propriétés photochimiques des composés **2.0x** et **2.0y**.

Composé	λ_{ex} (nm)	λ_{em} (nm)	Déplacement de Stokes (nm)	ε ($kL*mol^{-1}cm^{-1}$)	Φ_F [a]	Brilliance ($kL*mol^{-1}cm^{-1}$)[31]
2.0x	336	438	102	-	0.07	-
2.0y	410	556	146	-	0.005	-

2.4.3.Diarylimidazo[1,5-*a*]pyridines par cyclisation de thioamides et halogénation-couplage

Figure 17. Synthèse de 1,3-diarylimidazo[1,5-*a*]pyridines

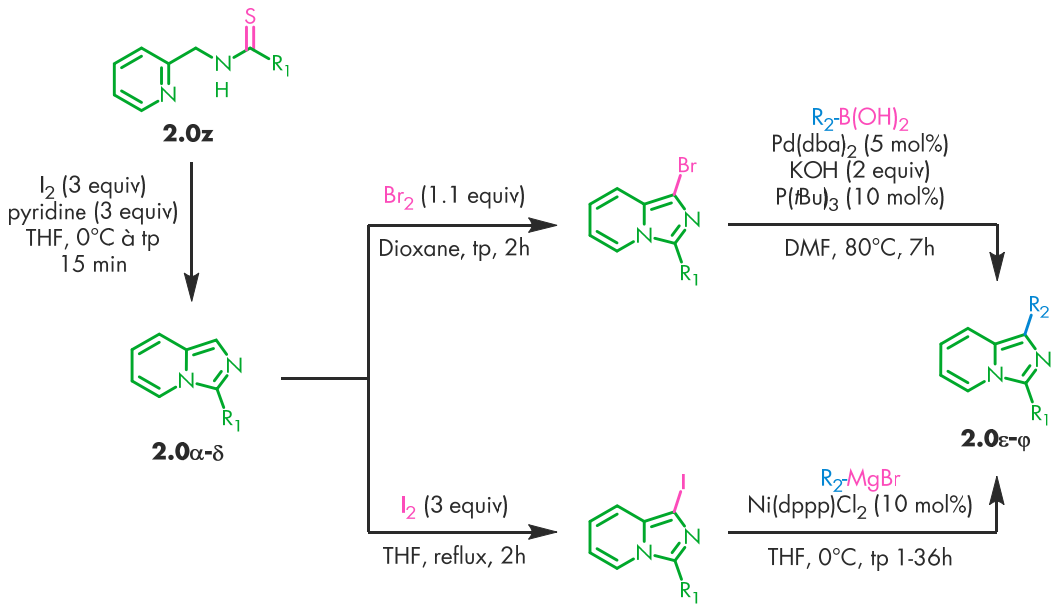

En effet, le bicycle imidazo[1,5-*a*]pyridine a lui aussi des propriétés émissives bien connues.[20] L'effet sur ces propriétés de la substitution en positions 1 et 3 par des groupements aromatiques a été exploré par le groupe de Murai[21] (**Figure 17**). Le groupement en position 1 (R^1) est introduit avant la fermeture du cycle imidazole, effectuée *via* l'oxydation de l'atome de soufre d'une thioamide (**2.0z**). Le groupement en position 3 (R_2) est ensuite ajouté par couplage aryl-aryl, après l'halogénation directe de cette position intrinsèquement nucléophile. Des mono- et diarylimidazo[1,5-*a*]pyridines variées ont été préparées et caractérisées (**2.0α-φ**). Une sélection de propriétés photophysiques montrant leur relation avec la substitution sur les groupements aryle est

présentée dans le **Tableau V**. Il est possible de remarquer pour les deux positions une tendance générale de déplacement bathochromique des maxima d'émission à mesure que la densité électronique des substituants aromatiques augmente (**2.0α**, **2.0β** et **2.0δ**; **2.0ε**, **2.0ϕ** et **2.0γ**). Par contre, ces effets ne sont pas très marqués et semblent peu cumulatifs (comparer **2.0ε**, **2.0γ**, **2.0η** et **2.0ι**). Ceci pourrait être expliqué par la déconjugaison en solution d'un ou l'autre des substituants par rotation autour du lien simple Csp^2-Csp^2, forcée par la répulsion stérique entre les hydrogènes *ortho* des substituants et ceux en position 4 et 7 sur l'imidazo[1,5-*a*]pyridine (**Figure 18**). Il est probable que cette conformation réduise l'impact électronique du cycle déconjugué sur les orbitales moléculaires frontières (OMF) du système, dont les différences énergétiques sont directement liées aux propriétés émissives.

Tableau V. Propriétés photophysiques des arylimidazo[1,5-*a*]pyridines

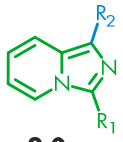

2.0α-φ

Composé	R_1	R_2	λ_{abs} (nm)	λ_{em} (nm)	Déplacement de Stokes (nm)	ε ($kL*mol^{-1}$ cm^{-1})	Φ_F[a]	Brilliance ($kL*mol^{-1}$ cm^{-1})[31]
2.0α	Ph	H	317	461	144	17.8	0.072	1.28
2.0β	4-OMe-C_6H_4	H	306	469	163	11.2	0.052	0.58
2.0χ	4-F-C_6H_4	H	312	465	153	12.9	0.060	0.77
2.0δ	4-NMe_2-C_6H_4	H	269 322	482	213 160	13.8 21.4	- 0.076	- 1.62
2.0ε	Ph	Ph	308	454	146	15.1	0.14	2.11
2.0ϕ	Ph	4-Me-C_6H_4	293	457	164	8.3	0.20	1.67
2.0γ	Ph	4-OMe-C_6H_4	308	471	163	22.4	0.17	3.81
2.0η	4-OMe-C_6H_4	Ph	301	465	164	17.8	0.18	3.20

2.0ι	4-OMe-C_6H_4	4-OMe-C_6H_4	303	479	176	20.4	0.22	4.49
2.0φ	4-OMe-C_6H_4	2-Thiophene	316	483	167	11.2	0.14	1.57

Figure 18. Minimisation *ab initio*[a] de l'état fondamental de la 1,3-diphénylimidazo[1,5-*a*]pyridine **2.0u** illustrant la déconjugaison partielle des substituants aromatiques

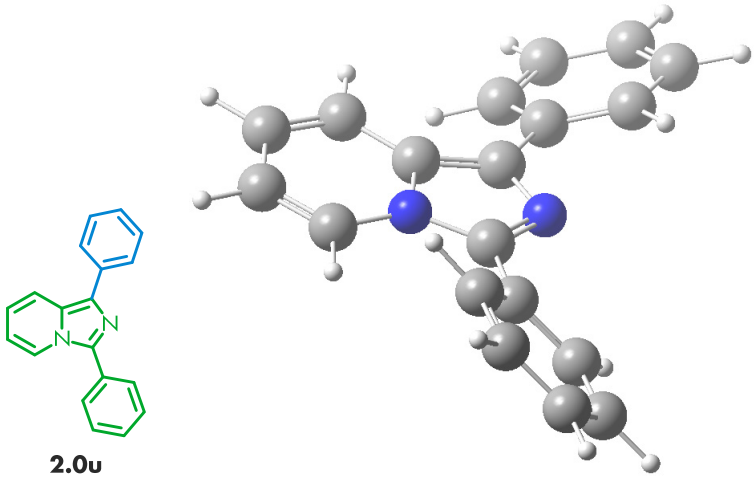

[a] Calculs DFT B3LYP 6.31G(d,p) dans le champ de solvant du méthanol effectués avec le logiciel Gaussian 09.

2.5.Article accepté dans le *Journal of Organic Chemistry*: General C–H Arylation Strategy for the Synthesis of Tunable Visible Light Emitting High Stokes Shift Benzo[*a*]imidazo[2,1,5-*c*,*d*]indolizines Fluorophores

Éric Lévesque, William S. Bechara†, Léa Constantineau-Forget†, Guillaume Pelletier, Natalie M. Rachel, Joelle N. Pelletier and André B. Charette*

Centre in Green Chemistry and Catalysis, Faculty of Arts and Sciences, Department of Chemistry, Université de Montréal, P.O. Box 6128, Station Downtown, Montréal, Québec, Canada, H3C 3J7

2.5.0.Participation des coauteurs

Éric Lévesque a optimisé les réactions de fonctionnalisation des tétracycles, a effectué les expériences de modélisation, les études cinétiques et le traitement des données produites, a rédigé le corps de l'article et a synthétisé et caractérisé la majeure partie des nouvelles molécules rapportées. Léa Constantineau-Forget, M. Sc. en a préparé et caractérisé environ le tiers. William S. Bechara, Ph. D. a effectué la synthèse de quelques structures (notamment les tricycles imidazo[2,1,5-*c*,*d*]indolizine) et assisté à la rédaction de la partie expérimentale et à l'organisation des données. Guillaume Pelletier, Ph. D. et William ont co-rédigé l'introduction de l'article. Léa, Éric et William ont travaillé sous la supervision du Pr. A. B. Charette. Natalie M. Rachel a effectué les expériences de bioconjugaison, sous la supervision de la Pr. Joëlle N. Pelletier.

2.5.1.Abstract:

Herein we report the discovery of the benzo[*a*]imidazo[2,1,5-*c*,*d*]indolizine motif displaying tunable full-color light emission. This new class of fluorescent dye is remarkable for its high chemical stability and unusually high Stokes shift. The tetracyclic fluorophores are synthesized from readily available amides *via* a chemoselective process involving Tf_2O-mediated amide cyclodehydration followed by intramolecular C–H arylation. The resulting aromatic structures are easily functionalized by electrophilic reagents to access a large library of fluorescent molecules with diversified substitution patterns. These compounds' photophysical properties were rationalized by DFT calculations. For some compounds, emission wavelengths can be predicted from the substituent's Hammett constants. Easily introduced nonconjugated reactive functional groups enable the labelling of biomolecules without modification of emissive properties.

2.5.2.Introduction

Organic fluorophores are privileged structures that have found pivotal applications in biological imaging, clinical diagnosis, and drug discovery.[4, 22] Such small molecules are routinely employed in stimulated emission depletion (STED) microscopy[23] and single-molecule microscopy,[24] tools extensively used in biochemistry for the precise tracking of specific molecules in complex biological systems.[25] In addition, the handling of water-soluble small-molecule fluorophores (i.e. rhodamine, benzopyrylium salts, fluorescein, BODIPY, etc.) is operationally attractive in contrast to fluorescent metal complexes or proteins (such as GFPs), which broadens their application in both medical and material sciences.[26,27,28] Specifically, fluorescent molecules have gained considerable popularity recently in material science due to their successful incorporation into organic light-emitting diodes (OLEDs).[29] Despite the wide spectrum of applications, few examples of organic, metal-free and color-tunable fluorescent cores are available in the literature. Most of the commonly employed dyes suffer from a narrow variability of the absorption and emission wavelengths and the effect of substituents on these wavelengths is often difficult to predict.[30] Furthermore, the methodical design of fluorescent scaffolds with specific predictable emission wavelengths and high brightness[31] is still a difficult task.[32]

The constant efforts to characterize and to understand each fluorophore's distinct properties are essential endeavors for both fundamental and commercial applications. A good

example of such innovation is characterized by the development of a series of tunable fluorescent 1,2-dihydropyrrolo[3,4-*b*]indolizin-3-ones, also called Seoul-Fluors, initiated by the Park group.[11] A combinatorial approach is used to synthesize a library of fluorophores from a single molecular framework. A significant variability of photophysical properties is achieved by installing substituents at specific positions on the fluorescent core. Density Functional Theory (DFT) calculations helped pinpoint such tunable areas on the dye. A challenging 1,3-dipolar cycloaddition reaction was needed to access the key tricyclic framework.

In order to address the challenges associated with small molecule fluorophore synthesis and applications, we report the discovery of a tetracyclic structure with previously unknown fluorescent properties. [17,19,33] Further chemical modifications of the tetracyclic scaffold, through a rational approach based on DFT calculations, enable the full-color-tuning of their emissive properties. These benzo[*a*]imidazo[2,1,5-*c*,*d*]indolizines are readily synthesized and functionalized in a practical, high-yielding and divergent synthetic pathway. This led to the elaboration of a library of fluorescent molecules with emission wavelengths covering the entire visible spectrum, featuring a high chemical stability and an unusually high Stokes shift (up to 281 nm). The synthesis of these fluorophores is described, followed by mechanistic, DFT and photophysical properties studies. Nonconjugated reactive functional groups can be appended to the aromatic core without affecting its innate photophysical properties. Such a group enabled the tagging of two target proteins through an enzyme-catalyzed glutamine transamidation.

2.5.3.Results and discussion

2.5.3.1.Synthetic approach.

Our group initially reported the synthesis of a single example of the benzo[*a*]imidazo[2,1,5-*c*,*d*]indolizine scaffold, obtained in 3 simple steps from 6-bromo-2-pyridinemethanamine.[16] However, this commercially available primary amine is prohibitively expensive. In order to broaden the accessibility of this methodology, an alternative and easily scalable 6-step procedure from commercially available and inexpensive chemicals was designed (**Figure 19**).

Figure 19. General Synthetic Pathway Toward Benzo[*a*]imidazo[2,1,5-*c,d*]indolizines Fluorophores

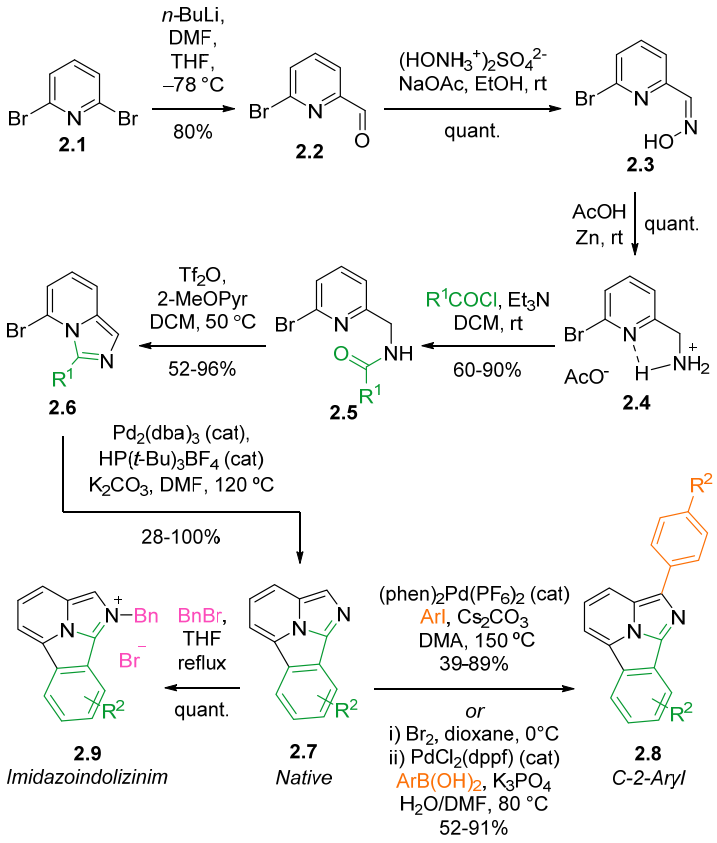

Commercially available 6-bromopicolinaldehyde (**2.2**) can either be purchased or generated from 2,6-dibromopyridine (**2.1**).[34] The previously reported synthetic pathway is intercepted by condensation of **2.2** with hydroxylammonium sulfate to yield the corresponding oxime (**2.3**), followed by treatment with powdered zinc metal in AcOH which reduces the oxime to the ammonium acetate salt (**2.4**). These last two steps quantitatively yield the primary ammonium on a multi-gram scale. The fluorophore's fused benzene ring, along with any desired substitution, is then introduced by acylation of the primary ammonium (**2.4**) with a benzoyl chloride derivative. The resulting secondary amides (**2.5**) are then treated under the optimized triflic anhydride-mediated cyclodehydration/aromatization conditions previously developed by our research group[16] to afford the corresponding imidazo[1,5-*a*]pyridines (**2.6**) (**Tableau VI**, amides **2.5** to imidazo[1,5-*a*]pyridines **2.6**). This step is the first in the sequence where some products require chromatographic purification.

The second cyclization, giving access to the fluorescent core, takes place *via* a palladium catalyzed intramolecular C–H arylation. This high-yielding transformation is triggered by a Pd(0) precatalyst, a bulky trialkylphosphine ligand, [35] and an excess of carbonate base (**Tableau VI**, imidazo[1,5-*a*]pyridines (**2.6**) to benzo[*a*]imidazo[2,1,5-*c*,*d*]indolizines (**2.7**)). Interestingly, KOH as base also promotes the reaction, albeit with lower reaction rates (>12 h needed to reach completion), indicating that the carbonate anion is beneficial but not necessary for the reaction to occur.[36] We decided to investigate this transformation by performing kinetic isotopic assays. A reaction rate comparison between fully deuterated (**2.6a**-d_5) and non-deuterated (**2.6a**) substrates results in a k_H/k_D ratio of 1.9. By analogy, an intramolecular competition reaction (**2.6a**-*ortho*-d_1) yields the C–H and C–D insertion products in a ratio of 2:1 which represent a 2.0 KIE value. These results support a mechanism where the turnover limiting step is either the C–H insertion step or the reductive elimination (in which case the former would be reversible) (**Figure 20**).[37] A concerted metalation-deprotonation (CMD) mechanism could be invoked when carbonate anions are present.[36] The rate decrease resulting from the absence of carbonate supports the hypothesis that C–H insertion step is turnover limiting, since the rate of that step is affected by the nature of the base/proton shuttle.

Figure 20. Proposed mechanism for the intramolecular C-H arylation

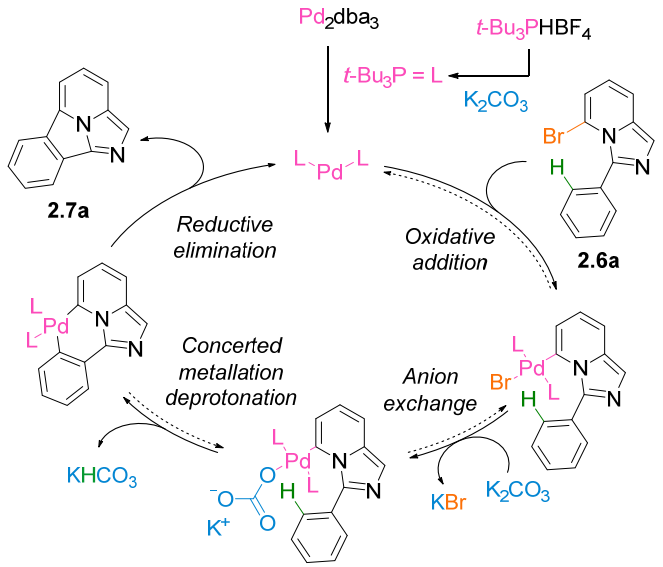

After efficient reaction conditions for both intramolecular cyclization steps were established, a large variety of benzo[*a*]imidazo[2,1,5-*c*,*d*]indolizines fluorophores were prepared

(**Tableau VI**). Gratifyingly, the overall process was shown to be efficient in the presence of various functional groups (R^2 in **Figure 19**). Both reactions are high yielding for both electron-poor and electron-rich amides (**Tableau VI**, entries 2-16). Another remarkable result is the formation of oxygen and sulfur-containing heterocycles **2.7q** and **2.7r**, albeit in lower yields for the C–H arylation step (entries 17-18). Alternatively, the methodology can also be extended to conjugated vinylic amides (entries 19-20). In this case, the second cyclization occurs *via* a carbometallation-elimination sequence. Unsurprisingly, an alkene whose geometry forces a *trans* β-hydride elimination gives a low yield (entry 20).

Tableau VI. Synthesis of "Native" Benzo[*a*]imidazo[2,1,5-*c*,*d*]indolizines: Cyclodehydration and C–H Arylation

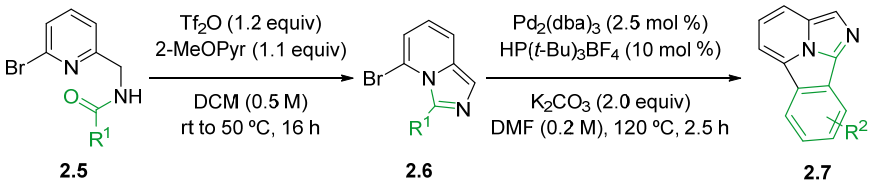

entry	amide (**2.5**)			imidazopyridine (**2.6**)		Benzoimidazo indolizines (**2.7**)		yield (**2.6**) (%)[a]	yield (**2.7**) (%)[b]
1		R^2 = H	2.5a		2.6a		2.7a	96	100
2		Ph	2.5b		2.6b		2.7b	87	100
3		*t*-Bu	2.5c		2.6c		2.7c	91	89
4		OBn	2.5d		2.6d		2.7d	91	90
5		$O(CH_2)_2OBz$	2.5e		2.6e		2.7e[c]	52	89[c]
6		NMe_2	2.5f		2.6f		2.7f	84	98
7		F	2.5g		2.6g		2.7g	90	98
8		Cl	2.5h		2.6h		2.7h	89	94
9		CO_2Me	2.5i		2.6i		2.7i	81	95
10		CN	2.5j		2.6j		2.7j[d]	88	99[d]
11			2.5k		2.6k		2.7k	88	93
12			2.5l		2.6l		2.7l	94	92
13			2.5m		2.6m		2.7m	93	66
14			2.5n		2.6n		2.7n	86	98
15			2.5o		2.6o		2.7o	86	97

16	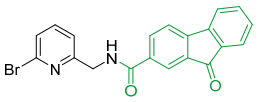	2.5p	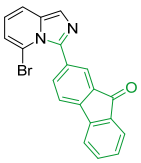	2.6p	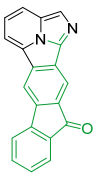	2.7p	65	61
17	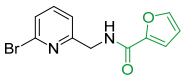	2.5q	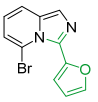	2.6q	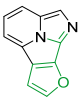	2.7q	84	40
18	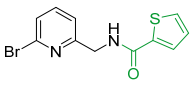	2.5r	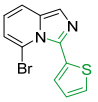	2.6r	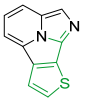	2.7r	90	65
19	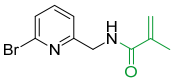	2.5s		2.6s		2.7s	74	87
20	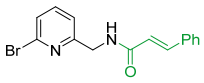	2.5t	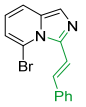	2.6t	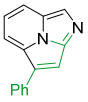	2.7t	94	28

[a] Isolated yield for the corresponding imidazo[1,5-*a*]pyridine (**2.6**) (%). [b] Isolated yield for the corresponding benzo[*a*]imidazo[2,1,5-*c*,*d*]indolizines (**2.7**) (%). [c] Yield of saponified product (primary alcohol) over 2 steps. [d] Made with no chromatographic purification over 6 steps. Overall yield from 2,6-dibromopyridine : 29%.

Figure 21. Elaboration of the C-2-Aryl Series: C–H arylation or Electrophilic Bromination/Suzuki-Miyaura Coupling

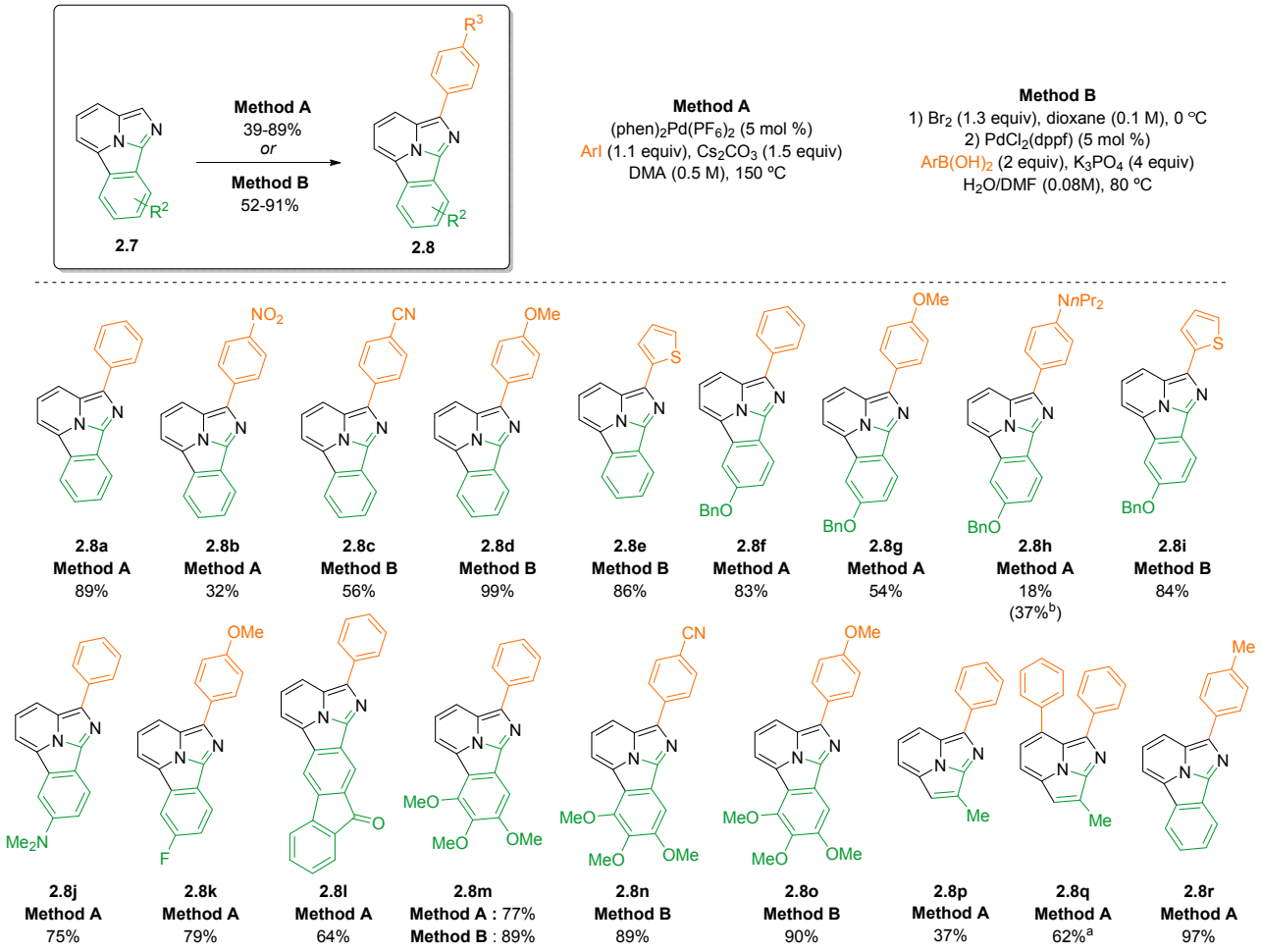

a 2.0 equiv of iodide used. *b* Corrected for recovered starting material.

The benzo[*a*]imidazo[2,1,5-*c,d*]indolizines (**2.7**) generated from the previous sequence are referred to as the *native* series. Similarly to the parent imidazo[1,5-*a*]pyridines,[21] they have an inherently nucleophilic character. For example, they successfully react at position C-2 under the cationic palladium-catalyzed arylation conditions reported by the Murai group[38] (**Figure 21**, method A). This allows for the synthesis of a second category of fluorophores, dubbed the *C-2-aryl* series (**2.8**). This arylation can also be achieved in two steps *via* a regioselective electrophilic bromination by the Br_2-dioxane complex followed by a Suzuki-Miyaura coupling[21] (**Figure 21**, method B). Both approaches provide good to excellent yields for most coupling partners. Interestingly, when tricycle **2.7s** was subjected to the direct arylation conditions, a significant amount of the diarylated

derivative **2.8q** was isolated along with a modest yield of **2.8p**, highlighting the tricyclic and tetracyclic scaffolds' distinct electronic properties.

Figure 22. Alkylation of Exocylic Nitrogen

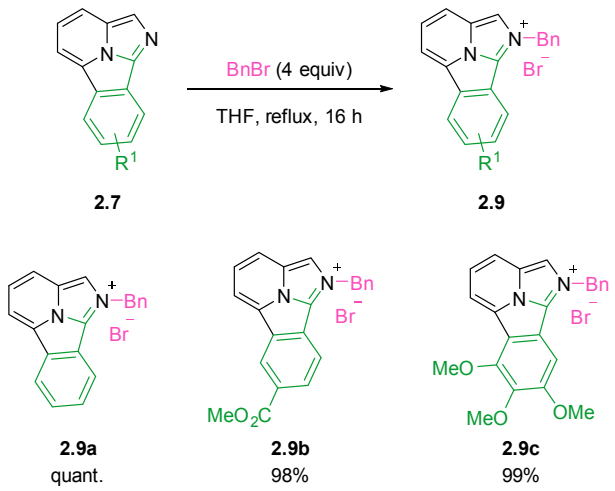

The *N*-alkylation or protonation of the exocyclic nitrogen produces a series of fluorescent *imidazoindolizinium* salts (**Figure 22**). Under electrophilic benzylation conditions, the desired salt precipitates quantitatively and can be filtered out, requiring no further purification.

Figure 23. (a) Crystal structure of **2.7k** (b) Approximate bond orders (*ref. 39*) and atom numbering

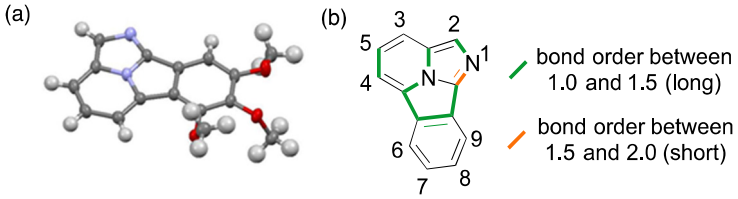

2.5.3.2.Structural properties.

The high crystallinity of benzo[*a*]imidazo[2,1,5-*c*,*d*]indolizines allows for the easy growth of single crystals (in the case of compound **2.7k**, a single 200 mg piece was obtained). X-ray diffraction spectroscopy revealed the main core is completely flat, with most outer bonds of order between 1.0 and 1.5 (elongated) (**Figure 23**). [39] The perfect planarity of the internal nitrogen indicates sp^2 hybridization, meaning the imidazopyridine's 10-electron aromaticity is conserved. However, the

fused benzene ring is distorted, the bridging bond being slightly longer than the other five. This suggests at least some 14-electron conjugation around all four fused rings.

2.5.3.3.Photophysical properties.

The members of the *native* series generally exhibit blue fluorescence, with a λ_{max} of emission between 461 nm and 489 nm. The excitation curves feature two to three well-defined peaks that all produce the same emission peak, ruling out fluorescence from higher excited states (**Tableau VII, 2.7a**).[5] The lowest wavelength peak exhibits an unusually high Stokes shift of 186 nm.[40] A direct excitation to a higher electronic level, followed by nonradiative relaxation to the first electronic excited state (S1) and radiative relaxation to ground state (S0) is a likely explanation.[5] Functional group modifications on the fused benzene ring can affect the emissive properties, especially if resonance is possible. The most noticeable effect is a bathochromic shift of emission caused by electron-donating groups at the C-7 or C-9 positions (*para* and *ortho* positions of the initial benzoyl chloride) (**Tableau VIII,** compounds **2.7d-2.7f** and **2.7n**). Interestingly, adding two more methoxy groups on the *meta* positions C-6 and C-8 (**Tableau VIII,** compound **2.7k**) had the opposite effect, bringing back the emission band close to that of the unsubstituted **2.7a** (**Figure 25**) *via* inductive effects. The presence of an electron-withdrawing group at C-7 (**Tableau VII, 2.7i**) does not shift the emission band significantly, but alters the excitation curve to feature three well-defined peaks.

Arylation of the core with a phenyl group at the C-2 position causes a bathochromic shift of both spectra and some changes to the excitation spectrum (**Tableau VII, 2.8a**). The high-energy excitation peak (315 nm) widens and exhibits higher light output (brightness)[31] than its lower energy counterpart (469 nm).

Figure 24. Excitation curve (λ_{em} = 464nm) of **2.7a** in function of pH in aqueous media. [a] Relative normalized fluorescence intensity.

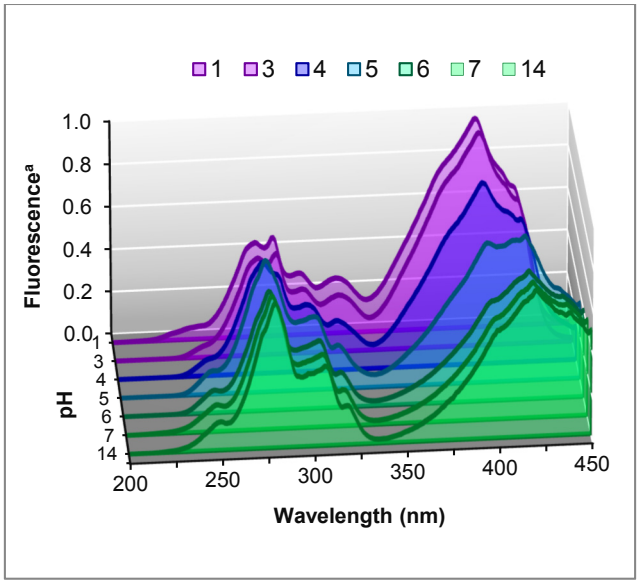

Imidazole ring *N*-alkylation significantly alters the photophysical properties. The emission and lowest-energy excitation peaks shift towards the violet (hypsochromic shift) while the latter becomes more intense. An almost identical spectrum can be obtained by exposing *native* **2.7a** to aqueous HCl, showing that the positive charge on the exocyclic nitrogen is responsible for the changes. When acquiring spectra in aqueous buffer solutions of varying pH, this spectrum change can be observed taking place between pH = 5 and pH = 3 (**Figure 24**). This observation is in line with the expected pK_a of the exocyclic nitrogen atom.[20b]

These empirical observations prompted us to turn to computational methods in order to locate the frontier molecular orbitals for all three systems. This should facilitate substituent effect prediction, enabling the rational modification of the fluorescent core to obtain specific emissive properties.[41]

Tableau VII. Photophysical and Computational Data of Representative Benzo[*a*]imidazo[2,1,5-*c,d*]indolizines

Structure and color[a]	Fluorescence Data	Calculated HOMO[b]	Calculated LUMO[b]
2.7a (*Native*) 	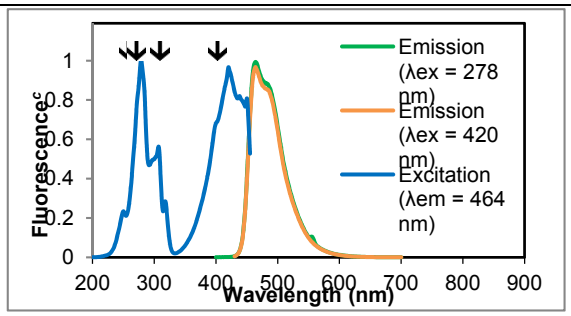	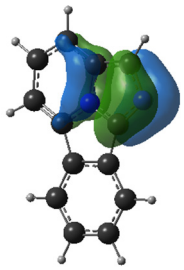	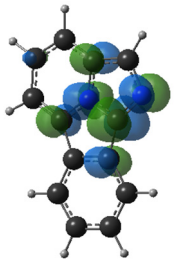
2.7i (*Native*) 	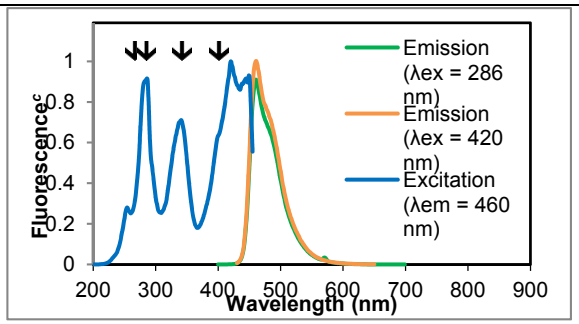	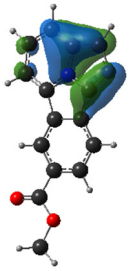	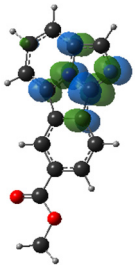
2.8a (C-2-Aryl) 	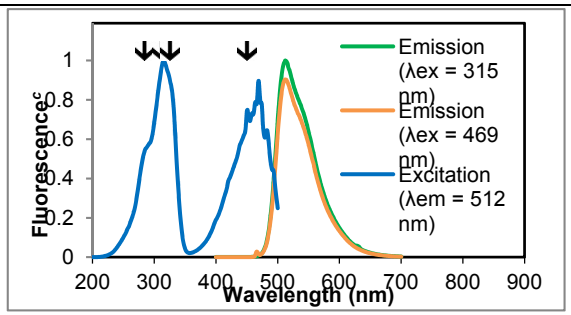	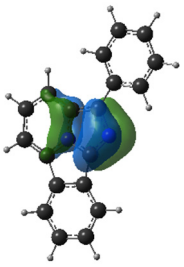	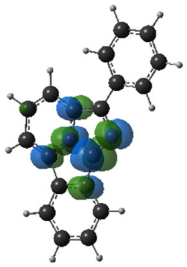
2.9d[d] (*Imidazoindolizinium*) 	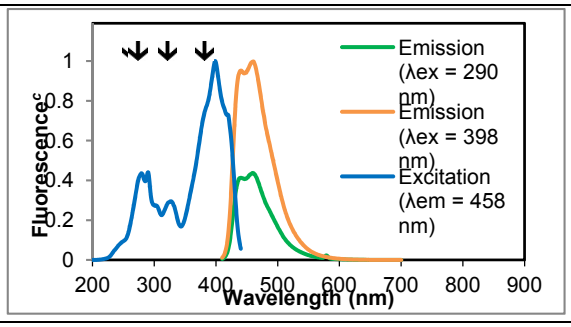	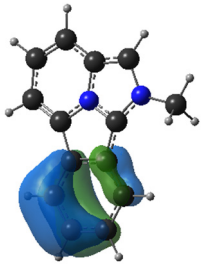	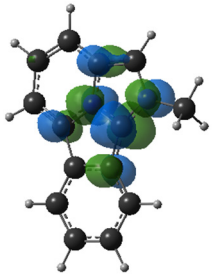

[a] Observed under an UVA-emitting low pressure mercury-vapor gas-discharge lamp ("blacklight blue") [b] See ref. 42 for basis set. [c] Normalized fluorescence intensity. [d] The N-methyl derivative was used in calculations to shorten computing time.

The resulting orbital representation of *native* **2.7a** (**Tableau VII**, **2.7a**)[42] shows that both the HOMO and LUMO are mostly centered on the imidazole ring. This explains why the two *meta* methoxy groups in compound **2.7k** counteract the bathochromic shift observed for the *para* or *ortho* alkoxy groups (compare with **2.7d** and **2.7n**). Moreover, the LUMO representation features a node at the C-2 position. This hints at a straightforward way to modulate the emission wavelength, as substitution at this position should influence the HOMO's energy level with minimal effect on the LUMO.

Frontier orbitals on the *C-2-aryl* core exhibit very little change, suggesting that the extra aryl group and its substituents can be a good handle to control the C-2 position's electron density. Time-dependent DFT (TD-DFT) calculations[42] allow the prediction of excitation wavelengths, which are in general agreement with the experimental results (**Tableau VII**, black arrows on graphs), adding validity to the employed model.[43]

Similar calculations performed on the *imidazoindolizinium* core show, in agreement with the measured fluorescence spectra, a completely different system. While the LUMO is still located on the imidazole ring, the neutral system's HOMO is stabilized by the positive charge on the ring and gets relegated to the HOMO^{-7} position. A π-orbital on the fused benzene ring takes the place of the HOMO, yielding a system where the frontier orbitals are separated, indicating the possibility of intramolecular charge transfer (ICT) fluorescence.[44] These theoretical results were not only verified by correlation between TD-DFT predictions and experimental excitation maxima, but also by substituent effect variation on the fused benzene ring. Since the HOMO is on that ring in the *imidazoindolizinium* series, all positions can contribute to its electron enrichment, not just the *ortho* (C-9) and *para* positions (C-7). Indeed, the addition of three methoxy groups at the positions C-6, C-7 and C-8 (**2.9c**) induces a bathochromic shift of 45 nm (Figure 25, **2.9a** and **2.9c**). This is in stark contrast with the *native* series, where that same modification had almost no effect on the photophysical properties (**Figure 25**, **2.7a** and **2.7k**).

Figure 25. Different effect of fused benzene ring substitution on *native* and *imidazoindolizinium* series.

	2.9a	2.9c	2.7a	2.7k
Structure	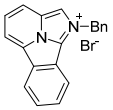	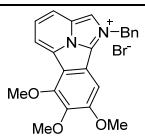	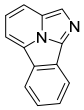	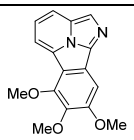
Color[a]	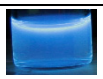		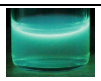	
λ_{em} (nm)	458	503	464	471

[a] Observed under an UVA-emitting low pressure mercury-vapor gas-discharge lamp ("blacklight blue").

As predicted for the *C-2-aryl* series, *para*-substitution on the exocyclic benzene ring has a significant effect on the emission peak, with donating groups effectively destabilizing the HOMO and reducing the emission energy. In fact, in this series, substitution at both C-2 and C-7 positions with electron-donating groups results in a bathochromic shift of the emission wavelength. A similar effect was reported on structurally related diarylimidazo[1,5-*a*]pyridines.[21] The effect of substituents at these positions appears cumulative (**Tableau VIII**, compare **2.8a**, **2.8d** and **2.8g**). The decrease of the emitted photons' energy was found to have a linear relationship with the sum of the Hammett constants[45] of the groups at positions C-2 and C-7, allowing the mathematical prediction of compound **2.8r**'s emission maximum (**Figure 26**) (Predicted λ_{em}: 525 nm; measured λ_{em}: 524 nm). This is particularly useful as it enables precise knowledge of a fluorophore's emissive properties before synthesis, avoiding lengthy trial-and-error when attempting to obtain probes tailor-made for specific applications.

Figure 26. Linear relationship between the substituents' Hammett constants and emitted photon energy.

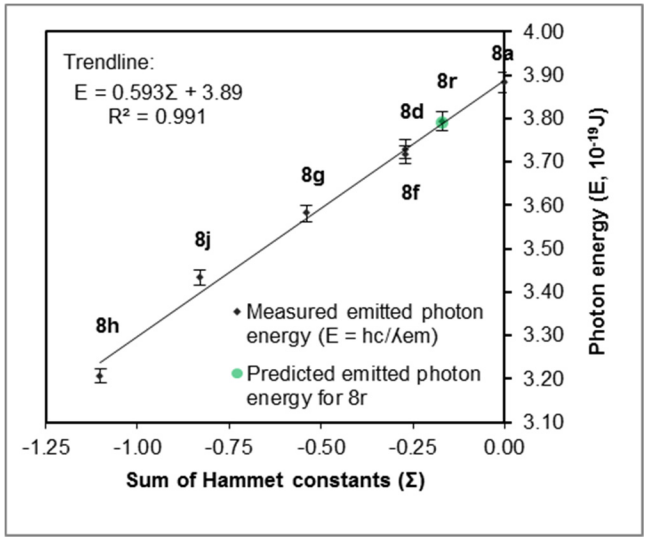

Interestingly, the high energy excitation peaks' maxima are not as affected by the electron enrichment as the emission peaks, leading to higher and higher Stokes shifts, up to 281 nm for compound **2.8h**. High Stokes shift fluorophores are desirable as their use greatly reduces the possibility of self-quenching and interference from excitation light diffusion. They can also be combined in a single sample with lower Stokes shift probes having similar excitation maxima. This enables the activation of multiple, differently colored probes with a single wavelength of incident light.[40]

As shown in **Figure 27** and **Figure 28**, simple one- or two-step structural modifications on the benzo[*a*]imidazo[2,1,5-*c*,*d*]indolizine core enable the synthesis of a fluorophore library whose emission maxima cover the entire visible spectrum. In most similar libraries, conjugated fused cycles must be added to access the higher wavelengths,[12] significantly lengthening the synthetic pathway.

Figure 27. Emission spectra of selected compounds. [a] Normalized fluorescence intensity.

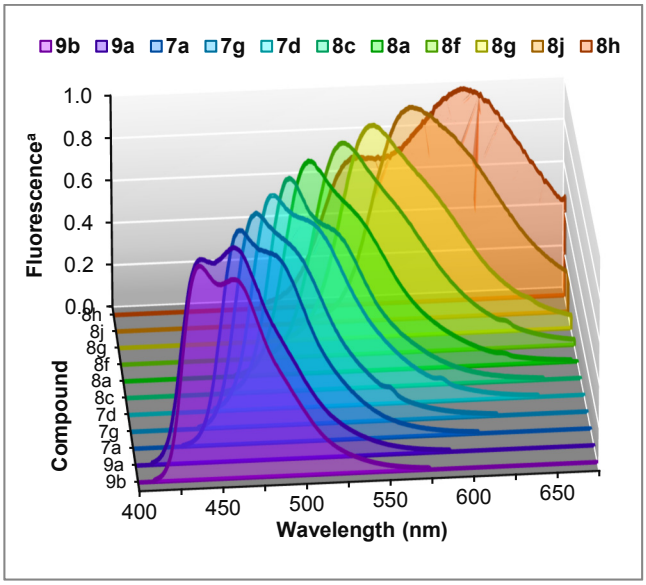

Figure 28. Luminescence of selected compounds under an UVA-emitting low pressure mercury-vapor gas-discharge lamp ("blacklight blue").

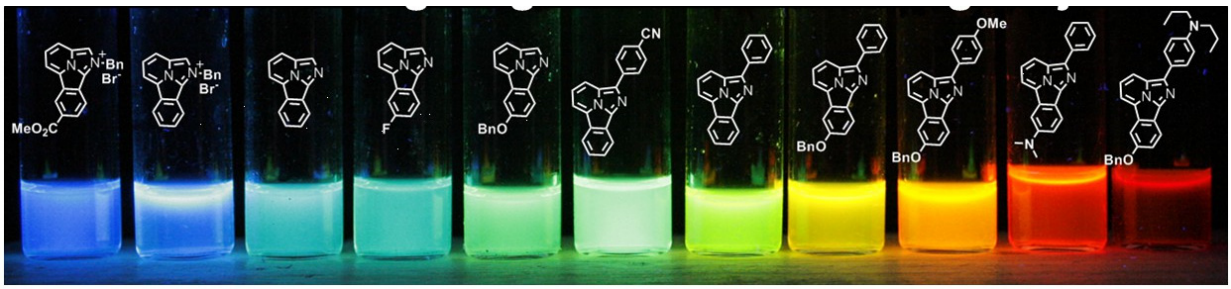

Tableau VIII. Photophysical Data of Selected Fluorophores

Compound	λ_{ex} (nm)	λ_{em} (nm)	Stokes shift (nm)	ε (kL*mol^{-1}cm^{-1})	Φ_F[a]	Brightness (kL*mol^{-1}cm^{-1})[31]
2.7a	278 421	464	186 43	24.8 5.9	0.08 0.34	2.1 2.0
2.7e	295 438	489	194 51	14.8 4.7	0.13 0.27	2.0 1.3
2.7k	289 420	471	182 51	28.0 7.3	0.10 0.27	2.7 2.0
2.7s	299 411	450	151 39	7.2 4.9	0.04 0.08	0.3 0.4

2.8a	315 469	512	197 43	22.4 11.0	0.18 0.33	4.1 3.7
2.8c	352 469	498	146 29	5.1 2.8	0.24 0.22	1.2 0.6
2.8d	317 469	535	218 66	22.0 11.1	0.14 0.23	3.0 2.6
2.8g	325 469	555	230 86	23.0 8.1	0.11 0.18	2.5 1.5
2.8h	339	620	281	20.4	0.02	0.4
2.8j	343 469	579	236 110	29.7 7.1	0.06 0.09	1.9 0.6
2.8q	285 468	529	244 61	27.1 14.7	0.10 0.31	2.7 4.5
2.8r	285 484	524	239 40	22.2 10.3	0.16 0.30	3.6 3.1
2.9a	398	458	60	6.1	0.39	2.4
2.9b	399	437	38	12.8	0.40	5.2
2.9c	399	503	104	8.9	0.16	1.4
2.10b	287 420	464	177 44	25.9 8.4	0.18 0.48	4.7 4.0
2.10e	280 424	467	187 43	10.6 3.0	0.12 0.37	1.3 1.1

[a] From the integration of emission peaks, using quinine hemisulfate as reference material ($\Phi_{quinine}$ = 0.546).

2.5.3.4.Tether groups and biolabelling.

Most applications of small molecule fluorophores involve their grafting onto biomolecules *via* a covalent tether. The fused benzene ring of benzo[*a*]imidazo[2,1,5-*c*,*d*]indolizines is a very convenient attaching point for tethering group precursors introduced through the acyl chloride building block (**Figure 29**). Unconjugated tether groups have very little effect on the photophysical properties (**Tableau VIII,** compare **2.7a** with **2.10e**). The fluorescent core is relatively inert to heat, acids or bases, allowing traditional functional group manipulations without degradation. The nitrile **2.7j** is readily reduced to the corresponding primary benzylic ammonium chloride, making the molecule highly water soluble.[46] The methyl ester **7i** can be hydrolyzed to the acid **2.10a**, substituted for an amide group (**2.10b**) or reduced to the benzylic alcohol **2.10c**. The sodium salt of **2.10a** is also highly water soluble.[46] Another primary alcohol (**2.7e**) can be obtained from hydrolysis of a

benzoyl protecting group, allowing the tethering of electron-richer fluorophores similar to compounds **2.7d** and **2.8f-2.8i**.

Figure 29. Post-cyclization derivatizations to include reactive tether groups.

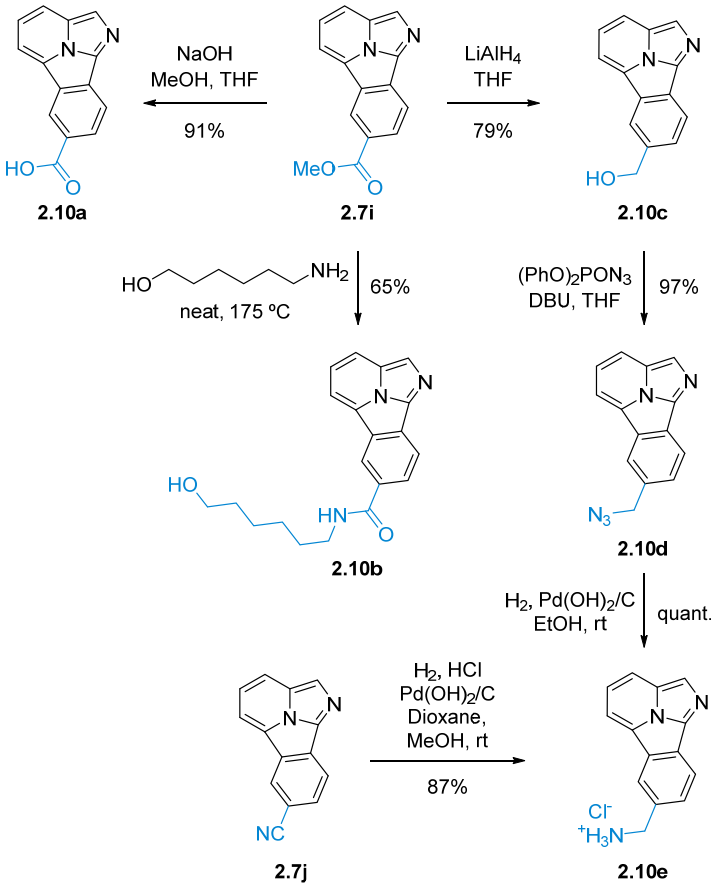

In light of these results, we sought to demonstrate the applicability of our fluorophores as probes for biological targets. Site-specific protein labelling remains a field of high interest within biotechnology, with biocatalysis representing a promising alternative to traditional metal-catalyzed conjugation.[47] Advantages include high specificity, as well as compatibility with biological media. Microbial transglutaminase (MTG) was selected to serve this purpose.[48] The acyl-transfer reaction catalyzed by MTG forms an amide linkage between a primary amine and a glutamine residue on the substrate protein. Here, we were able to take advantage of MTG's specificity for primary amines[49] in conjunction with the highly customizable nature of our fluorophores. The primary ammonium salt **2.10e** was both reactive with MTG and soluble in aqueous media. We selected α-lactalbumin and the immunoglobulin-binding domain B1 of streptococcal protein G (GB1) as model glutamine-

containing protein substrates. The reactivity of MTG with α-lactalbumin has been extensively characterized, including for chemoenzymatic protein labelling.[50] Its reactivity with protein GB1 has not yet been reported. To prevent non-specific labelling with other glutamine-containing substrates, the reactions were carried out *in vitro* with purified protein substrates. (**Tableau IX**) Both proteins were successfully labelled, illustrating the biological compatibility of benzo[*a*]imidazo[2,1,5-*c,d*]indolizines and the potential that these fluorophores have in the field of biocatalyzed bio-conjugation.

Tableau IX. Fluorophore-conjugated α-LA and GB1 proteins.

Target Protein	α-LA		GB1	
MTG	-	+	-	+
Coomassie staining				
UVA irradiation	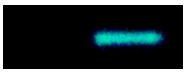		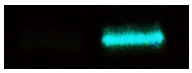	

Target protein and **2.10e** were incubated overnight in presence or absence of MTG in pH 7.4 buffer and resolved by gel electrophoresis.

2.5.4.Conclusion

In summary, we have developed an efficient divergent synthesis yielding a series of strained heteroaromatic fluorophores. Choice of building blocks for the amidation and electrophilic arylation steps enables the introduction of diverse functional groups. DFT calculations and empirical data allow the prediction of emission maxima before synthesis. Full visible spectra coverage was achieved by varying the substituents on three series of molecules based on the same core. Reactive functional groups can be linked to the tetracyclic core without affecting photophysical properties, enabling covalent tethering to biomolecules and materials. We believe benzo[*a*]imidazo[2,1,5-*c,d*]indolizines' high chemical stability, Stokes shift and tunability make them promising tools for the fields of fluorescent microscopy and photoactive materials and devices.

2.5.5.Associated content

Experimental procedures, full characterization of the products, fluorescence spectra, Gaussian input files and single crystal diffraction data are included as Supplementary Information. This material is available free of charge *via* the Internet at http://pubs.acs.org."

2.5.6.Author information

Corresponding Authors

* Department of Chemistry, University of Montreal

P.O. Box 6128 Stn Downtown, Montreal, Quebec, H3C 3J7 (Canada)

andre.charette@umontreal.ca

† These authors contributed equally.

2.5.7.Acknowledgement

The authors would like to thank A. Therrien and Prof. M. Lafleur for the use of their fluorimeter; C. Y. Legault and J.-P. Cloutier for help with the DFT calculations. This work was supported by the Natural Science and Engineering Research Council of Canada (NSERC), the Canada Foundation for Innovation, the Canada Research Chair Program, the FRQNT Centre in Green Chemistry and Catalysis (CGCC), the FQRNT Network for Research on Protein Function, Engineering and Applications (PROTEO) and Université de Montréal. E. L., W. S. B., G. P. and N. M. R. are grateful to NSERC, FQRNT, and Université de Montréal for postgraduate scholarships.

2.6.Commentaires et détails supplémentaires

2.6.1.Photostabilité

Voir les résultats de l'étude de photostabilité dans l'annexe 1 (page - 174 - **Figure 75**).

2.6.2.Étude comparative des propriétés photophysiques

Tableau X. Comparaison entre les propriétés photophysiques des benzo[*a*]imidazo[2,1,5-*c*,*d*]indolizines et celles de fluorophores commerciaux et structurellement semblables

Composé	λ_{ex} (nm)	λ_{em} (nm)	Déplacement de Stokes (nm)	ε ($kL*mol^{-1}cm^{-1}$)	Φ_F[a]	Brilliance ($kL*mol^{-1}cm^{-1}$)
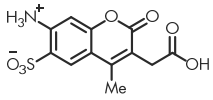 **Alexafluor 350**[7]	340	458	100	19	0.55	10.5
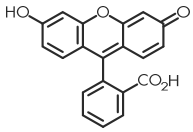 **Fluorescéine**[8]	494	521	18	90	0.92	83
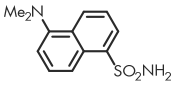 **Dansyl Amide**[9]	335	516	181	4.2	0.37	1.6
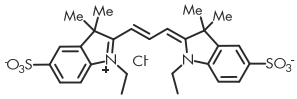 **Cy3**[10]	560	575	15	150	0.09	13.5
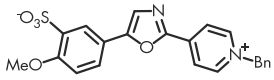 **Cascade Yellow**[32a]	409	558	149	24	0.56	13
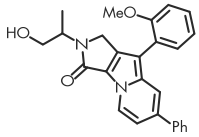 Séoulfluor représentatif (**2.0m**)[11]	381	489	108	12	0.55	6.7

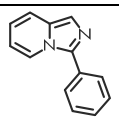 Analogue acyclique de **2.7a** (**2.0α**)[21]	317	461	144	17.8	0.072	1.28
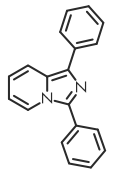 Analogue acyclique de **2.8a** (**2.0ε**)[21]	308	454	146	15.1	0.14	2.11
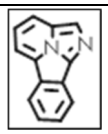 **2.7a**	278 421	464	186 43	24.8 5.9	0.08 0.34	2.1 2.0
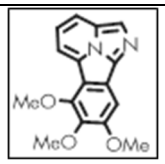 **2.7k**	289 420	471	182 51	28.0 7.3	0.10 0.27	2.7 2.0
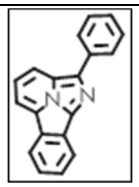 **2.8a**	315 469	512	197 43	22.4 11.0	0.18 0.33	4.1 3.7
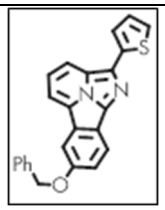 **2.8i**	336 469	557	221 88	38.5 15.6	0.12 0.16	4.5 2.4
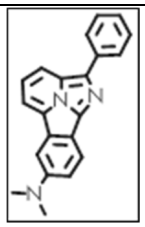 **2.8j**	343 469	579	236 110	29.7 7.1	0.06 0.09	1.9 0.6

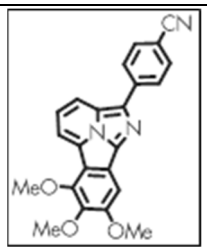 **2.8n**	356 469	497	141 28	18.4 15.7	0.35 0.38	6.4 5.9
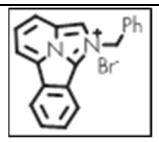 **2.9a**	398	458	60	6.1	0.39	2.4

Les propriétés photophysiques d'une sélection de fluorophores précédemment rapportés ou commerciaux sont comparées à celles des benzo[*a*]imidazo[2,1,5-*c*,*d*]indolizines. On peut remarquer que ces dernières ont la particularité d'avoir des déplacements de Stokes très élevés, même en comparaison avec les structures semblables non cyclisées **2.0α** et **2.0ε** ou avec un fluorophore commercial reconnu pour son déplacement de Stokes élevé tel que **Cascade Yellow**. De plus, la capacité d'obtenir des maxima d'émission prévisibles répartis sur toute la largeur du spectre visible par de simples modifications de groupements fonctionnels est rarement observée pour d'autres cœurs.[32a] Par contre, les benzo[*a*]imidazo[2,1,5-*c*,*d*]indolizines présentent des brillances plus faibles que la plupart des fluorophores commerciaux.

2.6.3.Ligand bidentate fluorescent

Figure 30. Couplage de Neigishi avec une 2-métallopyridine.

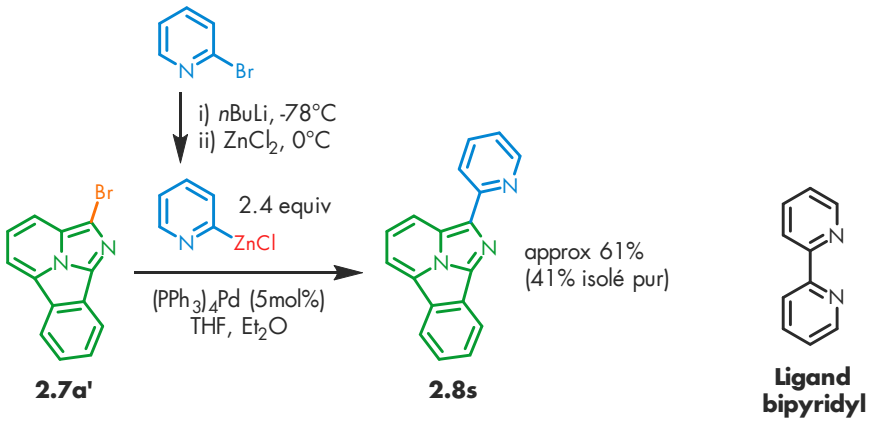

En plus des molécules présentées dans l'article, le produit **2.8s** ci-dessus a été synthétisé dans le but de produire un analogue fluorescent du ligand bipyridyl, avec un angle de morsure (*bite angle*) plus grand. Un couplage de Neigishi non optimisé avec la 2-bromozincopyridine a été réalisé. La structure a des propriétés photophysiques intéressantes, avec un rendement quantique et une brillance élevés (λ_{ex} = 332, 469 nm; λ_{em} = 493 nm; déplacement de Stokes = 161, 24 nm; ε = 16.8, 11.1 kL/(mol*cm); Φ = 0.35, 0.49; brillance = 5.9, 5.4 kL/(mol*cm)), mais son potentiel en tant que ligand n'a pas été testé.

2.6.4. Mécanisme de la cyclisation catalysée au palladium sur un alcène

Figure 31. Intermédiaires de la carbométallation-β-élimination avec un alcène.

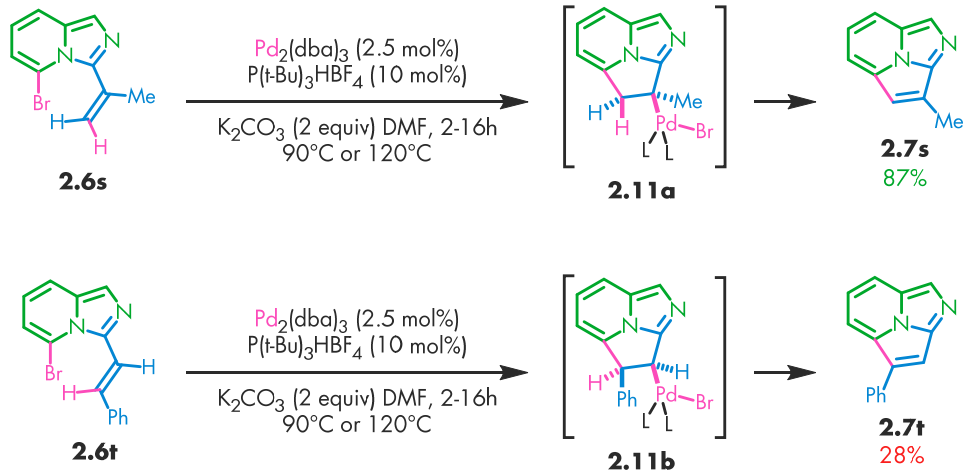

Les intermédiaires **2.11a** et **2.11b** illustrés à la **Figure 31** expliquent la différence de rendement entre **2.7s** et **2.7t**, les deux exemples de cyclisation catalysée au palladium impliquant un alcène plutôt qu'un cycle aromatique. Dans le cas de l'intermédiaire **2.11a**, un des protons de l'alcène de départ est parfaitement éclipsé avec l'atome de palladium, menant à une élimination réductrice efficace car elle est peu énergétiquement demandante. Inversement, l'atome de palladium de l'intermédiaire **2.11b** est éclipsé avec le groupement phényl. Le seul proton pouvant être éliminé est *trans* par rapport au métal.[51] De plus, la conformation *anti* (180° d'angle dièdre) nécessaire à la β-élimination *trans* est difficile à atteindre dans ce système sans augmenter la tension dans le cycle pyrrolidine. Ces contraintes rendent la réaction de β-élimination beaucoup plus difficile (lente), augmentant les chances de dégradation de l'intermédiaire organopalladium **2.11b** et menant à un rendement modeste.

2.7.Conclusion

Enfin, l'origine de la fluorescence des benzo[*a*]imidazo[2,1,5-*c*,*d*]indolizines a été explorée et une quantité suffisante de propriétés et d'informations ont été compilées pour mettre en évidence leur potentiel. Nous espérons que ces fluorophores ajustables, thermo- et chimiostables à déplacement de Stokes élevé soient à la hauteur des critères désirés par les experts des domaines où les petites molécules fluorescentes sont un outil indispensable.

3.Amélioration de la réaction de Simmons-Smith catalysée au zinc. Accès à des arylcyclopropanes 1,2,3-trisubstitués

3.1.Les carbénoïdes de zinc et la réaction de Simmons-Smith

3.1.1.Découverte et mécanisme général

Figure 32. Cycloaddition de Simmons-Smith : Découverte initiale

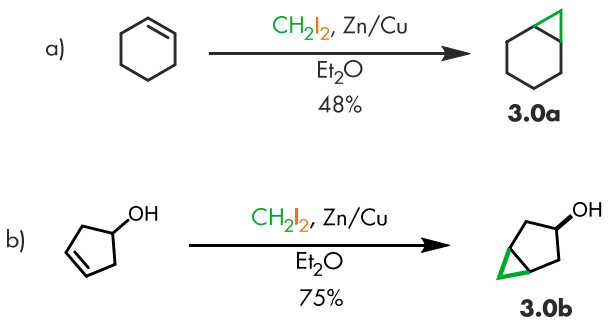

La réaction de Simmons-Smith a été rapportée pour la première fois en 1958[52] (**Figure 33** a). La combinaison du diiodométhane, d'un alliage cuivre/zinc et d'un alcène dans un solvant éthéré produit un cyclopropane par un procédé de type cycloaddition [2+1] chélétropique, une cycloaddition concertée lors de laquelle les deux nouvelles liaisons sont formées sur le même atome. Le puissant effet directeur du groupement alcool a été découvert peu après[53] (**Figure 33** b). Un carbénoïde de zinc électrophile (**3.0c**) est habituellement proposé comme intermédiaire clé.[54]

Figure 33. Mécanisme général de la cyclopropanation de Simmons-Smith.

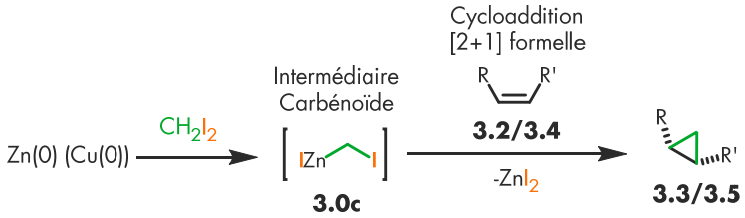

3.1.2.Propriétés générales des carbènes et carbénoïdes

Tableau XI. Comparaison entre les carbènes de Fisher et les carbénoïdes

	Carbène de Fisher	**Carbénoïde**
Lobes de la HOMO et de la LUMO	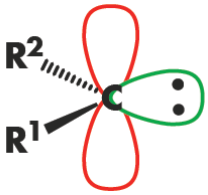	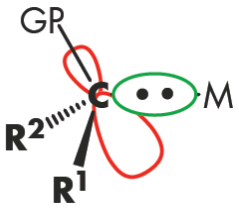
Hybridation de **C**	sp^2	sp^3
HOMO	doublet non-liant sur le carbone	σ du lien C-M
LUMO	*p* vide sur le carbone	σ* du lien C-GP
Charge du carbone	Neutre : Peut être libre ou stabilisé par un métal	Anionique : Toujours associé à un métal
Orbitales moléculaires frontières impliquées dans une cycloaddition [2+1] avec un alcène	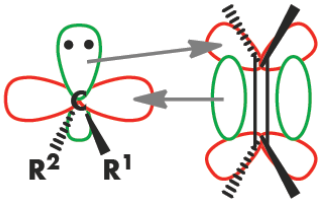	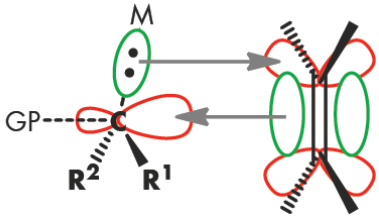

GP = Groupe Partant.

Les carbénoïdes, comme leur nom l'indique, ont de nombreux aspects en commun avec les carbènes. Un carbone portant un groupe partant et un métal électropositif est en effet à une élimination de former un carbène métallique, mais dans certains systèmes la configuration carbénoïde est plus stable. Comme le carbène, le carbénoïde peut réagir de manière concertée avec un alcène. L'orbitale anti-liante du lien carbone-groupe partant (GP) joue le rôle de l'orbitale *p* vide du carbène et le lien σ carbone-métal celui du doublet non-liant.[55]

3.1.3.Les carbénoïdes de zinc : Propriétés

Figure 34. Propriétés structurales et chimiques des carbénoïdes de zinc électrophiles.

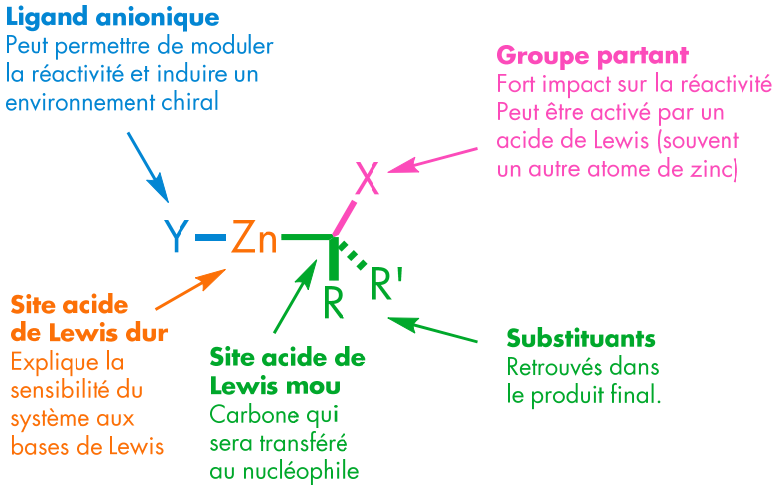

Les différents composants caractérisant les carbénoïdes de zinc et leurs influences respectives sont détaillés dans la **Figure 34**.[54,56] L'atome de carbone central, qui sera transféré au nucléophile, porte un atome de zinc et un groupe nucléofuge.

Cet atome de zinc représente le site acide de Lewis dur du système. Il est facilement coordiné par les bases de Lewis, principalement *via* les doublets d'électrons libres de l'oxygène et l'azote. Cette particularité rend les réactions de Simmons-Smith particulièrement sensibles aux bases de Lewis telles que l'eau et les solvants coordinants, mais elle permet aussi d'avoir un point d'ancrage très efficace pour le substrat ou un ligand chiral. Entre autres, cette acidité de Lewis explique les diastéréosélectivités élevées observées lors de cyclopropanation d'alcools et d'éthers allyliques.[57]

L'atome de zinc étant généralement à l'état d'oxydation II, il porte un second ligand anionique. Ce second ligand peut être un autre carbone carbénoïde,[58] un groupement alkyl,[59] un halogène,[60] ou un anion basé sur l'oxygène (carboxylate,[61] phosphate,[62]) ou l'azote (carbamate[63]). Les propriétés électroniques de ce ligand ont un effet notable sur l'acidité de Lewis de l'atome de zinc, donc sur la réactivité du carbénoïde. La librairie d'anions tolérés permet d'ajuster précisément cette réactivité aux besoins de la réaction à effectuer. En l'absence de ligands neutres additionnels, l'angle entre les deux ligands anioniques du zinc est généralement proche de 180°C, une géométrie de type sp.[64] La géométrie tétraédrique (hybridation sp^3), incluant deux ligands neutres

supplémentaires est considérée représentative de l'environnement du zinc en présence de bases de Lewis.[65]

L'atome de carbone adjacent au zinc est le site de réaction désiré. C'est le site acide de Lewis mou du système, le site avec lequel le nucléophile, généralement un alcène, doit réagir. S'il porte des substituants, ces derniers sont retrouvés dans le produit de réaction. Ils influencent aussi l'énergie et la géométrie de l'état de transition. De plus, la nature de leur interaction avec le nucléophile a un profond effet sur la stéréosélectivité observée.[66]

La seconde fonctionnalité essentielle à tout carbénoïde est le groupe partant, lié au même carbone que le métal. Généralement un halogène, il influence surtout la réactivité et l'acidité de Lewis du carbone adjacent.[67] Son départ peut être accéléré par un autre équivalent d'acide de Lewis, souvent l'halogénure de zinc produit par la réaction d'une autre molécule de carbénoïde.[64] La facilité à former le carbénoïde est aussi un facteur important dans le choix de l'élément qui formera le groupe partant. L'iode est souvent utilisé pour cette raison, étant donné qu'il est relativement simple de briser un lien carbone-iode pour y installer un atome de zinc.

3.1.4.Les carbénoïdes de zinc : Formation

Figure 35. Réactions permettant la formation de carbénoïdes de zinc

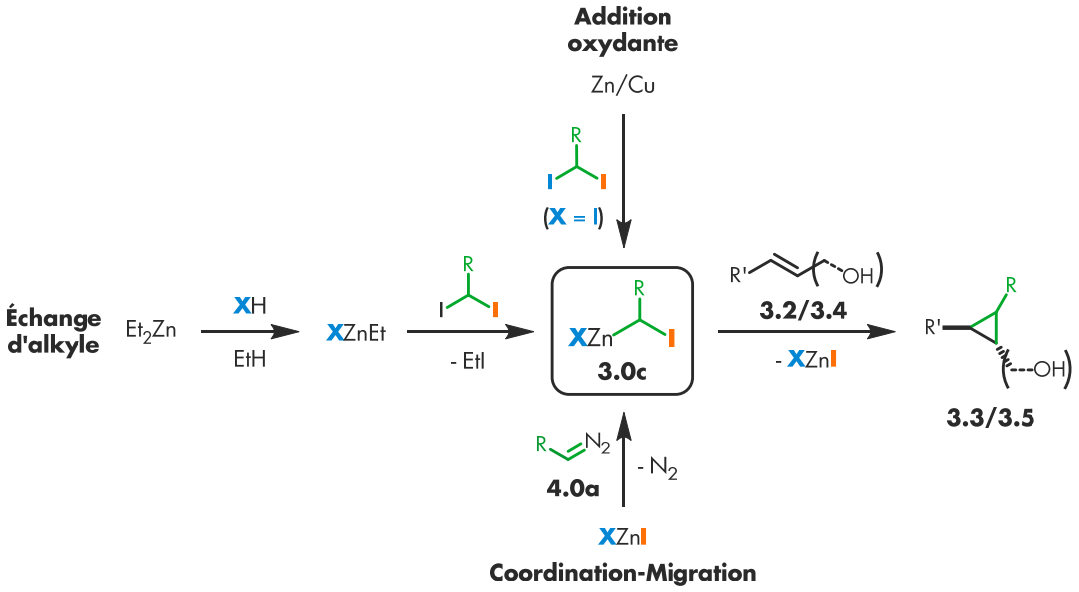

Les carbénoïdes de zinc peuvent être formés par plusieurs approches (**Figure 35**). La méthode originale rapportée par Simmons et Smith exploite l'addition oxydante formelle du zinc

(0) dans la liaison carbone-iode, accélérée par la présence de cuivre à la surface des grains métalliques. La présence d'un éther est généralement nécessaire à cette réaction.[52]

Il est aussi possible de transmétaller un composé alkylzinc avec un dihaloalcane, ce qui permet d'éviter l'utilisation de solvant éthéré.[68] Le diéthylzinc, un réactif pyrophorique, est habituellement utilisé comme source de zinc pour cette approche. Réagissant rapidement avec l'eau pour produire de l'éthane gazeux et de l'oxyde de zinc insoluble, il a comme avantage connexe la capacité d'assécher le milieu réactionnel sans le contaminer.

Une manière moins connue d'accéder aux carbénoïdes de zinc implique la réaction rapide entre un composé diazo nucléophile et un sel halozincique.[69]. L'efficacité de cette réaction dépend fortement de la nature du composé diazo, les composés diazo riches en électrons étant les plus réactifs.

3.2. Réaction de Simmons-Smith catalytique

Un des problèmes récurrents des méthodologies de cyclopropanation de Simmons-Smith est la quantité superstoechiométrique de zinc généralement requise. En effet, les méthodes d'addition oxydante et d'échange d'alkyles (**Figure 35**) ne permettent pas une régénération simple de l'intermédiaire carbénoïde. L'accumulation de quantités significatives de sels de zinc (II) acides de Lewis dans le milieu réactionnel nuit à la généralité de la réaction et complique les purifications. De plus la catalyse énantiosélective est compliquée par le fait que la fonction carbénoïde peut échanger d'un noyau zincique à l'autre par équilibre de Shlenk.[59] En effet, la plupart des versions énantiosélectives de la réaction de Simmons-Smith utilisent des quantités stœchiométriques de ligand chiral, nuisant à l'accessibilité économique de cette réaction.[54,62]

3.2.1. Approches pour reformer le carbénoïde *in situ*

Figure 36. Cyclopropanation de Simmons-Smith catalytique en zinc : Stratégies potentielles

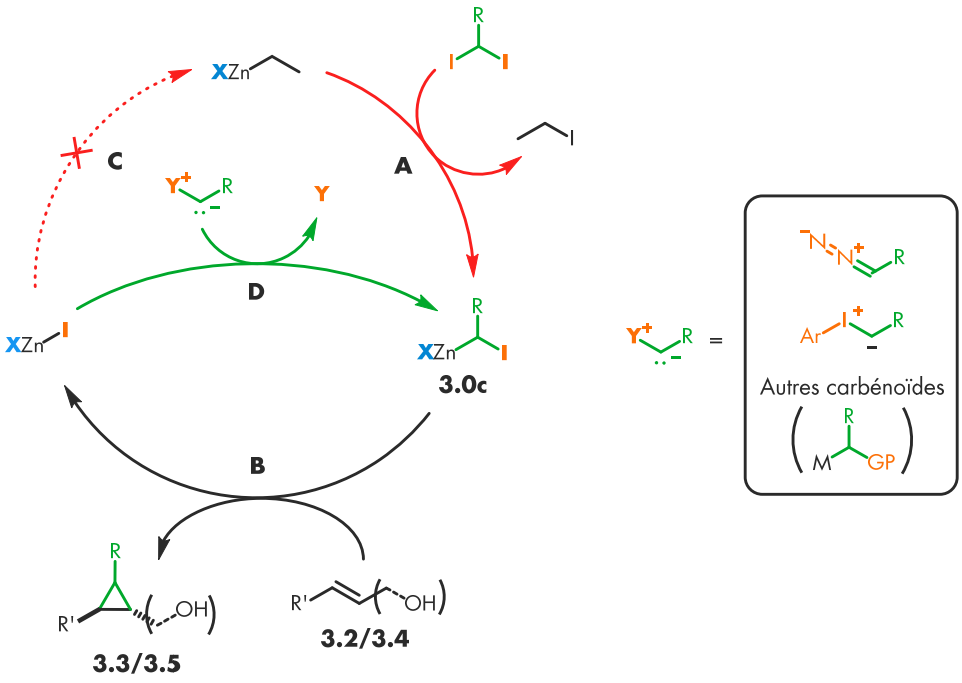

Supposons un cycle catalytique hypothétique utilisant le chemin réactionnel **B** (**Figure 36**) pour préparer un cyclopropane. Si l'approche par échange d'alkyle (**A**), habituellement la plus versatile, est utilisée, la force motrice de la formation du carbénoïde **3.0c** provient de la réactivité

du composé alkylzinc. Or, il existe peu de réactifs chimiosélectifs capable de régénérer cette réactivité en transférant efficacement un nouveau groupement alkyle sur le sous-produit halogénure de zinc (II) (**C**). De manière générale, seuls d'autres composés alkylmétal tels que les alkyllithiums effectuent cette transformation.[70] L'utilisation stœchiométrique d'alkylmétaux nucléophiles n'est pas idéale car elle limite fortement la tolérance aux groupements fonctionnels d'une réaction.

En contrepartie, l'approche par coordination-migration (**D**) utilise l'énergie d'un précurseur de carbène comme force motrice.[69] Les précurseurs de carbène sont caractérisés par un carbone nucléophile portant un groupe partant. Ils incluent les composés diazo, les ylures nucléophiles tels que les ylures d'iodonium et les carbénoïdes nucléophiles. Le principal intérêt de cette approche dans l'optique d'élaborer un système catalytique est que l'halogénure de zinc produit après la formation du cyclopropane peut réagir à nouveau avec un précurseur de carbénoïde, reformant le carbénoïde et bouclant le cycle.

3.2.2.Activation de précurseurs de carbène par les sels de zinc (II)

Figure 37. Mécanisme général de la réaction entre un halogénure de zinc (II) et un précurseur de carbène.

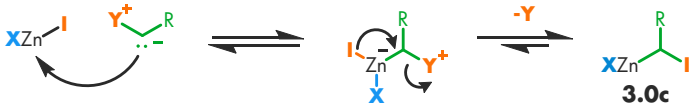

De manière générale, un précurseur de carbène (un nucléophile porteur d'un groupe nucléofuge) peut former un carbénoïde de zinc par le mécanisme décrit dans la **Figure 37**. Le précurseur de carbène coordine d'abord le noyau de zinc (II). L'intermédiaire « ate » ainsi formé possède alors un groupe partant en α d'un atome de zinc chargé négativement portant deux autres ligands anioniques. Le ligand le plus labile, généralement l'halogène, migre rapidement vers le carbone, permettant le départ du nucléofuge.

Figure 38. Formation d'un carbénoïde de zinc à partir d'un diazo nucléophile et d'un halogénure de zinc(II)

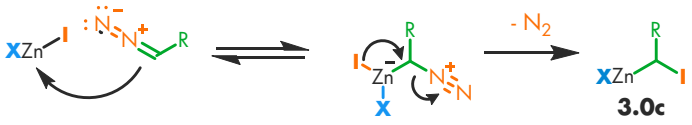

Dans le cas spécifique du zinc, les composés diazo sont les seuls précurseurs de carbène dont la capacité à former des carbénoïdes est connue. La **Figure 38** résume le mécanisme de cette transformation, dont le largage d'une molécule de diazote est la principale force motrice.

Figure 39. Exemple du mécanisme de coordination-migration : Carbénoïde de zinc à partir de diazométhane

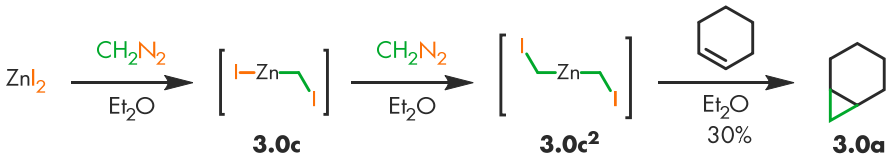

Le premier exemple de cette transformation a été rapporté l'année suivant la première publication de la réaction de Simmons-Smith[69] (**Figure 39**). La réaction entre deux équivalents de diazométhane et le diiodure de zinc permet la formation d'un complexe de zinc portant deux carbones carbénoïdes **3.0c²**. Ce même carbénoïde peut aussi être obtenu à partir de diéthylzinc et de diiodométhane par échange d'alkyle.[58] Une réactivité similaire avec les alcènes est observée pour les deux méthodes de préparation.

3.3.Arylcyclopropanation à partir d'aryldiazométhanes

Dans beaucoup de situations, il reste plus simple et sécuritaire de manipuler des diiodures et des composés organozinciques que de synthétiser, purifier et utiliser des composés diazo nucléophiles, qui sont sujets à dégrader, parfois violemment, suite au contact avec un acide ou à un choc mécanique. Une exception notable est lorsqu'un carbénoïde portant un groupement aromatique (carbénoïde de type benzylique) doit être préparé. En effet, les dihalogénures benzyliques sont difficiles à préparer et à utiliser à cause de leur instabilité à la chaleur et la lumière.[71] L'utilisation d'aryldiazométhanes devient alors une alternative avantageuse.

3.3.1.Exemples précédemment rapportés

Figure 40. Arylcyclopropanation d'alcènes simples utilisant des aryldiazométhanes et des halogénures de zinc.

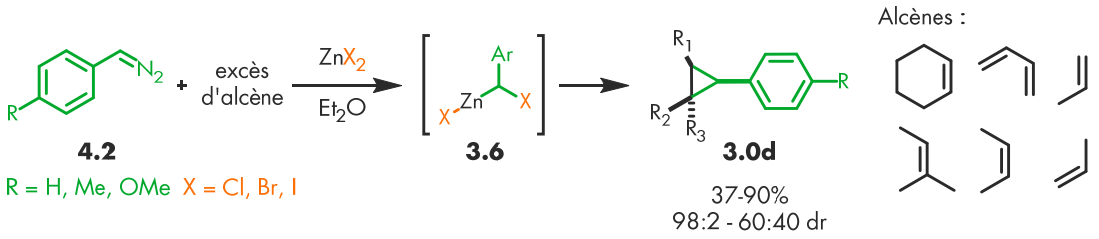

La première instance de cette utilisation a été rapportée en 1969.[72] Des solutions éthérées d'aryldiazométhanes sont traitées avec des halogénures de zinc en présence d'excès d'alcènes simples, résultant en la formation d'arylcyclopropanes (**Figure 40**).

Figure 41. Étude cinétique de la réaction entre un aryldiazométhane et un halogénure de zinc

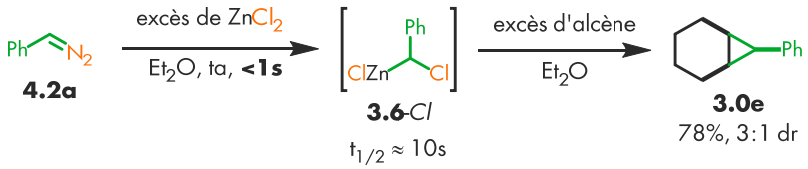

Le suivi de la réaction avec le dichlorure de zinc permet de conclure que la réaction entre le composé diazo et le sel de zinc est quasi instantanée et que le temps de demi-vie du carbénoïde

chloré est d'environ 10 secondes. Ceci explique l'importance d'un excès d'alcène dans cette réaction, pour piéger le carbénoïde avant sa dégradation rapide.

Figure 42. Formation de stilbène par la réaction entre le phényldiazométhane et le carbénoïde de zinc correspondant.

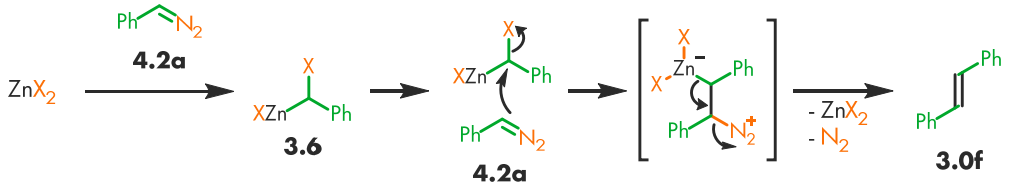

Un excès de sel de zinc a aussi été utilisé dans l'exemple de la **Figure 41** pour minimiser l'impact de la réaction entre le diazo nucléophile **4.2a** et le carbénoïde **3.6** dont le mécanisme est présenté à la **Figure 42**. L'alcène **3.0f** produit par cette réaction est un type de sous-produit communément observé dans des systèmes où un diazo est utilisé comme précurseur de carbénoïde/carbène. Heureusement pour un potentiel système catalytique, cette réaction indésirée, tout comme la cyclopropanation désirée, régénère le dihalogénure de zinc.

3.3.2. Travaux précédents au sein du groupe Charette

Figure 43. Arylcyclopropanation énantiosélective utilisant les aryldiazométhanes

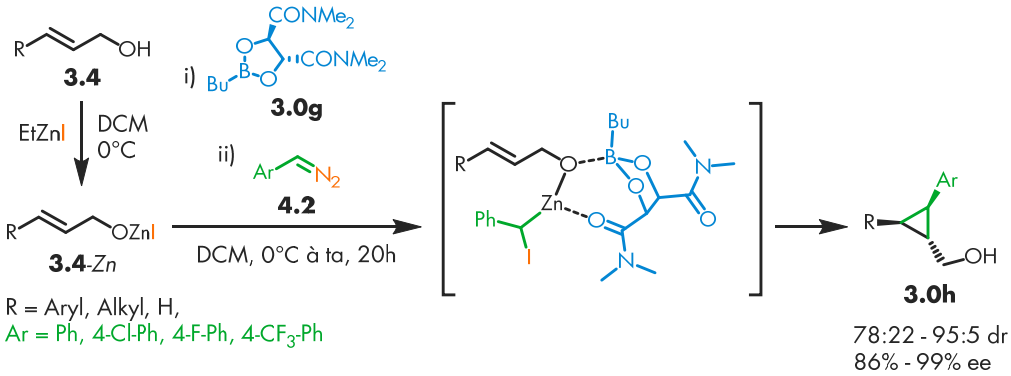

Une version énantiosélective de l'arylcyclopropanation décrite ci-haut a été développée au sein du groupe par S. Goudreau, Ph. D (**Figure 43**).[73] Une quantité stœchiométrique d'iodoéthylzinc est combinée à un alcool allylique. L'alcoolate de zinc **3.4**-*Zn* obtenu est coordiné au dioxaborolane chiral **3.0g**. Ensuite, une solution d'aryldiazométhane est ajoutée goutte à goutte.

Le carbénoïde résultant peut alors réagir de manière intramoléculaire avec l'alcène dans un environnement chiral, formant une variété de cyclopropylméthanols énantioenrichis **3.0h**.

Figure 44. Premier exemple de cyclopropanation de Simmons Smith catalytique en zinc avec un groupe directeur Lewis basique.

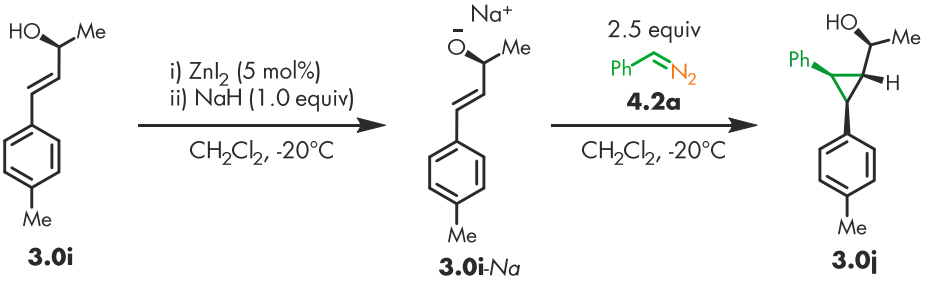

Un seul exemple utilisant une quantité catalytique de zinc sans ligand chiral a aussi été publié[73] (**Figure 44**). Le cyclopropane **3.0j** est obtenu avec un ratio diastéréomérique de 4:1 et un rendement combiné de 95%. Dans ce cas, l'hydrure de sodium a été utilisé pour déprotoner le groupement alcool du substrat **3.0i**.

3.3.3. Optimisation de la version catalytique

Figure 45. Relation entre la charge en zinc et le rendement pour différents groupes directeurs

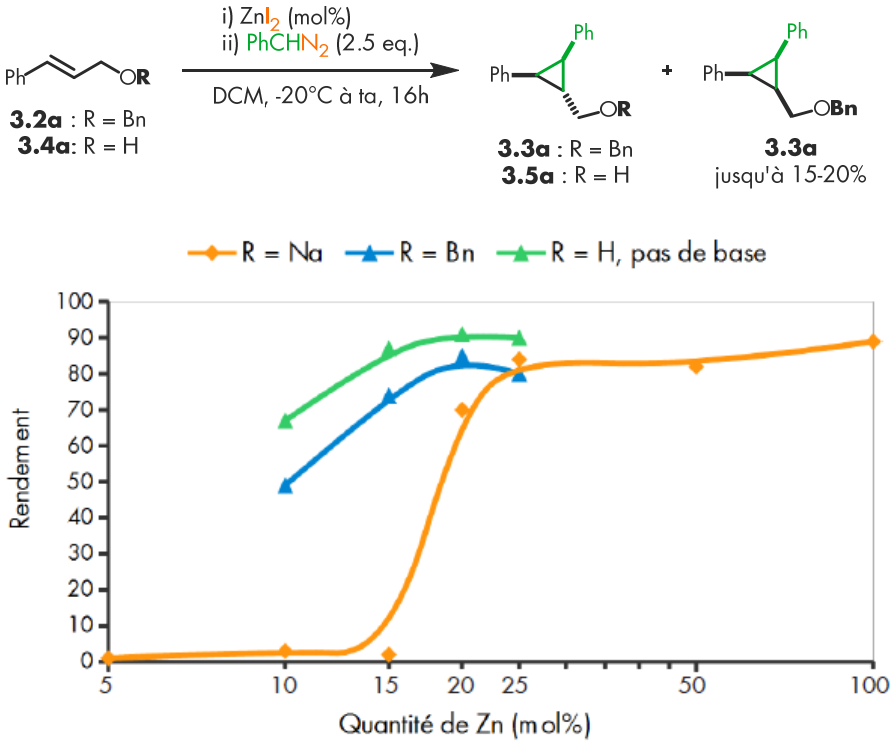

Le résultat décrit ci-haut s'est avéré difficile à reproduire. Le rendement de la cyclopropanation des alcoolates de sodium allyliques avec le phényldiazométhane **4.2a** apparaît fortement dépendant de la charge en zinc (**Figure 45**). De plus, l'hétérogénéité de la mixture réactionnelle empire les problèmes de reproductibilité. Le résultat de la réaction semble dépendant des propriétés de la phase solide (granulométrie, composition, propriétés de la surface), qui sont difficiles à contrôler d'un essai à l'autre. Il est possible que l'iode, essentiel à la formation du carbénoïde, se retrouve sous forme de NaI insoluble par échange d'anion entre le sodium et le zinc. Enfin, une quantité significative d'éther benzylique **3.3a** est observée. Il est formé par la réaction de l'anion alcoolate avec soit le carbénoïde, soit l'iodure de benzyle provenant de la protolyse du carbénoïde (voir **Figure 51**, page - 67 - dans l'article).

L'omission de la base alcaline (**Figure 45**, R = H) augmente le rendement et règle les problèmes de solubilité et de séquestration de l'iode, mais l'éther benzylique **3.3a** est encore présent.

La génération d'iodure de benzyle *via* la protolyse du carbénoïde par l'alcool libre **3.4a** accélérée par l'acidité de Lewis du zinc est probablement le mécanisme principal derrière leur formation.

Une manière facile de contourner ce problème était de choisir un éther allylique comme substrat modèle pour l'optimisation de cette réaction catalytique. De cette manière, la basicité de Lewis du groupe directeur alcool était partiellement conservée, mais pas son proton acide. L'éther allylique benzylique **3.2a** a été choisi pour le début de l'étude, puis remplacé par les éthers méthoxyméthyliques (MOM) pour faciliter l'éventuelle déprotection du groupement alcool en présence du cyclopropane.

Les conditions optimales de cette réaction se sont aussi avérées efficaces pour l'arylcyclopropanation d'alcènes peu activés tels que les styrènes. La transformation procède avec de hautes diastéréosélectivités malgré l'absence de base de Lewis directrice. Une modification du catalyseur permet aussi l'utilisation des alcools libres **3.2.** La formation indésirée d'iodure de benzyle menant à la benzylation problématique a été minimisée en réduisant l'acidité de Lewis du catalyseur avec un ligand phénolate. Les travaux d'optimisation et d'étude de cette cyclopropanation de Simmons-Smith catalytique en zinc sont décrits dans l'article ci-dessous.

3.4.Article publié dans le journal *Organic Letters* : Improved Zinc-Catalyzed Simmons-Smith Reaction: Access to Various 1,2,3-Trisubstituted Cyclopropanes[74]

Éric Lévesque, Sébastien R. Goudreau and André B. Charette*

Centre in Green Chemistry and Catalysis, FAS-Department of Chemistry, Université de Montréal, P.O. Box 6128, Station Downtown, Montréal, Québec, Canada, H3C 3J7

andre.charette@umontreal.ca

DOI: 10.1021/ol500267w

3.4.0.Participation des coauteurs

Éric Lévesque a effectué les expériences rapportées et rédigé l'article sous la supervision du Pr. A. B. Charette. Sébastien R. Goudreau, Ph. D. est le découvreur initial de la réaction de Simmons-Smith catalytique avec un substrat alcoolate allylique.

3.4.1.Abstract

Figure 46. Improved Zinc-Catalyzed Simmons-Smith Reaction: Abstract graphic

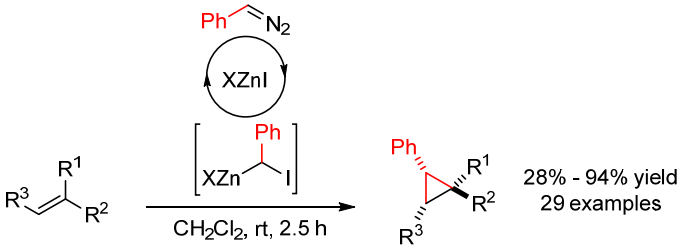

The Simmons-Smith reaction of zinc carbenoids with alkenes is a powerful method to access cyclopropanes containing various substitution patterns. This work exploits the high reactivity of aryldiazomethanes towards zinc halides to catalytically generate aryl-substituted carbenoids. These carbenoids are able to diastereoselectively cyclopropanate various alkenes, including unfunctionalized substrates such as styrenes. The zinc catalyst can be modified to tolerate the use of free allylic alcohols.

3.4.2.Results and Discussion

Cyclopropanes are important structural units in the field of synthetic chemistry. They are present in many natural and bioactive products[54] and can also participate in useful chemical reactions taking advantage of their unique ring strain.[75] The zinc-mediated reaction of *gem*-diiodoalkanes with alkenes, first reported by Simmons and Smith,[52] is among the most widely used approaches to access complex cyclopropanes.[76] The typical procedure[54,66,77] involves generating an excess of the desired zinc carbenoid[59,78] (**3.1**) before introducing the substrate alkene (**Figure 47**). Such a procedure can suffer from solubility issues, as coordinating additives are often required to solubilize the zinc reagent.[Erreur ! Signet non défini.,Erreur ! Signet non défini.] On a larger scale, the handling of air-sensitive organozinc compounds[54] and the generation of metal-containing waste also become problematic. Using only a catalytic amount of zinc would be a straightforward way to circumvent these issues.

Figure 47. Typical Simmons-Smith Procedure

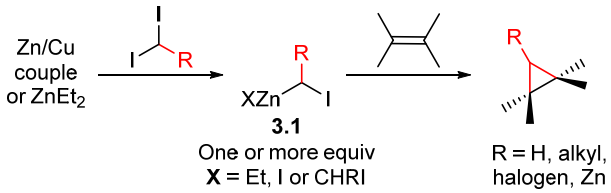

The key for the establishment of a viable catalytic cycle would be to use a precursor able to regenerate the reactive carbenoid from the zinc halide produced after the cyclopropanation. Alkyl-[69] and aryl-[72] diazo reagents have been demonstrated to fit such a requirement. Recently, our group successfully used this approach to generate enantioenriched arylcyclopropanes using stoichiometric amounts of both zinc halide and chiral tartrate-derived dioxaborolane. Furthermore, a few examples of this transformation using catalytic amounts of zinc halides have been reported, but they either require a large excess of alkene[72] or are limited to sodium allyloxides.[73] Herein we report the scope and applications study of the first zinc-catalyzed system to efficiently cyclopropanate styrenes[79] and allylic ethers (**Figure 48**). Also, a simple modification of the catalyst enables direct cyclopropanation of free allylic alcohols without deprotonation.

Figure 48. Arylcyclopropanations Using a Catalytic Amount of Zinc

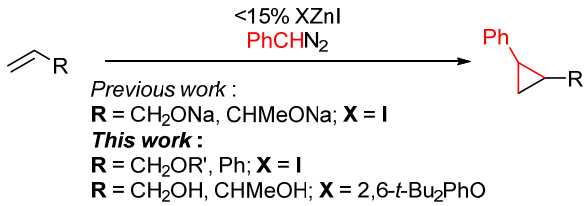

We started our investigation by treating the benzyl ether of cinnamyl alcohol (**3.2a**) with zinc iodide[80] and slowly adding phenyldiazomethane at –20 °C (**Tableau XII**, entry 1). During the addition, significant accumulation of the deep red diazo reagent was noticed, only fading away when the mixture was warmed up to room temperature. As zinc carbenoids react faster with diazo compounds than with alkenes,[72] this led to poor conversions and undesired formation of stilbenes. Adding the diazo reagent at room temperature increased turnover rate enough to keep its concentration low at all times (**Tableau XII**, entry 2), thus favoring the desired quantitative formation of cyclopropane. This also has the advantage of reducing reaction times such that complete conversion was reached shortly after the end of the diazo compound addition.

Tableau XII. Optimization of the Cyclopropanation Conditions

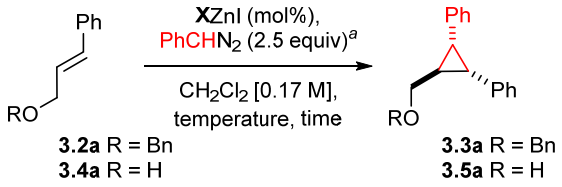

entry	initial R	temp (°C)	Zn (mol %)	**X** anion	time (h)	yield **3.5a** (%)[b]	yield **3.3a** (%)[b]
1	Bn	-20 to rt	10	I^-	16	-	48
2	Bn	rt	10	I^-	2.5	-	99
3	H	rt	10	I^-	2.5	60	23
4	H	rt	10	$(BuO)_2PO_2^-$	2.5	65	8
5	H	rt	10	PhO^-	2.5	65	5
6	H	rt	10	2,6-*t*-Bu_2PhO^-	2.5	70	5
7	H	rt	13	2,6-*t*-Bu_2PhO^-	2.5	81	8

[a] 0.75 M solution in DCM, added dropwise over 1.5 h. [b] Yields determined on the crude reaction mixture by ^1H NMR analysis using Ph_3CH as an internal standard.

In order to explore substrate generality, a series of protected allylic alcohols were submitted to the ZnI_2-catalyzed reaction (**Figure 49**).[81] It is noteworthy that aryl-substituted allylic ethers (**3.3a-c**) reacted with higher yields and higher diastereoselectivity than alkyl-substituted allylic ethers (**3.3d-g**). This led us to believe that styrenes may be sufficiently reactive to undergo this reaction without a Lewis basic directing group. Indeed, various styrene derivatives reacted smoothly (**3.3h-n**), only needing a slight increase in catalyst loading to improve the conversion (**Figure 49**). To our knowledge, this is the first report of a zinc-catalyzed cyclopropanation of styrene derivatives. While similar transformations can be performed with other metals such as Rh,[82] Fe,[83] Ru[84] or Os,[85] the diazo is always the limiting reagent, and large excesses (5-10 equiv) of the substrate are often required. Here the alkene is the limiting reagent and the required excess of diazo (2.5 equiv) is relatively small. This is probably due to the reactivity difference between zinc carbenoids and the carbenes usually formed with other metals.

Figure 49. Synthesis of Phenylcyclopropanes from Protected Allylic Alcohols and Styrenes[a]

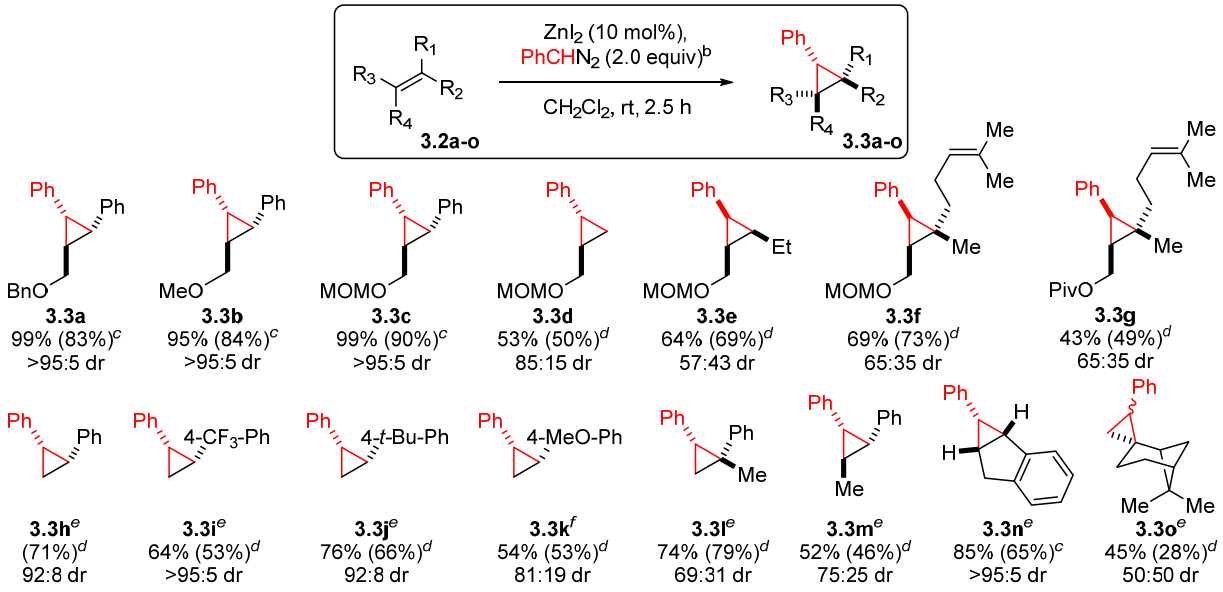

a Yields measured by ^{1}H-NMR of crude mixture using Ph_3CH or DMAP as an internal standard. *b* 0.75 M solution in CH_2Cl_2, added dropwise over 1.5 h. c Isolated yield, major diastereomer. *d* Isolated yield, both diastereomers combined. *e* 15 mol % of ZnI_2 and 2.5 equiv of phenyldiazomethane were used. *f* 13 mol % of 2,6-*t*-Bu_2PhOZnI were used instead of ZnI_2.

When free allylic alcohol **3.4a** was treated with similar conditions, the undesired *O*-benzylated cyclopropane **3.3a** was observed (**Tableau XII**, entry 3). This product putatively arises from protonolysis of the carbenoid C-Zn bond by the alcohol (*vide infra*), a reaction usually considered fast and quantitative.[64,86] The S_N2 reaction between the resulting benzyl iodide and zinc alkoxide yields the benzyl ether **3.3a**. As only one Zn-I bond is necessary to generate the carbenoid, we envisioned modulating its reactivity by replacing the catalyst's second iodide with another anion.[87] A screening of common anionic ligands[88] showed that zinc iodophosphates (entry 4) and iodophenoxides (entries 5-7) were suitable catalysts for this reaction. The hindered zinc phenoxide obtained from the deprotonation of 2,6-di-*tert*-butylphenol (2,6-*t*-Bu_2PhOZnI) gave the best results (entries 6-7).[89]

This catalyst enabled us to cyclopropanate allylic alcohols of various substitution patterns (**Figure 50**) with reduced amount of benzylated by-products. Furthermore, some substrates (**3.4c-e**) only required 1.6 equiv of diazo reagent to achieve complete conversion and no significant

amount of benzyl iodide or alcohol was observed in the crude mixtures. These results suggest that the decreased Lewis acidity of the zinc phenoxide catalyst leads to less acidification of the substrate's OH when it is complexed to the carbenoid, making cyclopropanation more prevalent than protonolysis. A similar effect has already been reported for zinc phosphate-derived carbenoids.[88b]

Throughout the reported products, the relative configuration of the introduced phenyl group was found to be dependent on the alkene's substitution pattern. For monosubstituted alkenes, the results show a *trans*-directing effect from an allylic oxygen (**3.3d, 3.5h**), while aryl substituents are *cis*-directing (**3.3h-k**). These effects are reversed or diminished when an alkyl group is *trans* to an aryl (**3.3l-m**) or *cis* to an allylic oxygen (**3.3e-g, 3.5l-n**), suggesting alkyls also exhibit a *cis*-directing effect. The inversion of diastereoselectivity between **3.5l** and **3.5n** and the sharp decrease in dr between **3.5k** and **3.5l** also highlight the *cis*-directing effect of the primary or secondary alkyl groups. These observations are correlated to earlier results using alkyl-substituted zinc carbenoids.[77a,90]

Figure 50. Synthesis of Phenylcyclopropanes from Allylic Alcohols[a]

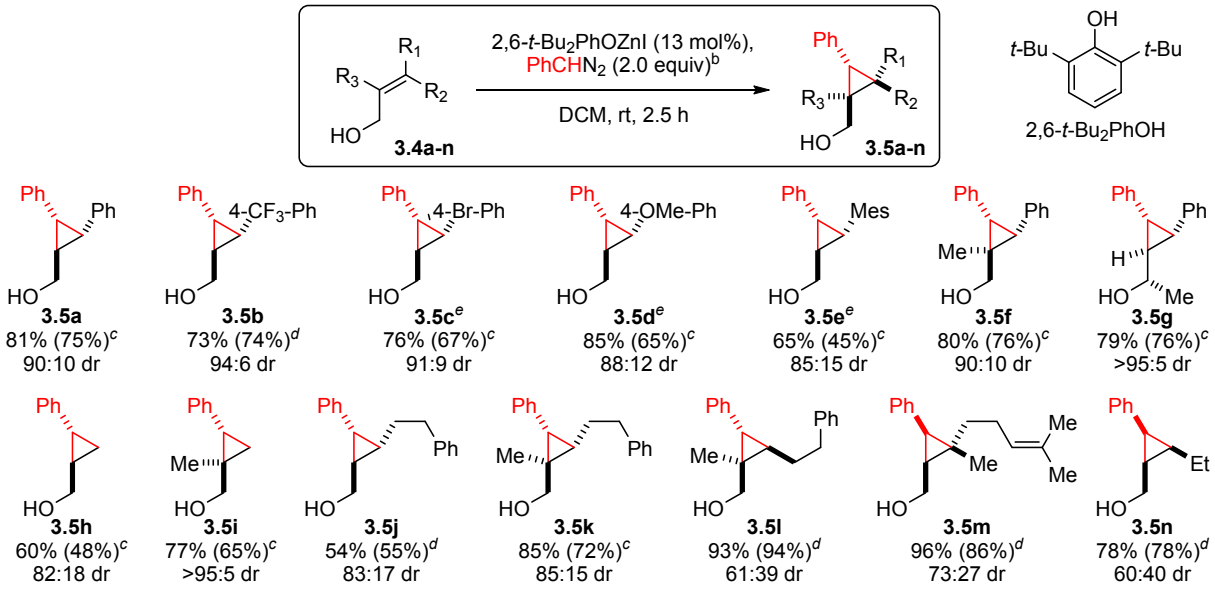

a Yields measured by ^{1}H-NMR of crude mixture using Ph_3CH as an internal standard. *b* 0.75 M solution in CH_2Cl_2, added dropwise over 1.5 h.

c Isolated yield, major diastereomer. *d* Isolated yield, both diastereomers combined. *e* Only 1.6 equiv of diazo used.

Figure 51. Proposed Mechanism for the Zinc-Catalyzed Cyclopropanation and Side Reactions

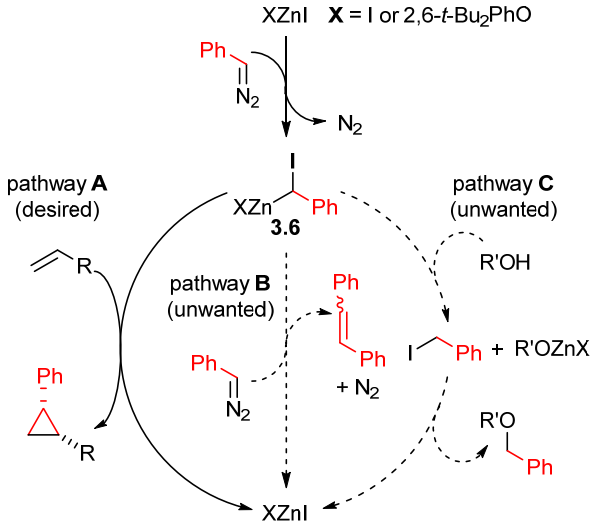

As previously reported,[73] the proposed mechanism for this reaction involves the formation of an iodo(phenyl)methylzinc carbenoid (**3.6**, **Figure 51**) *via* double nucleophilic displacement[5] between phenyldiazomethane and the iodozinc catalyst **XZnI**. This carbenoid can either react with

the substrate alkene to yield the desired cyclopropane (pathway A), with another equivalent of diazo reagent to yield a stilbene molecule (pathway B), or with a free hydroxyl group (if present) to yield a benzyl ether (pathway C). All of these reactions regenerate the starting **XZnI** catalyst. The two undesired pathways were minimized respectively by slowly adding the diazo at room temperature and by reducing the carbenoid's Lewis acidity. The cyclopropanation is believed to proceed through a transition state similar to the classic Simmons-Smith reaction of halomethylzinc species with alkenes.[54] In the cases where the alkene possesses a vicinal Lewis basic group, pre-complexation of the zinc salt to the substrate is probably involved.

In summary, we have developed a catalytic Simmons-Smith reaction able to rapidly convert allylic ethers and styrenes into the corresponding phenylcyclopropanes. A modified catalyst even tolerates free allylic alcohols. Furthermore, this system theoretically allows the introduction of a chiral anionic ligand on the catalyst, enabling the potential development of the first enantioselective Simmons-Smith reaction using catalytic amounts of both zinc and chiral mediator. The search for efficient chiral ligands is being pursued and will be reported in due course.

3.4.3.Acknowledgment.

This work was supported by the Natural Science and Engineering Research Council of Canada (NSERC), the Canada Research Chair Program, the FRQNT Centre in Green Chemistry and Catalysis and Université de Montréal. E. L. is grateful to NSERC and Université de Montréal for postgraduate scholarships. The authors would like to thank Louis-Philippe B. Beaulieu, Ph. D., Jakob F. Schneider, Ph. D. and Vincent N. G. Lindsay, Ph. D. for the synthesis of some allylic alcohols and styrenes.

3.4.4.Supporting Information Available.

Experimental procedures, NMR spectra, and compound characterization data. This material is available free of charge via the Internet at http://pubs.acs.org.

3.5.Commentaires et détails supplémentaires

3.5.1.Diastéréosélectivité observée

Figure 52. Ratios diastéréomériques observés en fonction des substituants de l'alcène (BL = base de Lewis)

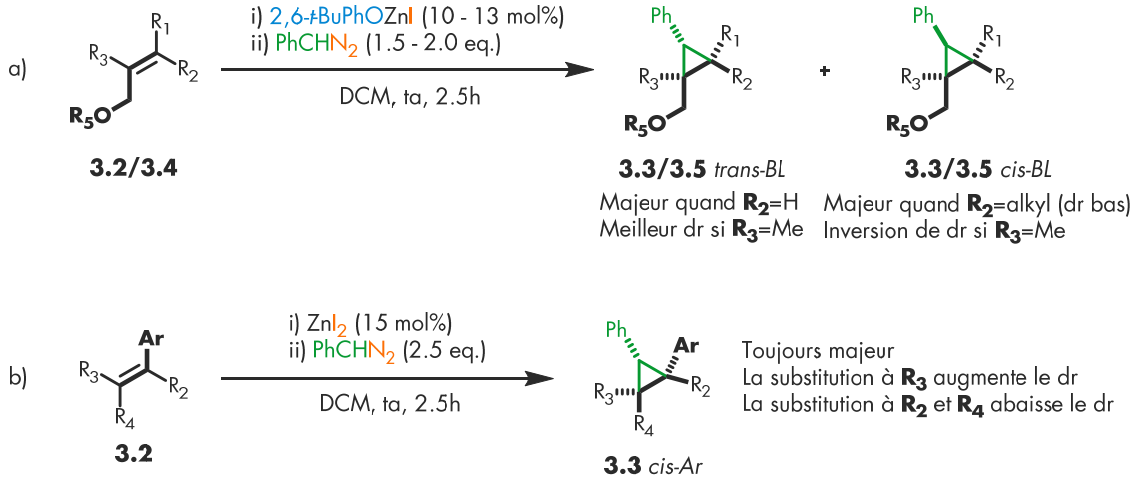

Le ratio diastéréomérique des mélanges observés varie beaucoup en fonction de l'alcène utilisé. Ces effets sont résumés dans la **Figure 52**. La tendance générale semble attribuer un effet *trans*-directeur aux groupements coordinants comme l'alcool et les éthers (BL) et un effet *cis*-directeur aux groupements alkyle ou aryle (Ar). Un modèle a été élaboré pour tenter de rationaliser ces effets.

3.5.2.Modèle d'état de transition

Figure 53. États de transition basés sur les modèles du groupe Nakamura

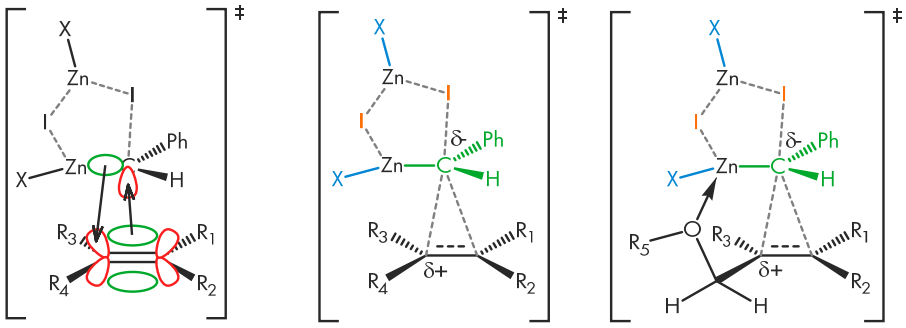

Heureusement, l'état de transition principal impliqué dans la réaction de Simmons-Smith a été extensivement modélisé par le groupe Nakamura en 2003.[64] Le modèle présenté ci-dessous est calqué sur la structure des états de transitions jugés les plus probables (**Figure 53**). Il est par contre à noter que les états de transition modélisés n'incluaient pas le groupement phényl sur le carbénoïde.

Figure 54. Modèle rationalisant les ratios diastéréomériques observés

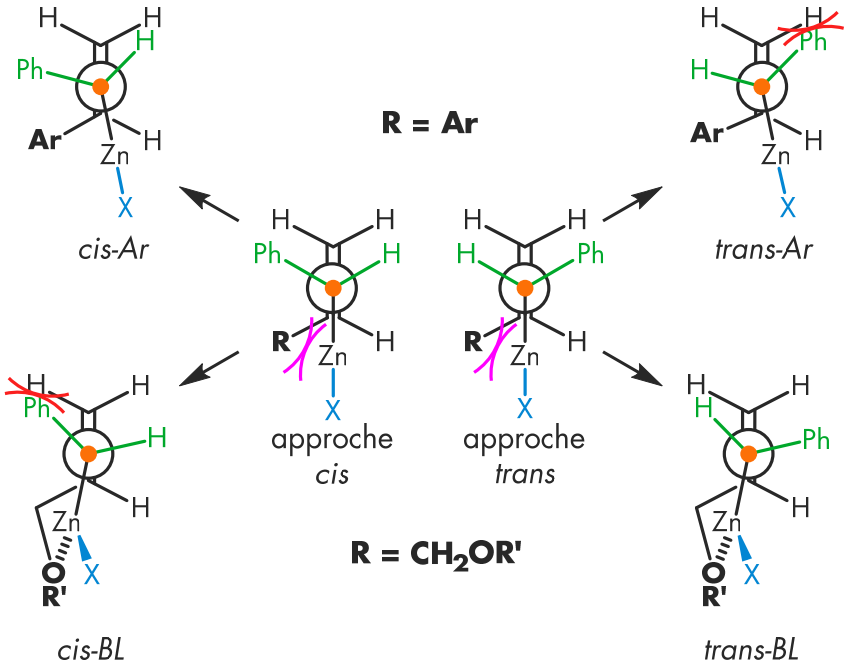

Les projections de Newman (l'axe orthogonal est celui du lien carbone-iode en train de se briser) présentée à la **Figure 54** illustrent les situations menant à un ou l'autre des diastéréoisomères. La liaison σ carbone-zinc doit être alignée avec un des lobes anti-liants de l'alcène, donc parallèle à la liaison π. Par contre, des effets stériques ou électroniques devraient être en mesure de déformer légèrement cet alignement. Posons que l'atome de zinc, avec sa cage de solvatation, est l'espèce la plus encombrée autour du carbone carbénoïde (cercle orange).

Si l'alcène ne porte pas de groupement base de Lewis, il est attendu que le zinc soit situé du côté du groupement de plus électrodonneur. En effet, l'état de transition n'est pas symétrique et il y a une accumulation significative de charge partielle positive sur le carbone proximal à l'approche du métal.

Il est possible que ce groupement (dans le cas ci-haut, le groupement aryl) déforme l'état de transition pour minimiser la répulsion électronique avec l'atome de zinc. Dépendamment de la face d'approche, le groupement phényl porté par le carbénoïde **3.6** peut alors soit se retrouver éclipsé avec un des substituants de l'alcène (*trans-Ar*, défavorisé), soit se placer dans l'espace libre entre deux substituants de l'alcène (*cis-Ar*, favorisé), ce qui mène à la prédominance de l'isomère *cis* tel qu'observé.

Dans le cas où le substituant porte une base de Lewis, telle un alcool ou un éther, la situation inverse se produit. L'interaction oxygène-zinc est stabilisante, donc le zinc se retrouve du côté du substituant directeur. Cet effet l'emporte sur la stabilisation de la charge partielle positive. La déformation de l'état de transition se produit dans l'autre sens. Le zinc s'approche de l'oxygène, poussant le phényl soit en face d'un substituant de l'alcène (*cis-BL*, défavorisé) ou entre deux substituants (*trans-BL*, favorisé), générant l'isomère *trans* observé en majorité.

3.6.Limitations liées aux composés diazo

Malheureusement, les composés aryldiazométhanes utilisés dans la cyclopropanation décrite ci-haut peuvent s'avérer problématiques en chimie conventionnelle. En effet, cette fonction chimique a le potentiel de libérer rapidement du diazote et de former des carbocations en milieu acide, deux propriétés qui en font des molécules explosives et toxiques, respectivement.[91] La synthèse et la purification du phényldiazométhane impliquait de nombreuses manipulations, augmentant le risque d'exposition. Les autres aryldiazométhanes, demandant encore plus de manipulations, n'ont pas été synthétisés. Une méthode plus sécuritaire pour accéder à des solutions propres de ces composés aurait permis d'explorer le potentiel de cette cyclopropanation bien plus en profondeur.

4.Génération et purification en flux continu de solutions réactives d'aryldiazométhanes via la fragmentation d'hydrazones

4.1.Introduction

Les risques associés au contact avec les composés aryldiazométhane ont nui à l'exploration du potentiel de la réaction de Simmons-Smith catalytique. Pour réduire ces risques et augmenter l'accessibilité de ces composés, une méthode permettant de les générer et les purifier en flux continu a été développée. De cette manière, le composé dangereux est consommé à mesure qu'il est généré, dans un système fermé, sans intervention de l'expérimentateur. Cette méthode permet, par la simple pression d'un bouton, d'obtenir un écoulement continu d'aryldiazométhanes variés dans des conditions limitant les risques d'exposition et de dégradation explosive. La compatibilité de ces solutions avec trois systèmes catalytiques a été démontrée, confirmant ainsi leur utilité face à des problèmes de synthèse réalistes.

4.2.Les composés diazo : Généralités

4.2.1.Propriétés des composés diazo

Figure 55. Extrêmes de résonance de la fonction diazo

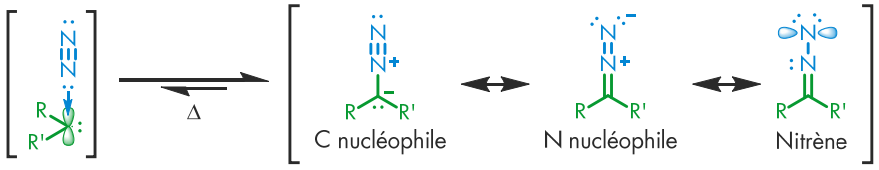

La fonction diazo, qui peut être imaginée comme un complexe formel entre un carbène et une molécule de diazote, possède plusieurs extrêmes de résonance qui expliquent sa réactivité (**Figure 55**).[92] Bien que rarement dessinée, la forme C-nucléophile est impliquée dans la plupart des réactions impliquant des composés diazo (**Figure 56**). Le carbone est le site base de Lewis mou de la fonction diazo. L'azote terminal est quant à lui le site base de Lewis dur. La réactivité N nucléophile est surtout observée avec des électrophiles métalliques et dans des systèmes encombrés.

La forme nitrène est rarement invoquée pour expliquer la réactivité, mais elle aide à comprendre le mécanisme de formation de certains diazos. Sa contribution à l'hybride de résonance est très faible car l'azote terminal a un octet incomplet.

4.2.2. Réactivité des composés diazo

Figure 56. Réactivité générale des composés diazo

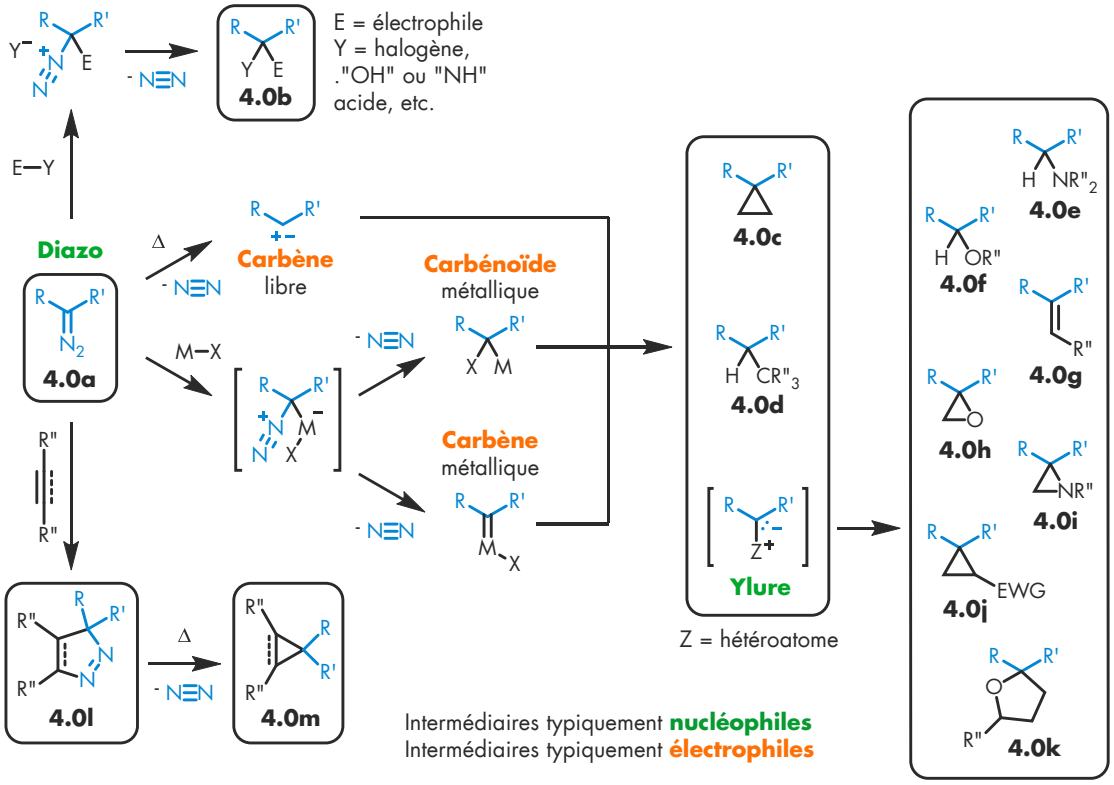

Les composés diazo (**Figure 56**, **4.0a**) réagissent généralement en tant que nucléophiles. Leur combinaison avec l'électrophile le plus simple, le proton, donne un agent alkylant très puissant, l'équivalent formel d'un carbocation vu le départ très favorisé de la molécule de diazote.[93] Dans la majorité des cas, la base conjuguée de l'acide initial réagit instantanément avec cet agent alkylant, formant un composé avec la structure générale **4.0b**. Sinon l'ion diazonium, qui peut aussi être formé par la réaction avec d'autres électrophiles, a la réactivité habituelle des carbocations, pouvant subir des éliminations[94] et des réarrangements.[95]

Des complexes métalliques acides de Lewis peuvent aussi réagir avec les composés diazo. Le diazote est rapidement expulsé après l'attaque initiale, menant à la formation de carbénoïdes[72,73,74]

ou de carbènes[96] métalliques. Ces espèces ont une réactivité semblable aux carbènes libres qui peuvent être générés par simple chauffage. De puissants électrophiles, ils peuvent réagir avec des systèmes π,[97] des liaisons C-H[98] ou des paires d'électrons libres,[99] formant respectivement des cyclopropanes (**4.0c**) des liens carbone-carbone (**4.0d**) ou des liens carbone-hétéroatome. Par contre les propriétés des carbénoïdes et carbènes métalliques peuvent être modulées par la structure et la composition du complexe, permettant d'effectuer des transformations beaucoup plus chimio-, régio-, diastéréo- et énantiosélectives.[100]

Quand un hétéroatome portant un doublet d'électrons réagit avec le carbène ou carbénoïde, un ylure est formé. Si l'hétéroatome porte un proton, ce dernier migre rapidement et l'ylure est neutralisé, menant aux produits d'insertions N-H (**4.0e**) ou O-H (**4.0f**) formelles.[99] Sinon, cet ylure peut réagir comme nucléophile avec des cétones, des imines ou des accepteurs de Michael, donnant accès à des alcènes (**4.0g**, oléfination de type Wittig[101]), des époxydes[102] (**4.0h**) des aziridines[103] (**4.0i**) et des cyclopropanes[104] (**4.0j**, Fermeture de Cycle Induite de Michael (MIRC en anglais)). Après protonation d'un ylure dérivé d'éther, un oxonium peut être obtenu, puis fragmenté.[105] Si l'ylure est formé par l'attaque d'un dérivé de carbonyl, un dipôle (1,3) réactif est formé,[106] ouvrant la porte aux cycloadditions avec des dipolarophiles variés (exemple avec un alcène : **4.0k**).

Enfin, les composés diazo sont aussi eux-mêmes des dipôles (1,3). Ils peuvent subir une cycloaddition avec des dipolarophiles tels que les alcènes et les alcynes.[107] La dihydropyrazole **4.0l** ainsi obtenue peut dégrader thermiquement si elle n'est pas aromatique, extrudant la molécule de diazote et produisant le cyclopropane **4.0m** correspondant.

4.2.3.Synthèse des composés diazo

Figure 57. Méthodologies pour la génération de composés diazo

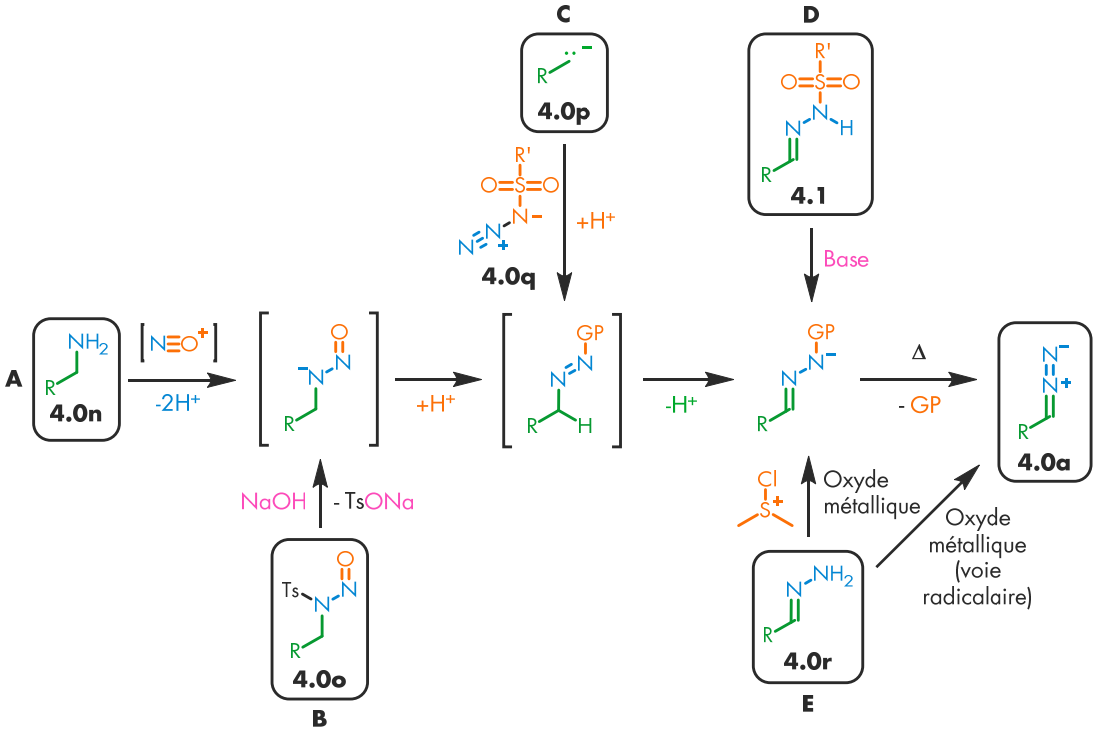

La fonction diazo peut être formée de multiples façons (**Figure 57**). La majorité d'entre elles cherchent à installer un groupe partant sur l'azote terminal de la fonction hydrazone d'une manière ou d'une autre. L'anion de cette structure particulière peut éliminer et former l'extrême de résonance nitrène du diazo. La vitesse de cette fragmentation dépend de la nature du groupe partant. Ce groupe partant peut être installé par oxydation de l'hydrazone correspondante[108] **4.0r** (chemin **E**) ou préinstallé sur cette dernière[94] (**4.1**, chemin **D**). L'hydrazone oxydée peut aussi être obtenue via un transfert de protons à partir du composé azo correspondant, qui peut être formé par l'attaque d'un nucléophile carboné **4.0p** sur l'azote terminal d'un azoture pauvre[109] **4.0q** (chemin **C**). Ce composé azo avec le groupement hydroxyle comme groupe partant (GP = OH) peut être formé par l'hydrolyse basique d'un N-nitrososulfonamide[110] **4.0o** (chemin **B**). Le N,4-diméthyl-N-nitrosobenzènesulfonamide (**4.0o** avec R = H) est vendu sous le nom Diazald® pour la production de diazométhane par cette approche. L'hydroxydiazène est aussi un intermédiaire dans une série de transferts de proton suivant l'addition d'une amine **4.0n** sur le cation nitrosonium,[111] habituellement généré *in situ via* l'acide nitreux, lui-même obtenu en traitant le nitrite de sodium avec un acide (chemin **A**).

4.3.Synthèse d'aryldiazométhanes en chimie conventionnelle

4.3.1.Aryldiazométhanes : approches synthétiques

La fonction aryldiazométhane, où le diazo est en position benzylique, est généralement formée à partir d'une hydrazone obtenue par condensation. L'hydrazone libre **4.0r**, produit de la réaction entre l'hydrazine et un aldéhyde ou une cétone, peut être directement oxydée par un oxyde métallique[112] ou une source d'ion chloronium (de manière analogue à une oxydation de Swern)[113] (chemin **E**). Alternativement, le produit de condensation avec un sulfonylhydrazide (**4.0t**) peut être traité avec une base et chauffé. L'anion de la sulfonylhydrazone **4.1** fragmente alors en sulfinate **4.0u** et en aryldiazométhane **4.2** (chemin **D**). Un analogue du Diazald® (chemin **B**, **4.0o** avec R = Ph) a aussi déjà été utilisé pour générer du phényldiazométhane.[114]

4.3.2.Fragmentation de sulfonylhydrazones

Figure 58. Synthèse de sulfonylhydrazones et fragmentation de leur base conjuguée en aryldiazométhanes

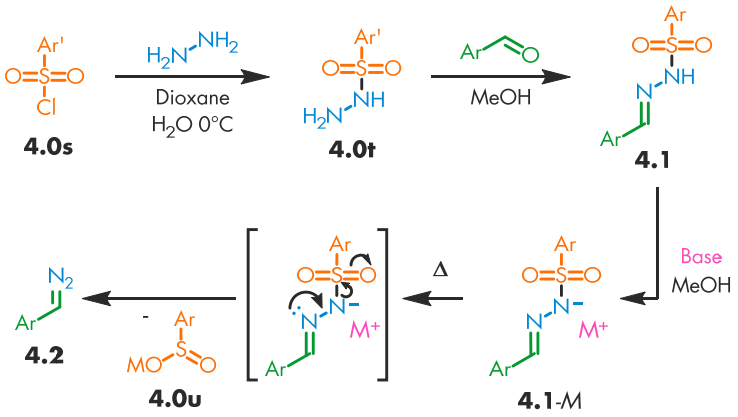

Un des avantages principaux de l'utilisation des sulfonylhydrazones (**4.1)** est la facilité de leur manipulation. Généralement peu solubles en milieu organique, elles précipitent spontanément du milieu réactionnel où elles sont formées (réaction de condensation), ce qui simplifie la purification. Les solides ainsi obtenus sont stables à l'air et résistants à l'hydrolyse, et peuvent être conservés à température ambiante sans dégradation après plusieurs mois.

Figure 59. Aryldiazométhanes par fragmentation de sels de sulfonylhydrazones

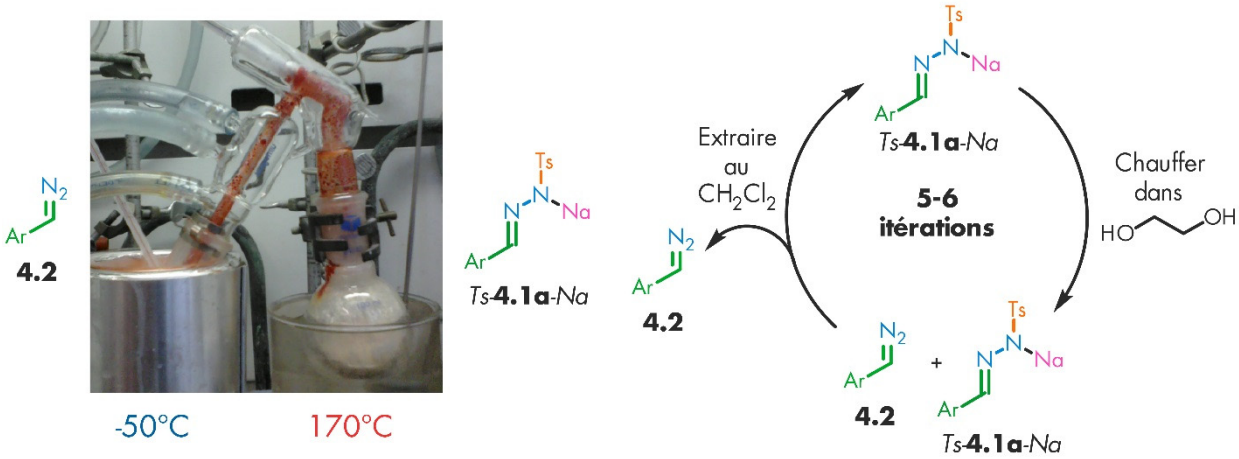

La méthode utilisée pour obtenir le phényldiazométhane[115] (**4.2a**) utilisé lors du projet précédent consiste à traiter la tosylhydrazone du benzaldéhyde (*Ts*-**4.1a**) avec du méthoxyde de sodium. Le sel (*Ts*-**4.1a**-*Na*) ainsi formé est concentré à sec à basse température pour empêcher la formation prématurée de diazo, facilement reconnaissable à sa couleur rouge sang. Enfin, pour produire le diazo, ce sel sodique est chauffé à sec sous pression réduite dans un montage à distillation. Le diazo généré en phase gazeuse est condensé à -50 °C, juste au-dessus de son point de fusion, laissant le sulfinate de sodium **4.0u** dans le ballon chauffé. Le phényldiazométhane **4.2a** pur est ensuite dilué, séché au sulfate de sodium (le produit réagit avec le sulfate de magnésium) et entreposé à -20°C sur des pastilles d'hydroxyde de potassium. Une solution ainsi préparée sera utilisable pendant environ 3 semaines sans chute de rendements avant de devoir être neutralisée avec de l'acide acétique.

Malheureusement, les aryldiazométhanes substitués ne sont généralement pas assez volatils pour obtenir un bon rendement lors de la distillation, et doivent être générés en solution.[115] Cette procédure implique une boucle itérative de courtes périodes de chauffage suivies d'extractions au dichlorométhane, qui est immiscible avec la solution de sulfonylhydrazonate de sodium (*Ts*-**4.1a**-*Na*) dans l'éthylène glycol. L'itération est nécessaire car l'aryldiazométhane réagit rapidement avec l'éthylène glycol à haute température (90 °C), formant un éther benzylique. Cette procédure, impliquant un significatif danger d'exposition pour l'expérimentateur vu les nombreuses manipulations, n'a pas été utilisée pour le projet précédent. Cette embûche nous a convaincu qu'il était nécessaire de développer une méthode plus conviviale et sécuritaire permettant d'utiliser les réactifs aryldiazométhanes.

4.4.Potentiel de la chimie en flux continu dans un contexte de réactifs dangereux/instables

4.4.1.Avantages de la chimie en flux continu

La synthèse en flux continu permet de contourner beaucoup des inconvénients reliés à l'utilisation de composés tels que les aryldiazométhanes.[116] En effet, le besoin d'entreposer le réactif de manière sécuritaire est éliminé vu qu'il est fabriqué sur demande. De plus, un tel système évite l'accumulation de quantités dangereuses de réactif puisque ce dernier est consommé à mesure qu'il est généré. Enfin, comme toutes les opérations se déroulent dans un système fermé, les risques d'exposition au réactif sont grandement réduits. Par contre, il est nécessaire d'adapter les conditions réactionnelles pour les rendre compatibles avec les technologies de manipulation de liquides et les méthodes de purification propres aux systèmes en flux continu.

4.4.2.Contraintes de la chimie en flux continu

En effet, les systèmes en continu ne sont pas aussi simples d'utilisation que les méthodes de chimie conventionnelle et ont des limitations inhérentes au fait que des liquides doivent être pompés sans interruptions dans des conduits, des connecteurs et des valves.

Une contrainte évidente est que toutes les matières pompées doivent être soit des fluides, soit des solides piégés dans une partie isolée du système, généralement une colonne cylindrique. Les précipitations qui peuvent se produire lors de la réaction et du parachèvement sont particulièrement problématiques. Si une étape inclut plusieurs fluides immiscibles, la vitesse du transfert de masse est fortement dépendante de la nature et de l'aire des interfaces entre les phases.

De plus, les méthodes de purification typiques à la chimie conventionnelle, telles que l'évaporation, l'extraction liquide-liquide, la filtration, la chromatographie et la distillation ne peuvent pas être réalisées aussi simplement en continu et ont toutes leurs contraintes spécifiques, si elles sont même possibles. Heureusement, il existe des techniques spécifiques au flux continu pour séparer les constituants d'un mélange. Ces techniques utilisent des membranes, des colonnes et des montages particuliers pour réaliser les mêmes opérations que les techniques conventionnelles réalisent avec de la verrerie, des pompes à vide, des filtres et des phases stationnaires chromatographiques.

4.5.Méthodes précédemment rapportées pour la synthèse et la purification de composés diazo en flux continu

Plusieurs méthodes ont déjà été rapportées pour obtenir des solutions de composés diazo en respectant les contraintes propres aux techniques de flux continu. La purification étant le principal défi d'une telle entreprise, les exemples présentés ont été sélectionnés en fonction des méthodes utilisées pour séparer les composés diazo des mixtures nécessaires à leur formation.

4.5.1.Séparation gaz-liquide

Figure 60. Utilisation d'un réacteur « tube dans tube » pour séparer le diazométhane d'un milieu réactionnel

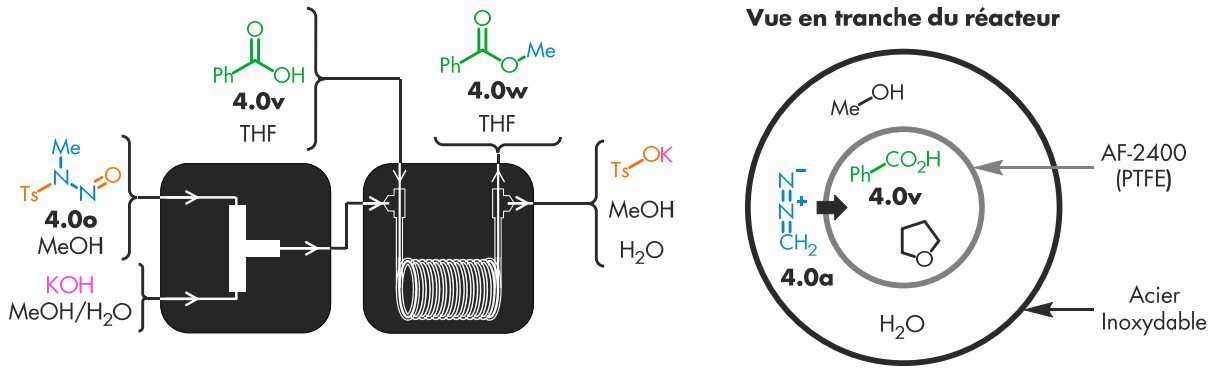

Une méthode de purification particulièrement sélective exploite les propriétés des membranes de PTFE de type AF-2400, qui sont uniquement perméables aux gaz de petit poids moléculaire.[117a] Le composé diazo le plus simple, le diazométhane, a un point d'ébullition de -23°C[118] et est suffisamment petit pour s'infiltrer dans les interstices du polymère fluoré. Ceci permet le générer ce diazo en phase aqueuse par hydrolyse du Diazald® (chemin **B** de la **Figure 57**), puis de le faire réagir de l'autre côté de la membrane dans un milieu anhydre. De cette manière, le diazométhane n'est présent dans le système que pour un petit laps de temps, toujours en très petite quantité. Le réacteur est composé d'un tube d'AF-2400 à l'intérieur d'un tube en acier inoxydable, avec la capacité de pomper un liquide dans les deux espaces concentriques ainsi créés. Cette méthode a aussi été utilisée pour la synthèse de 2,2,2-trifluorodiazoéthane.[117b]

4.5.2.Séparation liquide-solide

Figure 61. Utilisation d'une colonne de silice en ligne pour séquestrer un sous-produit polaire

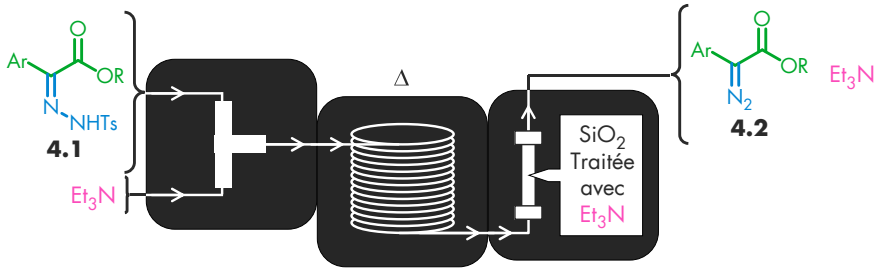

Une méthode de purification plus versatile communément employée en flux continu est l'utilisation de colonnes remplies d'un réactif insoluble capable de soustraire à une mixture liquide des composés indésirés spécifiques. Ces réactifs sont typiquement des bases ou acides inorganiques, des matériaux adsorbants ou des molécules fixées à une matrice insoluble.

Cette méthode a entre autres été utilisée avec une colonne de silice (**Figure 61**) pour retirer le sulfinate (**4.0u**) de triéthylammonium produit lors de la génération d'aryldiazoesters par fragmentation de sulfonylhydrazones en milieu basique[119] (chemin **D** de la **Figure 57**). Par contre, l'excès de base triéthylamine n'est pas retiré par la colonne, limitant les réactions pouvant être effectuées avec cette solution sans purification supplémentaire. De plus, après un certain temps d'opération, l'accumulation de sulfinate sur la silice cause des problèmes d'écoulement et de contamination.

Figure 62. Utilisation d'une colonne d'oxydant stœchiométrique insoluble. Aucune purification

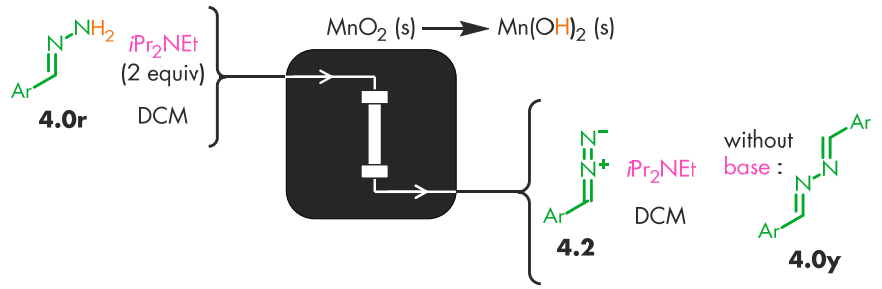

Une alternative à la purification en flux continu de la solution de diazo produite est de concevoir un système qui produit directement un réactif suffisamment pur pour être utilisé dans la

réaction subséquente. Cette situation idéale est difficile à atteindre, mais il est possible de limiter la nature et la quantité des impuretés. Ce compromis implique que le système ne sera compatible qu'avec des réactions pouvant tolérer la présence des impuretés sélectionnées. Un système de ce type a été rapporté en 2015 pour la synthèse des aryldiazométhanes **4.2** (**Figure 62**).[120a] Ces diazos nucléophiles sont formés par l'oxydation d'une solution d'hydrazone libre en présence d'un excès de base sur une colonne de dioxyde de manganèse insoluble (chemin **E** de la **Figure 57**). Le dihydroxyde de manganèse produit est lui aussi insoluble et ne contamine pas la solution. Par contre la surface de l'oxydant doit être conditionnée par le passage de réactif sacrificiel. De plus, il est consommé de manière stœchiométrique, forçant l'arrêt du système pour régénérer la colonne ou en remplacer le contenu. Enfin, l'excès de base diisopropyléthylamine (*i*Pr_2NEt, DIPEA), nécessaire à l'obtention d'un bon rendement et à l'élimination du sous-produit dibenzylidènehydrazine, reste dans la mixture. Les réactions utilisant les solutions de diazo produites par cette méthode doivent donc tolérer la présence de ces deux équivalents de base de Lewis.[120]

4.5.3.Séparation liquide-liquide

L'extraction liquide-liquide est une des rares méthodes de chimie conventionnelle qui peut être plus ou moins directement transférée au flux continu sans trop de complications. Les phases sont typiquement séparées non pas par différence de densité, mais par différence d'affinité pour une membrane microporeuse.[121] Les membranes les plus communes sont composées de polymères fluorés et sont percées de trous de l'ordre du micromètre à la centaine de nanomètres. Les phases aqueuses ou très polaires sont incapables de mouiller la membrane, défavorisant leur traversée, alors que les phases apolaires recouvrent la membrane et traversent sans résistance. Une grande tension de surface entre les deux phases facilite la séparation. L'ajustement du gradient de pression de part et d'autre de la membrane permet de ralentir ou d'accélérer la perméation.

Cette méthode a été utilisée en 2011 pour la synthèse et purification de solutions de diazoacétate d'éthyle (EDA, *Ethyl DiazoAcetate*).[122] Le diazo est produit par diazotization du chlorure d'éthylglycinium par le nitrite de sodium (chemin **A** de la **Figure 57**) dans un système biphasique eau/toluène. Une fois formé, le diazo migre dans la phase organique, laissant derrière le chlorure de sodium et les autres sels présents dans la phase aqueuse. La séparation des phases par membrane permet donc de récupérer une solution propre d'EDA dans le toluène.

Figure 63. Utilisation d'une membrane poreuse hydrophobe pour séparer une phase organique réactive d'une phase aqueuse

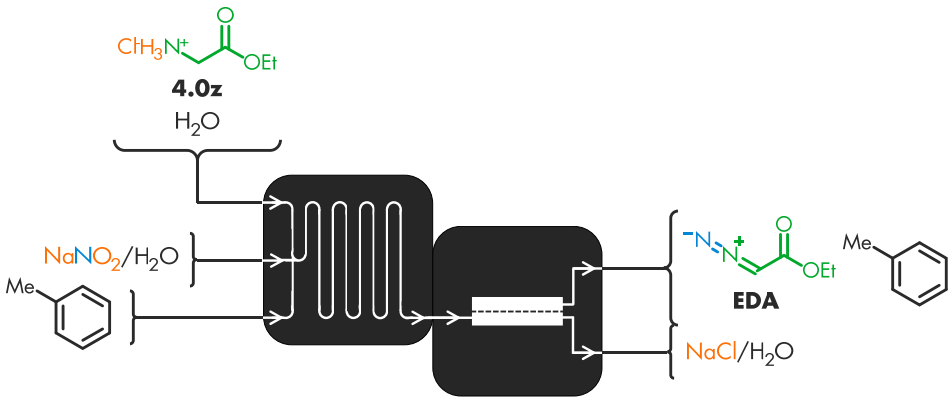

La méthode de séparation liquide-liquide nous semblait la plus appropriée pour l'application aux aryldiazométhanes. Ses principaux attraits sont la possibilité d'avoir un système applicable à de nombreux substrats qui fonctionne réellement en régime continu, sans nécessiter d'interruptions périodiques pour régénérer ou changer une colonne. De plus, étant donné la versatilité de cette approche pour différents systèmes chimiques, l'expérience acquise en l'adaptant à la synthèse d'aryldiazométhanes pourra être appliquée à d'autres réactions générant d'autres intermédiaires hautement réactifs d'intérêt.

Les étapes du développement d'une méthode de génération et de purification d'une librairie d'aryldiazométhanes en flux continu et l'utilisation directe de ces réactifs dans trois systèmes catalytiques sensibles aux bases de Lewis sont relatées dans l'article ci-dessous.

4.6.Article publié dans *Angewandte Chemie International Edition* : Continuous flow synthesis and purification of aryldiazomethanes via hydrazone fragmentation

Éric Lévesque, Simon T. Laporte, and André B. Charette*

DOI: 10.1002/anie.201608444

4.6.0.Participation des coauteurs

Éric Lévesque a effectué les expériences rapportées et rédigé l'article sous la supervision du Pr. A. B. Charette. Simon T. Laporte, B. Sc. a travaillé en tant que stagiaire sous la supervision de É. Lévesque lors des débuts du projet. Beaucoup d'éléments du montage en flux continu qu'il a développé sont présents dans le système final.

4.6.1.Abstract

Figure 64. Continuous flow synthesis and purification of aryldiazomethanes: Abstract graphic

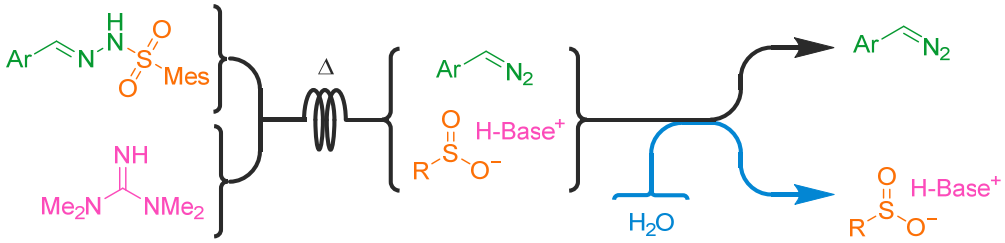

Electron-rich diazo compounds, such as aryldiazomethanes, are powerful reagents for the synthesis of complex structures, but the risks associated with their toxicity and instability often limit their use. Flow chemistry techniques make these issues avoidable, as the hazardous intermediate can be used as it is produced, avoiding accumulation and handling. Unfortunately, the produced stream is often contaminated with other reagents and by-products, making it incompatible with many applications, especially in catalysis. Herein is reported a metal-free continuous flow method for the production of aryldiazomethane solutions in a non-coordinating solvent from easily-prepared, bench-stable sulfonylhydrazones. All by-products are removed by an in-line aqueous wash, leaving a clean, base-free diazo stream. Three successful sensitive metal-catalyzed transformations demonstrated the value of the method.

Diazo compounds are versatile intermediates in organic synthesis. Driven by the release of dinitrogen, this unique structure gives access to highly reactive carbenes,[123] carbenoids[72,73,74] or carbocations.[124] However, the toxicity and instability inherent to these compounds usually discourage the exploitation of their chemical potential, especially on large scale applications.[91] Continuous flow chemistry can circumvent these risks.[116] Flow systems allow reagent mixing and product generation with minimal operator intervention, reducing the risk of exposure. Furthermore, simultaneous reagent production and consumption enables processes to be scaled up without increasing the maximum reagent accumulation.

Electron-rich diazo compounds, such as alkyl- or aryldiazomethanes, are of particular interest because of their inherent nucleophilicity and basicity, allowing alkylations[124] and homologations[125] under mild conditions. However, these same properties increase their Lewis or Brønsted acid sensitivity, complicating their synthesis, storage and use.[126]

Figure 65. Alternate approaches for the continuous synthesis of aryldiazomethanes: hydrazone oxidation by metal oxides[120] and sulfonylhydrazone fragmentation (this work).

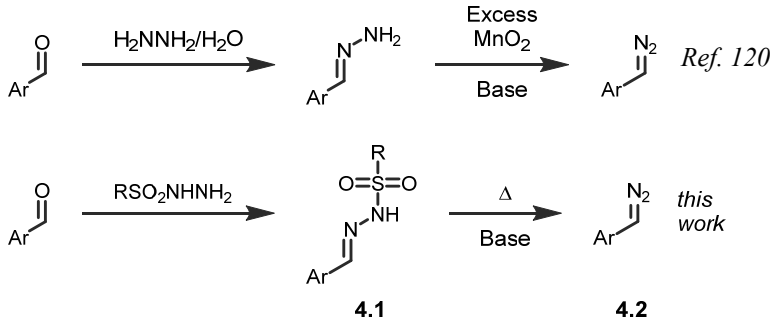

A straightforward approach for the continuous flow generation of aryldiazomethanes was recently reported by Ley and co-workers.[120] The reagents are obtained by running a CH_2Cl_2 solution of free hydrazine and diisopropylethylamine through a column packed with an excess of solid manganese dioxide. Unfortunately, the resulting diazo solutions still contain a superstoichiometric amount of base which is incompatible with catalytic systems involving base-sensitive transition metals. Furthermore, the solid oxidizer needs to be conditioned before use and gets reduced and contaminated as the reaction proceeds, requiring interruption of production for column repacking or regeneration. The free hydrazones used as starting materials are also problematic due to their tendency to self-condense into azines,[127] especially when derived from aldehydes.

The base-mediated fragmentation of sulfonylhydrazones is an alternative, metal-free approach to aryldiazomethane synthesis. These innocuous,[128] solid and bench-stable[129] compounds readily form via condensation of a sulfonylhydrazide with the corresponding aldehyde and are purified by simple precipitation. Under heat, their conjugate base undergoes sulfinate anion elimination, generating the diazo functional group (**Figure 65**).[94]

Figure 66. Flow setup concept and expected solution compositions.

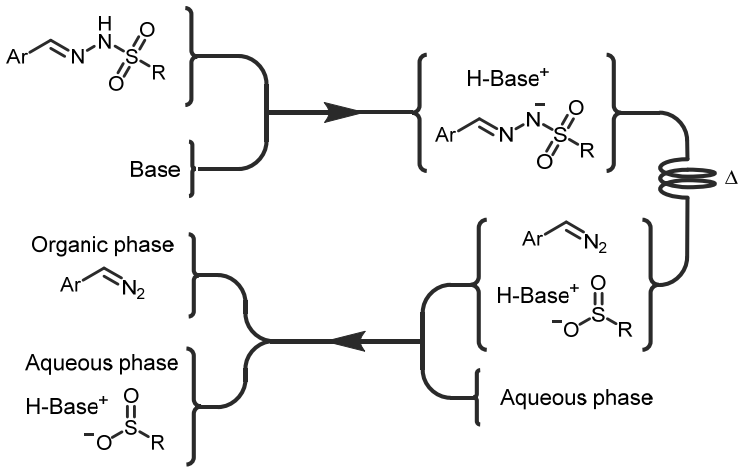

To be compatible with the most stringent catalytic applications, aryldiazomethanes must be base- and contaminant-free and dissolved in a non-coordinating solvent.[130] Continuous flow production of such solutions requires removal of the base and the sulfinate by-product from the stream. Several methods have previously been employed to purify specific classes of diazo reagents in flow systems, such as SiO_2-filled scavenger columns ($R_1C(N_2)COOR_2$),[119] AF-2400 tube-in-tube reactors (CH_2N_2 and CF_3CHN_2)[117] and membrane-based phase separation (CH_2N_2).[122b] An aqueous wash followed by a phase separation was deemed the most suitable approach for the preparation of aryldiazomethanes, as it is compatible with most substrates and allows unlimited continuous flow.

The system design for such a reaction-purification sequence includes base and sulfonylhydrazone feeds meeting before entering a heated reactor. The reactor's output is then cooled before addition of an aqueous stream. After sufficient biphasic extraction, the mixture runs through a Zaiput® phase separator, leaving all the reaction by-products behind in the aqueous phase. The cleaned reactive organic phase is then added to the reaction mixture intended to consume the diazo reagent (**Figure 66**). In order for such a system to operate properly, chemicals must be chosen or designed to satisfy its associated constraints. Namely, all reagents and by-products must be soluble at all times to avoid clogging, and everything but the desired aryldiazomethane must be transferred into the aqueous layer upon extraction. Since the most common reagents for aryldiazomethane preparation do not satisfy those constraints, a *de novo* approach had to be designed.

Tableau XIII. Optimisation of the sulfonylhydrazone fragmentation into phenyldiazomethane and subsequent purification.

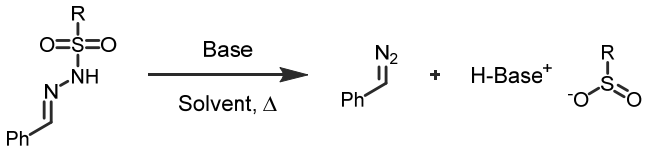

4.1 **4.2**

Entry	Exp. Type	Solvent(s)	R	Base	Quench/ wash	Yield **4.2a**[a]	By-product[b]
1[c]	Batch	MeOH/ Toluene	4-Tolyl	LiOMe	H_2O	7%	**4.1**
2[c]	Batch	MeOH/ Toluene	Mes	LiOMe	H_2O	47%	BnOMe[h]
3[c]	Batch	MeOH/ Toluene	Trip	LiOMe	H_2O	48%	$TripSO_2Li$
4[d]	Batch	CH_2Cl_2	Mes	LiO*i*Pr	H_2O	35%	**4.1**
5[d]	Batch	CH_2Cl_2	Mes	TMG	H_2O	55%	**4.1** + TMG[i]
6[d]	Batch	$HCONH_2$/ CH_2Cl_2[g]	Mes	TMG	H_2O	60%	**4.1** + TMG[i]
7[e]	Flow	$HCONH_2$/ CH_2Cl_2[g]	Mes	TMG	H_2O	63%	**4.1** + TMG[i]
8[f]	Flow	$HCONH_2$/ CH_2Cl_2[g]	Mes	TMG	H_2O	79%	TMG[i]
9[f]	Flow	$HCONH_2$/ CH_2Cl_2[g]	Mes	TMG	NH_4Cl/ H_2O	78%	NH_3[j]
j10[f]	Flow	$HCONH_2$/ CH_2Cl_2[g]	Mes	TMG	NH_5CO_3/ H_2O	79%	None[k]

a Titrated with BzOH or AcOH and corresponding ester isolated or quantified by ^{1}H-NMR using 1,3,5-trimethoxybenzene or triphenylmethane as internal standard. *b* Major by-product(s). *c* 55 °C, 30 min, 1.0 equiv base. *d* 45 °C, 30 min, 1.0 equiv base. *e* Unoptimized flow conditions (50 °C, 20 min, 1.0 equiv base). *f* Optimized flow conditions (65°C, 6 min, 2 equiv base). *g* 1.0 equiv of formamide. *h* From benzylation of MeOH by phenyldiazomethane. *i* Up to 15% TMG *j* Ammonium benzoate observed after titration. *k* no impurity >3%, no TMG.

At first, the optimal sulfonyl substituent was selected. The 4-tolyl group commonly used for batch synthesis[115] fragments very slowly into the diazo at temperatures compatible with the sensitive

aryldiazomethanes (**Tableau XIII**, entry 1). Sterically congested sulfonylhydrazones have been reported to undergo elimination more readily,[131] a process probably accelerated by steric decompression. The mesityl (Mes) group (entry 2) was optimal, as the equally efficient triisopropylphenyl (Trip) yielded a water-insoluble sulfinate (entry 3).

The typically used alkoxide/alcohol base and solvent system proved problematic. Alcohols can react with diazo reagents (entry 2), and alkali salts tend to be poorly soluble in organic media (entry 4). Dichloromethane was chosen as a non-Lewis-basic solvent. Common organic bases, such as triethylamine and DBU, were unsatisfactory, but tetramethylguanidine (TMG)[108] turned out to have the perfect combination of a high pK_b[132] and a hydrophilic conjugate acid (entry 5).

At this point, the only remaining issue was the insolubility of the sulfonylhydrazone precursor in CH_2Cl_2 before base addition. Fortunately, it was discovered that one to five equivalents of water-soluble formamide ensured the complete dissolution of most sulfonylhydrazones in CH_2Cl_2 without negatively impairing the product yield or purity (entry 6).

The reaction conditions were then suitable to be tested in the flow reactor (**Figure 67**). While conditions imitating the batch reaction gave a similar result (entry 7), the higher temperature and short reaction time made possible in the pressurized flow reactor increased the yield to a satisfactory 79% (entry 8). The only major impurity still present in the diazo stream was the excess base. Several mild aqueous proton sources were then tested (entries 9-10), and ammonium bicarbonate yielded a clean, uncontaminated aryldiazomethane stream (entry 10).

Figure 67. Final flow setup to generate and purify aryldiazomethanes.

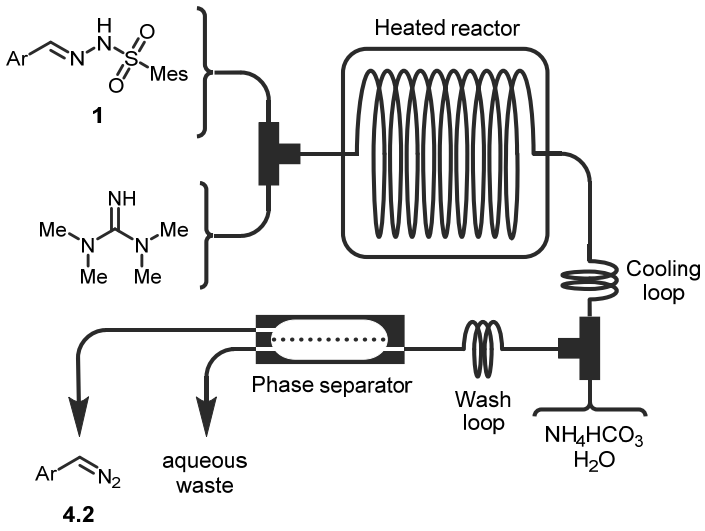

Diazo-consuming reactions often use slow addition rates that are usually achieved via syringe pump.[123] To accommodate this constraint, the system was tested at different concentrations and flow rates, adjusting the reactor volume to keep the reaction time constant. Aryldiazomethanes can be produced at rates between 1.0 to 10.0 mmol/h[133] and at concentrations between 0.50 M and 0.25 M[134] without significant variations in the yield or purity.

The methodology was shown to be quite general, giving excellent yields of electron-poor aryldiazomethanes (**4.2b-4.2i** and **4.2s-4.2t**) and acceptable yields of their highly reactive electron-rich counterparts (**4.2j-4.2n**).[135] Diaryldiazomethanes (**4.2u-4.2w**) could also be accessed, as well as complex heterocyclic diazo compounds (**4.2o-4.2p**), showcasing the excellent chemoselectivity of the method.

Figure 68. Flow synthesis of aryldiazomethanes: Scope study using various aldehydes and ketones. Yields are calculated from the isolated benzoic ester.

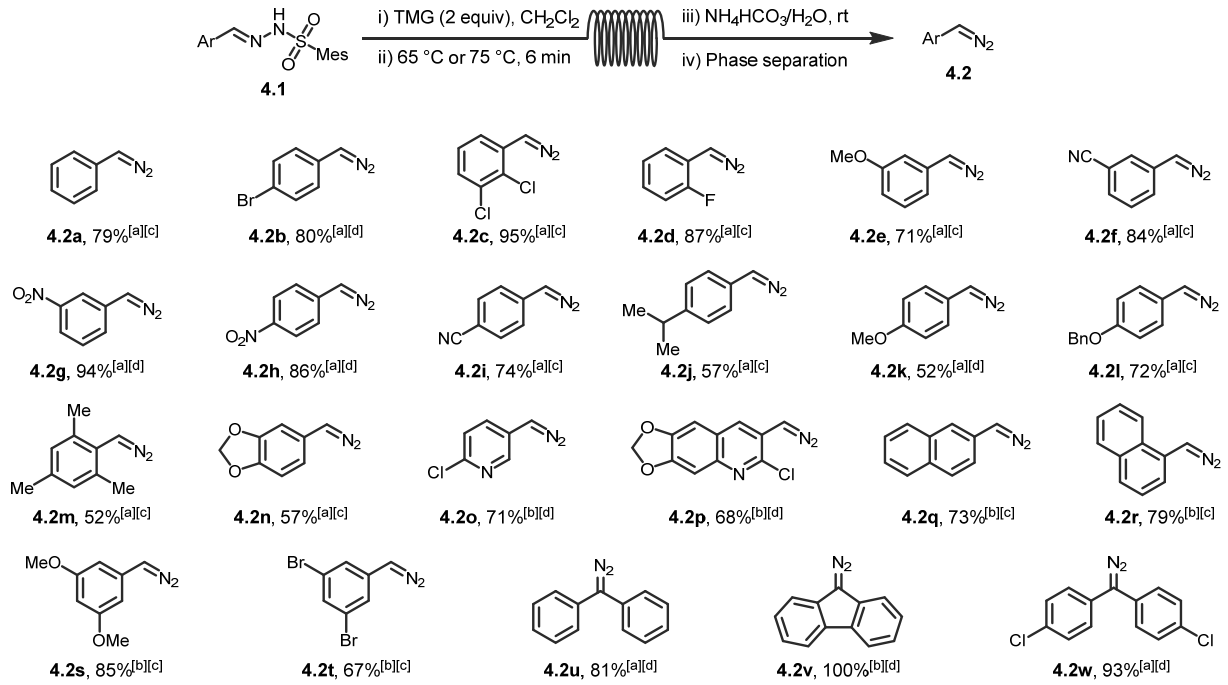

a 1 to 5 equiv formamide added in sulfonylhydrazone (**4.1**) solution. *b* Sulfonylhydrazone (**4.1**) was premixed with TMG before injection. *c* Reactor temperature = 65 °C. *d* Reactor temperature = 75 °C.

No precautions were taken to exclude water and oxygen from the solvents and reagents, as these did not increase the yield and purity of the streams. However, if the diazo's intended use involves an air- and water-sensitive reagent system, the stream can be passed through a column packed with a 1:1 mixture of dried Celite® and 4Å molecular sieves with no loss of yield.[136]

Figure 69. $Sc(OTf)_3$-catalyzed ring expansion of cycloheptanone.

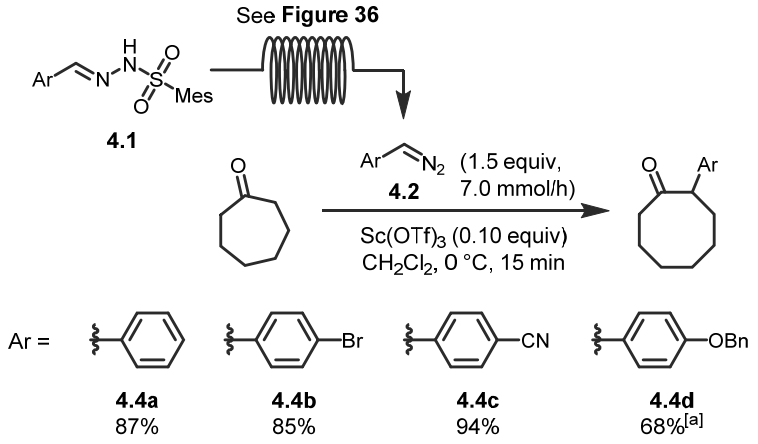

0.23 mmol scale, 0.35 M diazo, 333 μL/min. *a* Reaction run at –78 °C.

To investigate the produced aryldiazomethanes' applicability to metal-catalyzed reactions, three reagent systems known for their sensitivity to Lewis-basic contaminants were selected. In all cases, the output stream from the flow apparatus was added directly to a stirred reaction mixture.

First, the scandium-catalyzed cyclic ketone ring expansion developed by Kingsbury and co-workers was reported to fail when the diazo nucleophile solution is not of high purity.[137] This semipinacol rearrangement was successfully performed with 4 different continuously produced diazo compounds in good yields (**Figure 69**).

Figure 70. $Cu(acac)_2$-catalyzed epoxidation of 4-NO_2-benzaldehyde.

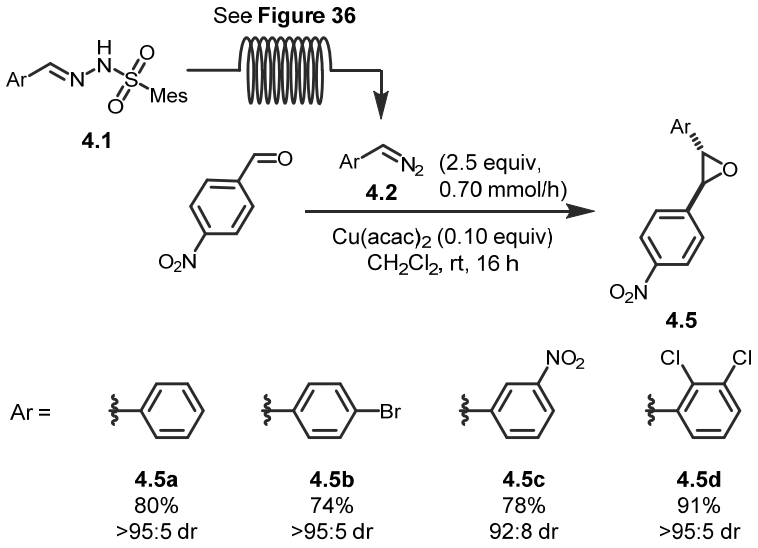

0.28 mmol scale, 0.18 M diazo, 66 μL/min.

Second, the copper-catalyzed epoxidation of aldehydes reported by Aggarwal and coworkers[123a] involves a typically water-sensitive copper carbene and a sulphur ylide as intermediates and requires a very slow addition of the diazo reagent. Nonetheless, the selected aromatic aldehyde underwent smooth epoxidation with 4 different diazo partners (**Figure 70**).

Finally, the catalytic Simmons-Smith cyclopropanation previously developed in our group[74] requires the formation of a notoriously Lewis-base sensitive zinc carbenoid.[54] The protected allylic alcohol substrate still underwent cyclopropanation in moderate to excellent yields (**Figure 71**).

Figure 71. ZnI_2-catalyzed cyclopropanation of MOM-protected cinnamyl alcohol.

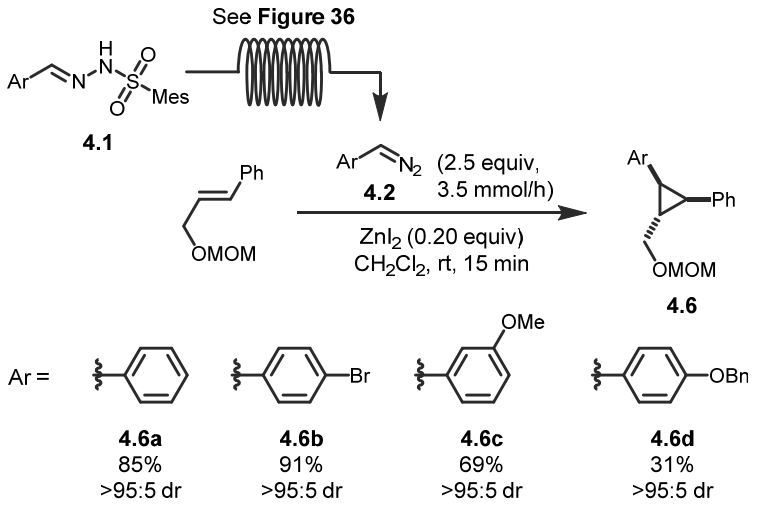

0.14 mmol scale, 0.35 M diazo, 166 μL/min.

In summary, a safe and efficient method for the on-demand production of clean, uncontaminated reactive aryldiazomethane solutions was developed. The sulfonylhydrazone precursors are safe, bench-stable solids easily prepared from the corresponding aldehydes. The diazo stream's concentration and flow rate can be modulated to suit the subsequent reaction. Three typically sensitive reactions were performed on multiple aryldiazomethanes to demonstrate the applicability of this method on real synthetic problems usually requiring extensively purified reagents. We are hopeful that this technology will allow a more widespread exploitation of diazo reagents' chemical potential.

4.6.2.Experimental Section

Typical procedure for the synthesis of mesitylsulfonylhydrazones from aldehydes: Mesitylsulfonylhydrazide (1.00 equiv) was suspended in EtOH in a 20 mL vial open to air and aldehyde (1.01 equiv) was added at once, followed by AcOH (0.005 equiv). Heterogeneous mixture was kept under strong agitation for 90 min. Excess hexanes were added and the resulting off-white solid was recovered by filtration (washing with hexanes).

Typical procedure for the continuous flow synthesis and purification of aryldiazomethanes: Stream 1 (0.24 mL inj. loop, 0.5 M **4.1a,** 0.5 M formamide in CH_2Cl_2, 1.0 equiv, 166 µL/min pumped CH_2Cl_2) and stream 2 (0.24 mL inj. loop, 1.0 M tetramethylguanidine in CH_2Cl_2, 2.0 equiv, 166 µL/min pumped CH_2Cl_2) meet in a "T" connector, run through a 2.0 mL coiled tube reactor heated at 65 °C and a 0.25 mL room temperature cooling loop. Stream 3 (1.00 mL/min pumped 1.0 M NH_4HCO_3/H_2O) is added via a second "T" connector. Biphasic stream runs in a 0.25 mL loop, phases are separated in a Zaiput® phase separator (1.0 µm pores PTFE membrane). Zaiput® back pressure regulators are set at 3 atm. Organic stream (333 µL/min, approx. 0.2 M phenyldiazomethane in CH_2Cl_2) is added directly to the target reaction mixture.

4.6.3.Acknowledgements

This work was supported by the Natural Science and Engineering Research Council of Canada (NSERC) under the CREATE Training Program in Continuous Flow Science, the Canada Foundation for Innovation, the Canada Research Chair Program, the FRQNT Centre in Green Chemistry and Catalysis and Université de Montréal. E.L. is grateful to NSERC and Université de Montréal for postgraduate scholarships.

Éric Lévesque, Simon T. Laporte, and André B. Charette, Department of Chemistry, University of Montreal, P.O. Box 6128, Stn Downtown, Montreal, Quebec, H3C 3J7 (Canada). E-mail: andre.charette@umontreal.

Supporting information for this article is available on the WWW under (link)

Keywords: Continuous flow • Cyclopropanation • Diazo compounds • Hydrazones • Ring expansion

5.Conclusion et travaux futurs

En résumé, une série d'hétérocycles fluorescents à déplacement de Stokes élevé et à émission ajustable a été synthétisée et étudiée. Ensuite, une version catalytique de la réaction de Simmons-Smith a été optimisée pour cyclopropaner efficacement des styrènes, des éthers allyliques et des alcools allyliques de manière diastéréosélective. Enfin, un système en flux continu a été développé pour accéder sécuritairement aux solutions purifiées d'aryldiazométhane nécessaires à la réaction de Simmons-Smith catalytique ainsi qu'à bien d'autres procédés.

5.1.Fluorophores benzo[*a*]imidazo[2,1,5-*c*,*d*]indolizine : exploration des propriétés et expansion des applications

Pour le projet des fluorophores benzo[*a*]imidazo[2,1,5-*c*,*d*]indolizine, la suite logique serait d'explorer leurs propriétés plus en profondeur, particulièrement comment leur interaction avec d'autres espèces chimiques affectent la fluorescence. En effet, l'intérêt principal d'un grand nombre de fluorophores est la possibilité d'observer une modification de la fluorescence (changement marqué de l'intensité émise ou déplacement du maximum d'émission) en présence de certaines molécules,[138] métaux[139] ou environnements biochimiques.[140]

Le degré d'interaction entre un fluorophore et des désactivateurs (*quenchers*)[141] ou des accepteurs de FRET[142] (transfert d'énergie par résonance de type Förster) dépendent de la distance intermoléculaire. L'observation du changement de fluorescence permet d'obtenir une précision de l'ordre du nanomètre sur la position spatiale moyenne des fluorophores par rapport à ces molécules. Les désactivateurs absorbent l'énergie du fluorophore excité et la dissipent en tant que chaleur, résultant en une baisse d'intensité d'émission quand les molécules sont rapprochées. Les accepteurs de FRET absorbent l'énergie du fluorophore excité, se retrouvent eux-mêmes dans un état excité puis émettent de la lumière à une longueur d'onde maximale différente. On observe alors l'apparition d'une nouvelle bande d'émission quand les molécules sont rapprochées. Une manière simple de tester si les benzo[*a*]imidazo[2,1,5-*c*,*d*]indolizines sont susceptibles à ce genre d'interaction serait de les lier de manière covalente à des désactivateurs ou des accepteurs de FRET absorbant les longueurs d'ondes appropriées et de mesurer leur effet sur les spectres d'émission.

Certains fluorophores sont aussi utilisés pour la détection d'ions métalliques en solution. La coordination à ces métaux, en altérant les propriétés électroniques du système, affecte les propriétés émissives, généralement par déplacement marqué des maxima d'émission. L'analogue fluorescent de bipyridyl **2.8s** (page - 45 -) semble un bon candidat pour l'observation de ce phénomène.

Dans le contexte des études de biologie cellulaire, les fluorophores ayant une affinité intrinsèque pour certaines biomolécules ou pour certaines structures (membranes, microtubules, etc.) sont de puissants outils. Vu leur structure planaire et hydrophobe, les benzo[*a*]imidazo[2,1,5-*c*,*d*]indolizines ont le potentiel d'agir comme intercalants à ADN.[140] Cette interaction pourrait même affecter les propriétés émissives, permettant de différentier le fluorophore libre du fluorophore intercalé. La distribution d'un tel fluorophore hydrophobe au sein d'une cellule entière pourrait aussi révéler des affinités intéressantes pour certaines membranes ou certains organelles.

Figure 72. Exemples de fluorophores permettant l'étiquetage covalent de biomolécules

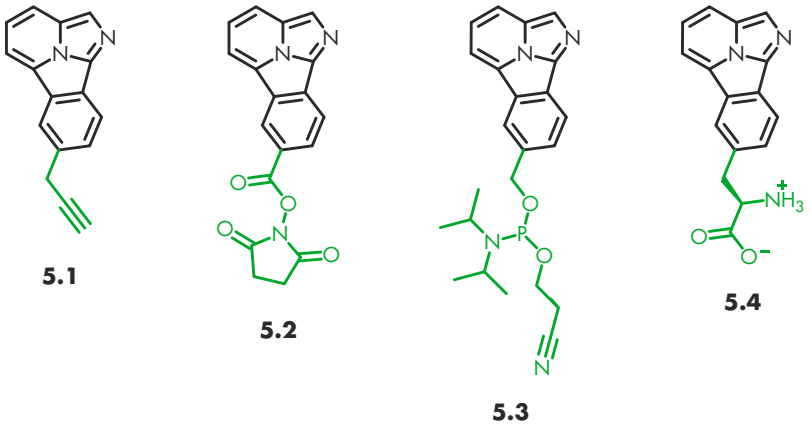

Pour faciliter l'usage des benzo[*a*]imidazo[2,1,5-*c*,*d*]indolizines en tant qu'étiquettes fluorescentes, il serait intéressant d'effectuer la synthèse d'autres exemples portant des groupements de bioconjugaison tels que l'alcyne **5.1** (cycloaddition de Huisgen « click »),[143] l'ester succinimidique **5.2** (addition-élimination en milieu aqueux)[144] la phosphoramidite **5.3** (monomère d'ADN synthétique)[145] et l'acide aminé **5.4** (monomère de protéines).[146]

Figure 73. Structure hypothétique pour un colorant à DSSC. Des espaceurs de type 1,4-phényl ou 2,5,thiophène peuvent être insérés à plusieurs endroits sur la structure.

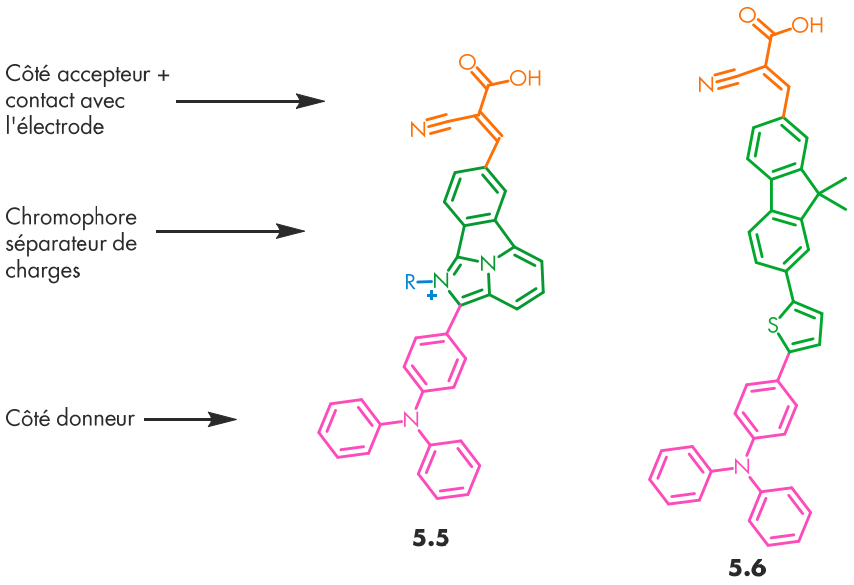

5.5 **5.6**

Enfin, les composés *imidazoindolizinium* (**2.9**) pourraient avoir une application en DSSC[147] (*Dye Sensitized Solar Cells*, ou cellules à pigment photosensible). En effet, les chromophores utilisés dans ces cellules doivent être en mesure de séparer les électrons des « trous » (transfert de charge) lorsque qu'ils absorbent un photon. Avec ses orbitales moléculaires frontières séparées, le noyau *imidazoindolizinium* devrait être en mesure d'effectuer cette séparation, qui sera accentuée en attachant un groupement électroattracteur et un groupement électrodonneur de part et d'autre de la molécule. La structure **5.5** ci-dessus est proposée, par analogie avec le composé **5.6** précédemment rapporté.[148] La fonction cyanoacrylate sert à faciliter l'interaction entre le chromophore et une électrode en oxyde de titane.

5.2. Réaction de Simmons Smith catalysée par un halogénure de zinc : Version énantiosélective catalytique en ligand chiral

Figure 74. Cyclopropanation énantiosélective catalytique en zinc et en ligand chiral

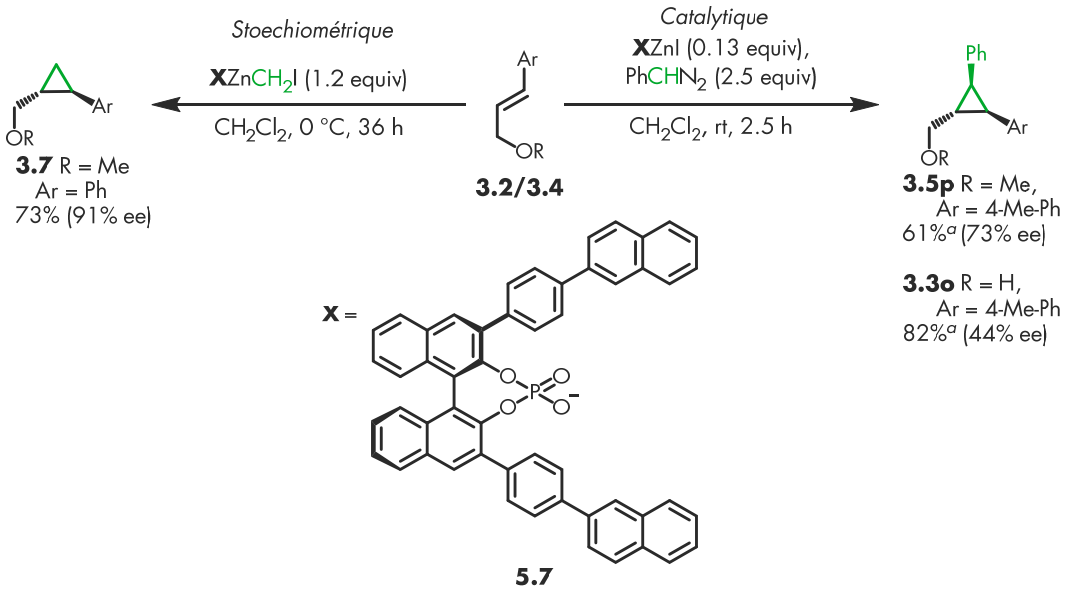

[a]Produits isolés. [b]Déterminé par analyse SFC sur une phase stationnaire chirale.

Un avantage évident à effectuer une cyclopropanation avec une quantité catalytique de métal est que théoriquement une quantité catalytique de ligand chiral est suffisante pour que l'état de transition ait lieu dans un environnement chiral. Une cyclopropanation énantiosélective impliquant une quantité stœchiométrique d'un anion phosphate chiral a déjà été développée par M.-C. Lacasse, Ph. D. en 2005.[62] Le même ligand, dérivé du BINOL, a été incorporé dans un sel iodozincique et exposé à du phényldiazométhane dans un milieu contenant un alcool ou un éther allylique. Les meilleurs résultats obtenus sont présentés dans la **Figure 74**. Avec l'accès aux aryldiazométhanes garanti par la méthode de flux continu, différents substrats pourraient être explorés pour mieux comprendre l'origine de l'énantioinduction. Cette dernière pourrait ensuite être améliorée par un design rationnel du ligand.

5.3.Plateforme générale pour la synthèse et la purification de composés diazo en flux continu

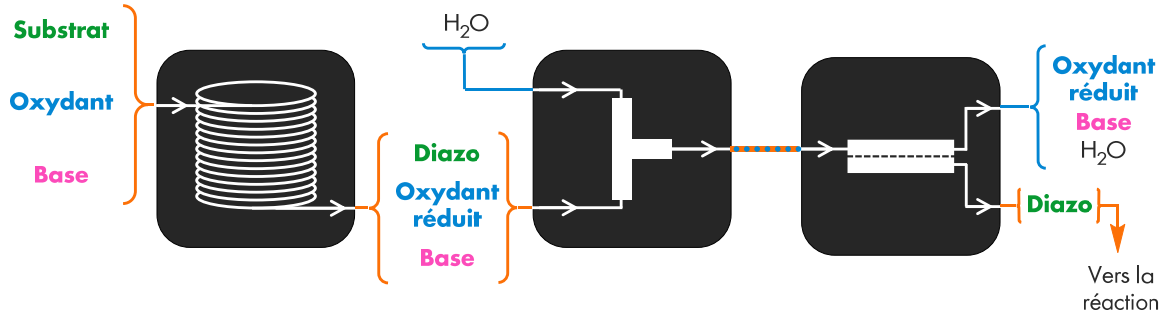

Finalement, la méthode de synthèse d'aryldiazométhanes en flux continu a une application évidente pour les réactions utilisant ces intermédiaires. Pendant longtemps l'exploration de cette chimie a été négligée à cause de la réticence à préparer, manipuler et entreposer les réactifs diazo riches en électrons. La procédure développée ci-haut ouvre la porte à la découverte de nouvelles réactions utilisant l'énergie emmagasinée dans un composé diazo de manière sécuritaire. La pureté des solutions produites devrait être compatible avec la plupart des réactifs, catalyseurs et intermédiaires réactionnels activés. Les aryldiazométhanes ont une réactivité et une nucléophilie intermédiaire entre celles du diazoacétate d'éthyle (EDA) et du diazométhane.[126] Les systèmes réactionnels utilisant l'un ou l'autre de ces diazos communs ont des chances d'être aussi applicables aux aryldiazométhanes.

De plus, l'approche générale utilisée pour la synthèse thermique et la purification par lavage aqueux pourrait être appliquée à la synthèse d'autres types de composés diazo et de réactifs à risque. La plupart des réactions menant à la formation de composés diazo ont le potentiel d'être adaptées aux contraintes du flux continu.

Annexe 1 : Informations supplémentaires associées à l'article « General C–H Arylation Strategy for the Synthesis of Tunable Visible Light Emitting High Stokes Shift Benzo[*a*]imidazo[2,1,5-*c*,*d*]indolizines Fluorophores »

A1.1.General considerations

Unless otherwise stated, all glassware was stored in the oven and/or was flame-dried prior to use. All reactions were set up under an argon atmosphere[149] while adding reagents and were run with the exclusion of moisture. All reaction flasks were kept closed with a septum during the reaction time. Anhydrous solvents were obtained either by filtration through alumina or molecular sieves on a GlassContour system (Irvine, CA) (THF, CH_2Cl_2, DMF, CH_3CN, toluene) or by distillation over CaH_2 (MeOH), BaO (DMA) or Na (1,4-Dioxane). Anhydrous EtOH and AcOH were used as is from commercial bottles. Analytical thin-layer chromatography (TLC) was performed on precoated, glass-backed silica gel (Merck 60 F254). Visualization of the developed chromatogram was performed by UV absorbance (254 nm), UV fluorescence (368 nm), aqueous potassium permanganate ($KMnO_4$) or cerium ammonium molybdate (CAM). Flash column chromatography was performed on a Teledyne Isco Combiflash® Companion automatic purification system. Prepacked normal phase silica gel columns (12 g, 24 g, 40 g, 80 g and 120 g) from Teledyne Isco (RediSep® Rf High Performance Gold) or from Grace (Reveleris®) were used for separation of products. Melting points were obtained on a Buchi melting point apparatus and are uncorrected. Nuclear magnetic resonance spectra (^{1}HNMR, ^{13}CNMR, ^{19}FNMR) were recorded on three Avance AV300 MHz AV400 MHz and AV500 MHz spectrometers. Chemical shifts for ^{1}H NMR spectra are recorded in parts per million from tetramethylsilane using the central peak of chloroform ($CHCl_3$) (δ = 7.26 ppm), MeOH (δ = 3.31 ppm) or HDO (δ = 4.79 ppm) as the internal standard. Chemical shifts for ^{13}C NMR spectra are recorded in parts per million from tetramethylsilane using the central peak of $CDCl_3$ (δ = 77.16 ppm) or MeOH (δ = 49.15 ppm), as the internal standard. All ^{13}C NMR spectra were obtained with complete proton decoupling. Chemical shifts for ^{19}F NMR spectra are recorded in parts per million from trichlorofluoromethane using the central peak of

trifluorotoluene (δ = -63.72 ppm) as the internal standard. Data are reported as follows: chemical shift, multiplicity (s = singlet, d = doublet, t = triplet, q = quartet, qn = quintet, sx = sextet, h = heptet, m = multiplet and br = broad), coupling constant in Hz and integration. Infrared spectra were taken on a Bruker Vertex Series FTIR (neat) and are reported in reciprocal centimeters (cm^{-1}). High resolution mass spectra were performed by the Centre régional de spectroscopie de masse de l'Université de Montréal.

A1.2.Reagents

Unless otherwise stated, commercial reagents were used without purification. Triethylamine (Et_3N) was distilled over calcium hydride and kept under argon before use. Trifluoromethanesulfonic anhydride (Tf_2O) was made by heating TfOH on P_4O_{10}, distilled and kept under argon in a Schlenk flask before use. 6-bromopyridine-2-carbaldehyde[150], 4-(2-hydroxy-ethoxy)-benzoic acid[151], benzoic-2-*d* acid[152] and $[Pd(phen)_2][PF_6]_2$[153] were synthesized according to previously reported procedures.

A1.3.Experimental procedures and characterization data

A1.3.1.Synthesis of starting material

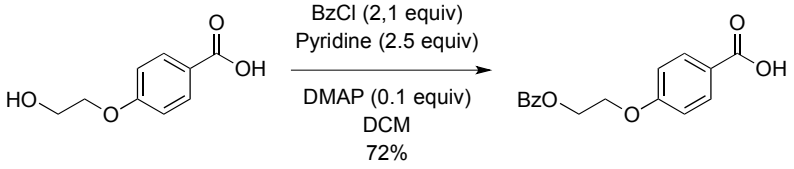

4-[2-(Benzoyloxy)ethoxy]benzoic acid: To a flame-dried 50 mL round bottom flask equipped with a magnetic stirbar and a rubber septum were dissolved 4-(2-hydroxyethoxy)benzoic acid (0.75 g, 4.1 mmol, 1.0 equiv), pyridine (0.83 mL, 10 mmol, 2.5 equiv) and 4-dimethylaminopyridine (50 mg, 0.41 mmol, 0.10 equiv) in CH_2Cl_2 (12 mL, 0.34 M). Benzoyl chloride (1.0 mL, 8.6 mmol, 2.1 equiv) was added dropwise and mixture was stirred at room temperature for 20 h. 1.0 M HCl (20 mL) was added and mixture was stirred for 1 h. Phases were separated and the aqueous layer was extracted with CH_2Cl_2 (3x). The combined organic layers were washed with 2.0 M HCl and dried over anhydrous $MgSO_4$, filtered over a sintered funnel and evaporated to dryness. The residue was purified by flash chromatography using a gradient of 0% to 15% MeOH in 0.5 % AcOH/CH_2Cl_2.

The fractions containing the pure product were combined and evaporated to dryness. 4-[2-(benzoyloxy)ethoxy]benzoic acid was isolated as a white solid (0.85 g, 72% yield). **mp**: 170-173 °C; **^{1}H NMR** ($CDCl_3$, 500 MHz): δ 8.04-8.01 (m, 2H), 8.00-7.96 (m, 2H), 7.63-7.58 (m, 1H), 7.49-7.45 (m, 2H), 7.07-7.03 (m, 2H), 4.68 (t, J = 4.5 Hz, 2H), 4.43 (t, J = 4.5 Hz, 2H); **^{13}C NMR** ($CDCl_3$, 125 MHz): δ 169.9, 167.9, 164.0, 134.4, 132.9, 131.2, 130.6, 129.6, 124.8, 115.4, 67.4, 64.6; **FTIR** (cm^{-1}) (neat): 2931, 1716, 1685, 1603, 1425, 1278, 1248, 1170, 708; **HRMS** (ESI, Pos): calcd for $C_{16}H_{15}O_5$ $[M+H]^+$: 287.0914 m/z, found 287.0914 m/z.

A1.3.2.Literature synthesis of (6-bromopyridin-2-yl)methanamine[16,154]

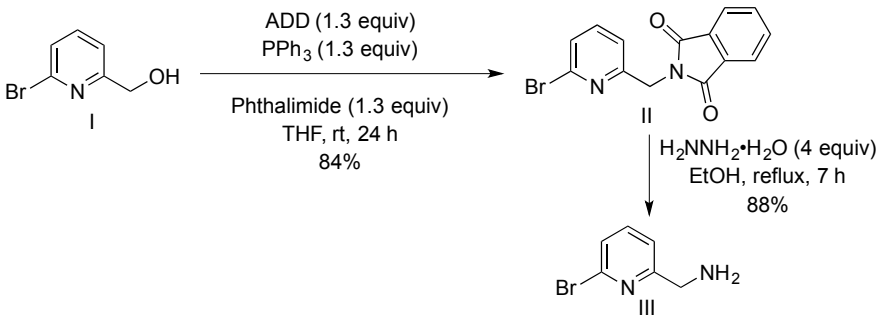

2-[(6-Bromopyridin-2-yl)methyl]-2,3-dihydro-1*H*-isoindole-1,3-dione (II): To a flame-dried 1000 mL round bottom flask equipped with a magnetic stirbar and a rubber septum was added 2-bromo-6-hydroxymethylpyridine (8.7 g, 46 mmol, 1.0 equiv). The alcohol was diluted with anhydrous THF (0.46 L, 0.10 M) and then 1,1'-(azodicarbonyl)dipiperidine (15 g, 60 mmol, 1.3 equiv) was added. The orange solution was then stirred at room temperature for 2 min. Then, triphenylphosphine (16 g, 60 mmol, 1.3 equiv) and phthalimide (8.9 g, 60 mmol, 1.3 equiv) were added successively. The reaction was then stirred for 24 h at room temperature (the solution was clear and orange). The reaction was then cooled to 0 °C and a solid precipitate was formed. The cooled suspension was then filtered on a Buchner filter and the cake was washed thoroughly with cold THF. The filtrate was then evaporated to dryness. The residue was then quenched by addition of a saturated aqueous solution of $NaHCO_3$ (30 mL) and diluted with EtOAc (100 mL). The biphasic layers were transferred to a 250 mL extraction funnel and the aqueous layer was then extracted with EtOAc (3x). The organic layers were combined and dried over anhydrous Na_2SO_4, filtered over a sintered funnel and evaporated to dryness. The residue was then purified by flash chromatography using a gradient of 30% to 100% EtOAc in hexanes while using a drypack to inject

the crude mixture. The fractions containing the pure product were combined and evaporated to dryness. 2-[(6-Bromopyridin-2-yl)methyl]-2,3-dihydro-1H-isoindole-1,3-dione was obtained as a crystalline white solid (12.3 g, 84% yield). **mp**: 118-119 °C; **^{1}H NMR** ($CDCl_3$, 500 MHz): δ 7.92-7.91 (m, 2H), 7.78-7.76 (m, 2H), 7.50 (t, *J* = 7.5 Hz, 1H), 7.38 (d, *J* = 8.0 Hz, 1H), 7.18 (d, *J* = 7.5 Hz, 1H), 5.01 (s, 2H); **^{13}C NMR** ($CDCl_3$, 125 MHz): δ 167.9, 156.9, 141.9, 139.0, 134.2, 132.1, 127.0, 123.6, 119.9, 42.5; **FTIR** (cm^{-1}) (neat): 2972, 2922, 2865, 2843, 1700, 1585, 1557, 1470, 1438, 1422, 1388, 1346; **HRMS** (ESI, Pos): calcd for $C_{14}H_{10}N_2O_2Br$ $[M+H]^+$: 316.9926 *m/z*, found 316.9910 *m/z*.

(6-Bromopyridin-2-yl)methanamine (III): A suspension of 2-[(6-bromopyridin-2-yl)methyl]-2,3-dihydro-1*H*-isoindole-1,3-dione (12.3 g, 38.6 mmol, 1.0 equiv) in absolute ethanol (0.39 L, 0.10 M) was charged in a 1000 mL round bottom flask equipped with a magnetic stirbar and a condenser and heated to reflux until complete dissolution (around 15 min). To the homogeneous solution was added hydrazine monohydrate 65% (11.5 mL, 154 mmol, 4.0 equiv). Within a minute, the reaction mixture became yellow. The reaction mixture was heated at reflux for 7 h during which time the mixture solidified into a white thick suspension. An additional 50 mL of ethanol was added, and the mixture was kept stirring for an extra 2 h. The reaction was cooled down to 0 °C to precipitate the hydrazine/phthalimide adduct. The precipitate was filtered on a Buchner and washed with absolute ethanol. The filtrate was partially concentrated. Remaining solids in the suspension were again filtered off and washed with cold EtOH. The filtrate was concentrated to dryness. The product (**III**) was recuperated as an orange oil. (6.3 g, 87% yield). **^{1}H NMR** ($CDCl_3$, 500 MHz): δ 7.57-7.50 (m, 1H), 7.40-7.35 (m, 1H), 7.31-7.27 (m, 1H), 3.98 (br s, 2H), 1.73 (br s, 2H); **^{13}C NMR** ($CDCl_3$, 75 MHz): δ 163.8, 141.8, 138.9, 126.2, 120.0, 47.4; **FTIR** (cm^{-1}) (neat): 3367, 3297, 2921, 2865, 1582, 1554, 1434, 1407, 1161, 1117; **HRMS** (ESI, Pos): calcd for $C_6H_8N_2Br$ $[M+H]^+$: 186.9871 *m/z*, found: 186.9861 *m/z*.

A1.3.3. Revised synthesis of (6-bromopyridin-2-yl)methanamine

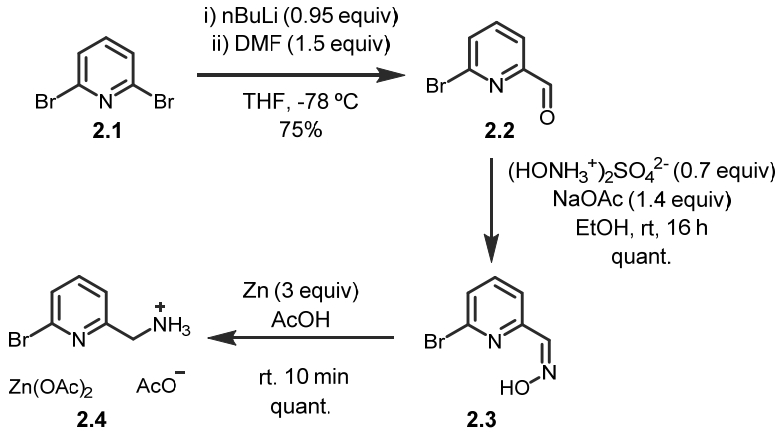

6-Bromopyridine-2-carbaldehyde (2.2): Following a literature procedure[2] the product was obtained as a beige solid (4.7 g, 80% yield). The crude mixture was purified by recrystallization from boiling hexanes (reflux to -20°C) instead of chromatography. **^{1}H NMR** ($CDCl_3$, 500 MHz): δ 10.01 (d, J = 0.5 Hz, 2H), 4.68 (dd, J = 7.0 Hz, J = 1.5 Hz, 2H), 7.78-7.71 (m, 2H).

6-Bromopyridine-2-carbaldehyde oxime (2.3): To a 10 mL round-bottom flask equipped with a magnetic stirbar and a rubber septum were added 6-bromopyridine-2-carbaldehyde (0.30 g, 1.6 mmol, 1.0 equiv), hydroxylammonium sulfate ($(NH_3OH)_2SO_4$) (0.19 g, 1.1 mmol, 0.7 equiv) and sodium acetate (0.20 g, 2.4 mmol, 1.5 equiv). EtOH (4.0 mL, 0.4 M) was added and heterogenous mixture was vigorously stirred at room temperature for 16h. $MgSO_4$ was added and mixture was filtered on cotton and concentrated under vacuum to yield a white solid. This was suspended in 2% $MeOH/CH_2Cl_2$ and filtered through a short silica plug. The filtrate was concentrated under vacuum to yield 6-bromopyridine-2-carbaldehyde oxime as a white solid (325mg, quantitative yield). **mp**: 164-166 °C; **^{1}H NMR** (DMSO, 500 MHz): δ 8.03 (s, 1H), 7.83 (dd, J = 7.5 Hz, J = 1.0 Hz, 1H), 7.69 (dt, J = 8.0 Hz, J = 0.5 Hz, 1H), 7.55 (dd, J = 8.0 Hz, J = 1.0 Hz, 1H); **^{13}C NMR** ($CDCl_3$, 125 MHz): δ 155.1, 148.8, 142.5, 140.6, 129.3, 120.3; **FTIR** (cm^{-1}) (neat): 3200, 3003, 1545, 1157, 1119, 976, 943, 786, 704; **HRMS** (ESI, Pos): calcd for $C_6H_6BrN_2O$ $[M+H]^+$: 200.9658 m/z, found 200.9665 m/z.

6-Bromopyridin-2-yl)methanammonium acetate (2.4): To a 5 mL round-bottom flask equipped with a magnetic stirbar and a rubber septum were added 6-bromopyridine-2-carbaldehyde oxime (50 mg, 0.25 mmol, 1.0 equiv) and AcOH (2.0 mL, 0.13 M). Zinc (49 mg, 0.75 mmol, 3.0 equiv) was poured in the flask in one portion. Mixture was stirred at room temperature for 10 min

and filtered over Celite. The filtrate was concentrated under vacuum to yield and off-white solid (140 mg) containing 6-bromopyridin-2-yl)methanammonium acetate (58 mg, 0.24 mmol, 95% yield) and zinc acetate (82 mg, 0.45 mmol). **mp**: 200-210 °C; **^{1}H NMR** ($CDCl_3$, 500 MHz): δ 7.81 (t, *J* = 8.0 Hz, 1H), 7.66 (dd, *J* = 8.0 Hz, *J* = 0.5 Hz, 1H), 7.46 (dd, *J* = 7.5 Hz, *J* = 1.0 Hz, 1H), 4.23 (s, 2H), 1.98 (s, 3H); **^{13}C NMR** ($CDCl_3$, 125 MHz): δ 180.2, 159.3, 142.1, 141.7, 129.3, 122.7, 44.2, 22.3; **FTIR** (cm^{-1}) (neat): 3264, 2997, 1544, 1388, 1333, 1169, 1019, 675, 613; **HRMS** (ESI, Pos): calcd for $C_6H_8BrN_2$ $[M+H]^+$: 186.9870 *m/z*, found 186.9871 *m/z*.

A1.3.4.General procedures for the synthesis of amides

Procedure A:

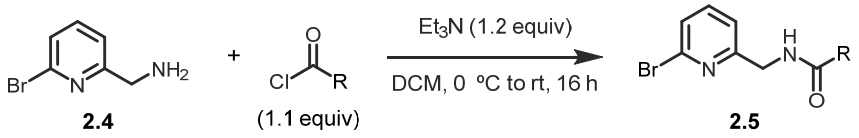

To a round bottom flask equipped with a magnetic stirrer and a rubber septum was added the (6-bromopyridin-2-yl)methanamine (1.0 equiv) as previously synthesized. The amine was diluted with CH_2Cl_2 (0.2 M) and cooled to 0 °C using an ice/water cooling bath. Triethylamine (1.2 equiv) was added via syringe followed by the acyl chloride (1.1 equiv). The reaction mixture was warmed to room temperature and stirred for 16 h. The reaction was quenched by addition of a saturated aqueous solution of Na_2CO_3, phases were separated and the aqueous layer was extracted with CH_2Cl_2 (3x). The combined organic layers were dried over anhydrous Na_2SO_4, filtered and evaporated to dryness.

Procedure B:

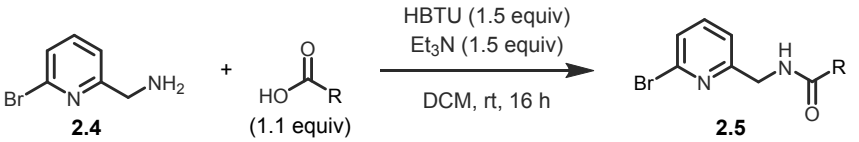

To a round bottom flask equipped with a magnetic stirrer and a rubber septum was added the (6-bromopyridin-2-yl)methanamine (1.0 equiv) as previously synthesized. The amine was diluted with CH_2Cl_2 (0.2 M). Triethylamine (1.5 equiv) was added via syringe followed by the carboxylic acid (1.1 equiv) and *N*,*N*,*N*',*N*'-tetramethyl-O-(1H-benzotriazol-1-yl)uronium hexafluorophosphate

(HBTU) (1.5 equiv). The reaction was quenched by addition of a saturated aqueous solution of Na_2CO_3, phases were separated and the aqueous layer was extracted with CH_2Cl_2 (3x). The combined organic layers were dried over anhydrous Na_2SO_4, filtered and evaporated to dryness.

Procedure C:

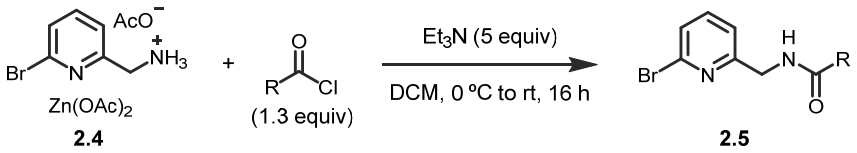

To a round bottom flask equipped with a magnetic stirrer and rubber septum was added the (6-bromopyridin-2-yl)methanammonium acetate salt (1.0 equiv). The amine was diluted with CH_2Cl_2 (0.2 M) and cooled to 0 °C using an ice/water cooling bath. Triethylamine (5.0 equiv) was added via syringe followed by the acyl chloride (1.3 equiv). The reaction mixture was warmed to room temperature and stirred for 16 h. The reaction was quenched by addition of a saturated aqueous solution of Na_2CO_3, phases were separated and the aqueous layer was extracted with CH_2Cl_2 (3x). The combined organic layers were dried over anhydrous $MgSO_4$, filtered and evaporated to dryness.

General procedure for acyl chloride synthesis:

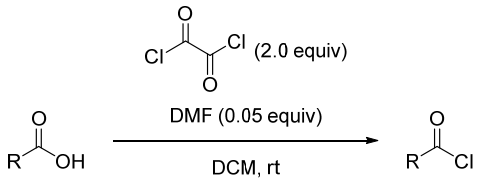

To a round-bottomed flask equipped with a magnetic stirrer and rubber septum was added the carboxylic acid (1.0 equiv), DMF (0.05 equiv) and CH_2Cl_2 (0.26 M). Oxalyl chloride (2.0 equiv) was added dropwise (gas evolution). Mixture was stirred for 2h, evaporated to dryness and used as is.

A1.3.5.Characterization data of amides

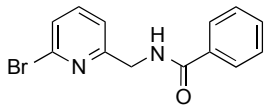

2.5a

***N*-((6-Bromopyridin-2-yl)methyl)benzamide (2.5a)**:[154a] Following **procedure A**. The crude amide was dissolved in a minimal amount of hot EtOAc and excess hexanes were added. The resulting precipitate was recovered by filtration and washed with hexanes, resulting in a white solid (0.81 g, 93% yield). **mp**: 130-131 °C, lit:[6a] 130-131 °C; **^{1}H NMR** ($CDCl_3$, 300 MHz): δ 7.87-7.81 (m, 2H), 7.55-7.29 (m, 7H), 4.71 (d, *J* = 5.5 Hz, 2H); **^{13}C NMR** ($CDCl_3$, 75 MHz): δ 167.5, 158.4, 141.6, 139.2, 134.0, 131.7, 128.6, 127.1, 126.8, 121.1, 44.5; **FTIR** (cm^{-1}) (neat): 3283, 2935, 1637, 1577, 1537, 1400, 1344, 1307, 1269; **HRMS** (ESI, Pos): calcd for $C_{13}H_{12}BrN_2O$ $[M+H]^+$: 291.0128 *m/z*, found: 291.0136 *m/z*.

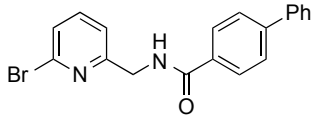

2.5b

***N*-((6-Bromopyridin-2-yl)methyl)-[1,1'-biphenyl]-4-carboxamide (2.5b):** Following **procedure A**. The crude amide was purified by flash chromatography over silica gel using a gradient of 30% to 100% EtOAc in hexanes. Fractions containing **2.5b** were concentrated to dryness, resulting in a white solid (0.78 g, 71% yield). **mp**: 168-169 °C; **^{1}H NMR** ($CDCl_3$, 500 MHz): δ 7.93-7.91 (m, 2H), 7.69-7.67 (m, 2H), 7.63-7.61 (m, 2H), 7.55 (t, *J* = 8.0 Hz, 1H), 7.48-7.45 (m, 2H), 7.43.7.34 (m, 2H), 7.35 (d, *J* = 7.5 Hz, 1H), 7.29 (br s, 1H), 4.76 (d, *J* = 5.0 Hz, 2H); **^{13}C NMR** ($CDCl_3$, 125 MHz): δ 136.2, 158.3, 144.5, 141.7, 140.0, 139.2, 132.7, 128.9, 128.0, 127.6, 127.3, 127.2, 126.9, 121.2, 44.5; **FTIR** (cm^{-1}) (neat): 3259, 1637, 1541, 781, 736, 690, 675; **HRMS** (ESI, Pos): calcd for $C_{19}H_{15}BrN_2O$ $[M+H]^+$: 367.0440 *m/z*, found: 367.0444 *m/z*.

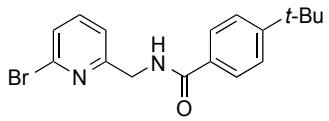

2.5c

***N*-((6-Bromopyridin-2-yl)methyl)-4-(*tert*-butyl)benzamide (2.5c)**: Following **procedure A**. The crude amide was purified by flash chromatography over silica gel using a gradient of 30% to 70% EtOAc in hexanes. Fractions containing **2.5c** were concentrated to dryness, resulting in a white solid (1.0 g, 96% yield). **mp**: 162-164 °C; **^{1}H NMR** ($CDCl_3$, 500 MHz): δ 7.79-7.77 (m, 2H), 7.54 (t, *J* = 8.0 Hz, 1H), 7.48-7.47 (m, 2H), 7.41 (d, *J* = 8.0 Hz, 1H), 7.33 (d, *J* = 7.5 Hz, 1H), 7.15 (br s, 1H), 4.73 (d, *J* = 5.5 Hz, 2H), 1.34 (s, 9H); **^{13}C NMR** ($CDCl_3$, 125 MHz): δ 167.4, 158.5, 155.2, 141.6, 139.2, 131.2, 126.9, 126.8, 125.6, 121.2, 44.5, 35.0, 31.2; **FTIR** (cm^{-1}) (neat): 3357, 3313, 2959, 2928, 2902, 1634, 1555, 1543, 1309, 982, 780, 658; **HRMS** (ESI, Pos): calcd for $C_{17}H_{19}BrN_2O$ $[M+H]^+$: 347.0754 *m/z*, found: 347.0755 *m/z*.

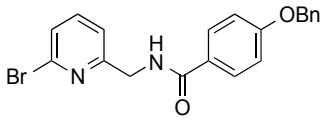

2.5d

4-(Benzyloxy)-N-((6-bromopyridin-2-yl)methyl)benzamide (2.5d): Following **procedure B**. The crude amide was purified by flash chromatography over silica gel using a gradient of 0% to 80% EtOAc in hexanes. Fractions containing **2.5d** were concentrated to dryness, resulting in a white solid (0.90 g, 76% yield). **mp**: 133-135 °C; **^{1}H NMR** ($CDCl_3$, 500 MHz): δ 7.82-7.79 (m, 2H), 7.53 (t, *J* = 7.5 Hz, 1H), 7.45-7.37 (m, 5H), 7.36-7.31 (m, 2H), 7.11 (br t, *J* = 4.5 Hz, 1H), 7.03-7.00 (m, 2H), 5.12 (s, 2H), 4.71 (d, *J* = 5.0 Hz, 1H); **^{13}C NMR** ($CDCl_3$, 125 MHz): δ 166.9 161.5, 158.5, 141.6, 139.2, 136.4, 129.0, 128.7, 128.2, 127.5, 126.8, 126.6, 121.2, 114.7, 70.1, 44.5; **FTIR** (cm^{-1}) (neat): 3362, 1637, 1604, 1537, 1501, 1248, 1113, 767, 734; **HRMS** (ESI, Pos): calcd for $C_{20}H_{17}BrN_2O_2$ $[M+H]^+$: 397.0546 *m/z*, found: 397.0541 *m/z*.

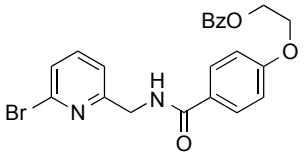

2.5e

2-(4-(((6-Bromopyridin-2-yl)methyl)carbamoyl)phenoxy)ethyl benzoate (2.5e): Following **procedure C**. The crude amide was dissolved in a minimal amount of hot EtOAc and excess hexanes were added. The resulting precipitate was recovered by filtration and washed with hexanes. The residue was dissolved in 25% EtOAc/CH_2Cl_2, washed with saturated $NaHCO_3$ (2X), dried

with MgSO4 and filtrated on a short silica gel column (washing with 25% EtOAc/CH_2Cl_2). Filtrate was concentrated to dryness, resulting in a beige solid (0.66 g, 90% yield). **mp**: 121-123 °C; **^{1}H NMR** ($CDCl_3$, 500 MHz): δ 8.04 (dd, *J* = 1.0 Hz, *J* = 8.5 Hz, 1H), 7.81 (d, *J* = 8.5 Hz, 1H), 7.58-7.50 (m, 2H), 7.45-7.37 (m, 3H), 7.32 (d, *J* = 7.5 Hz, 1H), 7.24 (br t, *J* = 5.0 Hz, 1H), 6.97 (d, *J* = 8.5 Hz, 2H), 4.71-4.66 (m, 4H), 4.35 (t, *J* = 5.0 Hz, 2H); **^{13}C NMR** ($CDCl_3$, 125 MHz): δ 167.0, 166.6, 161.4, 158.7, 141.6, 139.3, 133.3, 129.8 (2), 129.1, 128.5, 126.9 (2), 121.3, 114.6, 66.2, 63.2, 44.6; **FTIR** (cm^{-1}) (neat): 3313, 2968, 1708, 1278, 1248, 1119, 1069, 713, 665; **HRMS** (ESI, Pos): calcd for $C_{22}H_{20}BrN_2O_4$ $[M+H]^+$: 455.0608 *m/z*, found: 455.0601*m/z*.

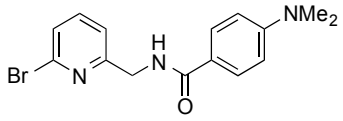

2.5f

***N*-((6-bromopyridin-2-yl)methyl)-4-(dimethylamino)benzamide (2.5f)**: Following **procedure A**. The crude amide was purified by flash chromatography over silica gel using a gradient of 30% to 70% EtOAc in hexanes. Fractions containing **2.5f** were concentrated to dryness, resulting in a white solid (0.56 g, 56% yield). **mp**: 155-157 °C; **^{1}H NMR** ($CDCl_3$, 400 MHz): δ 7.74 (d, *J* = 8.8 Hz, 2H), 7.52 (t, *J* = 7.5 Hz, 1H), 7.38 (d, *J* = 7.5 Hz, 1H), 7.32 (d, *J* = 7.5 Hz, 1H), 7.00 (br t, *J* = 5.5 Hz, 1H), 6.68 (d, *J* = 8.8 Hz, 2H), 4.70 (d, *J* = 6.0 Hz, 2H), 3.02 (s, 6H); **^{13}C NMR** ($CDCl_3$, 125 MHz): δ 167.4, 159.1, 152.6, 141.5, 139.1, 128.6, 126.6, 121.2, 120.8, 111.1, 44.5, 40.1; **FTIR** (cm^{-1}) (neat): 3276, 2921, 1626, 1604, 1514, 1302, 1115, 769, 665; **HRMS** (ESI, Pos): calcd for $C_{15}H_{17}BrN_3O$ $[M+H]^+$: 334.0550 *m/z*, found: 334.0544 *m/z*.

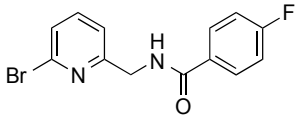

2.5g

***N*-((6-Bromopyridin-2-yl)methyl)-4-fluorobenzamide (2.5g)**: Following **procedure A**. The crude amide was purified by flash chromatography over silica gel using a gradient of 0% to 50% EtOAc in hexanes. Fractions containing **2.5g** were concentrated to dryness, resulting in a white solid (0.87 g, 94% yield). **mp**: 111-113 °C; **^{1}H NMR** ($CDCl_3$, 500 MHz): δ 7.87-7.83 (m, 2H), 7.54 (t, *J* = 7.5 Hz, 1H), 7.41 (d, *J* = 8.0 Hz, 1H), 7.32 (d, *J* = 7.5 Hz, 1H), 7.25 (br s, 1H), 7.15-7.10 (m,

2H), 4.71 (d, J = 5.5 Hz, 2H); **^{13}C NMR** ($CDCl_3$, 125 MHz): δ 166.4, 164.9 (d, $J_{C\text{-}F}$ = 250 Hz), 158.0, 141.7, 139.2, 130.3. 130.3, 129.4 (d, $J_{C\text{-}F}$ = 8.9 Hz), 126.9, 121.2, 115.7 (d, $J_{C\text{-}F}$ = 21.8 Hz); **^{19}F NMR** ($CDCl_3$, 282 MHz): δ -108.0 (s, F); **FTIR** (cm^{-1}) (neat): 3355, 1638, 1504, 847, 764, 599; **HRMS** (ESI, Pos): calcd for $C_{13}H_{10}BrFN_2O$ $[M+H]^+$: 309.0033 *m/z*, found: 309.0033 *m/z*.

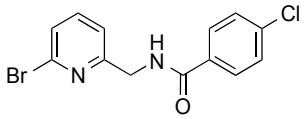

2.5h

***N*-((6-Bromopyridin-2-yl)methyl)-4-chlorobenzamide (2.5h)**: Following **procedure C**. The crude amide was dissolved in a minimal amount of hot EtOAc and excess hexanes were added. The resulting precipitate was recovered by filtration and washed with hexanes, resulting in a yellowish solid (30 mg, 92% yield). **mp**: 105-107 °C; **^{1}H NMR** ($CDCl_3$, 300 MHz): δ 7.79 (d, J = 8.7 Hz, 2H), 7.57 (t, J = 7.8 Hz, 1H), 7.43 (d, J = 8.7 Hz, 3H), 7.34 (d, J = 7.5 Hz, 1H), 4.72 (d, J = 5.4 Hz, 2H); **^{13}C NMR** ($CDCl_3$, 125 MHz): δ 166.5, 158.2, 141.7, 139.4, 138.0, 132.5, 129.0, 128.7, 127.0 121.3, 44.6; **FTIR** (cm^{-1}) (neat): 3328, 2923, 1636, 1542, 1310, 1093, 847, 774, 658; **HRMS** (ESI, Pos): calcd for $C_{13}H_{10}BrClN_2NaO$ $[M+Na]^+$: 346.95572 *m/z*, found: 346.95592 *m/z*.

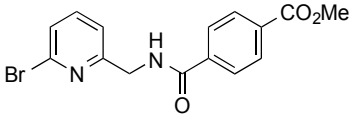

2.5i

Methyl 4-(((6-bromopyridin-2-yl)methyl)carbamoyl)benzoate (2.5i): Following **procedure A**. The crude amide was purified by flash chromatography over silica gel using a gradient of 30% to 100% EtOAc in hexanes. Fractions containing **2.5i** were concentrated to dryness, resulting in a white solid (0.88 g, 84% yield). **mp**: 149-151 °C; **^{1}H NMR** ($CDCl_3$, 500 MHz): δ 8.04-8.02 (m, 2H), 7.84-7.82 (m, 2H), 7.48 (t, J = 7.5 Hz, 1H), 7.35 (dd, J = 0.5, 8.0 Hz, 1H), 7.25 (dd, J = 0.5, J = 7.5 Hz, 1H), 4.66 (d, J = 5.5 Hz, 2H), 3.87 (s, 3H); **^{13}C NMR** ($CDCl_3$, 125 MHz): δ 166.7, 166.4, 158.0, 141.8, 139.4, 138.1, 133.0, 130.0,127.3, 127.1, 121.3, 52.5, 44.7; **FTIR** (cm^{-1}) (neat): 3275, 3040, 2959, 2864, 2844, 1721, 1637, 1279, 716; **HRMS** (ESI, Pos): calcd for $C_{15}H_{13}BrN_2O_3$ $[M+H]^+$: 349.0198 *m/z*, found: 349.0198 *m/z*.

Compound **5i** was also synthesized via **procedure C** (0.21 g, 59% yield).

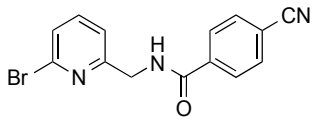

2.5j

***N*-((6-Bromopyridin-2-yl)methyl)-4-cyanobenzamide (2.5j)**: Following **procedure C**. The crude amide was dissolved in a minimal amount of hot EtOAc and excess hexanes were added. The resulting precipitate was recovered by filtration and washed with hexanes, resulting in a beige solid (0.90 mg, 71% yield). **mp**: 127-128 °C; **^{1}H NMR** ($CDCl_3$, 500 MHz): δ 7.89-7.87 (m, 2H), 7.70-7.68 (m, 2H), 7.50 (t, J = 7.5 Hz, 1H), 7.37-7.36 (m, 2H), 7.25 (dd, J = 0.5, J = 7.5 Hz, 1H), 4.66 (d, J = 5.0 Hz, 2H); **^{13}C NMR** ($CDCl_3$, 125 MHz): δ 165.7, 157.5, 141.8, 139.4, 138.1, 132.6, 127.9, 127.2, 121.3, 118.1, 115.4, 44.6; **FTIR** (cm^{-1}) (neat): 3304, 3066, 2973, 2939, 2933, 2864, 2844, 2825, 2230, 1643, 1554, 1306, 672; **HRMS** (ESI, Pos): calcd for $C_{14}H_{10}BrN_3O$ $[M+H]^+$: 316.0080 *m/z*, found: 316.0087 *m/z*.

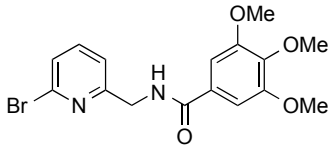

2.5k

***N*-((6-Bromopyridin-2-yl)methyl)-3,4,5-trimethoxybenzamide (2.5k)**: Following **procedure A**. The crude amide was dissolved in a minimal amount of hot EtOAc and excess hexanes were added. The resulting precipitate was recovered by filtration and washed with hexanes, resulting in a beige solid (1.0 g, 89% yield). **mp**: 115-117 °C; **^{1}H NMR** ($CDCl_3$, 400 MHz): δ 7.55 (t, J = 7.6 Hz, 1H), 7.41 (d, J = 8.0 Hz, 1H), 7.30-7.35 (m, 2H), 7.08 (s, 2H), 4.70 (d, J = 5.6 Hz, 2H), 3.90 (s, 6H), 3.88 (s, 3H); **^{13}C NMR** ($CDCl_3$, 125 MHz): δ 167.2, 158.4, 153.3, 141.6, 141.1, 139.5, 129.5, 127.0, 121.5, 104.5, 61.0, 56.4, 44.6; **FTIR** (cm^{-1}) (neat): 3303, 2937, 1580, 1496, 1410, 1325, 1230, 1119, 1000; **HRMS** (ESI, Pos): calcd for $C_{16}H_{18}BrN_2O_4$ $[M+H]^+$: 381.0445 *m/z*, found: 381.0451 *m/z*.

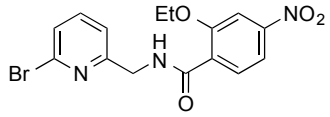

2.5l

***N*-((6-Bromopyridin-2-yl)methyl)-2-ethoxy-4-nitrobenzamide (2.5l)**: Following **procedure B**. The crude amide was purified by flash chromatography over silica gel using a gradient of 0% to 20% EtOAc in CH_2Cl_2. Fractions containing **2.5l** were concentrated to dryness, resulting in a white solid (0.75 g, 66% yield). **mp**: 136-138 °C; **^{1}H NMR** ($CDCl_3$, 400 MHz): δ 8.93 (s, 2H), 8.40 (d, J = 8.4 Hz, 1H), 7.91 (dd, J = 2.0, J = 8.4 Hz, 1H), 7.85 (s, 1H), 7.56 (t, J = 7.6 Hz, 1H), 7.43 (d, J = 8.0 Hz, 1H), 7.31 (d, J = 7.6 Hz, 1H), 4.80 (d, J = 4.8 Hz, 1H), 4.39 (q, J = 6.8 Hz, 1H), 1.65 (t, J = 6.8 Hz, 1H); **^{13}C NMR** ($CDCl_3$, 125 MHz): δ 163.5, 158.0, 157.3, 150.4, 141.9, 139.3, 133.5, 127.0, 126.8, 121.1, 115.8, 107.6, 66.1, 45.0, 14.9; **FTIR** (cm^{-1}) (neat): 3347, 1653, 1522, 1433, 1229, 1024, 866, 789, 735; **HRMS** (ESI, Pos): calcd for $C_{15}H_{15}BrN_3O_4$ $[M+H]^+$: 380.0241 m/z, found: 380.02518m/z.

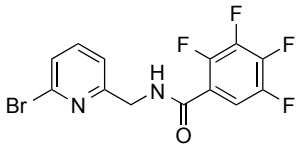

2.5m

***N*-((6-Bromopyridin-2-yl)methyl)-2,3,4,5-tetrafluorobenzamide (2.5m)**: Following **procedure A**. The crude amide was purified by flash chromatography over silica gel using a gradient of 50% to 80% EtOAc in hexanes. Fractions containing **2.5m** were concentrated to dryness, resulting in a white solid (0.91 mg, 84% yield). **mp**: 126-128 °C; **^{1}H NMR** ($CDCl_3$, 700 MHz): δ 7.82-7.76 (m, 2H), 7.59 (t, J = 10.5 Hz, 1H), 7.46 (dd, J = 0.7, 11.2 Hz, 1H), 7.33 (dd, J = 0.7, 10.5 Hz, 1H), 4.75 (d, J = 4.9 Hz, 2H); **^{13}C NMR** ($CDCl_3$, 175 MHz): δ 160.5, 157.1, 147.9 (d, $J_{C\text{-}F}$ = 7.0 Hz), 147.0 (d, $J_{C\text{-}F}$ = 9.3 Hz), 146.48 (d, $J_{C\text{-}F}$ = 9.8 Hz), 145.6 (d, $J_{C\text{-}F}$ = 9.5 Hz), 143.4 (ddd, $J_{C\text{-}F}$ = 3.5, 12.4, 16.5 Hz), 141.9 (ddd, $J_{C\text{-}F}$ = 3.5, 12.4, 16.5 Hz), 141.4 (ddd, $J_{C\text{-}F}$ = 3.5, 12.8, 18.9 Hz), 140.0 (ddd, $J_{C\text{-}F}$ = 3.2, 12.4, 18.4 Hz), 139.3, 127.1, 120.9, 117.2, 112.8 (d, $J_{C\text{-}F}$ = 2.8 Hz), 44.7; **^{19}F NMR** ($CDCl_3$, 282 MHz): δ -153.7 to -153.6 (m, F), -148.9 to -148.8 (m, F), -138.8 to -138.7 (m, F), -136.8 to -136.7 (m, F).; **FTIR** (cm^{-1}) (neat): 3392, 3078, 1667, 1503, 1474, 792, 772; **HRMS** (ESI, Pos): calcd for $C_{13}H_7BrF_4N_2O$ $[M+H]^+$: 362.9751 m/z, found: 362.9752 m/z.

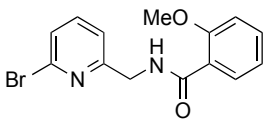

5n

Benzyl 4-(((6-bromopyridin-2-yl)methyl)carbamoyl)benzenesulfonate (2.5n): Following **procedure B**. The crude amide was purified by flash chromatography over silica gel using a gradient of 0% to 100% EtOAc in hexanes. Fractions containing **2.5n** were concentrated to dryness, resulting in a white solid (0.40 g, 42% yield). **mp**: 90-91 °C; **^{1}H NMR** ($CDCl_3$, 500 MHz): δ 9.11 (br t, *J* = 6.0 Hz, 1H), 8.24 (dd, *J* = 2.0, 8.0 Hz, 1H), 7.53 (t, *J* = 7.5 Hz, 1H), 7.46 (ddd, *J* = 1.5, 7.0, 7.5 Hz, 1H), 7.39 (dd, *J* = 0.5, 8.0 Hz, 1H), 7.32 (dd, *J* = 0.5, 7.5 Hz, 1H), 7.08 (dd, *J* = 1.5, 8.0 Hz, 1H), 7.00 (dd, *J* = 1.0, 8.0 Hz, 1H), 4.78 (d, *J* = 6.0 Hz, 2H), 4.07 (s, 3H); **^{13}C NMR** ($CDCl_3$, 125 MHz): δ 165.5, 159.0, 158.0, 141.6, 139.2, 133.1, 132.4, 126.6, 121.3, 121.2, 121.1, 111.5, 56.1, 44.8; **FTIR** (cm^{-1}) (neat):3348, 2922, 1638, 1511, 1434, 1233, 1158, 1023, 780, 753, 618; **HRMS** (ESI, Pos): calcd for $C_{14}H_{14}BrN_2O_2$ $[M+H]^+$: 321.0233 *m/z*, found: 321.0225 *m/z*.

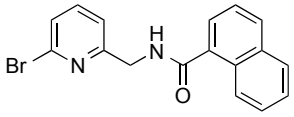

2.5o

***N*-((6-Bromopyridin-2-yl)methyl)-1-naphthamide (2.5o)**: Following **procedure A**. The crude amide was purified by flash chromatography over silica gel using a gradient of 10% to 50% EtOAc in hexanes. Fractions containing **2.5o** were concentrated to dryness, resulting in a white solid (0.90 g, 86% yield). **mp**: 154-155 °C; **^{1}H NMR** ($CDCl_3$, 500 MHz): δ 8.41-8.37 (m, 1H), 7.94 (d, *J* = 8.5 Hz, 1H), 7.89-7.86 (m, 1H), 7.70 (dd, *J* = 1.5, 7.0 Hz, 1H), 7.59-7.51 (m, 3H), 7.50-7.46 (m, 1H), 7.43 (dd, *J* = 0.5, 7.5 Hz, 1H), 7.38 (dd, *J* = 0.5, 7.5 Hz, 1H) 7.04 (br s, 1H), 4.83 (d, *J* = 5.5 Hz, 2H); **^{13}C NMR** ($CDCl_3$, 125 MHz): δ 169.6, 158.2, 141.7, 139.3, 134.0, 133.7, 130.9, 130.2, 128.3, 127.2, 126.9, 126.5, 125.5, 125.3, 124.8, 121.1, 44.5; **FTIR** (cm^{-1}) (neat): 3244, 1638, 1536, 1427, 1404, 1308, 778, 767, 714; **HRMS** (ESI, Pos): calcd for $C_{17}H_{13}BrN_2O$ $[M+H]^+$: 341.0284 *m/z*, found: 341.0292 *m/z*.

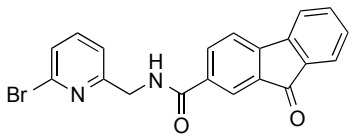

2.5p

***N*-((6-Bromopyridin-2-yl)methyl)-9-oxo-9H-fluorene-2-carboxamide (2.5p)**: Following **procedure A**. The crude amide was purified by flash chromatography over silica gel using a gradient of 20% to 80% EtOAc in hexanes. Fractions containing **2.5p** were concentrated to dryness,

resulting in a yellow solid (0.75 g, 74% yield). **mp**: 192-194 °C; **^{1}H NMR** ($CDCl_3$, 500 MHz): δ 8.10-8.06 (m, 2H), 7.71 (d, *J* = 5.0 Hz, 2H), 7.65-7.52 (m, 4H), 7.43 (d, 7.5 Hz, 1H), 7.39-7.33 (m, 2H), 7.22 (s, 1H), 4.75 (d, *J* = 5.5 Hz, 2H); **^{13}C NMR** ($CDCl_3$, 125 MHz): δ 192.8, 166.2, 158.0, 147.3, 143.5, 141.8, 139.3, 135.0, 134.9, 134.6, 134.3, 130.0, 127.0, 124.6, 122.4, 121.1 (2), 120.6, 44,6; **FTIR** (cm^{-1}) (neat): 3405, 1703, 1656, 1614, 1578, 1265, 738, 583; **HRMS** (ESI, Pos): calcd for $C_{20}H_{13}BrN_2O_2$ $[M+H]^+$: 393.0233 *m/z*, found: 393.0242 *m/z*.

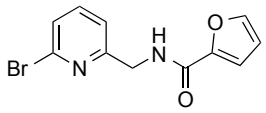

2.5q

***N*-((6-Bromopyridin-2-yl)methyl)furan-2-carboxamide (2.5q)**: Following **procedure A**. The crude amide was purified by flash chromatography over silica gel using a gradient of 40% to 70% EtOAc in hexanes. Fractions containing **2.5q** were concentrated to dryness, resulting in a white solid (0.73 g, 87% yield). **mp**: 117-118 °C; **^{1}H NMR** ($CDCl_3$, 500 MHz): δ 7.50-7.42 (m, 3H), 7.35 (d, *J* = 7.5 Hz, 1H), 7.28 (dd, *J* = 0.5, 7.5 Hz, 1H), 7.09 (dd, *J* = 1.0, 3.5 Hz, 1H), 6.46 (dd, *J* = 1.5, 3.0 Hz, 1H), 4.65 (d, *J* = 5.5 Hz, 2H); **^{13}C NMR** ($CDCl_3$, 125 MHz): δ 158.5, 158,5, 147.6, 144.3, 141.6, 139.2, 126.8, 120.9, 114.5, 112.1, 43.9; **FTIR** (cm^{-1}) (neat): 3235, 1636, 1526, 1014, 771, 762, 629, 601; **HRMS** (ESI, Pos): calcd for $C_{11}H_9BrN_2O_2$ $[M+H]^+$: 280.9920 *m/z*, found: 280.9921 *m/z*.

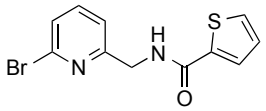

2.5r

***N*-((6-Bromopyridin-2-yl)methyl)thiophene-2-carboxamide (2.5r)**: Following **procedure A**. The crude amide was purified by flash chromatography over silica gel using a gradient of 40% to 100% EtOAc in hexanes. Fractions containing **2.5r** were concentrated to dryness, resulting in a white solid (0.75 g, 84% yield). **mp**: 123-127 °C; **^{1}H NMR** ($CDCl_3$, 500 MHz): δ 7.57 (dd, *J* = 1.5, 4.0 Hz, 1H), 7.54 (t, *J* = 8.0 Hz, 1H), 7.49 (dd, *J* = 1.0, 5.0 Hz, 1H), 7.41 (d, *J* = 7.5 Hz, 1H), 7.33 (d, *J* = 7.5 Hz, 1H), 7.10-7.05 (m, 2H), 4.69 (d, *J* = 5.5 Hz, 2H); **^{13}C NMR** ($CDCl_3$, 125 MHz): δ 161.9, 158.1, 141.6, 139.3, 138.5, 130.3, 128.4, 127.7, 126.9, 121.2, 44.4; **FTIR** (cm^{-1}) (neat): 3319,

3083, 2981, 2968, 2934, 1552, 1305, 721, 679; **HRMS** (ESI, Pos): calcd for $C_{11}H_9BrN_2OS$ $[M+H]^+$: 296.9692 *m/z*, found: 296.9690 *m/z*.

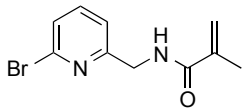

2.5s

***N*-((6-Bromopyridin-2-yl)methyl)-1-naphthamide (2.5s)**: Following **procedure A**. The crude amide was purified by flash chromatography over silica gel using a gradient of 40% to 100% EtOAc in hexanes. Fractions containing **2.5s** were concentrated to dryness, resulting in a white solid (0.74 g, 72% yield). **mp**: 53-54 °C; **^{1}H NMR** ($CDCl_3$, 500 MHz): δ 7.66 (d, *J* = 16.0 Hz, 1H), 7.54-7.50 (m, 3H), 7.40-7.34 (m, 4H), 7.30 (dd, *J* = 1.0, 7.5 Hz, 1H), 6.77 (br s, 1H), 6.52 (d, *J* = 15.5 Hz, 1H), 4.66 (d, *J* = 5.5 Hz, 2H); **^{13}C NMR** ($CDCl_3$, 125 MHz): δ168.4, 158.4, 141.6, 139.6, 139.2, 126.8, 121.1, 120.2, 44.2, 18.6; **FTIR** (cm^{-1}) (neat): 3327, 3083, 2924, 1657, 1616, 1583, 1556, 1521, 1435, 1405, 1121, 776; **HRMS** (ESI, Pos): calcd for $C_{10}H_{11}BrN_2O$ $[M+H]^+$: 255.0128 *m/z*, found: 255.0140 *m/z*.

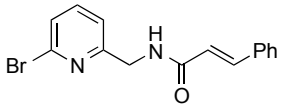

2.5t

***N*-((6-Bromopyridin-2-yl)methyl)cinnamamide (2.5t)**: Following **procedure A**. The crude amide was purified by flash chromatography over silica gel using a gradient of 40% to 100% EtOAc in hexanes. Fractions containing **2.5t** were concentrated to dryness, resulting in a white solid (0.77 g, 80% yield). **mp**: 120-122 °C; **^{1}H NMR** ($CDCl_3$, 500 MHz): δ 7.66 (d, *J* = 16.0 Hz, 1H), 7.54-7.50 (m, 3H), 7.40-7.34 (m, 4H), 7.30 (dd, *J* = 1.0, 7.5 Hz, 1H), 6.77 (br s, 1H), 6.52 (d, *J* = 15.5 Hz, 1H), 4.66 (d, *J* = 5.5 Hz, 2H); **^{13}C NMR** ($CDCl_3$, 125 MHz): δ 166.0, 158.3, 141.6, 141.6, 139.2, 134.7, 129.8, 128.8, 127.9, 126.8, 121.2, 120.28, 44.4; **FTIR** (cm^{-1}) (neat): 3232, 3064, 3032, 2982, 2970, 2946, 1652, 1613, 1578, 1551, 731, 684, 671; **HRMS** (ESI, Pos): calcd for $C_{15}H_{13}BrN_2O$ $[M+H]^+$: 317.0284 *m/z*, found: 317.0283 *m/z*.

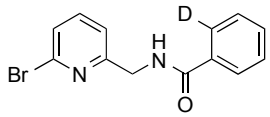

2.5a(*ortho*-d_1)

***N*-((6-Bromopyridin-2-yl)methyl)benzamide-2-*d* (2.5a(*ortho*-d_1))**: Following **procedure C**. The crude amide was dissolved in a minimal amount of hot EtOAc and excess hexanes were added. The resulting precipitate was recovered by filtration and washed with hexanes. resulting in a beige solid (0.11 g, 75% yield). **mp**: 127-128 °C; **^{1}H NMR** ($CDCl_3$, 500 MHz): δ 7.84 (dd, J = 1.0 Hz, J = 8.0 Hz, 1H), 7.54 (t, J = 10.0 Hz, 1H), 7.53-7.50 (m, 1H), 7.48-7.43 (m, 2H), 7.41 (d, J = 10.0 Hz, 1H), 7.33 (dd, J = 1.0 Hz, J = 7.5 Hz, 1H), 7.23 (br s, 1H), 4.73 (d, J = 5.5 Hz, 2H); **^{13}C NMR** ($CDCl_3$, 125 MHz): δ 167.6, 158.4, 141.8, 139.3, 134.1, 131.8, 128.8, 128.7, 127.2, 127.0 126.9 (t, $J_{C\text{-}D}$ = 23.4 Hz), 121.3, 44.6; **FTIR** (cm^{-1}) (neat): 3287, 3061, 2926, 1638, 1537, 1436, 1403, 1121, 770; **HRMS** (ESI, Pos): calcd for $C_{13}H_{11}DBrN_2O$ $[M+H]^+$: 292.01903*m*/*z*, found: 292.0191 *m*/*z*. Product is 90% *ortho*-deuterated, as was the starting acyl chloride.

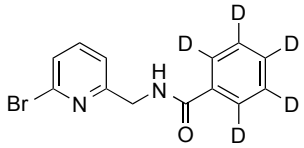

2.5a-d_5

***N*-((6-Bromopyridin-2-yl)methyl)benzamide-2,3,4,5,6-d_5 (2.5a-d_5)**: Following **procedure A**. The crude amide was was dissolved in a minimal amount of hot EtOAc and excess hexanes were added. The resulting precipitate was recovered by filtration and washed with hexanes, resulting in a beige solid (0.38 g, 85% yield). **mp**: 128-129 °C; **^{1}H NMR** ($CDCl_3$, 400 MHz): δ 7.55 (t, J = 7.6 Hz, 1H), δ 7.42 (d, J = 8.0 Hz, 1H), δ 7.34 (d, J = 7.2 Hz, 1H), δ 7.19 (s, 1H), δ 7.40 (d, J = 5.2 Hz, 2H); **^{13}C NMR** ($CDCl_3$, 125 MHz): δ 167.6, 158.4, 141.7, 139.3, 134.0, 131.3 (t, $J_{C\text{-}D}$ = 24.3 Hz), 128.2 (t, $J_{C\text{-}D}$ = 24.5 Hz), 127.0, 126.8 (t, $J_{C\text{-}D}$ = 24.3 Hz), 121.3, 44.6; **FTIR** (cm^{-1}) (neat): 3287, 3061, 2926, 1638, 1538, 1403, 1121, 770, 629; **HRMS** (ESI, Pos): calcd for $C_{13}H_7D_5BrN_2O$ $[M+H]^+$: 296.0441 *m*/*z*, found: 296.0453*m*/*z*.

A1.3.6.General procedure for the synthesis of imidazo[1,5-*a*]pyridines

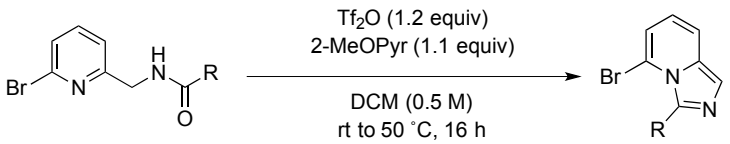

5 **6**

To a flame-dried and argon-flushed glass microwave (sealable) vial (VWR®) equipped with a magnetic stirrer and a rubber septum was added the amide (1.0 equiv) and anhydrous CH_2Cl_2 (0.50 M). 2-methoxypyridine (2-MeOPyr) (1.1 equiv) was added via syringe and Tf_2O (1.2 equiv) was added over 2 min via syringe. The reaction usually changed color (dark purple or dark blue) and was exothermic upon addition of the anhydride. The reaction mixture was slowly heated to 50 °C using an oil bath and stirred for 16 h. The mixture was cooled to room temperature and quenched by addition of saturated aqueous Na_2CO_3 and then stirred for 5 min. Phases were separated and the aqueous layer was extracted with CH_2Cl_2 (3x). The combined organic layers were dried over anhydrous $MgSO_4$, filtered and evaporated to dryness.

A1.3.7.Characterization data of imidazo[1,5-*a*]pyridines

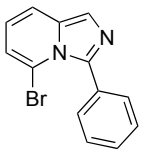

2.6a

5-Bromo-3-phenylimidazo[1,5-*a*]pyridine (2.6a):[6a] Following **general procedure**. The crude imidazo[1,5-*a*]pyridine was purified by flash chromatography over silica gel using a gradient of 10% to 80% EtOAc in hexanes. Fractions containing **2.6a** were concentrated to dryness, resulting in a green solid (0.50 g, 96% yield). **mp**: 80-81°C, lit:[6a] 80-81 °C; **^{1}H NMR** ($CDCl_3$, 400 MHz): δ 7.66 (s, 1H), 7.57-7.52 (m, 3H), 7.50-7.41 (m, 3H), 6.85 (app dt, J = 1.0, 7.0 Hz, 1H), 6.61 (dd, J = 7.0, 9.0 Hz, 1H); **^{13}C NMR** ($CDCl_3$, 100 MHz): δ 140.1, 133.3, 132.1, 131.1, 128.5, 126.7, 120.7, 119.1, 118.5, 117.6, 111.3; **FTIR** (cm^{-1}) (neat): 3064, 2922, 1623, 1565, 1537, 1492, 1456, 1444, 1408, 1360, 1320, 803, 760; **HRMS** (ESI, Pos): calcd for $C_{13}H_{10}N_2Br$ [M+H]+: 273.0022 *m/z*, found 273.0014 *m/z*.

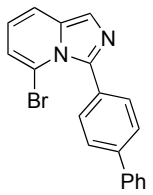

2.6b

3-([1,1'-Biphenyl]-4-yl)-5-bromoimidazo[1,5-*a*]pyridine (2.6b): Following **general procedure**. The crude imidazo[1,5-*a*]pyridine was purified by flash chromatography over silica gel using a gradient of 10% to 70% EtOAc in hexanes. Fractions containing **2.6b** were concentrated to dryness, resulting in a brown solid (0.61 g, 87% yield). **mp**: 164-166 °C; **^{1}H NMR** ($CDCl_3$, 400 MHz): δ 7.70-7.66 (m, 5H), 7.63-7.60 (m, 2H), 7.53 (dd, *J* = 0.8, 9.2 Hz, 1H), 7.49-7.45 (m, 2H), 7.40-7.36 (m, 1H), 6.85 (dd, *J* = 1.2, 6.8 Hz, 1H), 6.60 (dd, *J* = 6.8, 8.8 Hz, 1H); **^{13}C NMR** ($CDCl_3$, 100 MHz): δ 141.6, 140.6, 140.2, 133.8, 131.8, 131.4, 128.9, 127.6, 127.2, 125.8, 121.3, 119.6, 119.0, 118.0, 111.8; **FTIR** (cm^{-1}) (neat): 3057, 2964, 842, 807, 758, 691; **HRMS** (ESI, Pos): calcd for $C_{19}H_{13}BrN_2$ $[M+H]^+$: 349.0335 *m/z*, found: 349.0344 *m/z*.

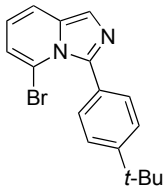

2.6c

5-Bromo-3-(4-(*tert*-butyl)phenyl)imidazo[1,5-*a*]pyridine (2.6c): Following **general procedure**. The crude imidazo[1,5-*a*]pyridine was purified by flash chromatography over silica gel using a gradient of 10% to 70% EtOAc in hexanes. Fractions containing **2.6c** were concentrated to dryness, resulting in a yellow solid (0.60 g, 91% yield). **mp**: 128-129 °C; **^{1}H NMR** ($CDCl_3$, 400 MHz): δ 7.61 (s, 1H), 7.49 (dd, *J* = 0.8, 8.8 Hz, 1H), 7.46-7.40 (m, 4H), 6.80 (dd, *J* = 1.2, 6.8 Hz, 1H), 6.55 (dd, *J* = 6.4, 8.8 Hz, 1H), 1.37 (s, 9H); **^{13}C NMR** ($CDCl_3$, 100 MHz): δ 152.1, 140.7, 133.6, 131.1, 129.5, 124.1, 121.0, 119.3, 118.7, 118.0, 111.8, 34.8, 31.4; **FTIR** (cm^{-1}) (neat): 2966, 2949, 2865, 2845, 822, 757, 686; **HRMS** (ESI, Pos): calcd for $C_{17}H_{17}BrN_2$ $[M+H]^+$: 329.0648 *m/z*, found: 329.0663 *m/z*.

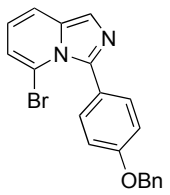

2.6d

3-(4-(Benzyloxy)phenyl)-5-bromoimidazo[1,5-*a*]pyridine (2.6d): Following **general procedure**. The crude imidazo[1,5-*a*]pyridine was purified by flash chromatography over silica gel using a gradient of 15% to 75% EtOAc in hexanes. Fractions containing **2.6d** were concentrated to dryness, resulting in a green solid (0.73 g, 91% yield). **mp**: 117-119 °C; **^{1}H NMR** ($CDCl_3$, 400 MHz): δ 7.61 (s, 1H), 7.50-7.44 (m, 5H), 7.40 (t, J = 5.6 Hz, 2H), 7.34 (d, J = 5.6 Hz, 1H), 7.02 (d, J = 7.2 Hz, 2H), 6.80 (dd, J = 0.8, J = 5.2 Hz, 1H), 6.55 (dd, J = 5.2, J = 7.2 Hz, 1H), 5.13 (s, 2H); **^{13}C NMR** ($CDCl_3$, 125 MHz): δ 159.5, 140.4, 136.8, 133.6, 132.8, 128.7, 128.1, 127.7, 125.2, 120.9, 119.4, 118.8, 118.1, 113.6, 111.9, 70.2; **FTIR** (cm^{-1}) (neat): 3057, 1450, 1238, 1172, 1027, 827, 814, 772, 691, ; **HRMS** (ESI, Pos): calcd for $C_{20}H_{16}BrN_2O$ $[M+H]^+$: 379.0441 *m/z*, found: 379.0458 *m/z*.

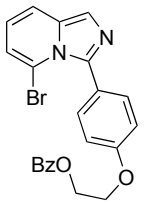

2.6e

2-(4-(5-Bromoimidazo[1,5-*a*]pyridin-3-yl)phenoxy)ethyl benzoate (2.6e): Following **general procedure**. The crude imidazo[1,5-*a*]pyridine was purified by flash chromatography over silica gel using a gradient of 10% to 75% EtOAc in hexanes. Fractions containing **2.6e** were concentrated to dryness, resulting in a green solid (0.20 g, 52% yield). **mp**: 109-111 °C; **^{1}H NMR** ($CDCl_3$, 500 MHz): δ 8.11-8.06 (m, 2H), 7.62 (s, 1H), 7.61-7.42 (m, 6H), 7.01-6.96 (m, 2H), 6.82 (dd, J = 1.5, 11.5 Hz, 1H), 6.61-6.54 (m, 1H), 4.71 (dd, J = 8.0 Hz, 2H), 4.38 (dd, J = 8.0 Hz, 2H); **^{13}C NMR** ($CDCl_3$, 125 MHz): δ 166.7, 159.4, 140.2 133.6, 133.3, 132.9, 130.0, 129.9, 128.5, 125.3, 120.9, 119.5, 118.9, 118.1, 113.4, 111.9, 66.2, 63.4; **FTIR** (cm^{-1}) (neat): 1712, 1455, 1273, 1241, 1112, 1062, 834, 804, 706; **HRMS** (ESI, Pos): calcd for $C_{22}H_{18}BrN_2O_3$ $[M+H]^+$: 437.0501 *m/z*, found: 437.0495 *m/z*.

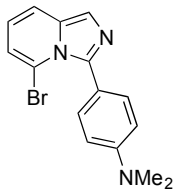

2.6f

4-(5-Bromoimidazo[1,5-*a*]pyridin-3-yl)-*N,N*-dimethylaniline (2.6f): Following **general procedure**. The crude imidazo[1,5-*a*]pyridine was purified by flash chromatography over silica gel using a gradient of 15% to 75% EtOAc in hexanes. Fractions containing **2.6f** were concentrated to dryness, resulting in a yellow solid (0.33 g, 84% yield). **mp**: 167-168 °C; **^{1}H NMR** ($CDCl_3$, 400 MHz): δ 7.59 (s, 1H), 7.46 (d, J = 8.4 Hz, 1H), 7.37 (d, J = 8.8 Hz, 2H), 6.78 (dd, J = 0.8 Hz, J = 6.8 Hz, 1H), 6.73 (dd, J = 2.0 Hz, J = 6.8 Hz, 2H), 6.52 (dd, J = 6.8, J = 8.8, Hz, 1H), 3.02 (s, 6H); **^{13}C NMR** ($CDCl_3$, 75 MHz): δ 150.9, 141.5, 133.5, 132.4, 120.8, 120.0, 119.3, 118.5, 118.1, 112.2, 110.7, 40.5; **FTIR** (cm^{-1}) (neat): 3077, 2889, 1609, 1439, 1359, 1231, 822, 805, 692; **HRMS** (ESI, Pos): calcd for $C_{15}H_{15}BrN_3$ $[M+H]^+$: 316.0444 *m/z*, found: 316.0459 *m/z*.

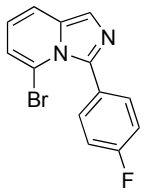

2.6g

5-Bromo-3-(4-fluorophenyl)imidazo[1,5-*a*]pyridine (2.6g): Following **general procedure**. The crude imidazo[1,5-*a*]pyridine was purified by flash chromatography over silica gel using a gradient of 10% to 70% EtOAc in hexanes. Fractions containing **2.6g** were concentrated to dryness, resulting in a grey solid (0.52 g, 90% yield). **mp**: 78-80 °C; **^{1}H NMR** ($CDCl_3$, 500 MHz): δ 7.61 (s, 1H), 7.51-7.48 (m, 3H), 7.12-7.09 (m, 2H), 6.82 (dd, J = 1.0, 7.0 Hz, 1H), 6.58 (dd, J = 7.0, 9.0 Hz, 1H); **^{13}C NMR** ($CDCl_3$, 125 MHz): δ 163.3 (d, $J_{C\text{-}F}$ = 296.9 Hz), 133.7, 133.3 (d, $J_{C\text{-}F}$ = 10.0 Hz), 128.6 (d, $J_{C\text{-}F}$ = 3.9 Hz), 121.0, 119.6, 119.0, 118.0, 114.2 (d, $J_{C\text{-}F}$ = 26.1 Hz), 111.5; **^{19}F NMR** ($CDCl_3$, 471 MHz): δ -112.2 (t, $J_{H\text{-}F}$ = 8.5 Hz, 1F); **FTIR** (cm^{-1}) (neat): 3057, 2964, 1214, 798; **HRMS** (ESI, Pos): calcd for $C_{13}H_8BrFN_2$ $[M+H]^+$: 290.9928 *m/z*, found: 290.9933 *m/z*.

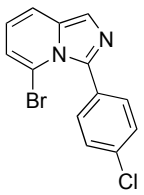

2.6h

5-Bromo-3-(4-chlorophenyl)imidazo[1,5-*a*]pyridine (2.6h): Following **general procedure**. The crude imidazo[1,5-*a*]pyridine was purified by flash chromatography over silica gel using a gradient of 10% to 75% EtOAc in hexanes. Fractions containing **2.6h** were concentrated to dryness, resulting in a green solid (45 mg, 95% yield). **mp**: 99-101 °C; **^{1}H NMR** ($CDCl_3$, 400 MHz): δ 7.63 (s, 1H), 7.52 (d, *J* = 8.8 Hz, 1H), 7.47 (d, *J* = 8.4 Hz, 2H), 7.40 (d, *J* = 8.4 Hz, 2H), 6.85 (d, *J* = 8.8 Hz, 1H), 6.61 (dd, *J* = 8.8 Hz, 6.8 Hz, 1H); **^{13}C NMR** ($CDCl_3$, 75 MHz): δ 139.3, 135.2, 134.0, 132.8, 131.1, 127.5, 121.4, 119.8, 119.3, 118.2, 111.7; **FTIR** (cm^{-1}) (neat): 3084, 1450, 1161, 1117, 1087, 967, 832, 791, 689; **HRMS** (ESI, Pos): calcd for $C_{13}H_9BrClN_2$ $[M+H]^+$: 306.9632 *m/z*, found: 306.9641 *m/z*.

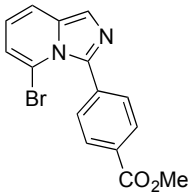

2.6i

Methyl 4-(5-bromoimidazo[1,5-*a*]pyridin-3-yl)benzoate (2.6i): Following **general procedure**. The crude imidazo[1,5-*a*]pyridine was purified by flash chromatography over silica gel using a gradient of 10% to 70% EtOAc in hexanes. Fractions containing **2.6i** were concentrated to dryness, resulting in a brown solid (0.54 g, 81% yield). **mp**: 134-135 °C; **^{1}H NMR** ($CDCl_3$, 400 MHz): δ 8.14-8.11 (m, 2H), 7.70 (s, 1H), 7.68-7.65 (m, 2H), 7.48 (dd, *J* = 0.8, 9.2 Hz, 1H), 6.90 (dd, *J* = 1.2, 6.8 Hz, 1H), 6.67 (dd, *J* = 6.8, 8.8 Hz, 1H), 4.0 (s, 3H); **^{13}C NMR** ($CDCl_3$, 100 MHz): δ 166.8, 139.2, 136.8, 134.1, 131.3, 130.3, 128.3, 121.7, 119.9, 119.4, 118.0, 111.6, 52.3; **FTIR** (cm^{-1}) (neat): 3086, 3071, 2987, 2942, 2923, 2858, 2845, 1753, 1276, 692; **HRMS** (ESI, Pos): calcd for $C_{15}H_{11}BrN_2O_2$ $[M+H]^+$: 331.0077 *m/z*, found: 331.0076 *m/z*.

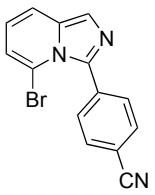

2.6j

4-(5-Bromoimidazo[1,5-*a*]pyridin-3-yl)benzonitrile (2.6j): Following **general procedure**. The crude imidazo[1,5-*a*]pyridine was dissolved in a minimal amount of hot EtOAc and excess hexanes were added. The resulting precipitate was recovered by filtration and washed with hexanes, resulting in a green solid (0.58 g, 88% Yield). **mp**: 148-149 °C; **^{1}H NMR** ($CDCl_3$, 500 MHz): δ 7.72-7.65 (m, 5H), 7.57 (dd, *J* = 1.0, 9.0 Hz, 1H), 6.91 (dd, *J* = 1.0, 6.5 Hz, 1H), 6.68 (dd, *J* = 7.0, 9.0 Hz, 1H); **^{13}C NMR** ($CDCl_3$, 125 MHz): δ 138.2, 136.8, 134.4, 131.8, 130.9, 122.1, 120.2, 119.8, 118.7, 118.1, 112.4, 111.3; **FTIR** (cm^{-1}) (neat): 2981, 2972, 2947, 2923, 2863, 2844, 2827, 842, 799, 781; **HRMS** (ESI, Pos): calcd for $C_{14}H_8BrN_3$ $[M+H]^+$: 297.9974 *m/z*, found: 297.9973 *m/z*.

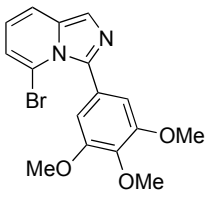

2.6k

5-Bromo-3-(3,4,5-trimethoxyphenyl)imidazo[1,5-*a*]pyridine (2.6k): Following **general procedure**. The crude imidazo[1,5-*a*]pyridine was purified by flash chromatography over silica gel using a gradient of 15% to 75% EtOAc in hexanes. Fractions containing **2.6k** were concentrated to dryness, resulting in a green solid (0.80 g, 88% Yield). **mp**: 101-102 °C; **^{1}H NMR** ($CDCl_3$, 500 MHz): δ 7.61 (s, 1H), 7.51 (dd, *J* = 1.0 Hz, 9.0 Hz, 1H), 6.84 (dd, *J* = 1.0 Hz, 6.5 Hz, 1H), 6.75 (s, 2H), 6.59 (dd, *J* = 6.5, 9.0 Hz, 1H), 3.91 (s, 3H), 3.87 (s, 6H); **^{13}C NMR** ($CDCl_3$, 125 MHz): δ 152.2, 140.3, 139.1, 133.7, 127.6, 120.9, 119.7, 119.1, 118.1, 111.9, 109.4, 61.2, 56.3; **FTIR** (cm^{-1}) (neat): 2935, 1582, 1463, 1409, 1233, 1118, 999, 760, 691; **HRMS** (ESI, Pos): calcd for $C_{16}H_{16}BrN_2O_3$ $[M+H]^+$: 363.0339 *m/z*, found: 363.0349 *m/z*.

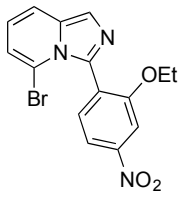

2.6l

5-Bromo-3-(2-ethoxy-4-nitrophenyl)imidazo[1,5-*a*]pyridine (2.6l): Following **general procedure**. The crude imidazo[1,5-*a*]pyridine was purified by flash chromatography over silica gel using a gradient of 15% to 75% EtOAc in hexanes. Fractions containing **2.6l** were concentrated to dryness, resulting in a green solid (0.42 mg, 94% Yield). **mp**: 158-159 °C; **^{1}H NMR** ($CDCl_3$, 400 MHz): δ 7.93 (dd, *J* = 2.0, 8.4 Hz, 1H), 7.74 (d, *J* = 10.0 Hz, 2H), 7.73 (d, *J* = 14.4 Hz, 1H) 7.55 (d, *J* = 9.2 Hz, 1H), 6.89 (dd, *J* = 1.0, 6.8 Hz, 1H), 6.67 (dd, *J* = 7.2, 9.2 Hz, 1H), 4.08 (q, *J* = 6.8 Hz, 2H), 1.20 (t, *J* = 6.8 Hz, 3H); **^{13}C NMR** ($CDCl_3$, 75 MHz): δ 158.7, 149.6, 135.6, 134.3, 132.0, 129.2, 122.0, 119.8, 119.4, 118.1, 115.2, 112.3, 105.7, 64.6, 14.5; **FTIR** (cm^{-1}) (neat): 3053, 1512, 1340, 1319, 1083, 1213, 868, 802, 734; **HRMS** (ESI, Pos): calcd for $C_{15}H_{13}BrN_3O_3$ $[M+H]^+$: 362.0145 *m*/*z*, found: 362.0135 *m*/*z*.

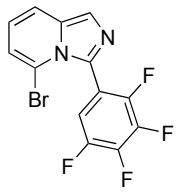

2.6m

5-Bromo-3-(2,3,4,5-tetrafluorophenyl)imidazo[1,5-*a*]pyridine (2.6m): Following **general procedure**. The crude imidazo[1,5-*a*]pyridine was purified by flash chromatography over silica gel using a gradient of 10% to 70% EtOAc in hexanes. Fractions containing **2.6m** were concentrated to dryness, resulting in a beige solid (0.64 g, 93% Yield). **mp**: 88-89 °C; **^{1}H NMR** ($CDCl_3$, 500 MHz): δ 7.69 (s, 1H), 7.56 (d, *J* = 9.0 Hz, 1H), 7.26-7.21 (m, 1H), 6.92 (d, *J* = 6.5 Hz, 1H), 6.70 (dd, *J* = 7.0, 9.0 Hz, 1H); **^{13}C NMR** ($CDCl_3$, 175 MHz): δ 147.4-147.1 (m), 146.0-145.7 (m), 142.3 (ddd, $J_{C\text{-}F}$ = 3.3, 12.6, 15.9 Hz), 141.1-140.8 (m), 139.5 (ddd, $J_{C\text{-}F}$ = 4.2, 12.6, 16.6 Hz), 134.5, 131.1, 122.1, 120.1, 119.9, 118.1, 117.7-117.5 (m), 113.9 (dd, $J_{C\text{-}F}$ = 2.3, 19.6 Hz); **^{19}F NMR** ($CDCl_3$, 470 MHz):

δ -156.9 to -155.8 (m, 1F), -153.2 to -153.0 (m, 1F), -139.7 to -139.6 (m, 1F), -134.7 to -134.6 (m, 1F); **FTIR** (cm^{-1}) (neat): 3107, 3039, 3012, 2956, 2847, 960, 799, 749, 700, 679; **HRMS** (ESI, Pos): calcd for $C_{13}H_5BrF_4N_2$ $[M+H]^+$: 344.9645 *m/z*, found: 344.9645 *m/z*.

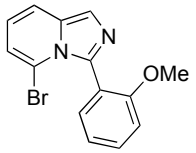

2.6n

5-Bromo-3-(2-methoxyphenyl)imidazo[1,5-*a*]pyridine (2.6n): Following **general procedure**. The crude imidazo[1,5-*a*]pyridine was purified by flash chromatography over silica gel using a gradient of 15% to 75% EtOAc in hexanes. Fractions containing **2.6n** were concentrated to dryness, resulting in a green solid (0.30 g, 86% Yield). **mp**: 129-131 °C; **^{1}H NMR** ($CDCl_3$, 500 MHz): δ 7.64 (s, 1H), 7.51-7.43 (m, 3H) 7.03 (dt *J* = 1.0, 9.0 Hz, 1H), 6.90 (d, *J* = 8.4 Hz, 1H), 6.79 (d, *J* = 6.4 Hz, 1H), 6.79 (dt, *J* = 1.0, 9.0 Hz, 1H), 3.72 (s, 3H); **^{13}C NMR** ($CDCl_3$, 125 MHz): δ 159.3, 137.6, 133.7, 132.3, 131.0, 122.4, 121.0, 120.0, 118.9 (2), 118.0, 112.3, 110.0, 55.3; **FTIR** (cm^{-1}) (neat): 2925, 1443, 1283, 1261, 1239, 1100, 1020, 796, 746; **HRMS** (ESI, Pos): calcd for $C_{14}H_{12}BrN_2O$ $[M+H]^+$: 303.0128 *m/z*, found: 303.0137 *m/z*.

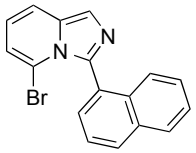

2.6o

5-Bromo-3-(naphthalen-1-yl)imidazo[1,5-*a*]pyridine (2.6o): Following **general procedure**. The crude imidazo[1,5-*a*]pyridine was purified by flash chromatography over silica gel using a gradient of 10% to 70% EtOAc in hexanes. Fractions containing **2.6o** were concentrated to dryness, resulting in a light greenish solid (0.76 g, 82% yield). **mp**: 152-153 °C; **^{1}H NMR** ($CDCl_3$, 500 MHz): δ 7.99 (d, *J* = 8.5 Hz, 1H), 7.91 (d, *J* = 8.5 Hz, 1H), 7.75 (s, 1H), 7.62 (dd, *J = 1.0,* 7.0 Hz, 1H), 7.58 (dd, *J* = 1.0, 9.0 Hz, 1H), 7.56-7.52 (m, 1H), 7.50-7.46 (m, 1H), 7.42-7.38 (m, 1H), 7.23-7.20 (m, 1H), 6.77 (dd, *J* = 1.0, 6.5 Hz, 1H), 6.64-6.60 (m, 1H); **^{13}C NMR** ($CDCl_3$, 125 MHz): δ 138.5, 134.8, 133.5, 132.9, 130.2 (2), 129.8, 128.2, 126.7, 126.0, 125.9, 124.5, 121.0, 119.2, 118.0, 111.7; **FTIR**

(cm^{-1}) (neat): 2966, 2865, 1055, 1033, 1013, 775, 758, 693; **HRMS** (ESI, Pos): calcd for $C_{17}H_{11}BrN_2$ $[M+H]^+$: 323.0178 *m/z*, found: 323.0194 *m/z*.

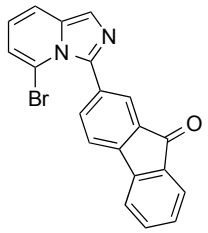

2.6p

2-(5-Bromoimidazo[1,5-*a*]pyridin-3-yl)-9*H*-fluoren-9-one (2.6p): Following **general procedure**. The crude imidazo[1,5-*a*]pyridine was purified by flash chromatography over silica gel using a gradient of 10% to 70% EtOAc in hexanes. Fractions containing **2.6p** were concentrated to dryness, resulting in a dark orange solid (0.45 g, 58% yield). **mp**: 198-199 °C; **^{1}H NMR** ($CDCl_3$, 500 MHz): δ 7.83-7.82 (m, 1H), 7.74-7.70 (m, 2H), 7.68 (s, 1H), 7.64-7.60 (m, 2H), 7.58-7.53 (m, 2H), 7.36 (dt, *J* = 1.0, 7.5 Hz, 1H), 6.90 (dd, *J* = 1.0, 6.5 Hz, 1H), 6.68-6.64 (m, 1H); **^{13}C NMR** ($CDCl_3$, 125 MHz): δ 144.6, 144.1, 139.1, 137.1, 134.8, 134.6, 134.0, 133.3, 132.9, 129.4, 127.1, 124.5, 121.5, 120.7, 119.9, 119.4, 119.2, 118.1, 111.6; **FTIR** (cm^{-1}) (neat): 1707, 1612, 1597, 1184, 769, 742, 685, 671; **HRMS** (ESI, Pos): calcd for $C_{20}H_{11}BrN_2O$ $[M+H]^+$: 375.0128 *m/z*, found: 375.0134 *m/z*.

2.6q

5-Bromo-3-(furan-2-yl)imidazo[1,5-*a*]pyridine (2.6q): Following **general procedure**. The crude imidazo[1,5-*a*]pyridine was purified by flash chromatography over silica gel using a gradient of 10% to 70% EtOAc in hexanes. Fractions containing **2.6q** were concentrated to dryness, resulting in a beige solid (0.44 mg, 84% yield). **mp**: 123-124 °C; **^{1}H NMR** ($CDCl_3$, 400 MHz): δ 7.64 (s, 1H), 7.60 (dd, *J* = 0.8, 1.6 Hz, 1H), 7.51 (dd, *J* = 0.8, 8.8 Hz, 1H), 6.89 (dd, *J* = 1.2, 6.8 Hz, 1H), 6.73 (dd, *J* = 0.8, 3.6 Hz, 1H), 6.64 (dd, *J* = 6.8, 8.8 Hz, 1H), 6.55 (dd, *J* = 2.0, 3.6 Hz, 1H); **^{13}C NMR** ($CDCl_3$, 100 MHz): δ 143.0, 142.9, 134.2, 130.4, 121.4, 120.0, 119.4, 117.7, 114.8, 112.0,

111.5; **FTIR** (cm^{-1}) (neat): 3126, 3109, 3091, 3076, 2968, 2939, 2922, 2867, 2844, 805, 760; **HRMS** (ESI, Pos): calcd for $C_{11}H_7BrN_2O$ $[M+H]^+$: 262.9815 *m/z*, found: 262.9819 *m/z*.

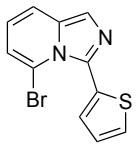

2.6r

5-Bromo-3-(thiophen-2-yl)imidazo[1,5-*a*]pyridine (2.6r): Following **general procedure**. The crude imidazo[1,5-*a*]pyridine was purified by flash chromatography over silica gel using a gradient of 10% to 70% EtOAc in hexanes. Fractions containing **2.6r** were concentrated to dryness, resulting in a brown solid (0.50 g, 90% yield). **mp**: 95-96 °C; **^{1}H NMR** ($CDCl_3$, 500 MHz): δ 7.64 (s, 1H), 7.53-7.50 (m, 2H), 7.25 (dd, *J* = 1.5, 4.0 Hz, 1H), 7.10 (dd, *J* = 3.5, 5.0 Hz, 1H), 6.87 (dd, *J* = 1.5, 7.0 Hz, 1H), 6.62 (dd, *J* = 7.0, 9.0 Hz, 1H); **^{13}C NMR** ($CDCl_3$, 125 MHz): δ 134.2, 132.9, 132.7, 132.0, 128.1, 126.1, 121.4, 119.9, 119.5, 118.0, 112.0; **FTIR** (cm^{-1}) (neat): 3080, 3065, 3008, 2981, 2967, 2949, 2938, 2922, 2866, 2844, 2829, 802, 712, 689; **HRMS** (ESI, Pos): calcd for $C_{11}H_7BrN_2S$ $[M+H]^+$: 278.9586 *m/z*, found: 278.9589 *m/z*.

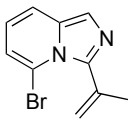

2.6s

5-Bromo-3-(prop-1-en-2-yl)imidazo[1,5-*a*]pyridine (2.6s): Following **general procedure**. The crude imidazo[1,5-*a*]pyridine was purified by flash chromatography over silica gel using a gradient of 5% to 60% EtOAc in hexanes. Fractions containing **2.6s** were concentrated to dryness, resulting in a green solid (0.76 g, 74% yield). **mp**: 76-77 °C; **^{1}H NMR** ($CDCl_3$, 500 MHz): δ 7.51 (s, 1H), 7.43 (dd, *J* = 1.0, 9.0 Hz, 1H), 6.81 (dd, *J* = 1.0, 7.0 Hz, 1H), 6.56-6.52 (m, 1H), 5.61-5.58 (m, 1H), 5.22-5.20 (m, 1H), 2.26 (d, *J* = 10.0 Hz, 3H); **^{13}C NMR** ($CDCl_3$, 75 MHz): δ 141.4, 136.6, 133.2, 122.1, 120.6, 119.2, 118.8, 117.8, 111.6, 25.2; **FTIR** (cm^{-1}) (neat): 3076, 3064, 1623, 1358, 1312,

1278, 1181, 814, 800, 762, 689; **HRMS** (ESI, Pos): calcd for $C_{10}H_9BrN_2$ $[M+H]^+$: 238.0052 *m/z*, found: 238.0059 *m/z*.

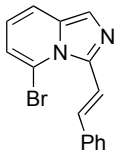

2.6t

(*E*)-5-Bromo-3-styrylimidazo[1,5-*a*]pyridine (2.6t): Following **general procedure**. The crude imidazo[1,5-*a*]pyridine was purified by flash chromatography over silica gel using a gradient of 10% to 70% EtOAc in hexanes. Fractions containing **2.6t** were concentrated to dryness, resulting in a green solid (0.57 g, 94% yield). **mp**: 91-93 °C; **^{1}H NMR** ($CDCl_3$, 300 MHz): δ 8. 31 (d, *J* = 15.9 Hz, 1H), 7.61-7.55 (m, 4H), 7.45 (dd, *J* = 0.9, 8.7 Hz, 1H), 7.40-7.35 (m, 2H), 7.31-7.27 (m, 1H), 6.88 (dd, *J* = 1.2, 6.9 Hz, 1H), 6.52 (dd, *J* = 6.6, 8.7 Hz, 1H); **^{13}C NMR** ($CDCl_3$, 75 MHz): δ 139.7, 137.3, 134.4, 131.5, 128.7, 127.9, 126.7, 122.5, 120.2, 118.8, 118.4, 117.0, 111.5; **FTIR** (cm^{-1}) (neat): 3107, 3055, 3039, 3012, 2954, 2847, 960, 799, 749, 700, 679; **HRMS** (ESI, Pos): calcd for $C_{15}H_{11}BrN_2$ $[M+H]^+$: 299.0178 *m/z*, found: 299.0183 *m/z*.

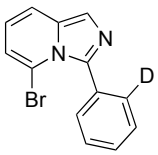

2.6a-*ortho*-d_1

5-Bromo-3-(phenyl-2-*d*)imidazo[1,5-*a*]pyridine (2.6a-*ortho*-d_1): Following **general procedure**. The crude imidazo[1,5-*a*]pyridine was purified by flash chromatography over silica gel using a gradient of 10% to 75% EtOAc in hexanes. Fractions containing **2.6a-*ortho*-d_1** were concentrated to dryness, resulting in a green solid (60 mg, 74% yield). **mp**: 59-61 °C; **^{1}H NMR** ($CDCl_3$, 500 MHz): δ 7.64 (s, 1H), 7.54-7.51 (m, 2H), 7.48-7.40 (m, 3H), 6.83 (dd, *J* = 1.0, 6.5 Hz, 1H), 6.59 (dd, *J* = 6.5, 9.1 Hz, 1H); **^{13}C NMR** ($CDCl_3$, 100 MHz): δ 140.5, 133.7, 132.3, 131.6, 131.3

(t, $J_{C\text{-}D}$ = 25.0 Hz), 129.1, 127.3, 127.2 121.0, 119.7, 119.1 118.1, 111.8; **FTIR** (cm^{-1}) (neat): 1623, 1445, 1360, 1320, 1185, 1105, 965, 804, 760, 688, 633; **HRMS** (ESI, Pos): calcd for $C_{13}H_9DBrN_2$ [M+H]+: 274.0085 *m/z*, found 274.0095 *m/z*.

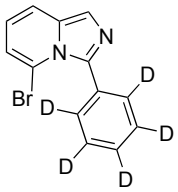

2.6a-*d*$_5$

5-Bromo-3-(phenyl-*d*5)imidazo[1,5-*a*]pyridine (2.6a-*d*$_5$): Following **general procedure**. The crude imidazo[1,5-*a*]pyridine was purified by flash chromatography over silica gel using a gradient of 15% to 75% EtOAc in hexanes. Fractions containing **2.6a-*d*$_5$** were concentrated to dryness, resulting in a green solid (0.26 g, 92% yield). **mp**: 72-74 °C; **^{1}H NMR** ($CDCl_3$, 500 MHz): δ 7.64 (s, 1H), 7.52 (dd, *J* = 1.0, 9.0 Hz, 1H), 6.83 (dd, *J* = 1.0, 7.0 Hz, 1H), 6.59 (dd, *J* = 6.5, 9.0 Hz, 1H); **^{13}C NMR** ($CDCl_3$, 125 MHz): δ 140.5, 133.7, 132.4, 131.1 (t, $J_{C\text{-}D}$ = 24.4 Hz), 128.5 (t, $J_{C\text{-}D}$ = 24.3 Hz), 126.7 (t, $J_{C\text{-}D}$ = 24.3 Hz), 121.1, 119.6, 119.0, 118.1, 111.8; **FTIR** (cm^{-1}) (neat): 3351, 3083, 1750, 1478, 1094, 809, 689, 562; **HRMS** (ESI, Pos): calcd for $C_{13}H_5D_5BrN_2$ [M+H]+: 278.0336 *m/z*, found 278.0342 *m/z*.

A1.3.8.General procedure for the synthesis of imidazo[2,1,5-*c,d*]indolizines

Procedure A:

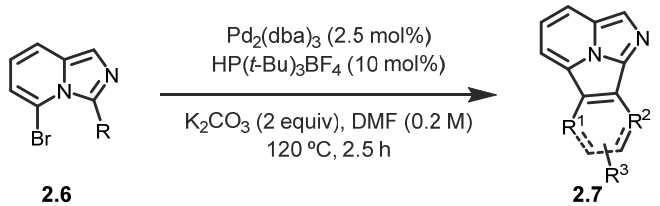

2.6 **2.7**

To a flame-dried microwave (sealable) vial (VWR®) equipped with a magnetic stirrer was added the corresponding 5-bromoimidazo[1,5-*a*]pyridine (1.0 equiv), as previously synthesized. Then, $Pd_2(dba)_3$ (0.025 equiv), HP(*t*-Bu)$_3BF_4$ (0.10 equiv), and K_2CO_3 (2.0 equiv) were added to the vial.

The vial was capped with a rubber septum and purged with argon. Anhydrous DMF (0.20M) was added and the reaction was quickly heated to 120 °C using an oil bath and stirred for 2.5 h. The reaction was cooled to room temperature and the crude mixture was diluted in EtOAc and a saturated aqueous solution of NaCl was added. The layers were separated and the aqueous layer was extracted with EtOAc (3x). The combined organic layers were washed with brine (2x) dried over anhydrous $MgSO_4$, filtered over a pad of silica gel, and evaporated to dryness. *Note: Preparing the reaction mixture in a glovebox produced similar results for several runs and is likely unnecessary for most substrates.*

Procedure B:

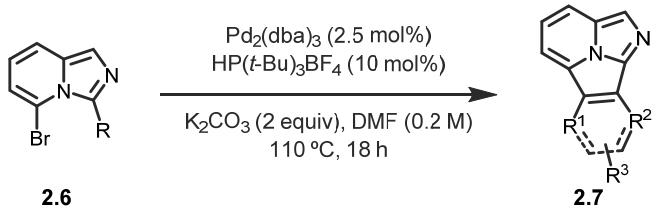

2.6 **2.7**

To a flame-dried microwave (sealable) vial (VWR®) equipped with a magnetic stirrer was added the corresponding 5-bromoimidazo[1,5-*a*]pyridine (1.0 equiv), as previously synthesized. The vial was then purged (2 x 10 min) with argon and transferred in an Ar-filled glovebox. Then, $Pd_2(dba)_3$ (0.025 equiv), HP(*t*-Bu)$_3BF_4$ (0.10 equiv), and K_2CO_3 (2.0 equiv) were added to the vial. The vial was capped with an aluminum microwave cap (VWR® with Teflon seal) and removed from of the glovebox. Anhydrous DMF (0.20 M) was added. The reaction was slowly heated to 110 °C using an oil bath and stirred for 16 h. The reaction was cooled to room temperature and uncapped. The crude mixture was diluted in CH_2Cl_2 (5 mL) and quenched by addition of a saturated aqueous solution of NaCl. The layers were separated and the aqueous layer was extracted with CH_2Cl_2 (2x). The combined organic layers were dried over anhydrous Na_2SO_4, filtered over a pad of silica gel and evaporated to dryness.

Procedure C:

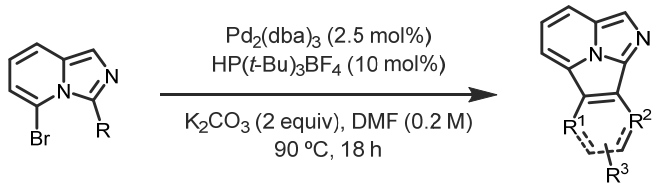

2.6 **2.7**

To a flame-dried microwave (sealable) vial (VWR®) equipped with a magnetic stirrer was added the corresponding 5-bromoimidazo[1,5-*a*]pyridine (1.0 equiv), as previously synthesized. The vial was then purged (2 x 10 min) with argon and transferred in an Ar-filled glovebox. Then, $Pd_2(dba)_3$ (0.025 equiv), HP(*t*-Bu)$_3BF_4$ (0.10 equiv), and K_2CO_3 (2.0 equiv) were added to the vial. The vial was capped with an aluminum microwave cap (VWR® with Teflon seal) and removed from of the glovebox. Anhydrous DMF (0.20 M) was added. The reaction was slowly heated to 90 °C using an oil bath and stirred for 16 h. The reaction was cooled to room temperature and uncapped. The crude mixture was diluted in CH_2Cl_2 (5 mL) and quenched by addition of a saturated aqueous solution of NaCl. The layers were separated and the aqueous layer was extracted with CH_2Cl_2 (2x). The combined organic layers were dried over anhydrous Na_2SO_4, filtered over a pad of silica gel and evaporated to dryness.

A1.3.9.Characterization data of imidazo[2,1,5-*c,d*]indolizines

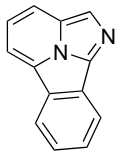

2.7a

Benzo[*a*]imidazo[2,1,5-*c,d*]indolizine (2.7a): Following **procedure A**. The crude imidazo[2,1,5-*c*,*d*]indolizine was purified by flash chromatography over silica gel using a gradient of 1% to 10% MeOH in CH_2Cl_2. Fractions containing **2.7a** were concentrated to dryness, resulting in a bright yellow solid (0.11 g, 100% yield). **mp**: 98-100 °C; **^{1}H NMR** ($CDCl_3$, 500 MHz): δ 8.44-8.41 (m, 2H), 8.25 (s, 1H), 8.15 (d, *J* = 8.5 Hz, 1H), 8.04 (d, *J* = 7.0 Hz, 1H), 7.80 (t, *J* = 7.0 Hz, 1H), 7.69 (dd, *J* = 7.0, 8.5 Hz, 1H), 7.63 (t, *J* = 7.5 Hz, 1H); **^{13}C NMR** ($CDCl_3$, 125 MHz): δ 137.6, 131.1, 129.2, 128.2, 127.4, 126.5, 125.7, 124.8, 123.1, 121.7, 119.9, 116.7, 110.3; **FTIR** (cm^{-1}) (neat): 3057, 2923, 1561, 1528, 1499, 1455, 1426, 1335, 1296; **HRMS** (ESI, Pos): calcd for $C_{13}H_9N_2$ $[M+H]^+$: 193.0766 *m*/*z*, found 193.0759 *m*/*z*.

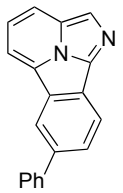

2.7b

7-Phenylbenzo[*a*]imidazo[2,1,5-*c,d*]indolizine (2.7b): Following **procedure B**. The crude imidazo[2,1,5-*c,d*]indolizine was purified by flash chromatography over silica gel using a gradient of 40% to 60% EtOAc in hexanes. Fractions containing **2.7b** were concentrated to dryness, resulting in a brown oil (0.13 g, 100% yield). **^{1}H NMR** ($CDCl_3$, 400 MHz): δ 8.58 (d, *J* = 0.8 Hz, 1H), 8.45 (d, *J* = 8.0 Hz, 1H), 8.24 (s, 1H), 8.14 (d, *J* = 8.4 Hz, 1H), 8.04 (d, *J* = 6.8 Hz, 1H), 8.02 (dd, *J* = 1.6, 8.4 Hz, 1H), 7.78-7.76 (m, 2H), 7.68 (dd, *J* = 6.8, 8.4 Hz, 1H), 7.55-7.51 (m, 2H), 7.44-7.40 (m, 1H); **^{13}C NMR** ($CDCl_3$, 100 MHz): δ 141.0, 138.2, 137.4, 131.8, 129.0, 128.6, 127.7, 127.5, 127.5, 127.0, 126.7, 125.9, 121.8, 121.6, 120.1, 116.9, 110.5; **FTIR** (cm^{-1}) (neat): 3054, 3024, 2954, 2922, 2852, 1067, 746, 694, 676; **HRMS** (ESI, Pos): calcd for $C_{19}H_{12}N_2$ $[M+H]^+$: 269.1073 *m/z*, found 269.1072 *m/z*.

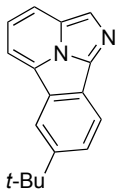

2.7c

7-(*tert*-Butyl)benzo[*a*]imidazo[2,1,5-*c,d*]indolizine (2.7c): Following **procedure C**. The crude imidazo[2,1,5-*c,d*]indolizine was purified by flash chromatography over silica gel using a gradient of 10% to 80% EtOAc in hexanes. Fractions containing **2.7c** were concentrated to dryness, resulting in a brown oil (0.11 g, 89% Yield). **^{1}H NMR** ($CDCl_3$, 500 MHz): δ 8.39 (dd, *J* = 1.0, 2.0 Hz, 1H), 8.33 (dd, *J* = 0.5, 8.5 Hz, 1H), 8.18 (s, 1H), 8.10 (d, *J* = 8.5 Hz, 1H), 8.01 (d, *J* = 7.0 Hz, 1H), 7.86 (dd, *J* = 1.5, 8.5 Hz, 1H), 7.65 (dd, *J* = 7.0, 8.5 Hz, 1H), 1.50 (s, 9H); **^{13}C NMR** ($CDCl_3$, 125 MHz): δ 148.3, 137.7, 131.4, 127.4, 126.9, 126.1, 125.7, 121.5, 119.4, 119.3, 116.5, 109.9, 35.2, 31.7; **FTIR** (cm^{-1}) (neat): 2955, 2903, 2863, 1363, 795, 677; **HRMS** (ESI, Pos): calcd for $C_{17}H_{16}N_2$ $[M+H]^+$: 249.1386 *m/z*, found 249.1380 *m/z*.

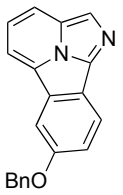

2.7d

7-(Benzyloxy)benzo[*a*]imidazo[2,1,5-*c,d*]indolizine (2.7d): Following **procedure A**. The crude imidazo[2,1,5-*c,d*]indolizine was purified by flash chromatography over silica gel using a gradient of 1% to 10% MeOH in CH_2Cl_2. Fractions containing **2.7d** were concentrated to dryness, resulting in a dark yellow solid (0.47 g, 90% yield). **mp**: 109-110 °C; **^{1}H NMR** ($CDCl_3$, 500 MHz): δ 8.58 (d, *J* = 0.8 Hz, 1H), 8.45 (d, *J* = 8.0 Hz, 1H), 8.24 (s, 1H), 8.14 (d, *J* = 8.4 Hz, 1H), 8.04 (d, *J* = 6.8 Hz, 1H), 8.02 (dd, *J* = 1.6, 8.4 Hz, 1H), 7.78-7.76 (m, 2H), 7.68 (dd, *J* = 6.8, 8.4 Hz, 1H), 7.55-7.51 (m, 2H), 7.44-7.40 (m, 1H); **^{13}C NMR** ($CDCl_3$, 125 MHz): δ 157.0, 137.7, 136.8, 132.7, 128.8, 128.3, 127.7, 126.8, 126.6, 125.8, 122.7, 121.2, 121.0, 118.7, 117.1, 110.4, 107.8, 70.9; **FTIR** (cm^{-1}) (neat): 3091, 1496, 1335, 1223, 1051, 974, 773, 743, 677; **HRMS** (ESI, Pos): calcd for $C_{20}H_{15}N_2O$ $[M+H]^+$: 299.1179 *m/z*, found 299.1187 *m/z*.

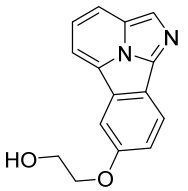

2.7e

2-(Benzo[*a*]imidazo[2,1,5-*c,d*]indolizin-7-yloxy)ethan-1-ol (2.7e): Following **procedure A**. The crude imidazo[2,1,5-*c,d*]indolizine was added to a 5-mL round-bottom flask equipped with a magnetic stir bar and a rubber septum. 2.0 M NaOH in water (0.7 mL, 1.4 mmol, 8.0 equiv), THF (0.4 mL) and MeOH (0.4 mL) were added. The resulting suspension was vigorously stirred at room temperature for 16h. CH_2Cl_2 and a saturated aqueous solution of NaCl were added. The layers were separated and the aqueous layer was extracted with CH_2Cl_2 (3x). The combined organic layers were washed with brine (2x) dried over anhydrous $MgSO_4$, filtered over a pad of silica gel, and evaporated to dryness. The crude alcohol was purified by flash chromatography over silica gel using a gradient of 1% to 10% MeOH in CH_2Cl_2. Fractions containing **7e** were concentrated to dryness, resulting in a yellow solid (38 mg, 89% yield). **mp**: 77-80 °C; **^{1}H NMR** ($CDCl_3$, 500 MHz): δ 8.23 (d, *J* =

8.5 Hz, 1H), 8.20 (d, *J* = 7.5 Hz, 2H), 8.11 (s, 1H), 8.08 (d, *J* = 2.5 Hz, 1H), 7.74 (dd, *J* = 7.0, 8.5 Hz, 1H), 7.46 (dd, *J* = 2.0, 8.5 Hz, 1H), 4.28 (t, *J* = 4.5 Hz, 2H), 3.99 (t, *J* = 4.5 Hz, 2H); **^{13}C NMR** ($CDCl_3$, 125 MHz): δ 159.0, 137.9, 134.1, 127.9, 126.8, 126.3, 123.3, 122.5, 121.2, 119.8, 118.4, 112.4, 108.6, 71.3, 61.7; **FTIR** (cm-1) (neat): 3302, 2919, 1712, 1602, 1562, 1438, 1210, 1058, 793; **HRMS** (ESI, Pos): calcd for $C_{15}H_{13}N_2O_2$ [M+H]+: 253.0972 m/z, found 253.0981 m/z.

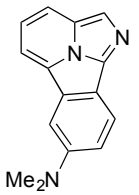

2.7f

***N,N*-Dimethylbenzo[*a*]imidazo[2,1,5-*c,d*]indolizin-7-amine (2.7f)**: Following **procedure A**. The crude imidazo[2,1,5-*c,d*]indolizine was purified by flash chromatography over silica gel using a gradient of 1% to 10% MeOH in CH_2Cl_2. Fractions containing **2.7f** were concentrated to dryness, resulting in a brown solid (0.12 g, 98% yield). **mp**: 118-120 °C; **^{1}H NMR** ($CDCl_3$, 500 MHz): δ 8.22 (d, *J* = 8.5 Hz, 1H), 8.07 (s, 1H), 8.03 (d, *J* = 8.5 Hz, 1H), 7.87 (d, *J* = 7.0 Hz, 1H), 7.61 (d, *J* = 2.5 Hz, 1H), 7.53 (dd, *J* = 6.5, 8.5 Hz, 1H), 7.22 (dd, *J* = 2.5, 9.0 Hz, 1H), 3.14 (s, 6H); **^{13}C NMR** ($CDCl_3$, 125 MHz): δ 149.0, 138.5, 133.6, 127.4, 125.7, 125.5, 120.9, 120.6, 119.3, 116.7, 115.8, 109.5, 105.5, 41.3; **FTIR** (cm^{-1}) (neat): 2888, 2802, 1623, 1496, 1432, 1342, 1054, 792, 673; **HRMS** (ESI, Pos): calcd for $C_{15}H_{14}N_3$ $[M+H]^+$: 236.1182 *m/z*, found 236.1189 *m/z*.

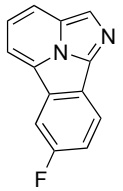

2.7g

7-Fluorobenzo[*a*]imidazo[2,1,5-*c,d*]indolizine (2.7g): Following **procedure B**. The crude imidazo[2,1,5-*c,d*]indolizine was purified by flash chromatography over silica gel using a gradient of 1% to 10% MeOH in CH_2Cl_2. Fractions containing **2.7g** were concentrated to dryness, resulting in a bright yellow solid (103.0 mg, 98% yield). **mp**: 129-130 °C; **^{1}H NMR** ($CDCl_3$, 400 MHz): δ 8.37 (dd, *J* = 4.8, 8.4 Hz, 1H), 8.23 (s, 1H), 8.18 (d, *J* = 8.4 Hz, 1H), 8.07-8.03 (m, 2H), 7.69 (dd, *J* = 7.2, 8.8 Hz, 1H), 7.53 (dt, *J* = 2.4, 8.8 Hz, 1H); **^{13}C NMR** ($CDCl_3$, 100 MHz): δ 161.5, 159.6, 137.0,

132.0, 127.6, 126.0, 124.7, 121.4, 121.2 (d, $J_{C\text{-}F}$ = 7.3 Hz), 117.5 (d, $J_{C\text{-}F}$ = 19.4 Hz), 117.5, 111.1, 109.3 (d, J = 19.4 Hz, $J_{C\text{-}F}$); **^{19}F NMR** ($CDCl_3$, 282 MHz): δ -115.7 to -115.6 (m, 1F); **FTIR** (cm^{-1}) (neat): 3064, 3015, 2952, 2920, 2851, 1006, 769; **HRMS** (ESI, Pos): calcd for $C_{13}H_7FN_2$ $[M+H]^+$: 211.0667 *m/z*, found 211.0660 *m/z*.

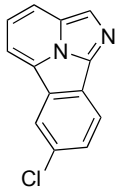

2.7h

7-Chlorobenzo[*a*]imidazo[2,1,5-*c,d*]indolizine (2.7h): Following **procedure A**. The crude imidazo[2,1,5-*c*,*d*]indolizine was purified by flash chromatography over silica gel using a gradient of 1% to 10% MeOH in CH_2Cl_2. Fractions containing **2.7h** were concentrated to dryness, resulting in a yellow solid (0.11 g, 94% yield). **mp**: 162-163°C; **^{1}H NMR** ($CDCl_3$, 500 MHz): δ 8.38 (dd, J = 0.5 Hz, 1.5 Hz, 1H), 8.33 (dd, J = 0.5 Hz, J = 8.5 Hz, 1H), 8.26 (s, 1H), 8.19 (d, J = 8.5 Hz, 1H), 8.06 (d, J = 7.0 Hz, 1H), 7.74 (dd, J = 2.0 Hz, 8.5 Hz, 1H), 7.71 (dd, J = 7.0 Hz, 8.5 Hz, 1H); **^{13}C NMR** ($CDCl_3$, 125 MHz): δ 137.0, 132.0, 130.8, 129.7, 128.3, 126.4, 126.1, 125.6, 123.1, 122.0, 121.0, 117.6, 111.4; **FTIR** (cm^{-1}) (neat): 3071, 2929, 1720, 1461, 1335, 1276, 1244, 962, 714; **HRMS** (ESI, Pos): calcd for C13H8ClN2 $[M+H]^+$: 227.0371 *m/z*, found 227.0380 *m/z*.

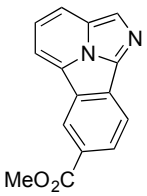

2.7i

Methyl benzo[*a*]imidazo[2,1,5-*c,d*]indolizine-7-carboxylate (2.7i): Following **procedure A**. The crude imidazo[2,1,5-*c*,*d*]indolizine was purified by flash chromatography over silica gel using a gradient of 1% to 10% MeOH in CH_2Cl_2. Fractions containing **2.7i** were concentrated to dryness, resulting in a yellow solid (0.17 g, 97% Yield). **mp:** 206-207 °C; **^{1}H NMR** ($CDCl_3$, 500 MHz): δ 9.13 (s, 1H), 8.44-8.35 (m, 3H), 8.22 (d, J = 8.5 Hz, 1H), 8.16 (d, J = 7.0 Hz, 1H), 7.79 (dd, J = 7.0, 8.0 Hz, 1H), 4.04 (s, 3H); **^{13}C NMR** ($CDCl_3$, 100 MHz): δ 167.1, 130.5, 130.4, 130.1, 129.5, 126.5,

126.3, 125.4, 122.7, 119.5, 117.4, 111.5, 52.5; **FTIR** (cm^{-1}) (neat): 3089, 3060, 3032, 3007, 2982, 2950, 2922, 2861, 2845, 1712; **HRMS** (ESI, Pos): calcd for $C_{15}H_{10}N_2O_2$ [M+H]+: 251.0815 *m/z*, found 251.0806 *m/z*.

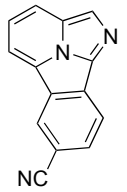

2.7j

Benzo[*a*]imidazo[2,1,5-*c,d*]indolizine-7-carbonitrile (2.7j): Following **procedure A**. The crude imidazo[2,1,5-*c*,*d*]indolizine was dissolved in a minimal amount of hot CH_2Cl_2 and excess hexanes were added. The resulting precipitate was recovered by filtration and washed with hexanes, resulting in a yellow solid (0.31 g, 84% yield). **mp:** 251-253 °C; **^{1}H NMR** ($CDCl_3$, 400 MHz): δ 8.73-8.72 (m, 1H), 8.47 (dd, *J* = 0.4, 8.0 Hz, 1H), 8.39 (s, 1H), 8.29 (d, *J* = 8.4 Hz, 1H), 8.20 (d, *J* = 7.2 Hz, 1H), 7.98 (dd, *J* = 1.2, 8.0 Hz, 1H), 7.84 (dd, *J* = 7.2, 8.4 Hz, 1H); **^{13}C NMR** ($CDCl_3$, 100 MHz): δ136.4, 131.6, 130.5, 130.1, 129.6, 127.9, 126.6, 125.2, 123.0, 120.6, 119.4, 118.2, 112.5, 107.6; **FTIR** (cm^{-1}) (neat): 3069, 3012, 2962, 2920, 2846, 2250, 820, 814; **HRMS** (ESI, Pos): calcd for $C_{14}H_7N_3$ [M+H]+: 218.0713 *m/z*, found 218.0719 *m/z*.

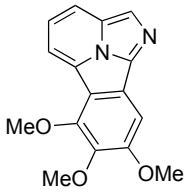

2.7k

6,7,8-Trimethoxybenzo[*a*]imidazo[2,1,5-*c,d*]indolizine (2.7k): Following **procedure A**. The crude imidazo[2,1,5-*c*,*d*]indolizine was purified by flash chromatography over silica gel using a gradient of 0% to 10% MeOH in CH_2Cl_2. Fractions containing **2.7k** were concentrated to dryness, resulting in a brown oil (0.54 g, 93% yield). **mp**: 118-120°C; **^{1}H NMR** ($CDCl_3$, 500 MHz): δ 8.95 (d, *J* = 2.0 Hz, 1H), 8.47 (s, 1H), 8.31 (d, *J* = 8.5 Hz, 1H), 8.26 (d, *J* = 7.0 Hz, 1H), 8.04 (d, *J* = 2.0 Hz, 1H), 7.86 (dd, *J* = 7.5 Hz, 8.5 Hz, 1H), 4.56 (q, *J* = 7.0 Hz, 2H), 1.72 (t, *J* = 7.0 Hz, 3H); **^{13}C NMR** ($CDCl_3$, 125 MHz): δ 152.7, 145.7, 135.4, 131.6, 130.2, 126.9, 126.2, 123.1, 121.6, 118.4,

113.2, 112.4, 105.3, 65.5, 14.8; **FTIR** (cm^{-1}) (neat): 2930, 1620, 1417, 1250, 1128, 1085, 1044, 999, 816; **HRMS** (ESI, Pos): calcd for $C_{16}H_{15}N_2O_3$ $[M+H]^+$: 283.1077 *m/z*, found 283.1086 *m/z*.

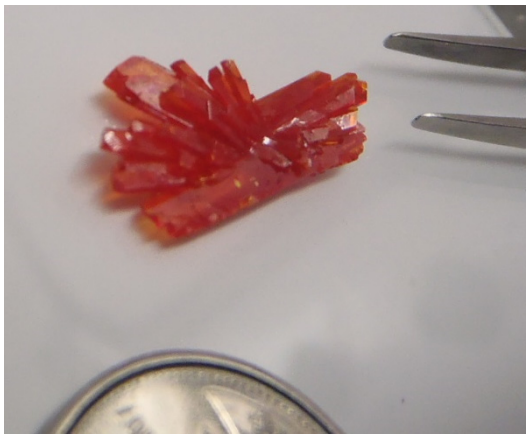

200 mg single crystal piece. Recrystallized from wet DMF

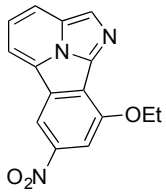

2.7l

9-Ethoxy-7-nitrobenzo[*a*]imidazo[2,1,5-*c,d*]indolizine (2.7l): Following **procedure A**. The crude imidazo[2,1,5-*c,d*]indolizine was purified by flash chromatography over silica gel using a gradient of 0% to 10% MeOH in CH_2Cl_2. Fractions containing **2.7l** were concentrated to dryness, resulting in a yellow solid (0.13 g, 92% yield). **mp**: 239-240 °C; **^{1}H NMR** ($CDCl_3$, 500 MHz): δ 8.95 (d, *J* = 2.0 Hz, 1H), 8.47 (s, 1H), 8.31 (d, *J* = 8.5 Hz, 1H), 8.26 (d, *J* = 7.0 Hz, 1H), 8.04 (d, *J* = 2.0 Hz, 1H), 7.86 (dd, *J* = 7.5 Hz, *J* = 8.5 Hz, 1H), 4.56 (q, *J* = 7.0 Hz, 2H), 1.72 (t, *J* = 7.0 Hz, 3H); **^{13}C NMR** ($CDCl_3$, 125 MHz): δ 152.7, 145.7, 135.4, 131.6, 130.2, 126.9, 126.2, 123.1, 121.6, 118.4, 113.2, 112.4, 105.3, 65.5, 14.8; **FTIR** (cm^{-1}) (neat): 3055, 1523, 1319, 1290, 1204, 1177, 1076, 976, 809; **HRMS** (ESI, Pos): calcd for $C_{15}H_{12}N_3O_3$ $[M+H]^+$: 282.0873 *m/z*, found 282.0884 *m/z*; This compound does not exhibit significant fluorescence

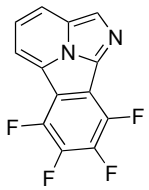

2.7m

6,7,8,9-Tetrafluorobenzo[*a*]imidazo[2,1,5-*c,d*]indolizine (2.7m): Following **procedure B**. The crude imidazo[2,1,5-*c,d*]indolizine was purified by flash chromatography over silica gel using a gradient of 30% to 50% EtOAc in hexanes. Fractions containing **2.7m** were concentrated to dryness, resulting in a bright yellow solid (87.3 mg, 66% yield). **mp:** 179-181 °C; **Rf**: 0.72 (100% EtOAc); **^{1}H NMR** ($CDCl_3$, 500 MHz): δ 8.34 (s, 1H), 8.28 (d, J = 8.4 Hz, 1H), 8.22 (d, J = 7.2 Hz, 1H), 7.80 (dd, J = 7.2, 8.4 Hz, 1H); **^{13}C NMR** ($CDCl_3$, 175 MHz): δ 142.6 (dd, $J_{C\text{-}F}$ = 15.2, 556.7 Hz), 141.3 (dt, $J_{C\text{-}F}$ = 23.8, 354.9 Hz), 139.0 (t, $J_{C\text{-}F}$ = 20.5 Hz), 137.0 (t, $J_{C\text{-}F}$ = 20.7 Hz), 133.8, 130.1, 126.3, 122.8, 122.4, 118.2, 115.0, 113.30 (ddd, $J_{C\text{-}F}$ = 8.05, 21.9, 385.9 Hz); **^{19}F NMR** ($CDCl_3$, 471 MHz): δ -159.0 (t, J = 23.1 Hz, 1F), -151.8 (t, J = 18.8 Hz, 1F), -142.8 (t, J = 16.0 Hz, 1F), -141.1 (t, J = 17.0 Hz, 1F); **FTIR** (cm^{-1}) (neat): 3055, 3006, 2981, 2967, 2949, 2938, 2922, 2865, 2844, 1024, 814; **HRMS** (ESI, Pos): calcd for $C_{13}H_4F_4N_2$ $[M+H]^+$: 265.0383 *m/z*, found 265.0389 *m/z*.

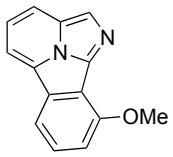

2.7n

9-Methoxybenzo[*a*]imidazo[2,1,5-*c,d*]indolizine (2.7n): Following **procedure A**. The crude imidazo[2,1,5-*c,d*]indolizine was purified by flash chromatography over silica gel using a gradient of 0% to 10% MeOH in CH_2Cl_2. Fractions containing **2.7n** were concentrated to dryness, resulting in a yellow solid (0.11 g, 98% yield). **mp**: 129-131 °C; **^{1}H NMR** ($CDCl_3$, 500 MHz): δ 8.26 (s, 1H), 8.16 (d, J = 8.0 Hz, 1H), 8.05 (d, J = 7.0 Hz, 1H), 8.00 (dd, J = 0.5 Hz, J = 7.0 Hz, 1H), 7.68 (dd, J = 7.0 Hz, J = 8.5 Hz, 1H), 7.56 (t, J = 8.0 Hz, 1H), 7.24 (d, J = 8.0 Hz, 1H), 4.23 (s, 3H); **^{13}C NMR** ($CDCl_3$, 125 MHz): δ 153.7, 136.8, 132.6, 127.9, 126.6, 126.4, 125.7, 121.6, 118.2, 117.0, 115.5, 111.1, 110.4, 56.2; **FTIR** (cm^{-1}) (neat): 2925, 1622, 1467, 1239, 1161, 1100, 1020, 796, 746; **HRMS** (ESI, Pos): calcd for $C_{14}H_{11}N_2O$ $[M+H]^+$: 223.0866 *m/z*, found 223.0869 *m/z*.

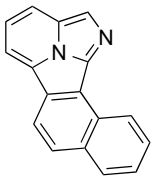

2.7o

Imidazo[2,1,5-*c,d*]naphtho[2,1-*a*]indolizine (2.7o): Following **procedure A**. The crude imidazo[2,1,5-*c,d*]indolizine was purified by flash chromatography over silica gel using a gradient of 20% to 50% EtOAc in hexanes. Fractions containing **2.7o** were concentrated to dryness, resulting in an yellow solid (138.0 mg, 97% yield). **mp:** 149-150 °C; **Rf**: 0.31 (100% EtOAc); **^{1}H NMR** ($CDCl_3$, 500 MHz): δ 9.22 (d, *J* = 8.5 Hz, 1H), 8.46 (s, 1H), 8.34 (d, *J* = 8.5 Hz, 1H), 8.25 (d, *J* = 8.0 Hz, 1H), 8.20 (d, *J* = 7.5 Hz, 1H), 8.06 (d, *J* = 8.0 Hz, 1H), 7.94 (d, *J* = 8.5 Hz, 1H), 7.81-7.77 (m, 2H), 7.71-7.67 (m, 1H); **^{13}C NMR** ($CDCl_3$, 100 MHz): δ 138.1, 133.6, 129.6, 128.3, 127.3, 127.1, 127.0, 126.9, 126.7, 126.0, 125.4, 122.0, 120.2, 116.5, 112.1 ; **FTIR** (cm^{-1}) (neat): 3042, 2920, 2851, 784, 723, 672, 468; **HRMS** (ESI, Pos): calcd for $C_{17}H_{10}N_2$ $[M+H]^+$: 243.0923 *m/z*, found 243.097 *m/z*.

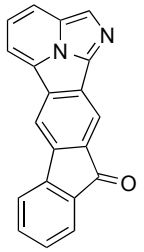

2.7p

11*H*-Fluoreno[3,2-*a*]imidazo[2,1,5-*c,d*]indolizin-11-one (2.7p): Following **procedure A**. The crude imidazo[2,1,5-*c,d*]indolizine was purified by flash chromatography over silica gel using a gradient of 0% to 3% MeOH in CH_2Cl_2. Fractions containing **2.7p** were concentrated to dryness, resulting in red solid (67 mg, 61% yield). **mp:** 297-300 °C; **^{1}H NMR** ($CDCl_3$, 700 MHz): δ 8.54 (s, 1H), 8.52 (s, 1H), 8.31-8.28 (m, 3H), 7.86-7.82 (m, 1H), 7.74 (d, *J* = 5.5 Hz, 1H), 7.66 (d, *J* = 5.5 Hz, 1H), 7.58 (t, *J* = 5.5 Hz, 1H), 7.33 (t, *J* = 5.5 Hz, 1H); **^{13}C NMR** ($CDCl_3$, 175 MHz): δ 192.8, 144.5, 140.5, 135.9, 135.4, 135.3, 135.1, 135.0, 129.4, 127.1, 126.7, 126.4, 125.9, 124.4, 123.7, 120.8, 119.0, 116.3, 115.1, 114.4; **FTIR** (cm^{-1}) (neat): 1701, 1598, 1327, 1303, 1061, 998, 797, 742, 737,

672; **HRMS** (ESI, Pos): calcd for $C_{20}H_{10}N_2O$ $[M+H]^+$: 295.0867 *m/z*, found 295.0866 *m/z*. This compound does not exhibit significant fluorescence because of limited solubility in MeOH.

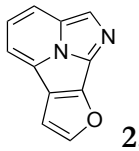

2.7q

Furo[3,2-*a*]imidazo[2,1,5-*c,d*]indolizine (2.7q): Following **procedure B**. The crude imidazo[2,1,5-*c,d*]indolizine was purified by flash chromatography over silica gel using a gradient of 0% to 50% EtOAc in hexanes. Fractions containing **2.7q** were concentrated to dryness, resulting in a bright green solid (36 mg, 40% yield). **mp:** 119-120 °C; **^{1}H NMR** ($CDCl_3$, 300 MHz): δ 8.34 (s, 1H), 8.16 (d, *J* = 8.4 Hz, 1H), 7.93 (d, *J* = 7.2 Hz, 1H), 7.77 (d, *J* = 2.4 Hz, 1H), 7.75-7.69 (m, 1H), 7.15 (d, *J* = 2.1 Hz, 1H); **^{13}C NMR** ($CDCl_3$, 75 MHz): δ 149.4, 146.7, 129.9, 127.5, 127.2, 121.6, 120.4, 120.4, 115.2, 112.6, 105.9; **FTIR** (cm^{-1}) (neat): 3127, 2981, 2968, 2921, 2908, 989, 797, 706, 671; **HRMS** (ESI, Pos): calcd for $C_{11}H_6N_2O$ $[M+H]^+$: 183.0553 *m/z*, found 183.0549 *m/z*.

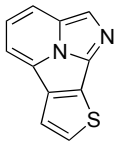

2.7r

Thieno[3,2-*a*]imidazo[2,1,5-*cd*]indolizine (2.7r): Following **procedure B**. The crude imidazo[2,1,5-*c,d*]indolizine was purified by flash chromatography over silica gel using a gradient of 30% to 50% EtOAc in hexanes. Fractions containing **2.7r** were concentrated to dryness, resulting in a bright orange solid (37.4 mg, 38% yield). **mp:** 150-152 °C; **^{1}H NMR** ($CDCl_3$, 500 MHz): δ 8.34 (s, 1H), 8.16 (d, *J* = 8.5 Hz, 1H), 8.00 (d, *J* = 7.0 Hz, 1H), 7.77 (d, *J* = 5.0 Hz, 1H), 7.73 (dd, *J* = 7.0, 8.5 Hz, 1H), 7.51 (d, *J* = 5.0 Hz, 1H); **^{13}C NMR** ($CDCl_3$, 125 MHz): δ 136.3, 134.9, 132.2, 129.3, 126.9, 126.5, 123.5, 121.7, 119.4, 115.4, 11.5; **FTIR** (cm^{-1}) (neat): 3085, 3068, 2921, 2850, 742, 730, 669; **HRMS** (ESI, Pos): calcd for $C_{11}H_6N_2S$ $[M+H]^+$: 199.0325 *m/z*, found 199.0329 *m/z*.

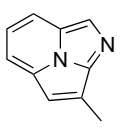

2.7s

7-Methylimidazo[2,1,5-*c,d*]indolizine (2.7s): Following **procedure A**. The crude imidazo[2,1,5-*c,d*]indolizine was purified by flash chromatography over silica gel using a gradient of 5% to 50% EtOAc in hexanes. Fractions containing **2.7s** were concentrated to dryness, resulting in a light green solid (0.10 g, 87% yield). **mp:** 68-70 °C; **^{1}H NMR** ($CDCl_3$, 500 MHz): δ 8.42 (s, 1H), 8.10 (d, *J* = 8.0 Hz, 1H), 7.86 (d, *J* = 7.5 Hz, 1H), 7.70 (t, *J* = 7.5 Hz, 1H), 7.19 (s, 1H), 2.84 (d, *J* = 1.0 Hz, 3H); **^{13}C NMR** ($CDCl_3$, 125 MHz): δ 141.1, 131.7, 131.0, 128.1, 127.0, 122.1, 114.4, 114.3, 113.0, 12.6; **FTIR** (cm^{-1}) (neat): 3384, 3075, 2964, 2901, 2833, 2765, 1117, 1028, 777; **HRMS** (ESI, Pos): calcd for $C_{10}H_8N_2$ $[M+H]^+$: 157.0766 *m/z*, found 157.0760 *m/z*.

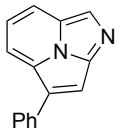

2.7t

6-Phenylimidazo[2,1,5-*c,d*]indolizine (2.7t): Following **procedure B**. The crude imidazo[2,1,5-*c,d*]indolizine was purified by flash chromatography over silica gel using a gradient of 10% to 60% EtOAc in hexanes. Fractions containing **2.7t** were concentrated to dryness, resulting in an orange oil (31 mg, 28% yield). **^{1}H NMR** ($CDCl_3$, 500 MHz): δ 8.55 (s, 1H), 8.32 (d, *J* = 7.0 Hz, 1H), 8.25 (d, *J* = 8.0 Hz, 1H), 7.93 (s, 1H), 7.91-7.89 (m, 2H), 7.84 (t, *J* = 7.5 Hz, 1H), 7.56-7.52 (m, 2H), 7.41-7.38 (m, 1H); **^{13}C NMR** ($CDCl_3$, 125 MHz): δ 135.4, 132.63, 130.8, 126.7, 126.4, 126.1, 125.1, 124.8, 124.0, 120.0, 114.2, 113.7, 111.3; **FTIR** (cm^{-1}) (neat): 3376, 3056, 2981, 2922, 2865, 2845, 1092, 1069, 769; **HRMS** (ESI, Pos): calcd for $C_{15}H_{10}N_2$ $[M+H]^+$: 219.0917 *m/z*, found 219.0913 *m/z*.

A1.3.10. General procedure for the arylation of imidazo[2,1,5-*c,d*]indolizines

Method A:

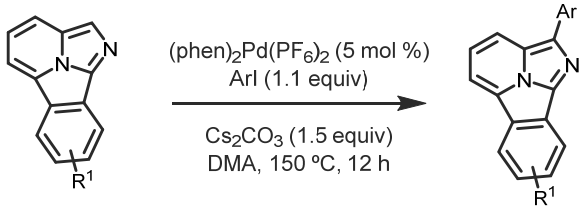

2.7 **2.8**

To a microwave (sealable) vial (VWR®) equipped with a magnetic stirbar and a rubber septum was added Cs_2CO_3 (1.5 equiv). The vial was heated to 150 °C in an oil bath under vacuum for 30 min. The tube was cooled to room temperature, flushed with argon and the corresponding iodide (1.1 equiv) and imidazo[2,1,5-*c,d*]indolizine (1.0 equiv) as previously synthesized were added. DMA (0.5 M) was used to cannulate $[Pd(phen)_2][PF_6]_2$ (0.05 equiv) from a dry vial into the reaction vessel. The vial was capped with an aluminum microwave cap (VWR® with Teflon seal) and heated to 150 °C in an oil bath for 20h. Brine and EtOAc were added. Phases were separated and aqueous phase was extracted with EtOAc (3x). The combined organic layers were washed with brine (2x), dried over $MgSO_4$ and evaporated to dryness.

Method B:

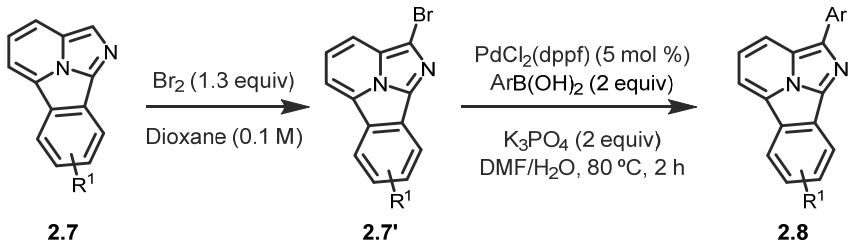

2.7 **2.7'** **2.8**

To a flame-dried round-bottom flask equipped with a magnetic stirbar and a rubber septum was added the corresponding imidazo[2,1,5-*c*,*d*]indolizine (1.0 equiv), as previously synthesized. 1,4-dioxane (0.2 M) was added and solution was frozen in a water/ice bath. In a flame-dried vial equipped with a rubber septum, bromine (1.3 equiv) was mixed with 1,4-dioxane (0.2M) and cannulated under argon into the round-bottom flask (freezes on top of the substrate solution). The ice bath was removed and both layers mixed together as they thawed. This mixture was stirred at room temperature for 20 min. A saturated solution of sodium thiosulfate in water was added and the resulting solution was transferred to a separatory funnel and extracted with CH_2Cl_2 (4x). The combined organic layers were washed with 2M NaOH, dried over $MgSO_4$ and evaporated to dryness to yield a yellow-orange solid. The crude bromoimidazo[2,1,5-*c*,*d*]indolizine was purified by flash chromatography over silica gel using a gradient of 5% to 30% EtOAc in hexanes. Fractions containing (**2.7a'**, **2.7d'**, **2.7k'**) were concentrated to dryness, resulting in a colorful solid.

To a microwave (sealable) vial (VWR®) equipped with a magnetic stirbar and a rubber septum was added the corresponding bromoimidazo[2,1,5-*c*,*d*]indolizine (1.0 equiv), the corresponding boronic acid (2.0 equiv), K_3PO_4*H_2O (4.0 equiv) and $PdCl_2$(dppf)* CH_2Cl_2 (0.05 equiv). 17% H_2O in DMF (0.08M) was added, vial was flushed with argon and mixture was heated to 80 °C and stirred for 90 min. EtOAc and saturated aqueous solutions of NaCl and $NaHCO_3$ were added and mixture was transferred to a separatory funnel. Phases were separated and aqueous phase was extracted with EtOAc (3x). The combined organic layers were washed with brine (2x), dried over $MgSO_4$ and evaporated to dryness.

A1.3.11 Characterization data of other Benzoimidazo[2,1,5-*cd*]indolizines

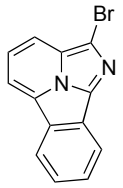

2.7a'

2-Bromobenzo[*a*]imidazo[2,1,5-*c,d*]indolizine (2.7a'): Following **method B**. Yellow-green solid (34 mg, 96% yield). **mp:** 155-157 °C; **^{1}H NMR** ($CDCl_3$, 500 MHz): δ 8.39-8.32 (m, 2H), 8.12-8.02 (m, 2H), 7.80-7.75 (m, 1H), 7.72-7.59 (m, 2H); **^{13}C NMR** ($CDCl_3$, 125 MHz): δ 136.0, 130.1, 129.7, 127.8, 127.1, 125.3, 124.6, 123.3, 122.4, 119.9, 116.1, 111.4, 111.2; **FTIR** (cm^{-1}) (neat): 2925, 1424, 1389, 1336, 1300, 1109, 1070, 743, 727; **HRMS** (ESI, Pos): calcd for $C_{13}H_8BrN_2$ $[M+H]^+$: 270.9865 *m/z*, found 270.9873 *m/z*. This compound does not exhibit significant fluorescence

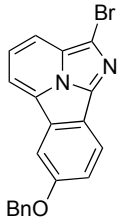

2.7d'

2-Bromo-7-benzyloxybenzo[*a*]imidazo[2,1,5-*c,d*]indolizine (2.7d'): Following **method B**. Yellow solid (114 mg, 90% yield). **mp:** 142-144°C; **^{1}H NMR** ($CDCl_3$, 500 MHz): δ 8.24 (d, *J* = 9.0 Hz, 1H), 8.00 (d, *J* = 8.5 Hz, 1H), 7.95 (d, *J* = 7.0 Hz, 1H), 7.87 (d, *J* = 2.5 Hz, 1H), 7.63 (dd, *J* = 7.5, 9.0 Hz, 1H), 7.53-7.50 (m, 2H), 7.45-7.42 (m, 3H), 7.39-7.35 (m, 1H), 5.26 (s, 2H); **^{13}C NMR** ($CDCl_3$, 125 MHz): δ 157.4, 136.6, 136.1, 131.7, 128.9, 128.4, 127.7, 127.2, 124.5, 122.1, 121.9, 121.0, 119.1, 116.4, 111.4, 110.1, 107.8, 70.9; **FTIR** (cm^{-1}) (neat): 3056, 1620, 1564, 1496, 1435, 1380, 1338, 1282, 1227, 1167, 1104, 1062; **HRMS** (ESI, Pos): calcd for $C_{20}H_{14}BrN_2O$ $[M+H]^+$: 377.0284 *m/z*, found 377.0288 *m/z*. This compound does not exhibit significant fluorescence

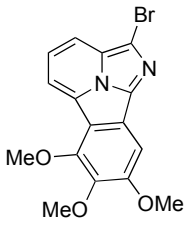

2.7k'

2-Bromo-6,7,8-trimethoxybenzo[*a*]imidazo[2,1,5-*cd*]indolizine (2.7k'): Following **method B**. Green solid (0.20 g, 80% yield). **mp:** 144-146 °C; **^{1}H NMR** ($CDCl_3$, 500 MHz): δ 8.01 (d, *J* = 7.0 Hz, 1H), 7.95 (d, *J* = 9.0 Hz, 1H), 7.67 (dd, *J* = 7.0, 9.0 Hz, 1H), 7.58 (s, 1H), 4.28 (s, 3H), 4.07 (s, 3H), 4.00 (s, 3H); **^{13}C NMR** ($CDCl_3$, 125 MHz): δ 156.9, 150.1, 140.0, 136.0, 126.2, 124.8, 124.1, 123.0, 117.1, 114.8, 112.9, 110.3, 97.6, 61.7, 61.3, 56.6; **FTIR** (cm^{-1}) (neat): 2939, 1617, 1454, 1416, 1275, 1140, 1111, 982, 756; **HRMS** (ESI, Pos): calcd for $C_{16}H_{14}BrN_2O_3$ $[M+H]^+$: 61.0182 *m/z*, found 361.0187 *m/z*. This compound does not exhibit significant fluorescence

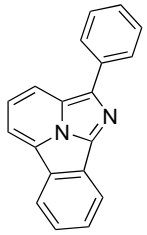

2.8a

2-Phenylbenzo[*a*]imidazo[2,1,5-*c,d*]indolizine (2.8a): Following **method B**. The crude imidazo[2,1,5-*c,d*]indolizine was purified by flash chromatography over silica gel using a gradient of 5% to 35% in hexanes. Fractions containing **2.8a** were concentrated to dryness, resulting in a yellow solid (48 mg, 89% yield). **mp:** 170-172 °C; **^{1}H NMR** ($CDCl_3$, 500 MHz): δ 8.43 (d, *J* = 7.9 Hz, 1H), 8.32 (d, *J* = 8.3 Hz, 2H), 8.24 (d, *J* = 7.6 Hz, 2H), 7.94 (d, *J* = 6.9 Hz, 1H), 7.76 (t, *J* = 7.5 Hz, 1H), 7.69-7.46 (m, 4H), 7.36 (t, *J* = 7.2 Hz, 1H).**^{13}C NMR** ($CDCl_3$, 125 MHz): δ 140.0, 137.0, 135.8, 130.8, 129.4, 129.1, 127.9, 127.2, 126.9, 126.6, 125.0, 123.1, 123.0, 122.4, 120.1, 117.7, 110.8; **FTIR** (cm^{-1}) (neat): 3043, 1600, 1388, 1336, 1102, 1070, 783, 756, 692, **HRMS** (ESI, Pos): calcd for $C_{19}H_{13}N_2$ $[M+H]^+$: 269.1073 *m/z*, found 269.1077 *m/z*.

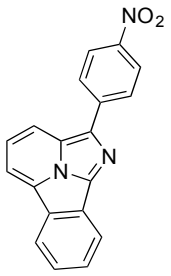

2.8b

2-(4-Nitrophenyl)benzo[*a*]imidazo[2,1,5-*c,d*]indolizine (2.8b): Following **method B**. The crude imidazo[2,1,5-*c*,*d*]indolizine was purified by flash chromatography over silica gel using a gradient of 5% to 35% EtOAc in hexanes. Fractions containing **2.8b** were concentrated to dryness, redissolved in boiling DCM, precipitated with hexanes, cooled to -78°C and filtrated, washing with -78°C hexanes. The residue was recovered as a yellow solid (20 mg, 32% yield). **mp:** 231-234 °C; **^{1}H NMR** ($CDCl_3$, 300 MHz): δ 8.49-8.41 (m, 7H), 8.09 (d, *J* = 7.0 Hz, 1H), 7.88 (d, *J* = 7.0 Hz, 1H), 7.84-7.81 (m, 1H), 7.69 (dd, *J* = 1.0, 7.5 Hz, 1H); **^{13}C NMR** ($CDCl_3$, 125 MHz): δ 146.1, 142.3, 138.5, 136.9, 131.7, 130.1, 128.1, 127.9, 126.2, 124.7, 124.4, 123.5, 120.6, 117.6, 111.1; **FTIR** (cm^{-1}) (neat): 1588, 1494, 1461, 1310, 1098, 1070, 847, 757, 701; **HRMS** (ESI, Pos): calcd for $C_{19}H_{12}N_3O_2$ $[M+H]^+$: 314.0924 *m/z*, found 314.0928 *m/z*; This compound does not exhibit significant fluorescence

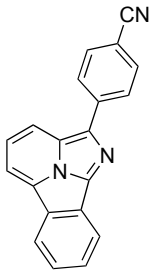

2.8c

4-(Benzo[*a*]imidazo[2,1,5-*c,d*]indolizin-2-yl)benzonitrile (2.8c): Following **method B**. The crude imidazo[2,1,5-*c*,*d*]indolizine was purified by flash chromatography over silica gel using a gradient of 5% to 40% EtOAc in hexanes. Fractions containing **2.8c** were concentrated to dryness, resulting in an yellow solid (17 mg, 58% yield). **mp:** 226-228 °C; **^{1}H NMR** ($CDCl_3$, 500 MHz): δ 8.48 (ddd, *J* = 0.5, 1.0, 8.0 Hz, 1H), 8.43 (ddd, *J* = 0.5, 1.0, 8.0 Hz, 1H), 8.42 (d, *J* = 8.5 Hz, 1H), 8.38 (d, *J* = 8.5 Hz, 2H), 8.10 (d, *J* = 7.0 Hz, 1H), 7.86 (d, *J* = 7.0 Hz, 1H), 7.84 (d, *J* = 7.5 Hz, 1H),

7.69 (d, J = 8.5 Hz, 2H), 7.70 (ddd, J = 1.0, 7.0, 8.0 Hz, 1H); **^{13}C NMR** ($CDCl_3$, 125 MHz): δ 140.1, 138.0, 137.1, 132.7, 131.4, 129.8, 127.9, 127.6, 126.2, 125.8, 124.0, 123.8, 123.3, 120.3, 119.4, 117.3, 110.9, 109.5; **FTIR** (cm^{-1}) (neat): 2926, 2214, 1605, 1414, 1336, 1102, 1072, 748, 838; **HRMS** (ESI, Pos): calcd for $C_{20}H_{12}N_3$ $[M+H]^+$: 294.1026 *m/z*, found 294.1033 *m/z*.

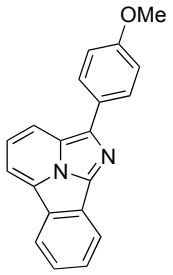

2.8d

2-(4-Methoxyphenyl)benzo[*a*]imidazo[2,1,5-*c,d*]indolizine (2.8d): Following **method B**. The crude imidazo[2,1,5-*c*,*d*]indolizine was purified by flash chromatography over silica gel using a gradient of 0% to 20% EtOAc in hexanes. Fractions containing **2.8d** were concentrated to dryness, resulting in an yellow solid (59 mg, 99% yield). **mp:** 148-151 °C; **^{1}H NMR** ($CDCl_3$, 500 MHz): δ 8.45 (d, J = 8.0 Hz, 1H), 8.41 (d, J = 8.0 Hz, 1H), 8.39 (d, J = 9.0 Hz, 1H), 8.20 (d, J = 8.5 Hz, 2H), 8.05 (d, J = 6.5 Hz, 1H), 7.79 (dd, J = 7.5, 8.0 Hz, 1H), 7.70 (dd, J = 7.0, 8.5 Hz, 1H), 7.61 (dd, J = 7.5, 8.0 Hz, 1H), 7.10 (d, J = 8.5 Hz, 2H), 3.91 (s, 3H); **^{13}C NMR** ($CDCl_3$, 75 MHz): δ 158.9, 140.0, 136.4, 130.4, 129.0, 128.6, 127.7, 127.5, 126.3, 124.5, 122.9, 122.2, 121.6, 119.7, 117.4, 114.5, 110.6, 55.4; **FTIR** (cm^{-1}) (neat): 1517, 1468, 1434, 1241, 1172, 1039, 975, 834, 623; **HRMS** (ESI, Pos): calcd for $C_{20}H_{15}N_2O$ $[M+H]^+$: 299.1179 *m/z*, found 299.1183 *m/z*.

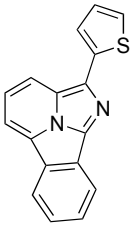

2.8e

2-(Thiophen-2-yl)benzo[*a*]imidazo[2,1,5-*c,d*]indolizine (2.8e): Following **method B**. The crude imidazo[2,1,5-*c*,*d*]indolizine was purified by flash chromatography over silica gel using a gradient of 0% to 20% EtOAc in hexanes. Fractions containing **2.8e** were concentrated to dryness,

resulting in a dark orange solid (13 mg, 86% yield). **mp:** 54-57 °C; **^{1}H NMR** ($CDCl_3$, 300 MHz): δ 8.41 (d, *J* = 8.0 Hz, 1H), 8.32 (d, *J* = 8.0 Hz, 1H), 8.27 (d, *J* = 8.5 Hz, 1H), 7.95 (d, *J* = 7.0 Hz, 1H), 7.78-7.56 (m, 4H), 7.35 (dd, *J* = 1.0, 5.0 Hz, 1H), 7.19 (dd, *J* = 3.5, 5.0 Hz, 1H); **^{13}C NMR** ($CDCl_3$, 125 MHz): δ 131.0, 129.6 (2), 128.1 (2), 127.8, 126.9, 125.2, 124.4, 123.3 (2), 123.2, 122.6, 122.3, 120.4, 117.3, 111.2; **FTIR** (cm^{-1}) (neat): 2922, 2852, 1721, 1423, 1393, 1333, 1063, 748, 699; **HRMS** (ESI, Pos): calcd for $C_{17}H_{11}N_2S$ $[M+H]^+$: 275.0638 *m/z*, found 275.0642 *m/z*.à

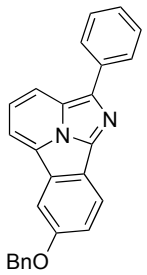

2.8f

7-(Benzyloxy)-2-phenylbenzo[*a*]imidazo[2,1,5-*c,d*]indolizine (2.8f): Following **method B**. The crude imidazo[2,1,5-*c*,*d*]indolizine was purified by flash chromatography over silica gel using a gradient of 5% to 35% EtOAc in hexanes. Fractions containing **2.8f** were concentrated to dryness, resulting in a yellow solid (62 mg, 83% yield). **mp:** 128-130 °C; **^{1}H NMR** ($CDCl_3$, 400 MHz): δ 8.32 (d, *J* = 8.0 Hz, 1H), 8.30 (d, *J* = 8.0 Hz, 1H), 8.23-8.21 (m, 2H), 7.87 (d, *J* = 7.0 Hz, 1H), 7.84 (d, *J* = 2.4 Hz, 1H), 7.58 (dd, *J* = 3.5, 7.0 Hz, 1H), 7.56-7.51 (m, 4H), 7.45-7.33 (m, 5H), 5.24 (s, 2H); **^{13}C NMR** ($CDCl_3$, 125 MHz): δ 157.1, 139.2, 137.0, 136.8, 135.9, 132.3, 129.8, 129.1, 128.8, 128.7, 128.3, 127.7, 127.0, 126.8, 126.5, 122.9, 122.2, 121.9, 121.1, 118.8, 118.0, 110.8, 107.6, 70.2; **FTIR** (cm^{-1}) (neat): 1563, 1497, 1439, 1282, 1059, 1023, 776, 734, 693, ; **HRMS** (ESI, Pos): calcd for $C_{26}H_{19}N2O$ $[M+H]^+$: 375.1492 *m/z*, found 375.1501 *m/z*.

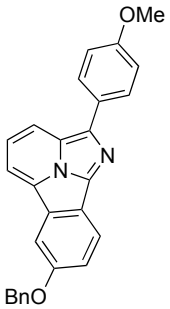

2.8g

7-(benzyloxy)-2-(4-methoxyphenyl)benzo[*a*]imidazo[2,1,5-*c,d*]indolizine (2.8g): Following **method A**. The crude imidazo[2,1,5-*c,d*]indolizine was purified by flash chromatography over silica gel using a gradient of 5% to 35% EtOAc in hexanes. Fractions containing **2.8g** were concentrated to dryness, resulting in an yellow solid (44 mg, 54% yield). **mp:** 121-124 °C; **^{1}H NMR** ($CDCl_3$, 500 MHz): δ 8.28 (d, *J* = 7.5 Hz, 1H), 8.20 (d, *J* = 7.5 Hz, 1H), 8.12 (d, *J* = 7.0 Hz, 2H), 7.81 (d, *J* = 7.0 Hz, 1H), 7.78 (d, *J* = 2.0 Hz, 1H), 7.51-7.35 (m, 7H), 7.06 (d, *J* = 7.0 Hz, 2H), 5.20 (s, 2H), 3.88 (s, 3H); **^{13}C NMR** ($CDCl_3$, 125 MHz): δ 159.0, 156.9, 139.3, 136.8, 136.5, 132.0, 128.8, 128.7, 128.2, 127.7, 127.6, 126.5, 122.3, 122.0, 121.2, 120.9, 118.7, 117.9, 114.6, 110.8, 107.4, 70.7, 55.5.; **FTIR** (cm^{-1}) (neat): 2923, 1607, 1498, 1439, 1233, 1173, 1058, 1019, 828, 694; **HRMS** (ESI, Pos): calcd for $C_{27}H_{21}N_2O_2$ $[M+H]^+$: 405.1598 *m/z*, found 405.1604 *m/z*.

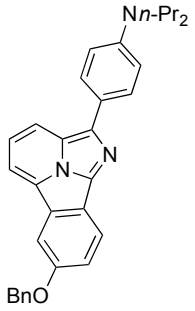

2.8h

4-(7-(Benzyloxy)benzo[*a*]imidazo[2,1,5-*c,d*]indolizin-2-yl)-*N,N*-dipropylaniline (2.8h): Following **method A**. The crude imidazo[2,1,5-*c,d*]indolizine was purified by flash chromatography over silica gel using a gradient of 5% to 35% EtOAc in hexanes. Fractions containing **2.8h** were concentrated to dryness, resulting in an yellow solid (17 mg, 18% yield, 37% corrected for recovered starting material). **mp:** 93-96 °C; **^{11}H NMR** ($CDCl_3$, 500 MHz): δ 8.34 (br d, *J* = 8.5 Hz, 1H), 8.31 (d, *J* = 8.5 Hz, 1H), 8.08 (d, *J* = 8.0 Hz, 1H), 7.92 (d, *J* = 7.0 Hz, 1H), 7.87 (d, *J* = 1.5 Hz, 1H), 7.53-7.35 (m, 7H), 6.82 (br s, 2H), 5.25 (s, 2H), 3.44-3.19 (m, 4H), 1.69 (app sx, *J* = 7.5 Hz, 4H), 0.98 (t, *J* = 7.5 Hz, 6H); **^{13}C NMR** ($CDCl_3$, 100 MHz): δ 156.7, 136.9, 131.7, 128.8 (3), 128.2, 127.8, 127.7 (3), 126.3, 122.1, 121.9 (2), 121.0, 120.5, 118.7, 118.3, 112.3, 111.1, 107.4, 70.8, 53.1, 20.7, 11.6; **FTIR** (cm^{-1}) (neat): 2955, 2871, 1609, 1521, 1438, 1468, 1364, 1235, 1193, 1060, 695; **HRMS** (ESI, Pos): calcd for $C_{32}H_{32}N_3O$ $[M+H]^+$: 474.2540 *m/z*, found 474.2547 *m/z*.

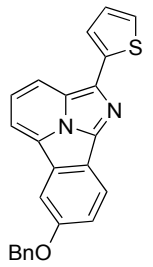

2.8i

7-(Benzyloxy)-2-(thiophen-2-yl)benzo[*a*]imidazo[2,1,5-*c,d*]indolizine (2.8i): Following **method B**. The crude imidazo[2,1,5-*c,d*]indolizine was purified by flash chromatography over silica gel using a gradient of 0% to 20% EtOAc in hexanes. Fractions containing **2.8i** were concentrated to dryness, resulting in a yellow solid (39 mg, 84% yield). **mp:** 127-130 °C; **^{1}H NMR** ($CDCl_3$, 300 MHz): δ 8.32 (d, *J* = 9.0 Hz, 1H), 8.28 (d, *J* = 8.5 Hz, 1H), 7.93 (d, *J* = 7.0 Hz, 1H), 7.87 (d, *J* = 2.5 Hz, 1H), 7.70 (br s, 1H), 7.62 (dd, *J* = 7.0, 8.5 Hz, 1H), 7.53-7.51 (m, 2H), 7.47-7.42 (m, 3H), 7.37 (m, 1H), 7.34 (dd, *J* = 1.0, 5.0 Hz, 1H), 7.19 (dd, *J* = 3.5, 5.0 Hz, 1H), 5.26 (s, 2H); **^{13}C NMR** ($CDCl_3$, 125 MHz): δ 157.3, 138.6, 136.7, 136.5, 133.8, 132.4, 128.8, 128.3, 128.1, 127.7, 126.8, 124.3, 123.1, 122.2, 122.0, 121.8, 121.5, 118.9, 117.5, 111.4, 107.7, 70.8; ; **FTIR** (cm^{-1}) (neat): 2920, 1619, 1562, 1494, 1434, 1382, 1332, 1282, 1202, 1171, 1131; **HRMS** (ESI, Pos): calcd for $C_{24}H_{17}N_2OS$ $[M+H]^+$: 381.1056 *m/z*, found 381.1065 *m/z*.

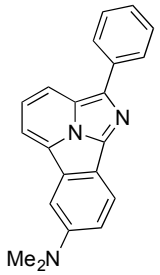

2.8j

N,N-Dimethyl-2-phenylbenzo[*a*]imidazo[2,1,5-*c,d*]indolizin-7-amine (2.8j): Following **method B**. The crude imidazo[2,1,5-*c,d*]indolizine was purified by flash chromatography over silica gel using a gradient of 5% to 35% EtOAc in hexanes. Fractions containing **2.8j** were concentrated to dryness, resulting in a red solid (47 mg, 76% yield). **mp:** 95-98 °C; **^{1}H NMR** ($CDCl_3$, 500 MHz): δ 8.30 (d, *J* = 8.5 Hz, 1H), 8.27 (d, *J* = 8.5 Hz, 1H), 7.88 (d, *J* = 7.0 Hz, 1H), 7.58 (dd, *J* = 7.0, 8.5 Hz, 1H), 7.55 (br s, 1H), 7.54-7.50 (m, 2H), 7.33 (tt, *J* = 1.0, 7.0 Hz, 1H), 7.18 (dd, *J* = 2.5, 8.5 Hz,

1H), 3.13 (s, 6H); **^{13}C NMR** ($CDCl_3$, 125 MHz): δ 149.2, 137.4, 135.4, 133.4, 129.1 (2), 128.0, 126.9, 126.3 (2), 122.4, 122.2, 121.2, 117.9, 115.8, 110.4, 105.4, 41.2; **FTIR** (cm^{-1}) (neat): 3060, 2924, 1624, 1562, 1499, 1436, 1063, 775, 698; **HRMS** (ESI, Pos): calcd for $C_{21}H_{18}N_3$ $[M+H]^+$: 312.1495 *m/z*, found 312.1502 *m/***FTIR** (cm^{-1}) (neat): 3060, 2924, 1624, 1562, 1499, 1436, 1063, 775, 698; **HRMS** (ESI, Pos): calcd for $C_{21}H_{18}N_3$ $[M+H]^+$: 312.1495 *m/z*, found 312.1502 *m/z*.

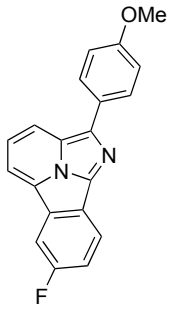

2.8k

7-Fluoro-2-(4-methoxyphenyl)benzo[*a*]imidazo[2,1,5-*c,d*]indolizine (2.8k): Following **method A**. The crude imidazo[2,1,5-*c*,*d*]indolizine was purified by flash chromatography over silica gel using a gradient of 5% to 35% EtOAc in hexanes. Fractions containing **2.8k** were concentrated to dryness, resulting in a blood red solid (44 mg, 79% yield). **mp:** 148-151 °C; **^{1}H NMR** (CD_2Cl_2, 300 MHz): δ 8.44 (d, *J* = 8.5 Hz, 1H), 8.37 (ddd, *J* = 0.3, 5.0, 8.5 Hz, 1H), 8.21-8.16 (m, 2H), 8.13-8.09 (m, 2H), 7.73 (dd, *J* = 7.0, 8.5 Hz, 1H), 7.55 (dt, *J* = 2.5, 9.0 Hz, 1H), 7.11-7.07 (m, 2H), 5.42 (s, 2H), 3.90 (s, 3H); **^{13}C NMR** (CD_2Cl_2, 125 MHz): δ 160.7 (d, *J* = 237.5 Hz, $J_{C\text{-}F}$) 159.4, 157.3, 139.8, 135.6, 131.6 (d, *J* = 10.0 Hz, $J_{C\text{-}F}$), 128.0, 126.2 (d, *J* = 5.0 Hz, $J_{C\text{-}F}$), 123.9, 122.5, 121.9, 121.7 (d, *J* = 10.0 Hz, $J_{C\text{-}F}$), 118.7, 117.8 (d, *J* = 25.0 Hz, $J_{C\text{-}F}$), 114.7, 112.1, 109.4 (d, *J* = 25.0 Hz, $J_{C\text{-}F}$), 55.5; 19F nmr NMR (CD2Cl2, 282 MHz): δ -115.3; **FTIR** (cm^{-1}) (neat): 1609, 1517, 1434, 1241, 1172, 1039, 975, 834, 623; **HRMS** (ESI, Pos): calcd for $C_{20}H_{14}FN_2O$ $[M+H]^+$: 317.10847 *m/z*, found 317.1091 *m/z*

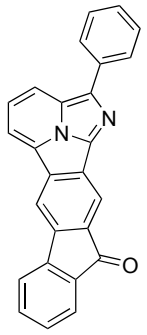

2.8l

2-Phenyl-11*H*-fluoreno[3,2-*a*]imidazo[2,1,5-*c,d*]indolizin-11-one (2.8l): Following **method A**. The crude imidazo[2,1,5-*c,d*]indolizine was purified by flash chromatography over silica gel using a gradient of 1% to 5% MeOH in DCM. Fractions containing **2.8l** were concentrated to dryness, resulting in a purple solid (53 mg, 64% yield). **mp:** 310-315 °C; **^{1}H NMR** (CD_2Cl_2, 500 MHz): δ 8.66 (s, 1H), 8.55-8.51 (m, 2H), 8.33-8.28 (m, 3H), 7.88 (dd, *J* = 7.0, 8.5 Hz, 1H), 7.77-7.72 (m, 2H), 7.62-7.59 (m, 3H), 7.45 (t, *J* = 7.0 Hz, 1H), 7.45 (dt, *J* = 0.5, 7.0 Hz, 1H); **^{13}C NMR** (DMF-d7, 175 MHz): δ 192.4, 145.0, 141.4, 139.5, 136.6, 135.8, 135.6, 135.0 (2x), 134.5, 129.5, 129.2, 127.6, 127.0, 126.5, 126.3, 124.2, 124.2, 123.9, 121.3, 120.0, 116.5, 115.5, 114.8; **FTIR** (cm^{-1}) (neat): 3053, 1714, 1587, 1333, 1301, 1052, 1020, 812, 743; **HRMS** (ESI, Pos): calcd for $C_{26}H_{15}N_2O$ $[M+H]^+$: 371.1184 *m/z*, found 371.1198 *m/z*. This compound does not exhibit significant fluorescence because of limited solubility in MeOH.

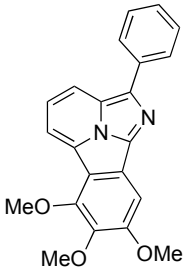

2.8m

4-(6,7,8-Trimethoxybenzo[*a*]imidazo[2,1,5-*c,d*]indolizin-2-yl)benzonitrile (2.8m): Following **method A**. The crude imidazo[2,1,5-*c,d*]indolizine was purified by flash chromatography over silica gel using a gradient of 0% to 20% EtOAc in hexanes. Fractions containing **8m** were concentrated to dryness, resulting in a dark orange solid (55 mg, 77% yield).

Following **method B**. The crude imidazo[2,1,5-*c,d*]indolizine was purified by flash chromatography over silica gel using a gradient of 0% to 20% EtOAc in hexanes. Fractions containing **2.8m** were concentrated to dryness, resulting in a dark orange solid (32 mg, 89% yield).

mp: 124-127 °C; **^{1}H NMR** ($CDCl_3$, 400 MHz): δ 8.32 (d, *J* = 8.5 Hz, 1H), 8.24 (d, *J* = 7.5 Hz, 1H), 8.00 (d, *J* = 7.0 Hz, 1H), 7.69 (s, 1H), 7.67 (dd, *J* = 7.0, 7.5 Hz, 1H), 7.53 (app t, *J* = 8.0 Hz, 2H), 7.35 (app t, *J* = 7.5 Hz, 1H), 4.29 (s, 3H), 4.08 (s, 3H), 4.01 (s, 3H); **^{13}C NMR** ($CDCl_3$, 75 MHz): δ 156.6, 150.1, 139.8, 139.6, 137.2, 135.9, 129.1, 127.1, 126.5, 125.9, 124.4, 123.3, 123.0, 117.7, 116.5, 112.3, 97.7, 61.7, 61.3, 56.7.; **FTIR** (cm^{-1}) (neat): 2927, 1617, 1502, 1452, 1417, 1276, 1238, 1192, 1136, 1102, 1049; **HRMS** (ESI, Pos): calcd for $C_{22}H_{19}N_2O_3$ $[M+H]^+$: 359.1390 *m/z*, found 359.1397 *m/z*.

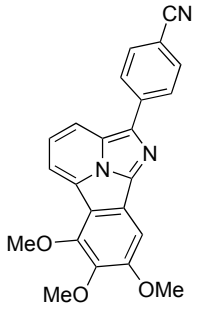

8n

4-(6,7,8-Trimethoxybenzo[*a*]imidazo[2,1,5-*c,d*]indolizin-2-yl)benzonitrile (2.8n): Following **method B**. The crude imidazo[2,1,5-*c,d*]indolizine was purified by flash chromatography over silica gel using a gradient of 0% to 20% EtOAc in hexanes. Fractions containing **2.8n** were concentrated to dryness, resulting in an orange (34 mg, 89% yield). **mp:** 209-212 °C; **^{1}H NMR** ($CDCl_3$, 400 MHz): δ 8.30 (d, *J* = 7.5 Hz, 2H), 8.25 (d, *J* = 8.5 Hz, 1H), 8.01 (d, *J* = 7.0 Hz, 1H), 7.76 (d, *J* = 7.5 Hz, 3H), 7.66 (s, 1H), 4.30 (s, 3H), 4.10 (s, 3H), 4.02 (s, 3H); **^{13}C NMR** ($CDCl_3$, 75 MHz): δ 157.0, 150.3, 140.4, 140.3, 138.2, 136.8, 132.9, 126.6, 126.3, 124.7, 124.4, 124.2, 119.5, 118.2, 116.1, 112.4, 109.5, 98.0, 61.7, 61.3, 56.7. **FTIR** (cm^{-1}) (neat): 2936, 2217, 1602, 1504, 1459, 1411, 1280, 1240, 1198, 1169, 1138, 1103; **HRMS** (ESI, Pos): calcd for $C_{23}H_{18}N_3O_3$ $[M+H]^+$: 384.1342 *m/z*, found 384.1349 *m/z*.

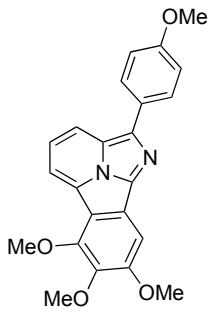

2.8o

6,7,8-Trimethoxy-2-(4-methoxyphenyl)benzo[*a*]imidazo[2,1,5-*c,d*]indolizine (2.8o): Following **method B**. The crude imidazo[2,1,5-*c,d*]indolizine was purified by flash chromatography over silica gel using a gradient of 0% to 20% EtOAc in hexanes. Fractions containing **2.8o** were concentrated to dryness, resulting in a deep red solid (35 mg, 90% yield). **mp:** 148-151 °C; **^{1}H NMR** ($CDCl_3$, 300 MHz): δ 8.28 (d, *J* = 8.5 Hz, 1H), 8.18-8.15 (m, 2H), 8.01 (d, *J* = 7.0 Hz, 1H), 7.68 (s, 1H), 7.65 (dd, *J* = 7.0, 8.5 Hz, 1H), 7.10-7.06 (m, 2H), 4.29 (s, 3H), 4.09 (s, 3H), 4.01 (s, 3H), 3.90 (s, 3H); **^{13}C NMR** ($CDCl_3$, 75 MHz): δ 159.1, 156.5, 150.1, 139.8, 139.6, 136.9, 128.8, 127.8, 125.6, 124.3, 122.8, 122.4, 117.5, 116.5, 114.6, 112.3, 97.6, 61.7, 61.3, 56.7, 55.5; **FTIR** (cm^{-1}) (neat): 2970, 1610, 1568, 1517, 1468, 1434, 1330, 1241, 1172, 1095; **HRMS** (ESI, Pos): calcd for $C_{23}H_{21}N_2O_4$ $[M+H]^+$: 389.1496 *m/z*, found 389.1504 *m/z*.

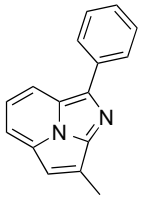

2.8p

7-Methyl-2-phenylimidazo[2,1,5-*c,d*]indolizine (2.8p): Following **method A**. The crude imidazo[2,1,5-*c,d*]indolizine was purified by flash chromatography over silica gel using a gradient of 10% to 60% EtOAc in hexanes. Fractions containing **2.8p** were concentrated to dryness, resulting in a yellow oil (72 mg, 61% yield). **^{1}H NMR** ($CDCl_3$, 500 MHz): δ 8.32 (d, *J* = 8.0 Hz, 1H), 8.29-8.25 (m, 2H), 7.85 (d, *J* = 7.5 Hz, 1H), 7.21 (t, *J* = 7.5 Hz, 1H), 7.54 (t, *J* = 7.5 Hz, 2H), 7.41-7.36 (m, 1H), 7.17-7.15 (m, 1H), 2.87 (d, *J* = 0.5 Hz, 1H); **^{13}C NMR** ($CDCl_3$, 125 MHz): δ 144.1, 140.4, 135.5, 130.7, 129.0, 128.5, 127.7, 127.0, 124.3, 122.6, 115.4, 114.6, 112.9, 12.6; **FTIR** (cm^{-1}) (neat):

3379, 3064, 2951, 2899, 2802, 2787, 1111, 1021, 779; **HRMS** (ESI, Pos): calcd for $C_{16}H_{13}N_2$ $[M+H]^+$: 233.1079 *m/z*, found 233.1084 *m/z*.

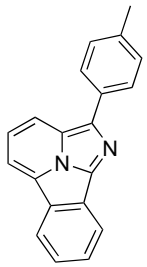

2.8r

2-(4-Methylphenyl)benzo[*a*]imidazo[2,1,5-*c,d*]indolizine (2.8r): Following **method A**. The crude imidazo[2,1,5-*c,d*]indolizine was purified by flash chromatography over silica gel using a gradient of 5% to 35% EtOAc in hexanes. Fractions containing **2.8p** were concentrated to dryness, resulting in a shiny orange foam (55 mg, 97% yield). **mp** = 51-54 °C; **^{1}H NMR** ($CDCl_3$, 400 MHz): δ 8.48 (d, *J* = 8.0 Hz, 1H), 8.40 (d, *J* = 8.5 Hz, 1H), 8.39 (d, *J* = 8.0 Hz, 1H), 8.15 (d, *J* = 8.0 Hz, 2H), 8.04 (d, *J* = 7.0 Hz, 1H), 7.79 (app dt, *J* = 1.0, 8.5 Hz, 1H), 7.72 (dd, *J* = 7.0, 8.5 Hz, 1H), 7.62 (app dt, *J* = 1.0, 8.5 Hz, 1H), 7.36 (d, *J* = 8.0 Hz, 2H), 2.45 (s, 3H); **^{13}C NMR** ($CDCl_3$, 101 MHz): δ 137.3, 130.7, 129.8 (2), 129.4, 127.4, 126.9, 126.5, 126.4, 125.1, 123.1 (2), 122.5, 122.4, 120.4, 118.0, 111.2, 21.4.**FTIR** (cm^{-1}) (neat): 3058, 2920, 1619, 1521, 1498, 1463, 1427, 1334, 1284, 1224, 1186, 1164; **HRMS** (ESI, Pos): calcd for $C_{20}H_{15}N_2$ $[M+H]^+$: 283.1230 *m/z*, found 283.1239 *m/z*.

A1.3.12.General procedure for double C-H arylation of imidazo[2,1,5-*c,d*]indolizine 2.8q

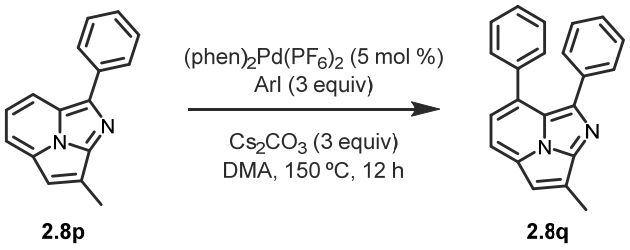

7-Methyl-2,3-diphenylimidazo[2,1,5-*c,d*]indolizine (2.8q): To a 5 mL microwave vial (VWR® 2-5 mL) equipped with a magnetic stirbar and a rubber septum was added Cs_2CO_3 (0.90 mmol, 3.0 equiv). The vial was heated to 150 °C in an oil bath under vacuum for 30 min. The tube was cooled

to room temperature, flushed with argon and iodobenzene (0.60 mmol, 2.0 equiv) and imidazo[2,1,5-*c*,*d*]indolizine (0.30 mmol, 1.0 equiv) as previously synthesized were added. DMA (0.6 mL, 0.5 M) was used to cannulate $[Pd(phen)_2][PF_6]_2$ (11 mg, 15 μmol, 0.05 equiv) from a dry 4 mL vial into the reaction vessel. The vial was capped with an aluminum microwave cap (VWR® with Teflon seal) and heated to 150 °C in an oil bath for 16 h. Brine and EtOAc were added and mixture was transferred to a separatory funnel. Phases were separated and aqueous phase was extracted with EtOAc (3X). The combined organic layers were washed with brine (2x), dried over $MgSO_4$ and evaporated to dryness. The crude imidazo[2,1,5-*c*,*d*]indolizine was purified by flash chromatography over silica gel using a gradient of 10% to 60% EtOAc in hexanes. Fractions containing **2.8q** were concentrated to dryness, resulting in an orange solid (53 mg, 65% yield). **mp:** 138-140 °C; **^{1}H NMR** ($CDCl_3$, 500 MHz): δ 8.37 (d, *J* = 8.0 Hz, 1H), 8.31-8.28 (m, 2H), 7.96 (d, *J* = 7.5 Hz, 1H), 7.76 (t, *J* = 8.0 Hz, 1H), 7.71-7.68 (m, 2H), 7.59-7.53 (m, 4H), 7.44-7.38 (m, 2H), 2.94 (s, 3H); **^{13}C NMR** ($CDCl_3$, 125 MHz): δ 144.0, 140.8, 135.5, 134.4, 129.6, 129.1, 128.9, 127.9, 127.7, 127.2, 127.0 (2), 126.1, 124.7, 123.0, 116.0, 114.7, 11.5; **FTIR** (cm^{-1}) (neat): 3386, 3055, 2975, 2903, 2847, 2733, 1114, 1038, 764; **HRMS** (ESI, Pos): calcd for $C_{22}H_{17}N_2$ $[M+H]^+$: 309.1392 *m/z*, found 309.1398 *m/z*.

A1.3.13. General procedure for the Neigishi Coupling

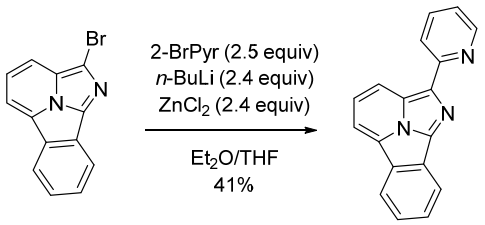

2.7a' **2.8s**

To a 25 mL flame-dried microwave (sealable) vial (VWR®) equipped with a magnetic stirrer and a rubber septum and cooled to -78°C was added *n*BuLi (1.0 mL, 1.3 M, 1.3 mmol, 2.4 equiv). A solution of 2-bromopyridine (0.13 mL, 1.4 mmol, 2.5 equiv) in Et_2O (1.0 mL) was added dropwise. Mixture was warmed to 0°C and a solution of $ZnCl_2$ (0.18 g, 1.3 mmol, 2.4 equiv) in THF (1.0 mL) was added. Mixture was warmed to room temperature and a suspension of **2.7a'** (0.15 g, 0.55 mmol, 1.0 equiv) and $(PPh_3)_4Pd$ (32 mg, 0.03 mmol, 0.05 equiv) in THF (2.0 mL) was added. Mixture was refluxed for 16h. EtOAc, H_2O and disodium EDTA were added. Phases were separated and and aqueous phase was extracted with EtOAc (3x). Organic phases were combined, washed with brine,

dried over $MgSO_4$, filtrated and evaporated to dryness. The crude orange-red solid was purified by flash chromatography over silica gel (0% - 50% EtOAc in hexanes). Fractions containing **2.8s** were concentrated to dryness, resulting in an orange solid. The solid was dissolved in boiling DCM and hexanes were added until cloudy. Mixture was slowly cooled to -20°C. Deep orange crystals (61 mg, 0.23 mmol, 41% yield) were recovered by filtration (washing with cold hexanes). **mp:** 136-138 °C; **^{1}H NMR** ($CDCl_3$, 500 MHz): δ 8.87 (d, *J* = 14.0 Hz, 1H), 8.74-8.71 (m, 1H), 8.47-8.38 (m, 3H), 8.05 (d, *J* = 11,5 Hz, 1H), 7.84-7.76 (m, 3H), 7.66-7.60 (m, 1H), 7.21-7.16 (m, 1H).**^{13}C NMR** ($CDCl_3$, 125 MHz): δ 155.2, 149.6, 139.3, 137.1, 136.6, 131.4, 129.3, 128.0, 126.9, 125.2, 124.9, 123.7, 123.2, 121.3, 120.4, 120.2, 119.9; 111.1 **FTIR** (cm^{-1}) (neat): 1589, 1455, 1317, 1104, 1068, 1000, 962, 793, 760, 750, 730, 697. **HRMS** (ESI, Pos): calcd for $C_{18}H_{12}N_3$ $[M+H]^+$: 270.10257 *m/z*, found 270.10322 *m/z*.

A1.3.14.General procedure for the *N*-alkylation of Benzo[*a*]imidazo[2,1,5-*c,d*]indolizines

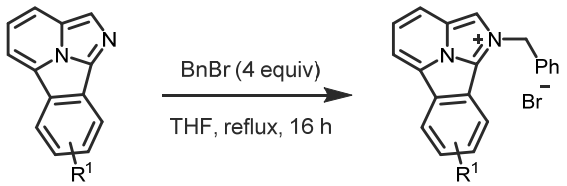

2.7 **2.9**

To a flame-dried microwave (sealable) vial (VWR®) equipped with a magnetic stirrer and a rubber septum was added the corresponding benzo[*a*]imidazo[2,1,5-*c,d*]indolizine (0.25 mmol, 1.0 equiv) as previously synthesized, THF (0.5 M) and benzyl bromide (1.0 mmol, 4.0 equiv). The vial was capped with an aluminum microwave cap (VWR® with Teflon seal) and heated to 60 °C in an oil bath for 16 h. Diethyl ether was added and the resulting slurry was filtered on fritted glass and washed with diethyl ether.

A1.3.15 Characterization data of benzoimidazo[2,1,5-*c,d*]indoliziniums

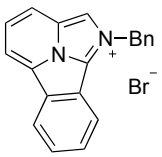

2.9a

1-Benzylbenzo[*a*]imidazo[2,1,5-*c,d*]indolizin-1-ium bromide (2.9a): Following general procedure. Product obtained as a bright yellow solid, (93 mg, quantitative yield). mp: 247-250 °C; **^{1}H NMR** (CD_3OD, 400 MHz): δ 8.78 (s, 1H), 8.70-8.66 (m, 1H), 8.65 (d; *J* = 7.0 Hz, 1H), 8.50 (d, *J* = 9.0 Hz, 1H), 8.16 (dd, *J* = 7.0, 7.5 Hz, 1H), 8.10-8.07 (m, 1H), 7.92-7.87 (m, 2H), 7.62-7.57 (m, 2H), 7.50-7.44 (m, 3H), 6.30 (s, 2H); **^{13}C NMR** (CD_3OD, 125 MHz): δ 135.3, 134.0, 132.7, 132.1, 130.6 (3), 130.1, 129.6, 129.6, 125.7, 125.3, 124.1, 122.7, 122.2, 120.7, 118.2, 55.6; **FTIR** (cm-1) (neat): 3021, 1510, 1450, 1429, 1354, 1178, 1160, 1128, 1081, 1015; **HRMS** (ESI, Pos): calcd for $C_{20}H_{15}N_2$ [M+H]+: 283.1230 m/z, found 283.1235 m/z

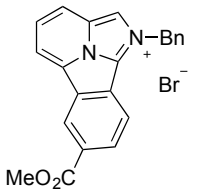

2.9b

1-Benzyl-7-(methoxycarbonyl)benzo[*a*]imidazo[2,1,5-*c,d*]indolizin-1-ium bromide (2.9b): Following general procedure. Product obtained as a bright yellow solid, (44 mg, 98% yield). **mp:** 215-218 °C; **^{1}H NMR** ($CDCl_3$, 400 MHz): δ 10.10 (s, 1H), 9.11 (d, *J* = 0.5 Hz, 1H), 8.59 (d, *J* = 7.0 Hz, 1H), 8.52 (d, *J* = 5.5 Hz, 1H), 8.42 (dd, *J* = 0.5, 6.5 Hz, 1H), 8.11 (dd, *J* = 6.0, 6.5 Hz, 1H), 7.98 (d, *J* = 6.8 Hz, 1H), 7.68 (dd, *J* = 1.0, 6.5 Hz, 2H), 7.34-7.26 (m, 3H), 6.73 (s, 2H), 4.01 (s, 3H); **^{13}C NMR** ($CDCl_3$, 125 MHz):δ 165.5, 133.6, 131.9, 131.5, 130.4, 129.6, 129.5, 128.9, 128.2, 127.9, 125.7, 125.3, 125.2 (2), 123.6, 121.9, 121.3, 117.6, 55.6, 52.9; **FTIR** (cm-1) (neat): 3024, 1716, 1430, 1348, 1321, 1290, 1249, 1167, 1130, 1069; **HRMS** (ESI, Pos): calcd for $C_{22}H_{17}N_2O_2$ [M+H]+: 341.1285 m/z, found 341.1291 m/z.

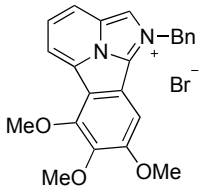

2.9c

1-Benzyl-6,7,8-trimethoxybenzo[*a*]imidazo[2,1,5-*c,d*]indolizin-1-ium bromide (2.9c): Following general procedure. Product obtained as a bright yellow solid, (118 mg, 99% yield). **mp**: 207-210 °C; **^{1}H NMR** ($CDCl_3$, 400 MHz): δ 9.76 (s, 1H), 8.30 (d, *J* = 9.0 Hz, 1H), 8.19 (d, *J* = 7.0

Hz, 1H), 7.92 (t, *J* = 8.0 Hz, 1H), 7.67 (d, *J* = 6.5 Hz, 2H), 7.33-7.26 (m, 3H), 7.15 (br s, 1H), 6.78 (s, 2H), 4.27 (s, 3H), 4.00 (s, 3H), 3.96 (s, 3H); **^{13}C NMR** ($CDCl_3$, 75 MHz): δ 157.6, 149.7, 141.8, 134.0, 130.2, 128.9 (2), 128.6, 127.9, 126.9, 122.7, 122.0, 118.3, 118.1, 117.9, 116.8, 100.4, 61.3, 61.1, 57.6, 54.5.; **FTIR** (cm-1) (neat): 3365, 3053, 2936, 1612, 1514, 1471, 1418, 1356, 1290, 1269, 1251, 1194, 1168, 1119, 1102, 1052; **HRMS** (ESI, Pos): calcd for $C_{23}H_{21}N_2O_3$ [M+H]+: 373.1547 m/z, found 373.1562 m/z.

A1.3.16 General procedures for the derivatization of imidazo[2,1,5-c,d]indolizines

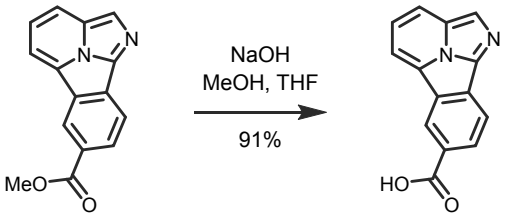

2.7i **2.10a**

Benzo[*a*]imidazo[2,1,5-*c,d*]indolizine-7-carboxylic acid (2.10a): To a 5 mL round-bottom flask equipped with a magnetic stirbar and a rubber septum was added methyl benzo[*a*]imidazo[2,1,5-*cd*]indolizine-7-carboxylate (**2.7i**) (22 mg, 0.09 mmol, 1.0 equiv) as previously synthesized. 2.0 M NaOH in water (0.35 mL, 0.70 mmol, 8.0 equiv), THF (0.22 mL) and MeOH (0.22 mL) were added. The resulting suspension was vigorously stirred at room temperature for 16 h (becomes homogenous after 2h). 12N HCl was added dropwise until pH = 2, causing precipitation. The residue was recovered by filtration, washing with 2N HCl, then with EtOAc, yielding a brown solid (19 mg, 0.08 mmol, 92% yield). **mp**: >310 °C; **1H NMR** ($CDCl_3$, 400 MHz): δ 9.35 (s, 1H), 8.74 (d, *J* = 7.0 Hz, 1H), 8.71 (s, 1H), 8.59 (d, *J* = 8.5 Hz, 1H), 8.49 (d, *J* = 8.5 Hz, 1H), 8.18 (t, *J* = 8.0 Hz, 1H); **^{13}C NMR** (CD_3OD, 125 MHz): δ 174.9, 136.1, 134.3, 130.8, 130.7, 128.3, 127.5, 126.6, 126.3, 124.8, 123.8, 118.7, 117.9, 112.3; **FTIR** (cm-1) (neat): 3130, 1703, 1420, 1349, 1293, 1267, 1226, 1156, 1114, 1074 ; **HRMS** (ESI, Pos): calcd for $C_{14}H_9N_2O_2$ [M+H]+: 237.0659 m/z, found 237.0667 m/z.

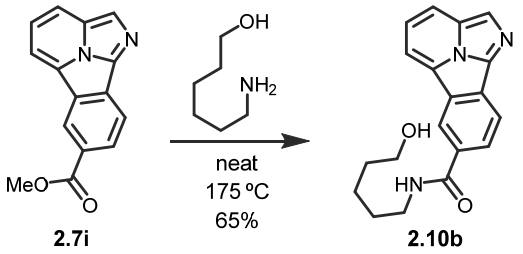

***N*-(6-Hydroxyhexyl)benzo[*a*]imidazo[2,1,5-*c,d*]indolizine-7-carboxamide (2.10b):** To a flame-dried 2 mL microwave vial (VWR® 0.5-2 mL) equipped with a magnetic stirrer and rubber septum were added methyl benzo[*a*]imidazo[2,1,5-*cd*]indolizine-7-carboxylate (**2.7i**) (50 mg, 0.20 mmol, 1.0 equiv) as previously synthesized and 6-aminohexanol (94 mg, 0.80 mmol, 4.0 equiv). The solids were heated to 175 °C in an oil bath (melts) and stirred for 4h under a light flow of argon. Mixture was cooled and dissolved in CH_2Cl_2 with a few drops of MeOH. Saturated aqueous NH_4Cl was added and phases were separated. Aqueous phase was extracted with DCM (4x), organic phases were combined, dried over $MgSO_4$ and evaporated to dryness. Purification by flash chromatography (2-10% MeOH/DCM) yielded a yellow powder (43 mg, 0.13 mmol, 64% yield). mp: 148-151 °C; **^{1}H NMR** (CD_3OD, 400 MHz): δ 9.06 (s, 1H), 8.40 (dd, *J* = 7.0, 9.0 Hz, 1H), 8.31 (s, 1H), 8.27 (dd, *J* = 1.5, 9.0 Hz, 1H), 7.91 (dd, *J* = 7.0, 9.0 Hz, 1H), 3.58 (t, *J* = 6.5 Hz,2H), 3.50 (t, *J* = 7.0 Hz, 2H), 1.73 (qn, *J* = 6.5 Hz, 2H), 1.59 (qn, *J* = 6.5 Hz, 2H), 1.50-1.47 (m, 4H); **^{13}C NMR** (CD_3OD, 100 MHz): δ 169.3, 136.0, 133.6, 132.4, 129.5, 128.9, 127.1, 126.8, 125.7, 124.2, 120.5, 119.6, 114.7, 62.9, 41.3, 33.6, 30.6, 28.0, 26.7; **FTIR** (cm-1) (neat): 3293, 2932, 2857, 1626, 1533, 1461, 1336, 1241, 1065; **HRMS** (ESI, Pos): calcd for $C_{20}H_{22}N_3O_2$ [M+H]+: 336.1707 m/z, found 336.1717 m/z.

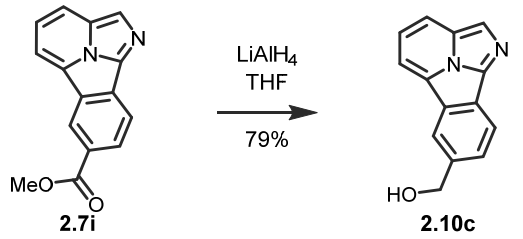

Benzo[*a*]imidazo[2,1,5-*c,d*]indolizin-7-ylmethanol (2.10c) : To a flame dried 5 mL round-bottom flask equipped with a magnetic stirbar and a rubber septum were added $LiAlH_4$ (19 mg, 0.50 mmol, 2.5 equiv) and THF (0.5 mL). This suspension was cooled at 0 °C before adding a solution of methyl benzo[*a*]imidazo[2,1,5-*cd*]indolizine-7-carboxylate (**2.7i**) (50 mg, 0.20 mmol, 1.0 equiv) as previously synthesized in THF (0.5 mL). The reaction mixture was stirred at 0 °C for 4 h. The mixture was poured in a saturated aqueous solution of sodium potassium tartrate cooled to 0

°C and stirred until gas evolution stops. DCM was added and phases were separated. Aqueous phase was extracted with DCM (2x), organic phases were combined, washed with brine, dried over $MgSO_4$ and evaporated to dryness. Purification by flash chromatography (0.5 - 10% MeOH/DCM) yielded a yellow powder (35 mg, 0.16 mmol, 79% yield). Single crystals were obtained by dissolving the product in boiling 1% MeOH/DCM, then adding hot hexanes (50 °C) until a slight cloudiness is observed and slowly cooling to -20 °C. mp: 154-155 °C; **^{1}H NMR** ($CDCl_3$, 400 MHz): δ 8.39 (s, 1H), 8.33 (d, *J* = 6.5 Hz, 1H), 8.22 (s, 1H), 8.14 (d, *J* = 7.0 Hz, 1H), 7.98 (d, *J* = 5.5 Hz, 1H), 7.74 (d, *J* = 5.5 Hz, 1H), 7.67 (dd, *J* = 5.5, 7.0 Hz, 1H); **^{13}C NMR** ($CDCl_3$, 125 MHz): δ 138.0, 137.5, 131.5, 128.5, 127.6, 127.5, 126.7, 125.9, 121.9, 121.5, 120.1, 117.0, 110.6, 65.6; **FTIR** (cm-1) (neat): 3121, 2909, 1435, 1410, 1333, 1298, 1277, 1238, 1168, 1080; **HRMS** (ESI, Pos): calcd for $C_{14}H_{11}N_2O$ [M+H]+: 223.0866 m/z, found 223.0876 m/z.

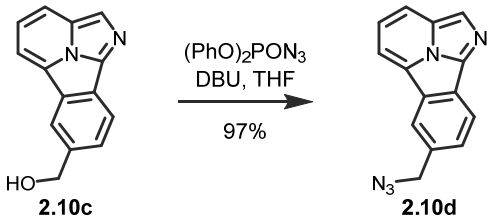

2.10c **2.10d**

7-(Azidomethyl)benzo[*a*]imidazo[2,1,5-*c,d*]indolizine (2.10d) : To a 5-mL round-bottom flask equipped with a magnetic stirbar and a rubber septum were added benzo[*a*]imidazo[2,1,5-*cd*]indolizin-7-ylmethanol (**2.10c**) (56 mg, 0.25 mmol, 1.0 equiv) as previously synthesized, diphenylphosphoryl azide (DPPA) (65 µL, 0.30 mmol, 1.2 equiv), 1,8-diazabicyclo[5.4.0]undec-7-ene (DBU) (45 mL, 0.30 mmol, 1.2 equiv) and THF (1.0 mL, 0.25 M). Mixture was stirred at room temperature for 16h. 1.0 mL of CH_2Cl_2 was added and the resulting solution was directly added on a silica column. Flash chromatography over silica gel using a gradient of 1% to 8% CH_2Cl_2 in hexanes. Fractions containing **2.10d** were concentrated to dryness, resulting in a yellow solid (60 mg, 0.24 mmol, 97% yield). mp: 110-112 °C; **^{1}H NMR** ($CDCl_3$, 500 MHz): δ 8.41 (d, *J* = 8.0 Hz, 1H), 8.34 (s, 1H), 8.25 (s, 1H), 8.16 (d, *J* = 8.5 Hz, 1H), 8.05 (d, *J* = 7.0 Hz, 1H), 7.71 (dd, *J* = 1.5, 8.0 Hz, 1H), 7.69 (dd, *J* = 7.0, 8.5 Hz, 1H), 4.63 (s, 2H); **^{13}C NMR** ($CDCl_3$, 125 MHz): δ 137.1, 132.3, 131.4, 129.5, 127.9, 127.8, 126.3, 126.0, 122.8, 122.0, 120.4, 117.3, 111.0, 55.2; **FTIR** (cm-1) (neat): 2933, 2107, 2080, 1623, 1531, 1450, 1433, 1411, 1336, 1295, 1237, 1199, 1167, 1157, 1078; **HRMS** (ESI, Pos): calcd for $C_{14}H_{10}N_5$ [M+H]+: 248.0931 m/z, found 248.094 m/z.

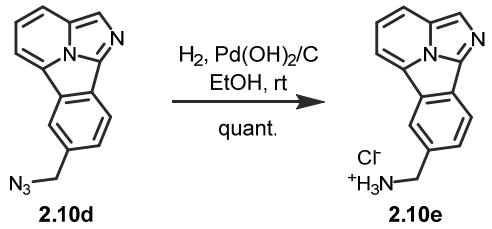

2.10d **2.10e**

Benzo[*a*]imidazo[2,1,5-*c,d*]indolizin-7-ylmethanaminium chloride (2.10e) : To a 5-mL round-bottom flask equipped with a magnetic stirbar and a rubber septum were added benzo[*a*]imidazo[2,1,5-*cd*]indolizine-7- (**2.7j**) (25 mg, 0.10 mmol, 1.0 equiv) as previously synthesized, 20% $Pd(OH)_2$ on carbon (4 mg, 5 μmol, 0.05 equiv) and EtOH (0.35 mL, 0.3 M). Hydrogen gas was bubbled in the suspension for 50 min and the mixture was stirred under an hydrogen atmosphere (1 bar) for 20 h. Excess 2N HCl was added and suspension was filtered on Celite. Filtrate was concentrated under vacuum to remove organic solvents. The resulting yellow aqueous phase was washed with DCM (4x) and concentrated to dryness. The solid was dissolved in DCM with 2-3 drops of MeOH and precipitated by the rapid addition of Et_2O. The residue was recovered by filtration of fritted glass, washing with ether, yielding a yellow solid (26 mg, 0.10 mmol, quantitative yield). mp: >310 °C; **^{1}H NMR** (D_2O, 500 MHz): δ 8.25-8.20 (m, 3H), 8.12 (d, J = 7.0 Hz, 1H), 7.98 (d, J = 8.5 Hz, 1H), 7.81 (app t, J = 8.5 Hz, 1H), 7.74 (d, J = 8.0 Hz, 1H), 4.39 (s, 2H); **^{13}C NMR** (D_2O, 125 MHz): δ 132.7, 131.6, 130.8, 127.3, 126.8, 124.1, 122.4, 121.0, 120.0, 118.4, 116.6, 42.9; **FTIR** (cm-1) (neat): 3401, 2855, 1613, 1489, 1421, 1377, 1353, 1226, 1082, 1056; **HRMS** (ESI, Pos): calcd for $C_{14}H_{12}N_3$ [M+H]+: 222.1026 m/z, found 222.1031 m/z.

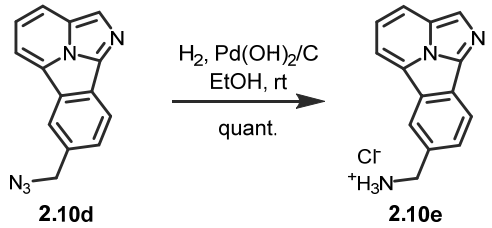

2.10d **2.10e**

Benzo[*a*]imidazo[2,1,5-*c,d*]indolizin-7-ylmethanaminium chloride (2.10e) : To a 5 mL round-bottom flask equipped with a magnetic stirbar and a rubber septum were added benzo[*a*]imidazo[2,1,5-*c,d*]indolizine-7-carbonitrile (**2.7j**) (30 mg, 0.14 mmol, 1.0 equiv) as previously synthesized, 20% $Pd(OH)_2$ on carbon (5 mg, 7 μmol, 0.05 equiv), methanol (1.2 mL), 1,4-dioxane (0.6 mL) and 12 M HCl (37 μL, 3.25 equiv). Hydrogen gas was bubbled in the suspension for 50 min, then the mixture was stirred under an hydrogen atmosphere (1 bar) for 20

h. H_2O was added and suspension was filtered on Celite. Filtrate was concentrated under vacuum to remove organic solvents. The resulting yellow aqueous phase was washed with CH_2Cl_2 (4x) and concentrated to dryness. The solid was dissolved in CH_2Cl_2 with 2-3 drops of MeOH and precipitated by the rapid addition of Et_2O. The residue was recovered by filtration, washing with ether, yielding a yellow-green solid (31 mg, 0.12 mmol, 87% yield).

A1.4.Fluorescence data

A1.4.1.Results

Compound	λ_{ex} (nm)	λ_{em} (nm)	Stokes shift (nm)	ε (kL/mol*cm)	Φ_F	Brightness (kL/mol*cm)	Excitation-emission graph
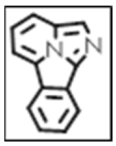 **2.7a**	278 421	464	186 43	24.8 5.9	0.08 0.34	2.1 2.0	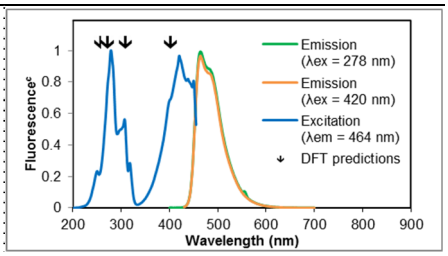
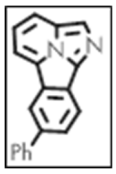 **2.7b**	290 430	476	186 46	17.8 5.4	0.08 0.23	1.5 1.2	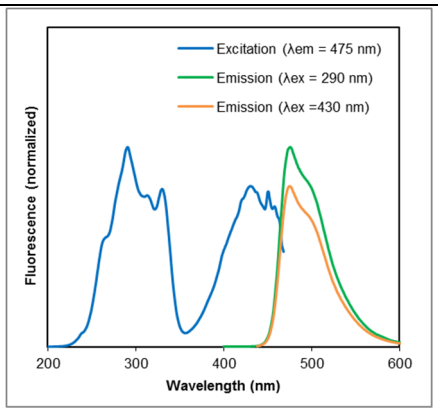
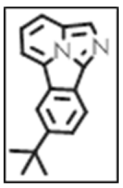 **2.7c**	282 424	469	187 45	26.2 5.9	0.05 0.17	1.3 1.0	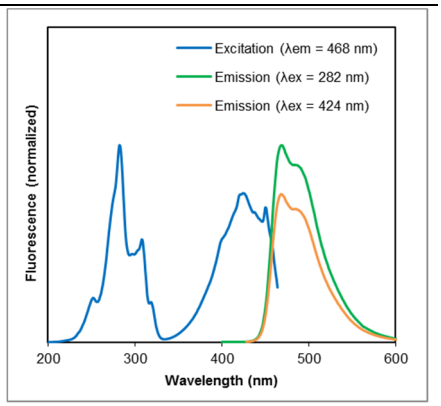

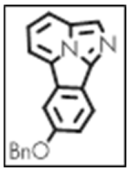 **2.7d**	295 438	486	191 48	15.2 4.7	0.11 0.25	1.6 1.2	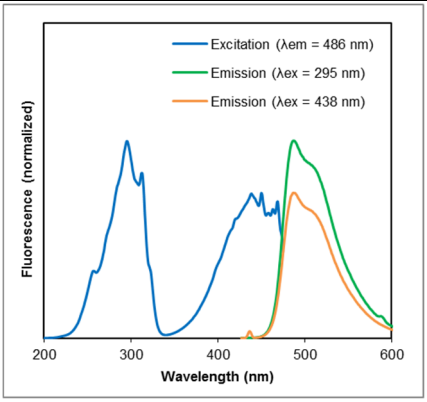
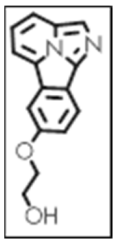 **2.7e**	295 438	489	194 51	14.8 4.7	0.13 0.27	2.0 1.3	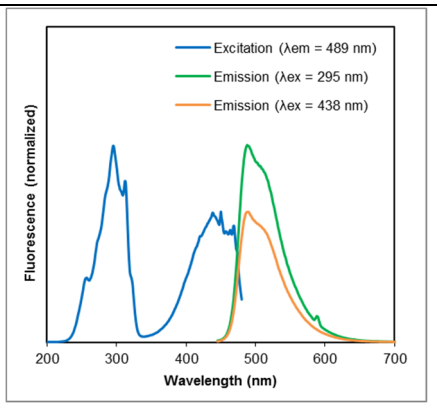
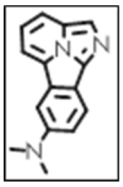 **2.7f**	277 329 469	552	275 223 83	28.7 17.0 4.9	0.01 0.04 0.06	0.4 0.6 0.3	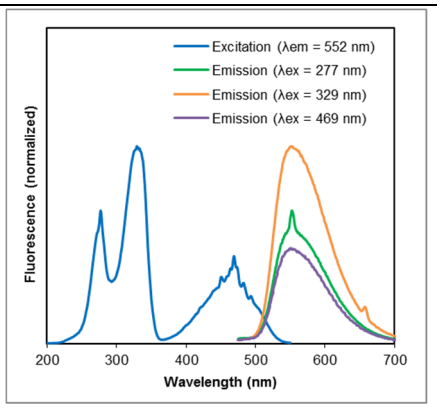
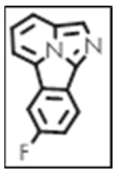 **2.7g**	279 430	476	197 46	21.0 5.6	0.07 0.24	1.4 1.4	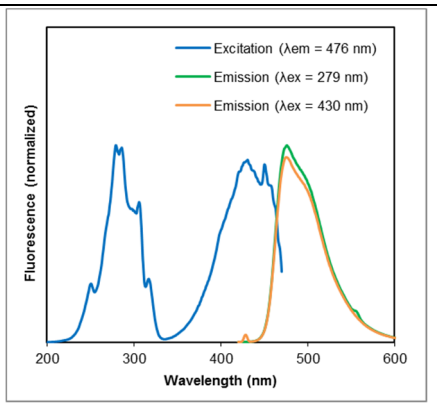

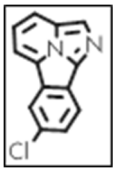 **2.7h**	288 428	473	185 45	20.8 6.5	0.08 0.21	1.6 1.4	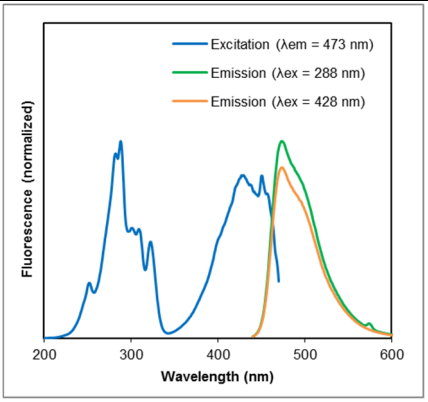
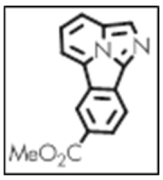 **2.7i**	286 420	461	175 41	18.0 6.6	0.08 0.24	1.4 1.6	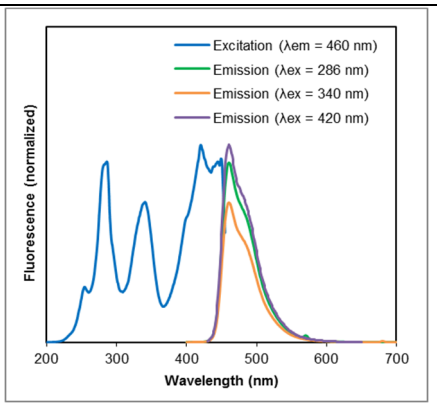
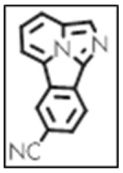 **2.7j**	287 341 450	463	176 122 13	23.9 8.8 9.7	0.09 0.21 0.24	2.2 1.8 2.3	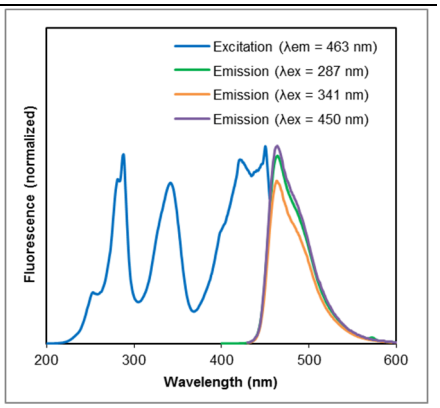
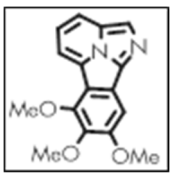 **2.7k**	289 420	471	182 51	28.0 7.3	0.10 0.27	2.7 2.0	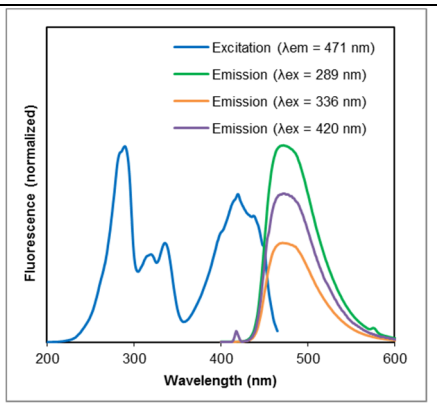

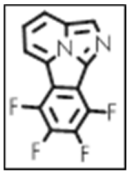 **2.7m**	273 450	467	194 17	13.9 5.1	0.06 0.26	0.8 1.4	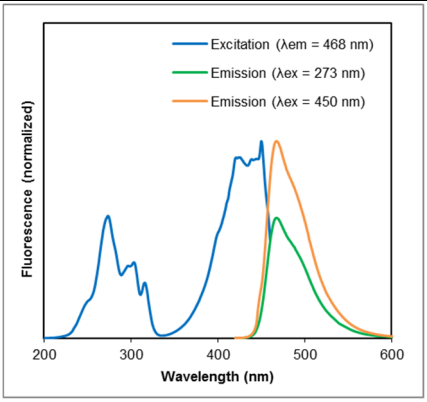
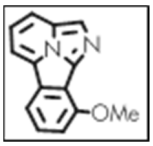 **2.7n**	275 438	480	205 42	7.6 1.8	0.04 0.18	0.3 0.3	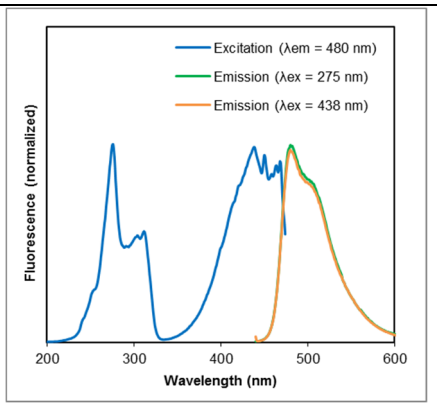
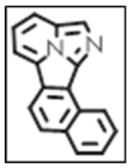 **2.7o**	305 327	487	182 160	20.9 14.5	0.10 0.14	2.0 2.0	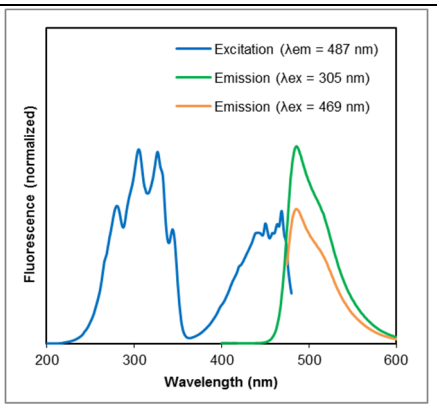
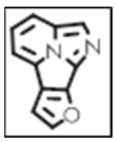 **2.7q**	274 413	480	206 67	9.5 3.1	0.03 0.14	0.3 0.4	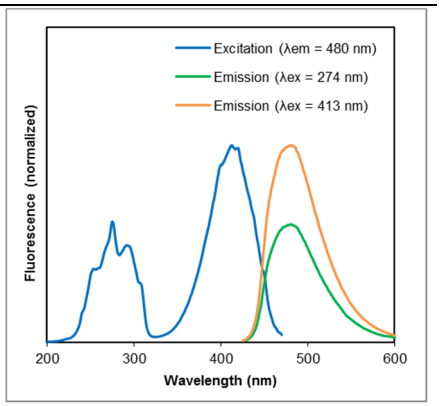

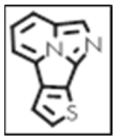 **2.7r**	283 420	478	195 58	16.8 4.9	0.02 0.06	0.3 0.3	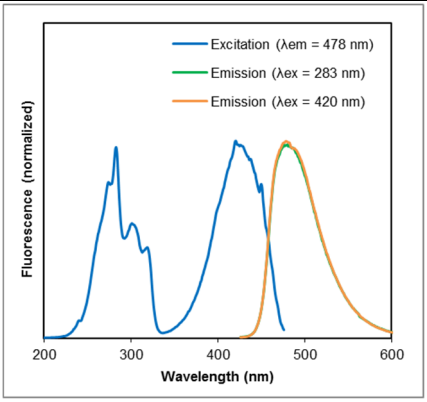
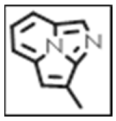 **2.7s**	299 411	450	151 39	7.2 4.9	0.04 0.08	0.3 0.4	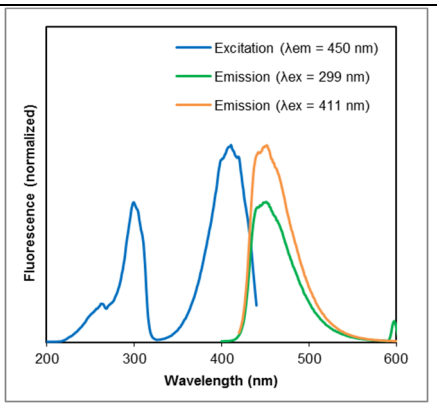
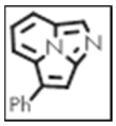 **2.7t**	296 450	506	210 56	12.4 10.7	0.05 0.12	0.6 1.3	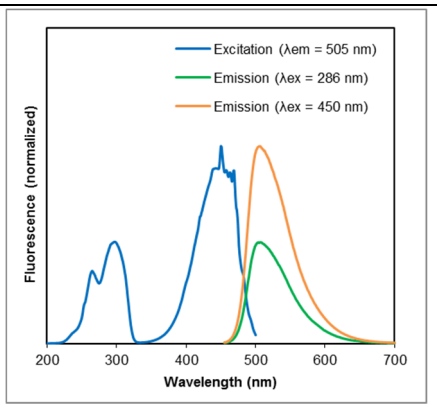
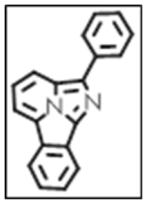 **2.8a**	315 469	512	197 43	22.4 11.0	0.18 0.33	4.1 3.7	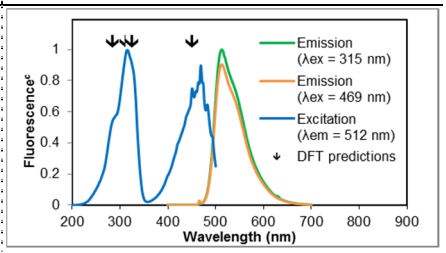

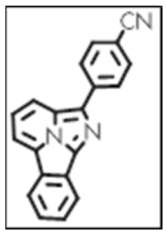 **2.8c**	352 469	498	146 29	5.1 2.8	0.24 0.22	1.2 0.6	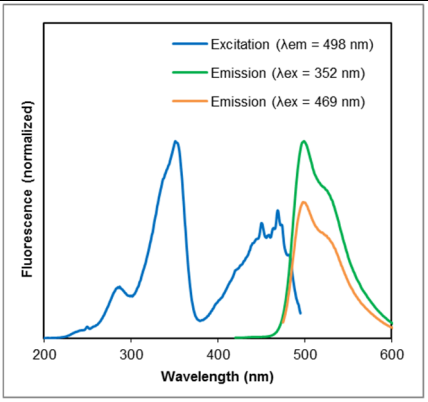
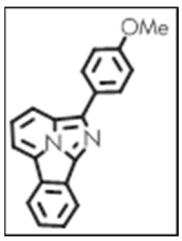 **2.8d**	317 469	535	218 66	22.0 11.1	0.14 0.23	3.0 2.6	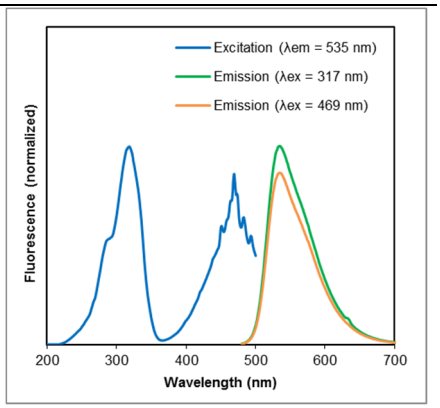
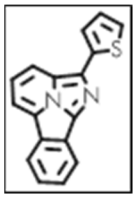 **2.8e**	332 469	538	206 69	15.0 8.4	0.16 0.20	2.4 1.6	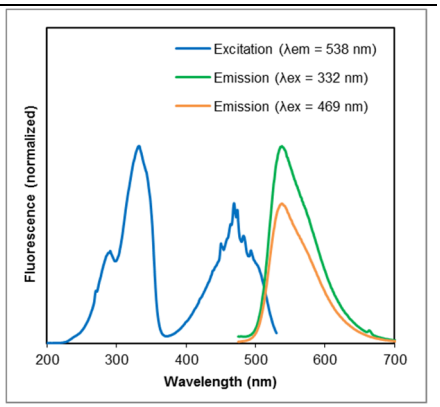
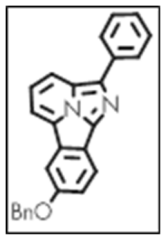 **2.8f**	323 469	533	210 64	22.0 8.9	0.16 0.27	3.5 2.4	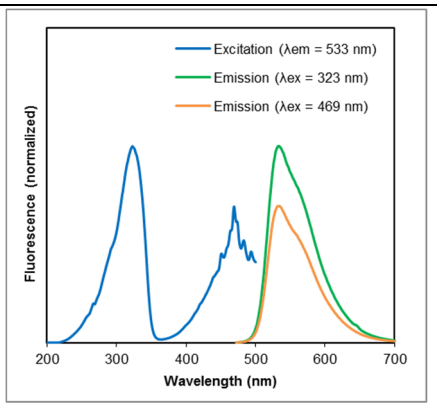

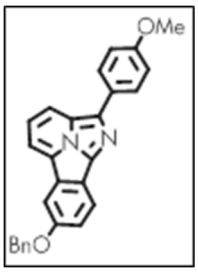 **2.8g**	325 469	555	230 86	23.0 8.1	0.11 0.18	2.5 1.5	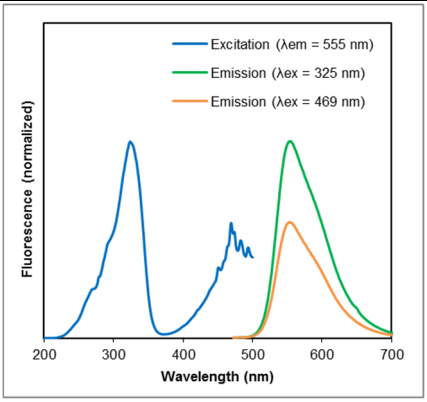
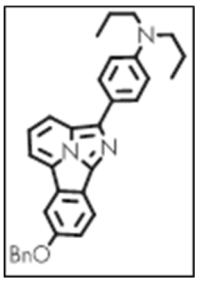 **2.8h**	339	620	281	20.4	0.02	0.4	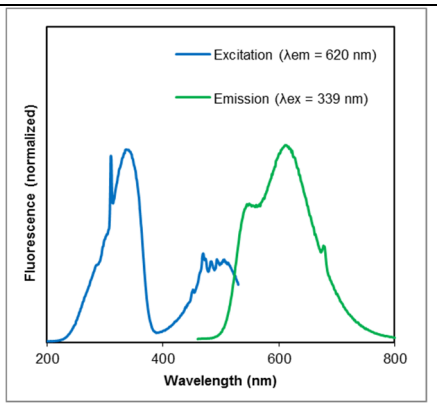
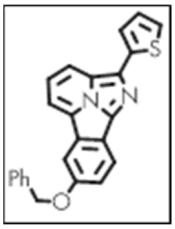 **2.8i**	336 469	557	221 88	38.5 15.6	0.12 0.16	4.5 2.4	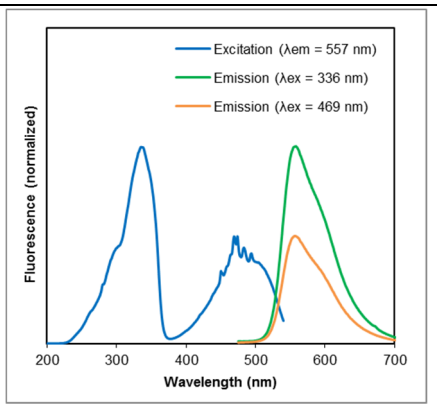
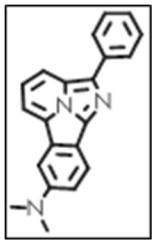 **2.8j**	343 469	579	236 110	29.7 7.1	0.06 0.09	1.9 0.6	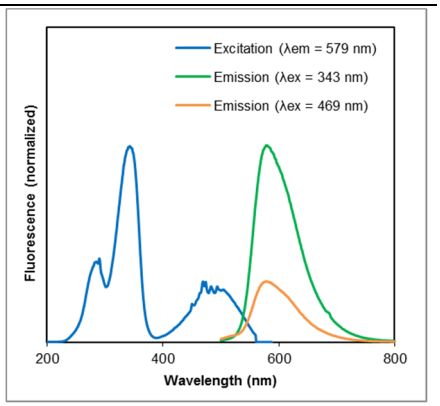

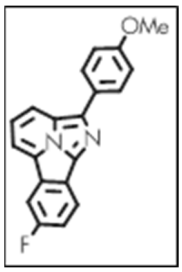 **2.8k**	321 469	550	229 81	9.9 4.1	0.11 0.18	1.1 0.7	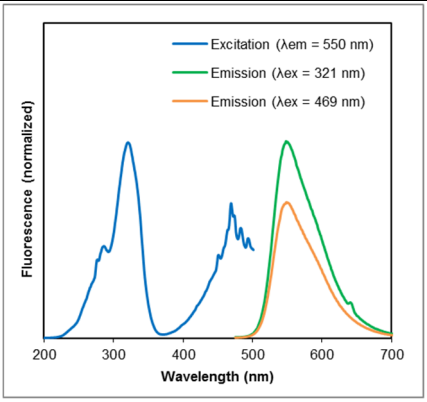
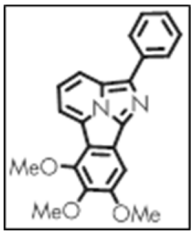 **2.8m**	308 469	507	199 38	29.3 11.8	0.15 0.31	4.3 3.7	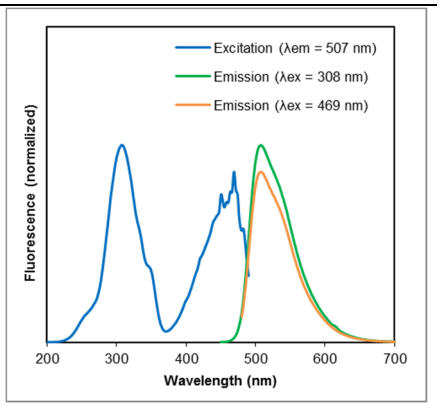
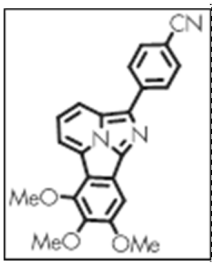 **2.8n**	356 469	497	141 28	18.4 15.7	0.35 0.38	6.4 5.9	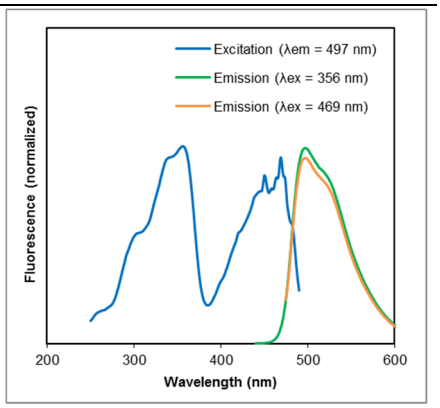
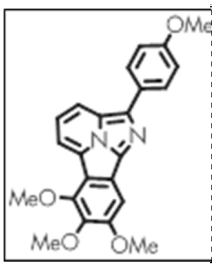 **2.8o**	310 469	526	216 57	28.3 11.3	0.13 0.26	3.6 3.0	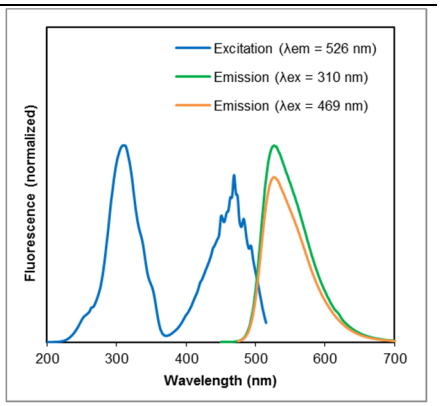

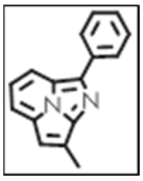 **2.8p**	313 450	490	177 40	12.5 11.6	0.15 0.23	1.9 2.7	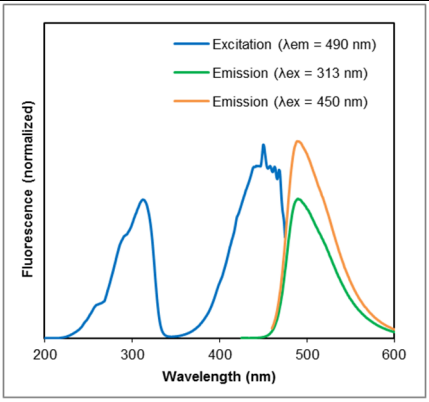
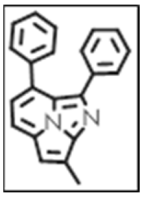 **2.8q**	285 468	529	244 61	27.1 14.7	0.10 0.31	2.7 4.5	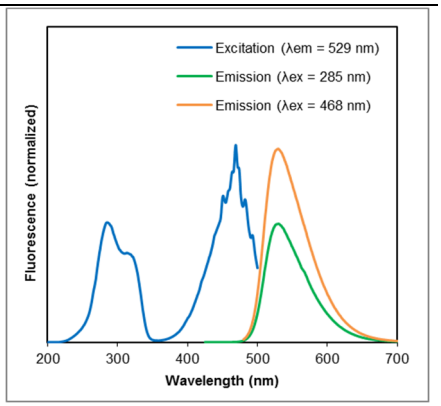
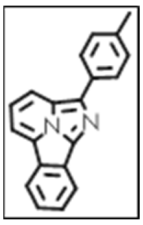 **2.8r**	285 484	524	239 40	22.2 10.3	0.16 0.30	3.6 3.1	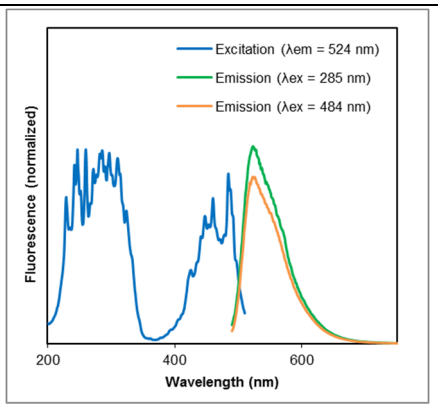
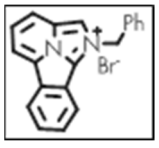 **2.9a**	398	458	60	6.1	0.39	2.4	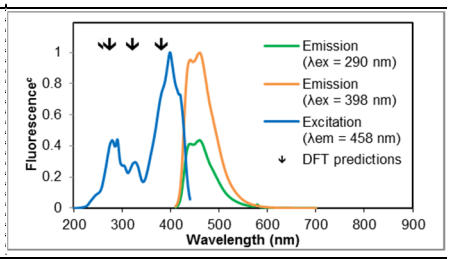

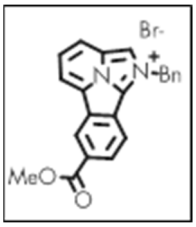 **2.9b**	399	437	38	12.8	0.40	5.2
 **2.9c**	399	503	104	8.9	0.16	1.4
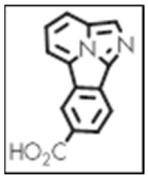 **2.10a**	285 329 420	462	177 133 42	7.9 2.6 2.3	0.10 0.14 0.28	0.8 0.4 0.6
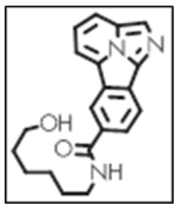 **2.10b**	287 420	464	177 44	25.9 8.4	0.18 0.48	4.7 4.0

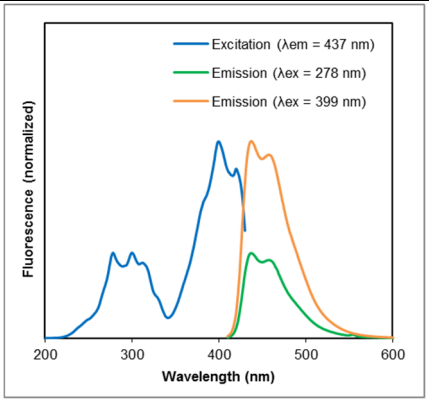

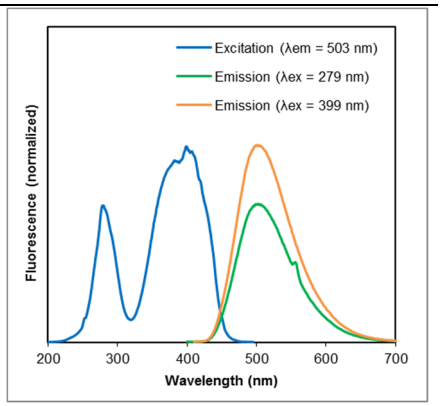

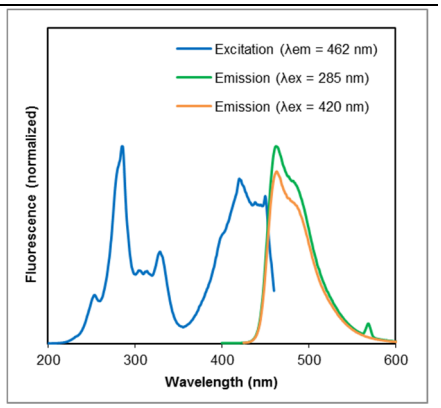

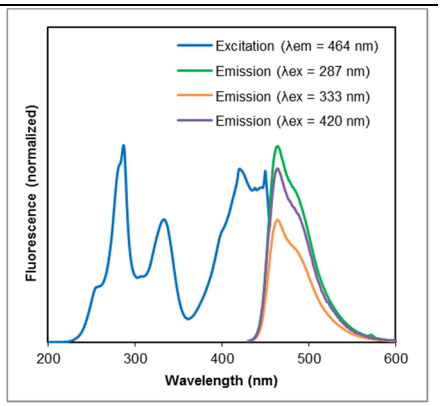

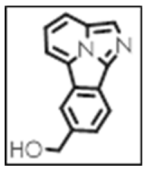 **2.10c**	282 423	468	186 45	26.2 6.8	0.09 0.30	2.4 2.0	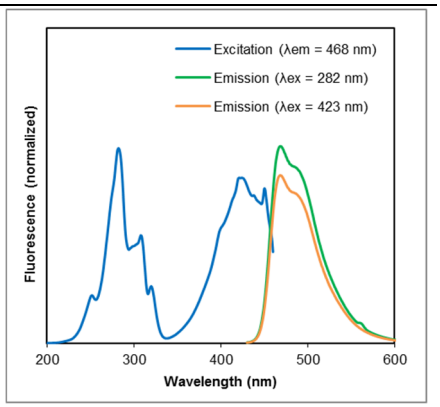
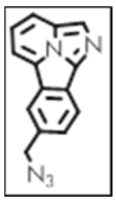 **2.10d**	281 423	468	187 45	23.6 6.4	0.12 0.40	2.8 2.5	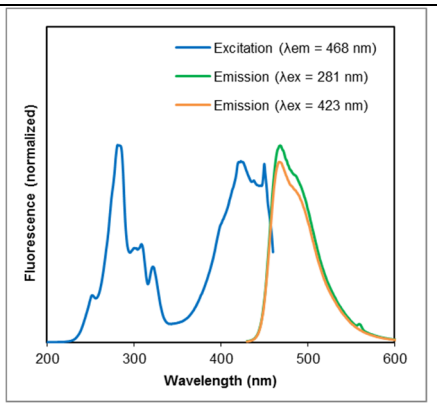
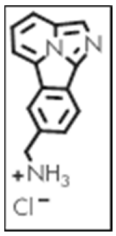 **2.10e**	280 424	467	187 43	10.6 3.0	0.12 0.37	1.3 1.1	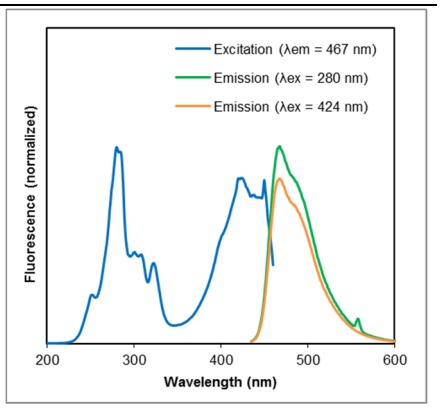

A1.4.2.Equations[6]

$$Stokes\ Shift\ = \lambda_{em} - \lambda_{ex}$$

$$\varepsilon = \frac{abs_{\lambda_{ex}}}{[sample]}$$

$$\frac{\Phi_F}{\Phi_{quinine}} = \frac{area_{sample}}{area_{quinine}} \cdot \frac{abs_{\lambda_{ex}\,quinine}}{abs_{\lambda_{ex}\,sample}} \cdot \frac{n_{sample}}{n_{quinine}}$$

$$\Phi_F = \frac{K \cdot area_{sample}}{abs_{\lambda_{ex}\,sample}} \cdot \frac{n_{sample}}{n_{quinine}}$$

$$K = \frac{\Phi_{quinine} \cdot abs_{\lambda_{ex}\,quinine}}{area_{quinine}}$$

$$Brightness = \Phi_F \cdot \varepsilon$$

A 5 mM solution of quinine in 0,5 M H_2SO_4 was used as quantum yield standard.

$Area_{quinine}$ was measured every experiment day.

$\Phi_{quinine}$ = 0.546[155] $abs_{\lambda_{ex}\,quinine}$ = 0.0266[156] $n_{quinine}$ = 1.347 (water) n_{sample} = 1.374 (MeOH)

A1.4.3.Hammett constants used in Figure 3[45]

H: 0.00

para-Me: -0.17

para-OMe: -0.27

para-$N(Pr)_2$: -0.83

Photon energy: $E = \frac{h \cdot c}{\lambda}$

A1.5.Photobleaching experiment

5 µM solutions of fluorescein, **2.7a**, **2.8a** and **2.9a** in glycerol were prepared. The fluorescein solution was buffered at pH = 7 (0.005M phosphate buffer). 3mL of each solution was added to quartz fluorescence vials with magnetic stirbars. Fluorescence spectra were acquired using the following excitation wavelengths: Fluorescein = 494 nm; **2.7a** = 421 nm; **2.8a** = 469 nm; **2.9a** = 398 nm. Vials were lined up on a rack and irradiated with a 500W tungsten-halogen filament in a quartz bulb. A computer fan was positioned behind the vials to prevent excessive temperature increase. Every 15 min, irradiation was stopped and spectra were acquired for each vial. Vials were shuffled around each time to limit position bias. The relative emitted light is the ratio of the emission peaks' integrations. Both **7a** (*native* series) and **2.8a** (*C-2-aryl* series) are more photostable than fluorescein.

Figure 75. Results of the comparative photobleaching experiment

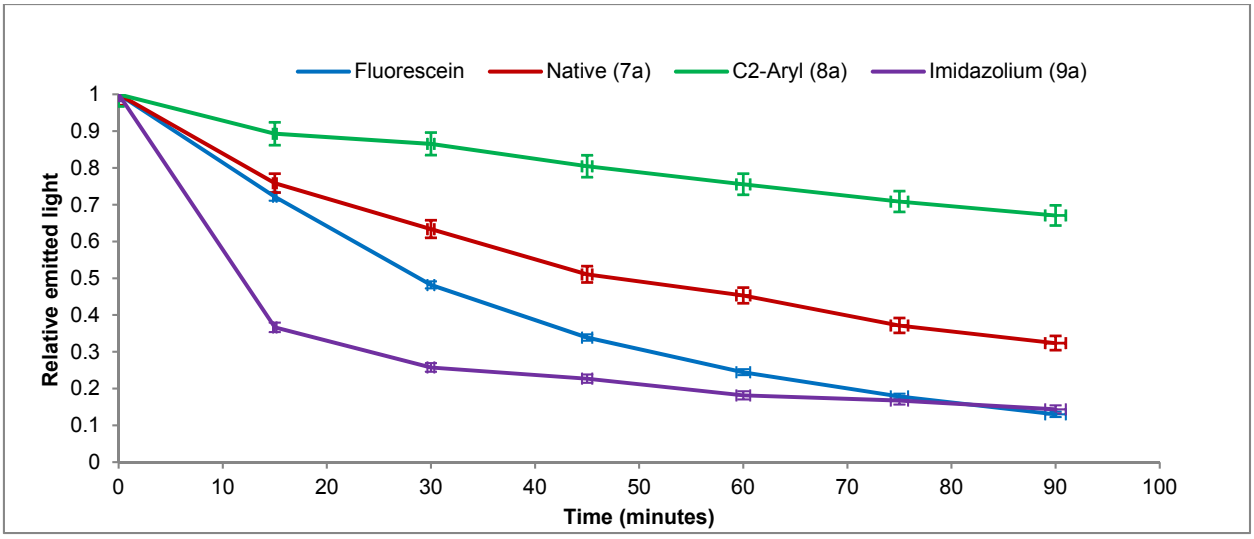

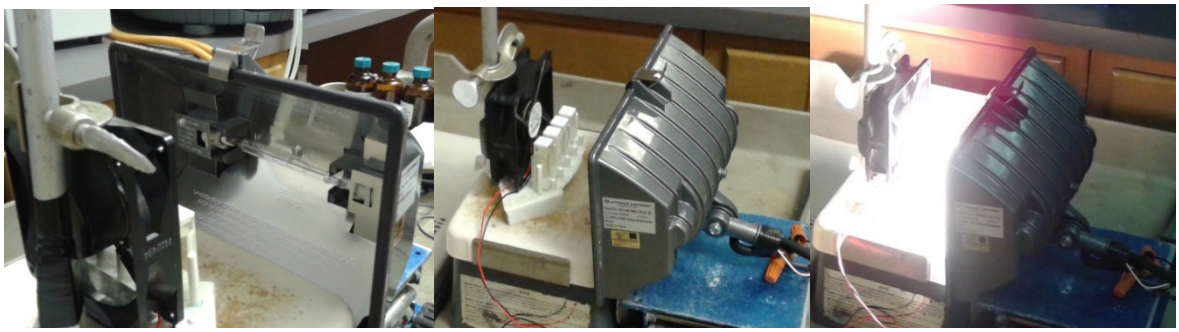

A1.6.Biocatalyzed biolabelling experiments

A1.6.1.MTG Expression and Purification

MTG was expressed and purified as previously described.[1] Briefly, a 5-mL starter culture of *E. coli* BL21 (DE3) containing the plasmid pET20b-MTG, which expresses a *C*-terminally 6-His-tagged version of MTG, was propagated overnight at 37°C in ZYP-0.8G medium and shaking at 240 rpm. It was used to inoculate 500 mL of autoinducing ZYP-5052 medium. After 2 h of incubation at 37 °C and 240 rpm, the temperature was reduced to 22 °C overnight. Cells were collected by centrifugation and resuspended in 0.2 M Tris-HCl, pH 6.0. The cells were lysed using a Constant Systems cell disruptor set at 37 kPSI and cooled to 4 °C. After further centrifugation to remove insoluble cellular matter, the inactive form of MTG was incubated with trypsin (1 mg/mL solution, 1:9 ratio of trypsin to MTG, v/v) for the purpose of cleaving its pro-sequence. Activated MTG was purified using a 5-mL His-trap nickel-nitrilotriacetic acid (Ni-NTA) column (GE Healthcare) equilibrated in 50 mM phosphate buffer, pH 8.0, with 300 mM NaCl, and eluted with an imidazole gradient (0 – 250 mM) using an Åtka FPLC (GE Healthcare). After purification, active MTG was dialyzed against 0.2 M Tris-HCl buffer, pH 6.0. The average yield was 25 mg of activated MTG per litre of culture, with ~ 85% purity as estimated by SDS-PAGE and revelation with Coomassie blue stain. Aliquots were snap frozen and stored at -80 °C in 15% glycerol.

A1.6.2.Expression and Purification of GB1

A 5-mL starter culture of *E. coli* BL21 (DE3) containing the plasmid pET15b-GB1, which expresses a *N*-terminally 6-His-tagged version of GB1, was propagated overnight at 37 °C in LB medium containing 100 μg/mL ampicillin and shaking at 240 rpm. It was used to inoculate 500 mL of LB + ampicillin. After approximately 3 h of incubation at 37°C and 240 rpm, the OD_{600} reached 0.6, and expression was induced by addition of 0.5 mM IPTG. GB1 was expressed for 4h at the same temperature and shaking speed. Cells were then collected by centrifugation and resuspended in buffer A (50 mM potassium phosphate, pH 7.4, 300 mM NaCl). The cells were lysed using a Constant Systems cell disruptor set at 37 kPSI and cooled to 4 °C. After further centrifugation to remove insoluble cellular matter, GB1 was purified using a 5-mL His-trap nickel-nitrilotriacetic acid (Ni-NTA) column (GE Healthcare) equilibrated in buffer A, and eluted with an imidazole gradient (0 – 250 mM) using an Åtka FPLC (GE Healthcare). After purification, Gb1 was dialyzed against

buffer A at 4 °C. The yields would vary between 50-80 mg of Gb1 per litre of culture, with ~ 85% purity as estimated by tricine SDS-PAGE[2] and revelation with Coomassie blue stain. If necessary, the purified GB1 was concentrated using an Amicon® Ultra regenerated cellulose centrifugal filter with a 3k MWCO (Merck-Millipore).

A1.6.3.Conjugation Assays with α-Lactalbumin and GB1

Fluorophore (10 mM), 5 mM glutathione were mixed with α-lactalbumin or GB1 such that its final concentration was 3 mg/mL, in 50 mM potassium phosphate buffer, pH 7.4. The final volume of each reaction was 200 µL. Reactions were incubated at 37 °C overnight. The reactions were washed 5 times over a Spin-X® UF microfuge concentrator, 5k MWCO (Corning), using 50 mM potassium phosphate buffer, pH 7.4, containing 2 mM EDTA. Washed sample was resolved using tricine SDS-PAGE.[2] The fluorescent bands were visualized and recorded using a Bio Rad ChemiDoc™ MP Imaging System using an excitation filter of 625 nm with a 30 nm bandpass, as well as photographed on a transilluminator. The gels were then stained with Coomassie brilliant blue to reveal the protein.

A1.6.4.High resolution MS spectra

Figure 76. Deconvoluted mass spectrum of **α-lactalbumin** in the control reaction containing buffer and fluorophore **2.10e**.

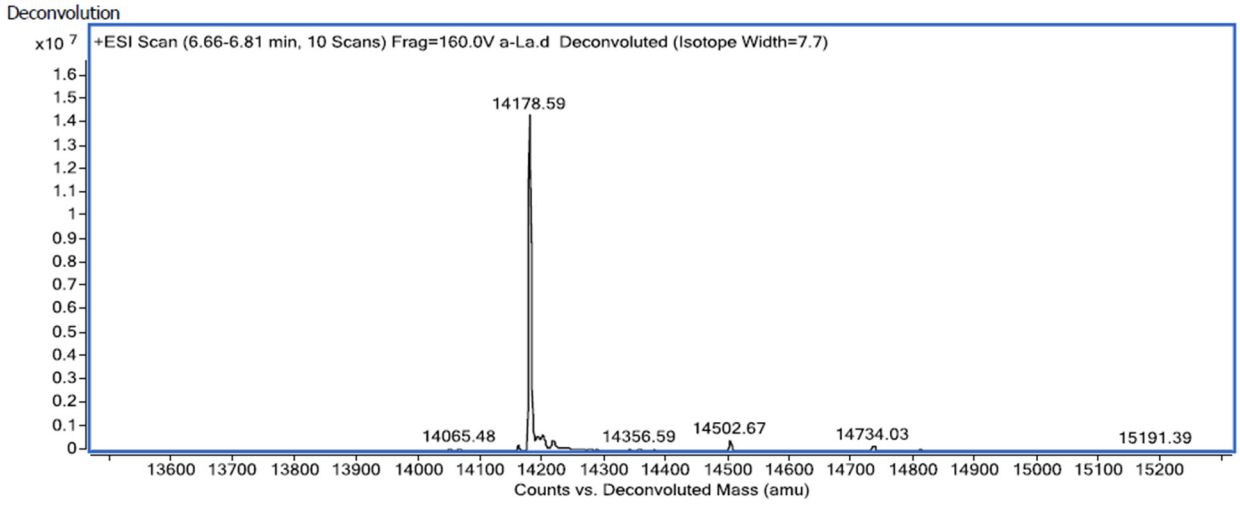

Figure 77. Deconvoluted mass spectrum of **α-lactalbumin** in the conjugation reaction containing buffer, fluorophore **2.10e**, and MTG. Mass per fluorophore unit : 204.1 amu.

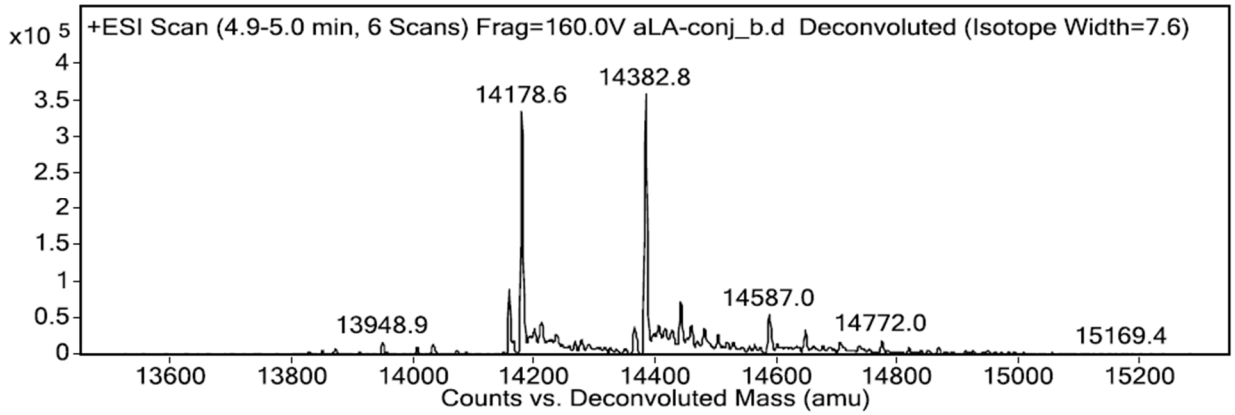

Figure 78. Deconvoluted mass spectrum of unconjugated GB1 in the control reaction containing buffer and fluorophore **2.10e**.

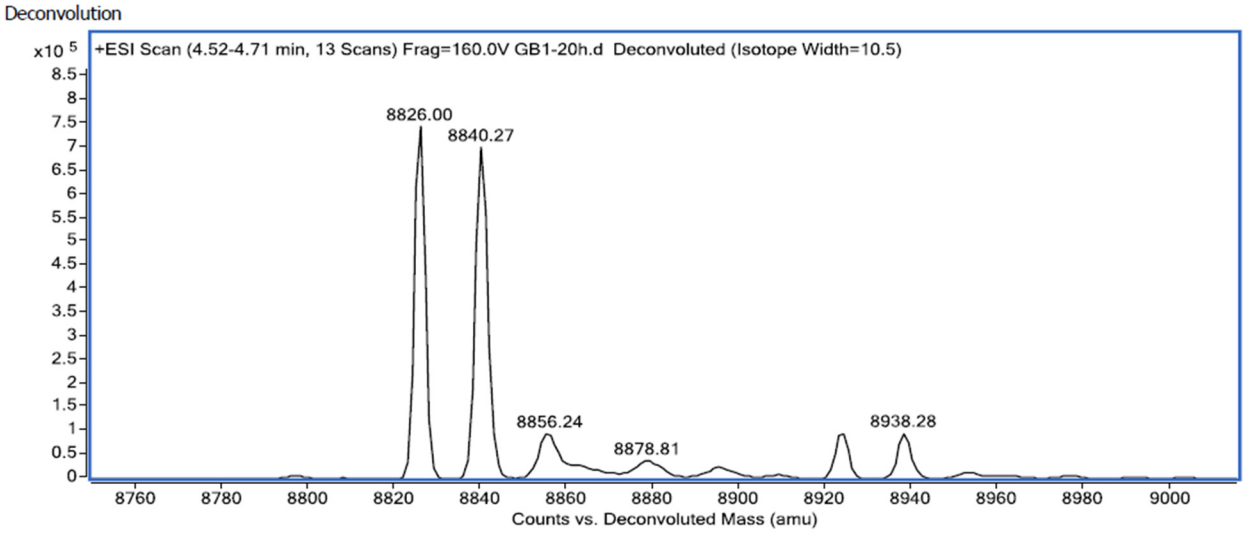

Figure 79. Deconvoluted mass spectrum of GB1 in the conjugation reaction containing buffer, fluorophore **2.10e**, and MTG. Mass per fluorophore unit : 204.1 amu

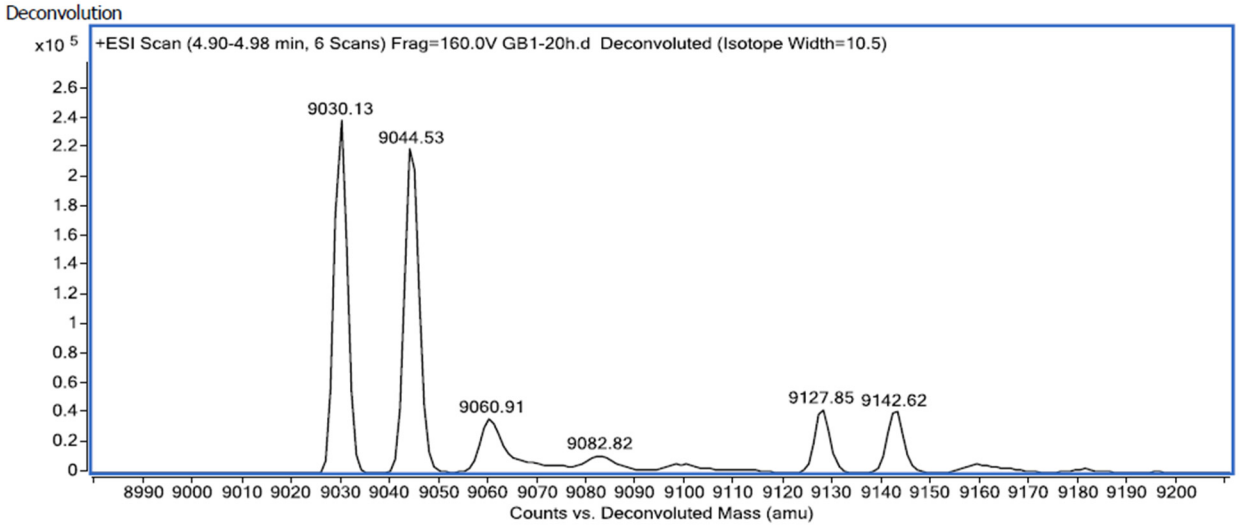

A1.7.X-ray data

A1.7.1.X-Ray of 6,7,8-trimethoxybenzo[*a*]imidazo[2,1,5-*c,d*]indolizine (2.7k)

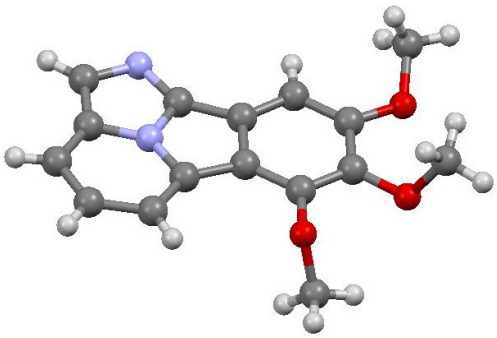

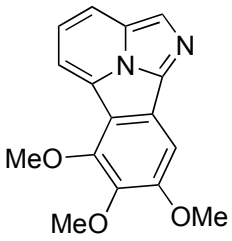

Crystal data and structure refinement for 2.7k

Identification code	SYLVA6
Empirical formula	$C_{16}H_{14}N_2O_3$
Formula weight	282.29
Temperature/K	100
Crystal system	monoclinic
Space group	$P2_1/n$
a/Å	10.4971(2)
b/Å	7.63330(10)
c/Å	16.6642(3)
α/°	90

β/°	93.3300(10)
γ/°	90
Volume/Å^3	1333.01(4)
Z	4
ρ_{calc}g/cm^3	1.407
μ/mm^{-1}	0.812
F(000)	592.0
Crystal size/mm^3	0.12 × 0.06 × 0.06
Radiation	CuKα (λ = 1.54178)
2Θ range for data collection/°	9.71 to 144.194
Index ranges	-12 ≤ h ≤ 12, -7 ≤ k ≤ 8, -20 ≤ l ≤ 20
Reflections collected	15306
Independent reflections	2569 [R_{int} = 0.0232, R_{sigma} = 0.0145]
Data/restraints/parameters	2569/0/193
Goodness-of-fit on F^2	1.051
Final R indexes [I>=2σ (I)]	R_1 = 0.0325, wR_2 = 0.0886
Final R indexes [all data]	R_1 = 0.0348, wR_2 = 0.0916
Largest diff. peak/hole / e Å^{-3}	0.30/-0.19

A1.7.2.X-Ray of 2-phenylbenzo[*a*]imidazo[2,1,5-*c,d*]indolizine (2.8a)

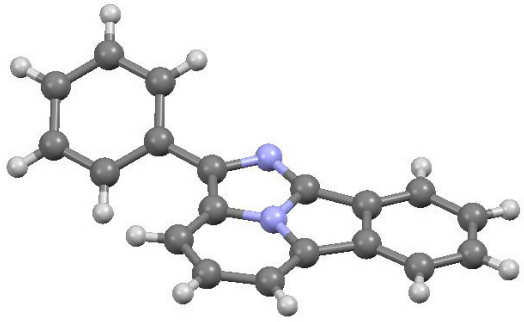

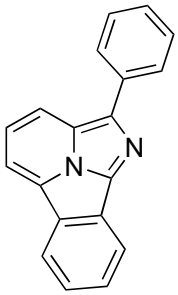

Crystal data and structure refinement for 2.8a

Identification code	SYLV11
Empirical formula	$C_{19}H_{12}N_2$
Formula weight	268.31
Temperature/K	150
Crystal system	monoclinic
Space group	$P2_1/c$
a/Å	12.6062(8)

b/Å	15.8957(10)
c/Å	6.5668(4)
α/°	90
β/°	99.593(3)
γ/°	90
Volume/Å^3	1297.48(14)
Z	4
ρ_{calc}g/cm^3	1.374
μ/mm^{-1}	0.636
F(000)	560.0
Crystal size/mm^3	0.4 × 0.03 × 0.03
Radiation	CuKα (λ = 1.54178)
2Θ range for data collection/°	7.112 to 140.294
Index ranges	-15 ≤ h ≤ 15, -19 ≤ k ≤ 19, -7 ≤ l ≤ 5
Reflections collected	22805
Independent reflections	2439 [R_{int} = 0.0747, R_{sigma} = 0.0456]
Data/restraints/parameters	2439/0/190
Goodness-of-fit on F^2	1.067
Final R indexes [I>=2σ (I)]	R_1 = 0.0505, wR_2 = 0.1300
Final R indexes [all data]	R_1 = 0.0638, wR_2 = 0.1414
Largest diff. peak/hole / e Å^{-3}	0.24/-0.31

A1.7.3.X-Ray of benzo[*a*]imidazo[2,1,5-*c,d*]indolizin-7-ylmethanol (2.10c)

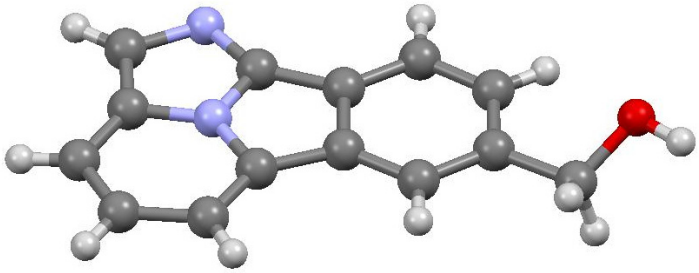

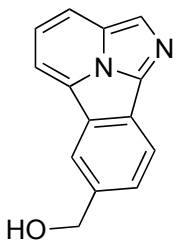

Crystal data and structure refinement for 2.10c

Identification code	SYLVA4
Empirical formula	$C_{14}H_{10}N_2O$
Formula weight	222.24

Temperature/K	100
Crystal system	orthorhombic
Space group	$Pna2_1$
a/Å	13.3138(14)
b/Å	18.7196(19)
c/Å	4.0464(5)
α/°	90
β/°	90
γ/°	90
Volume/Å^3	1008.48(19)
Z	4
ρ_{calc}mg/mm^3	1.464
m/mm^{-1}	0.488
F(000)	464.0
Crystal size/mm^3	0.1 × 0.02 × 0.02
Radiation	GaKα (λ = 1.34139)
2Θ range for data collection	7.088 to 121.27°
Index ranges	$-17 \leq h \leq 16$, $-24 \leq k \leq 24$, $-5 \leq l \leq 5$
Reflections collected	20940
Independent reflections	2251 [R_{int} = 0.0744, R_{sigma} = 0.0347]
Data/restraints/parameters	2251/1/158
Goodness-of-fit on F^2	1.094
Final R indexes [I>=2σ (I)]	R_1 = 0.0542, wR_2 = 0.1391
Final R indexes [all data]	R_1 = 0.0590, wR_2 = 0.1461
Largest diff. peak/hole / e Å^{-3}	0.36/-0.41

A1.8.Kinetic isotope effect in the C-H bond functionalization

A1.8.1.KIE determined from two parallel reactions

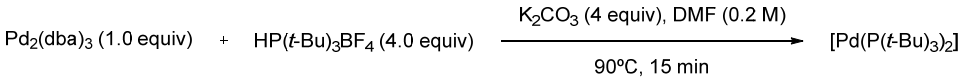

In an argon-pressurised glovebox, in a 4mL vial equipped with a magnetic stirbar and a rubber septum were added Pd_2dba_3 (9 mg, 9 μmol, 1.0 equiv), *t*-Bu_3PHBF_4 (11 mg, 38 μmol, 4.0 equiv) and K_2CO_3 (5 mg, 38 μmol, 4.0 equiv). Vial was taken out of the glovebox and DMF (2.3 mL, [Pd]

= 8 mM) was added. Mixture was heated to 90 °C for 15 min (turns from dark brown to clear green). Two equal volumes of solution are used as is in the two parallel reactions.

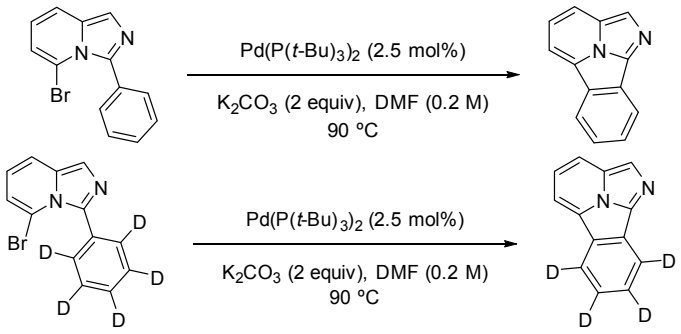

To a flame-dried 5 mL microwave (sealable) vial (VWR® 2-5 mL) equipped with a magnetic stirrer was added the corresponding 5-bromoimidazo[1,5-*a*]pyridine (0.25 mmol, 1.0 equiv), as previously synthesized, K_2CO_3 (69 mg, 0.5 mmol, 2.0 equiv) and triphenylmethane (10 mg, 41 µmol, 0.16 equiv). The palladium catalyst solution was added (0.75 mL, 6 µmol, 0.025 equiv) and mixture was heated to 90 °C. Samples were taken at regular intervals, filtered, diluted in $CDCl_3$ and analyzed by ^{1}H-NMR.

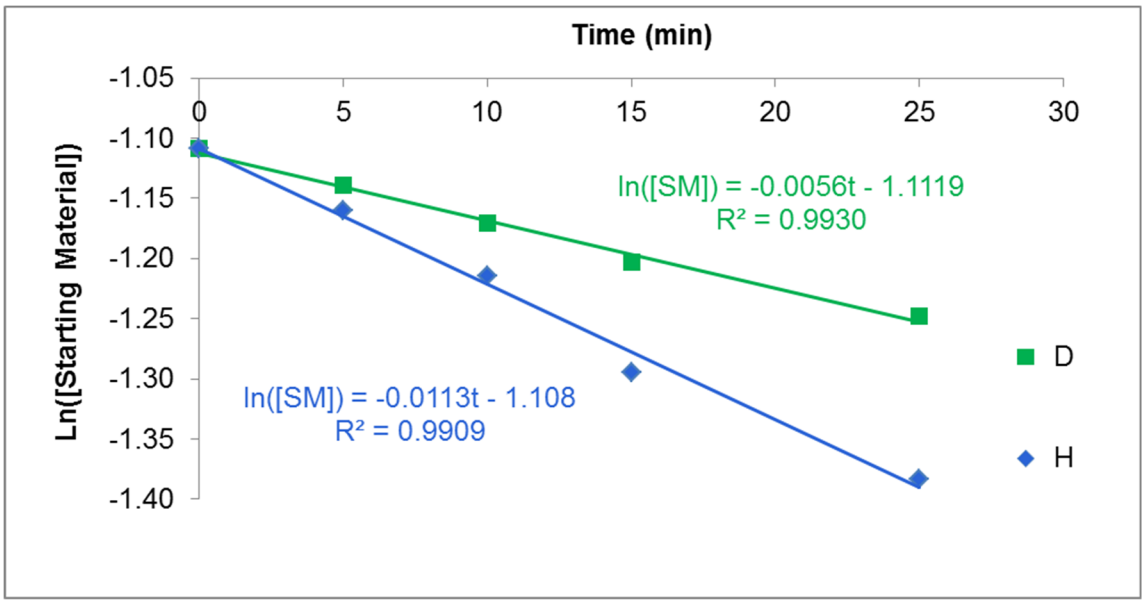

$$KIE = \frac{initial\ rate[H]}{initial\ rate[D]} = \frac{0.0113\frac{M}{min}}{0.0056\frac{M}{min}} = 2.02$$

A1.8.2.KIE determined from an intramolecular competition

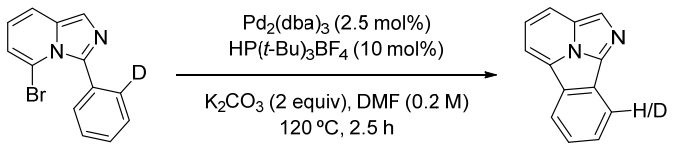

To a flame-dried 5 mL microwave (sealable) vial (VWR® 2-5 mL) equipped with a magnetic stirrer was added 5-bromo-3-(phenyl-2-*d*)imidazo[1,5-*a*]pyridine (26 mg, 95 μmol, 1.0 equiv), as previously synthesized. Then, $Pd_2(dba)_3$ (2.2 mg, 2.4 μmol, 0.025 equiv), $HP(t\text{-}Bu)_3BF_4$ (2.8 mg, 9.5 □ mol, 0.10 equiv), and K_2CO_3 (26 mg, 0.19 mmol, 2.0 equiv) were added to the vial. The vial was capped with a rubber septum and purged with argon. Anhydrous DMF (2.5 mL, 0.20M) was added and the reaction was quickly heated to 120 °C using an oil bath and stirred for 2.5 h. The reaction was cooled to rt and the crude mixture was diluted in CH_2Cl_2 (5 mL) and transferred to a 60-mL extraction funnel. A saturated aqueous solution of brine was added. The layers were separated and the aqueous layer was extracted with ethyl acetate (3x). The combined organic layers were washed with brine (2x) dried over anhydrous $MgSO_4$, filtered over a pad of silica gel, and evaporated to dryness. D/H ratio was determined by ^{1}H-NMR.

$$KIE = \frac{\%\,reacted\ C\text{-}H}{\%\,reacted\ C\text{-}D} = \frac{\%\,remaining\ D}{\%\,remaining\ H\text{-}\%\,nondeuterated\ SM} = \frac{(60\%)}{(40\%-10\%)} = 2.0$$

A1.9.Computational data

The Gaussian 09 Revision E.01 and Gaussview 5.0.9 software package (licensed to Université de Montréal) was used for *ab initio* calculations and frontier molecular orbital rendering and display. Calculations were performed on a Dell XPS L502X laptop computer.

Gaussian 09, Revision E.01, M. J. Frisch, G. W. Trucks, H. B. Schlegel, G. E. Scuseria, M. A. Robb, J. R. Cheeseman, G. Scalmani, V. Barone, B. Mennucci, G. A. Petersson, H. Nakatsuji, M. Caricato, X. Li, H. P. Hratchian, A. F. Izmaylov, J. Bloino, G. Zheng, J. L. Sonnenberg, M. Hada, M. Ehara, K. Toyota, R. Fukuda, J. Hasegawa, M. Ishida, T. Nakajima, Y. Honda, O. Kitao, H. Nakai, T. Vreven, J. A. Montgomery, Jr., J. E. Peralta, F. Ogliaro, M. Bearpark, J. J. Heyd, E. Brothers, K. N. Kudin, V. N. Staroverov, T. Keith, R. Kobayashi, J. Normand, K. Raghavachari, A. Rendell, J. C. Burant, S. S. Iyengar, J. Tomasi, M. Cossi, N. Rega, J. M. Millam, M. Klene, J. E. Knox, J. B. Cross, V. Bakken, C. Adamo, J. Jaramillo, R. Gomperts, R. E. Stratmann, O. Yazyev, A. J. Austin, R. Cammi, C. Pomelli, J. W. Ochterski, R. L. Martin, K. Morokuma, V. G. Zakrzewski, G. A. Voth, P. Salvador, J. J. Dannenberg, S. Dapprich, A. D. Daniels, O. Farkas, J. B. Foresman, J. V. Ortiz, J. Cioslowski, and D. J. Fox, Gaussian, Inc., Wallingford CT, 2013.

A1.9.1.Compound 2.7a

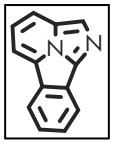

Gaussian input file for ground state optimization

%chk=C:\Program Files2\Gaussian\G09W\Scratch\TetracycleMinimOrb631Gdp.chk

%mem=7GB

%nprocshared=1

# opt b3lyp/6-31g(d,p) scrf=(solvent=methanol) guess=(always,local,save)
pop=(nbo,savemixed,full) geom=connectivity

TetracycleMinimOrb631Gdp

0 1

C	0.48526600	-1.18952800	0.00000000
C	1.04617300	-2.39714600	0.00000000
C	0.13258700	-3.57559800	0.00000000
C	-1.21385000	-3.41719300	0.00000000
C	-1.82714000	-2.05920200	0.00000000
C	-0.99437800	-1.02277500	0.00000000
C	-1.17014800	0.42558400	0.00000000
N	0.00000000	0.97803000	0.00000000
C	1.04942700	0.17867000	0.00000000
C	-0.07952900	2.28138600	0.00000000
C	1.19875000	3.01784800	0.00000000
C	2.33687500	2.25605800	0.00000000
C	2.27183200	0.73505000	0.00000000
C	-1.39210500	2.56985900	0.00000000
N	-2.12153400	1.30150000	0.00000000
H	-1.83851500	3.55508500	0.00000000
H	1.23576200	4.09921400	0.00000000
H	3.30358900	2.74198200	0.00000000
H	3.16770000	0.12881300	0.00000000
H	2.12136000	-2.51824000	0.00000000

H	0.55506100	-4.57196700	0.00000000
H	-1.85646300	-4.28798800	0.00000000
H	-2.90031200	-1.92169500	0.00000000

1 2 2.0 6 1.0 9 1.0

2 3 1.0 20 1.0

3 4 2.0 21 1.0

4 5 1.0 22 1.0

5 6 2.0 23 1.0

6 7 1.0

7 8 1.0 15 2.0

8 9 1.0 10 1.0

9 13 2.0

10 11 1.0 14 2.0

11 12 2.0 17 1.0

12 13 1.0 18 1.0

13 19 1.0

14 15 1.0 16 1.0

15

16

17

18

19

20

21

22

23

Frontier molecular orbitals from checkpoint file

HOMO: 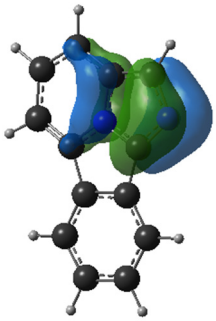 LUMO: 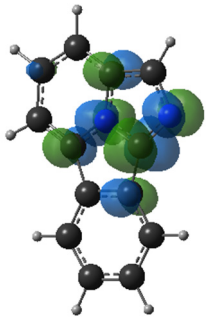

Gaussian input file for TD-DFT with optimized atomic coordinates

%chk=C:\Program Files2\Gaussian\G09W\Scratch\TetracycleTD631Gdp.chk

%mem=7GB

%nprocshared=1

td=(nstates=4) b3lyp/6-31g(d,p) scrf=(solvent=methanol) geom=connectivity

TetracycleTD631Gdp

0 1

C	0.48884500	-1.17586500	0.00000000
C	1.06088500	-2.45206600	0.00000000
C	0.22214200	-3.56372100	0.00000000
C	-1.17708800	-3.41343200	0.00000000
C	-1.77107100	-2.15383500	0.00000000
C	-0.94767500	-1.02230100	0.00000000
C	-1.21907100	0.40191700	0.00000000
N	0.00000000	0.98986500	0.00000000
C	1.09073200	0.15504000	0.00000000
C	-0.10095400	2.35954300	0.00000000
C	1.14974400	3.01457300	0.00000000
C	2.30645500	2.23801200	0.00000000
C	2.30435400	0.81071300	0.00000000
C	-1.50915200	2.54700600	0.00000000

N	-2.17167700	1.35538500	0.00000000
H	-2.04122300	3.48802100	0.00000000
H	1.21171700	4.09660400	0.00000000
H	3.26712200	2.74216000	0.00000000
H	3.24063300	0.26521900	0.00000000
H	2.13971600	-2.57381700	0.00000000
H	0.65191800	-4.56033900	0.00000000
H	-1.80581100	-4.29869900	0.00000000
H	-2.85122200	-2.04939200	0.00000000

1 2 1.5 6 1.5 9 1.0

2 3 1.5 20 1.0

3 4 1.5 21 1.0

4 5 1.5 22 1.0

5 6 1.5 23 1.0

6 7 1.0

7 8 1.5 15 1.5

8 9 1.5 10 1.5

9 13 2.0

10 11 1.5 14 1.5

11 12 1.5 17 1.0

12 13 1.5 18 1.0

13 19 1.0

14 15 1.5 16 1.0

15

16

17

18

19

20

21

22

23

TD-DFT predicted excitation energies and oscillator strengths

Excited State 1: Singlet-A' 3.0874 eV **401.59 nm** f=0.1228 <S**2>=0.000

50 -> 51 0.69243

This state for optimization and/or second-order correction.

Total Energy, E(TD-HF/TD-KS) = -609.608121336

Copying the excited state density for this state as the 1-particle RhoCI density.

Excited State 2: Singlet-A' 4.0189 eV **308.51 nm** f=0.0013 <S**2>=0.000

49 -> 51 -0.43505

50 -> 52 0.55146

Excited State 3: Singlet-A' 4.5795 eV **270.74 nm** f=0.5264 <S**2>=0.000

49 -> 51 0.47518

50 -> 52 0.39601

50 -> 53 -0.28800

Excited State 4: Singlet-A' 4.8013 eV **258.23 nm** f=0.0347 <S**2>=0.000

47 -> 51 -0.28629

48 -> 51 0.28007

49 -> 51 0.10476

49 -> 52 0.27496

50 -> 53 0.47779

A1.9.2 Compound 2.7i

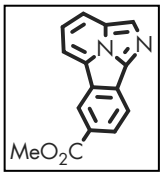

Gaussian input file for ground state optimization

%chk=C:\Program Files2\Gaussian\G09W\Scratch\EsterMinimOrb631Gdp.chk

%mem=7GB

%nprocshared=1

# opt b3lyp/6-31g(d,p) scrf=(solvent=methanol) guess=(always,local,save)
pop=(nbo,savemixed,full) geom=connectivity

EsterMinimOrb631Gdp

0 1

C	0.00000000	0.00000000	0.00000000
C	0.00000000	0.00000000	1.33861350
C	1.18128072	0.00000000	1.99373855
C	2.32985654	0.00039205	1.28088064
C	2.33842030	0.00046071	-0.06396723
C	1.16022044	0.00012529	-0.69264190
C	0.83188366	-0.00022260	-1.99000504
N	-0.42378723	-0.00066735	-2.00000768
C	-1.01016121	-0.00060446	-0.88673690
C	-0.88408045	-0.00113336	-3.16796093
C	-2.21677796	-0.00169275	-3.29431458
C	-2.93445109	-0.00169887	-2.14613205
C	-2.34973664	-0.00123312	-0.92453239
C	0.24167863	-0.00092880	-3.90512779
N	1.28710944	-0.00033170	-3.16935219
H	0.29227635	-0.00119637	-5.00177322
H	-2.69635347	-0.00220132	-4.28490773
H	-4.03617280	-0.00227388	-2.20835581
H	-2.94459117	-0.00123011	0.00171042
H	-0.97495225	-0.00030807	1.85059744

H	3.31502056	0.00040668	1.77687135
H	3.28073182	0.00060025	-0.63463024
C	1.23385616	-0.00058304	3.36230108
O	0.21006855	-0.00096964	4.01900353
C	2.44975718	-0.01140774	5.42531475
H	3.51077757	-0.01650187	5.76122062
H	1.95786658	0.90631253	5.81834880
H	1.95335445	-0.93188262	5.80641312
O	2.44342071	-0.00213643	4.01692394

1 2 1.0 6 2.0 9 1.0

2 3 2.0 20 1.0

3 4 1.0 23 1.0

4 5 2.0 21 1.0

5 6 1.0 22 1.0

6 7 1.0

7 8 1.0 15 2.0

8 9 1.0 10 1.0

9 13 2.0

10 11 1.0 14 2.0

11 12 2.0 17 1.0

12 13 1.0 18 1.0

13 19 1.0

14 15 1.0 16 1.0

15

16

17

18

19

20

21

22

23 24 2.0 29 1.0

24

25 26 1.0 27 1.0 28 1.0 29 1.0

26

27

28

29

Frontier molecular orbitals from checkpoint file

HOMO: 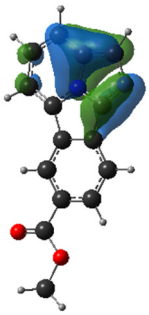 LUMO: 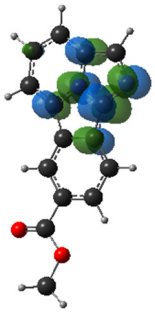

Gaussian input file for TD-DFT with optimized atomic coordinates:

%chk=C:\Program Files2\Gaussian\G09W\Scratch\EsterTD631Gdp.chk

%mem=7GB

%nprocshared=1

td=(nstates=4) b3lyp/6-31g(d,p) scrf=(solvent=methanol) geom=connectivity

EsterTD631Gdp

0 1

C	-0.18990766	0.29823234	0.00006182
C	1.10439649	0.80951239	0.00008964
C	2.18626498	-0.07678090	0.00010663
C	1.96885540	-1.47421264	0.00009776
C	0.68661094	-2.00540058	0.00008220

C	-0.40969395	-1.13289396	0.00005854
C	-1.83819793	-1.33785826	0.00001737
N	-2.37167057	-0.09152818	-0.00000766
C	-1.49128630	0.96065990	0.00001811
C	-3.74194667	-0.13040236	-0.00005444
C	-4.34290320	1.14537267	-0.00008268
C	-3.51627334	2.26805549	-0.00006147
C	-2.09208141	2.20312980	-0.00001092
C	-3.99277451	-1.53271581	-0.00005539
N	-2.83694835	-2.24691566	-0.00000896
H	-4.95768357	-2.02016023	-0.00008826
H	-5.42116728	1.25332585	-0.00012349
H	-3.97790287	3.24971364	-0.00008603
H	-1.50498278	3.11379943	0.00000385
H	1.29393492	1.87721994	0.00009471
H	2.82500756	-2.13800881	0.00010673
H	0.53597944	-3.07965423	0.00008348
C	3.55338868	0.50882186	0.00010624
O	3.78986508	1.70654122	0.00017620
C	5.87412036	0.06211897	-0.00021064
H	6.50731009	-0.82374884	0.00130661
H	6.06209666	0.66457720	-0.89153006
H	6.06125177	0.66712923	0.88953225
O	4.52076707	-0.43015620	-0.00019622

1 2 1.0 6 2.0 9 1.0

2 3 2.0 20 1.0

3 4 1.0 23 1.0

4 5 2.0 21 1.0

5 6 1.0 22 1.0

6 7 1.0

7 8 1.0 15 2.0

8 9 1.0 10 1.0

9 13 2.0

10 11 1.0 14 2.0

11 12 2.0 17 1.0

12 13 1.0 18 1.0

13 19 1.0

14 15 1.0 16 1.0

15

16

17

18

19

20

21

22

23 24 2.0 29 1.0

24

25 26 1.0 27 1.0 28 1.0 29 1.0

26

27

28

29

TD-DFT predicted excitation energies and oscillator strengths

Excited State 1: Singlet-A 3.0909 eV **401.12 nm** f=0.2019 <S**2>=0.000

64 -> 67 -0.11873

65 -> 66 0.67872

65 -> 67 0.12696

This state for optimization and/or second-order correction.

Total Energy, E(TD-HF/TD-KS) = -837.493968020

Copying the excited state density for this state as the 1-particle RhoCI density.

Excited State 2: Singlet-A 3.6277 eV **341.77 nm** f=0.1491 <S**2>=0.000

64 -> 66 0.16769

65 -> 66 -0.10516

65 -> 67 0.67305

Excited State 3: Singlet-A 4.3492 eV **285.07 nm** f=0.1851 <S**2>=0.000

63 -> 66 0.10250

64 -> 66 0.62094

64 -> 67 -0.13600

65 -> 67 -0.13860

65 -> 68 0.16386

65 -> 69 -0.15176

Excited State 4: Singlet-A 4.6361 eV **267.43 nm** f=0.4071 <S**2>=0.000

63 -> 66 -0.26141

64 -> 67 0.53613

65 -> 66 0.11386

65 -> 68 0.31184

A1.9.3.Compound 2.8a

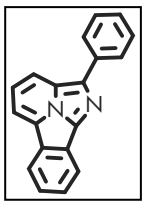

Gaussian input file for ground state optimization

%nosave

%chk=C:\Program Files2\Gaussian\G09W\Scratch\PhenylMinimOrb631Gdp.chk

%mem=7GB

# opt b3lyp/6-31g(d,p) scrf=(solvent=methanol) guess=(always,local,save)
pop=(nbo,savemixed,full) geom=connectivity

PhenylMinimOrb631Gdp

0 1

C	0.00000000	0.00000000	0.00000000
C	0.00000000	0.00000000	1.33824747
C	1.18898359	0.00000000	1.96664247
C	2.34415176	0.00000000	1.27498059
C	2.34771505	-0.00008740	-0.06959413
C	1.16255134	-0.00007842	-0.68856001
C	0.82198264	-0.00014822	-1.98174650
N	-0.43039066	-0.00017178	-2.01276973
C	-1.00516326	-0.00005787	-0.89148656
C	-0.86568961	-0.00033163	-3.19373900
C	-2.20797079	-0.00027663	-3.27389326
C	-2.92590995	-0.00026699	-2.12600832
C	-2.34281742	-0.00016482	-0.90725236
C	0.26202953	-0.00047142	-3.94980735
N	1.27209745	-0.00020695	-3.15772420
C	0.42910114	-0.00082239	-5.29239690
H	-2.75600041	-0.00018795	-4.22454245
H	-4.02814584	-0.00028930	-2.18355134
H	-2.93025242	-0.00003521	0.02338411
H	-0.94420718	-0.00005436	1.90549191

H	1.21682824	0.00000000	3.06962801
H	3.30418910	-0.00005553	1.81839951
H	3.28782241	-0.00020839	-0.64327477
C	1.67116654	-0.00039388	-5.82564445
C	1.88770883	-0.00071536	-7.15079576
C	0.85390434	-0.00160621	-8.00217639
C	-0.38970413	-0.00216373	-7.50497721
C	-0.58775424	-0.00176467	-6.17673853
H	-1.63576066	-0.00242607	-5.85727883
H	-1.25121292	-0.00308575	-8.19449765
H	1.02342996	-0.00187544	-9.09157428
H	2.91831288	-0.00029374	-7.54495730
H	2.57627633	0.00032426	-5.19500532

1 2 1.0 6 2.0 9 1.0

2 3 2.0 20 1.0

3 4 1.0 21 1.0

4 5 2.0 22 1.0

5 6 1.0 23 1.0

6 7 1.0

7 8 1.0 15 2.0

8 9 1.0 10 1.0

9 13 2.0

10 11 1.0 14 2.0

11 12 2.0 17 1.0

12 13 1.0 18 1.0

13 19 1.0

14 15 1.0 16 1.0

15

16 24 1.0 28 2.0

17

18

19

20

21

22

23

24 25 2.0 33 1.0

25 26 1.0 32 1.0

26 27 2.0 31 1.0

27 28 1.0 30 1.0

28 29 1.0

29

30

31

32

33

Frontier molecular orbitals from checkpoint file

HOMO: 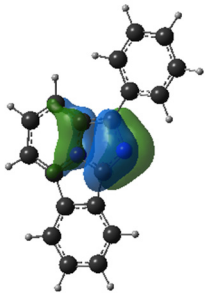 LUMO: 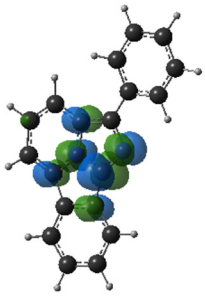

Gaussian input file for TD-DFT with optimized atomic coordinates

%chk=C:\Program Files2\Gaussian\G09W\Scratch\PhenylTD631Gdp.chk

%mem=7GB

%nprocshared=1

td=(nstates=4) b3lyp/6-31g(d,p) scrf=(solvent=methanol) geom=connectivity

PhenylTD631Gdp

0 1

C	2.96147300	0.21805700	0.00003000
C	4.35937500	0.23487800	0.00007500
C	5.04472000	-0.97747700	0.00029400
C	4.34990300	-2.20107900	0.00046300
C	2.95809200	-2.24407600	0.00042000
C	2.24959700	-1.03779900	0.00020800
C	0.83630300	-0.71875100	0.00010900
N	0.77770800	0.63430400	-0.00009700
C	1.98041800	1.29948500	-0.00019700
C	-0.51954300	1.08495500	-0.00021000
C	-0.60908500	2.49462400	-0.00063700
C	0.56610000	3.24493100	-0.00074900
C	1.87108200	2.67374300	-0.00050200
C	-1.26499900	-0.14549900	0.00001400
N	-0.40755600	-1.21627900	0.00016000
C	-2.71809300	-0.34831700	0.00007900
H	-1.56485400	3.00232000	-0.00097000
H	0.48478800	4.32668600	-0.00107300
H	2.74721500	3.31118600	-0.00060900
H	4.90168000	1.17540300	-0.00005600
H	6.13002800	-0.97981800	0.00033600
H	4.91141900	-3.13036100	0.00063100
H	2.43175300	-3.19306500	0.00055100
C	-3.24133400	-1.65659300	-0.00143400
C	-4.61574300	-1.87764400	-0.00142700
C	-5.50680500	-0.80044000	0.00009700
C	-5.00227800	0.50151000	0.00166300

C	-3.62635600	0.72654800	0.00168100
H	-3.26489800	1.74818900	0.00315900
H	-5.68142900	1.34916900	0.00293500
H	-6.57868800	-0.97361900	0.00009200
H	-4.99392100	-2.89605100	-0.00263700
H	-2.55111700	-2.49253900	-0.00265800

1 2 1.5 6 1.5 9 1.0

2 3 1.5 20 1.0

3 4 1.5 21 1.0

4 5 1.5 22 1.0

5 6 1.5 23 1.0

6 7 1.0

7 8 1.5 15 1.5

8 9 1.5 10 1.5

9 13 2.0

10 11 1.5 14 1.5

11 12 1.5 17 1.0

12 13 1.5 18 1.0

13 19 1.0

14 15 1.5 16 1.0

15

16 24 1.5 28 1.5

17

18

19

20

21

22

23

24 25 1.5 33 1.0

25 26 1.5 32 1.0

26 27 1.5 31 1.0

27 28 1.5 30 1.0

28 29 1.0

29

30

31

32

33

TD-DFT predicted excitation energies and oscillator strengths

Excited State 1: Singlet-A 2.7535 eV **450.29 nm** f=0.2696 <S**2>=0.000

70 -> 71 0.69686

This state for optimization and/or second-order correction.

Total Energy, E(TD-HF/TD-KS) = -840.690059447

Copying the excited state density for this state as the 1-particle RhoCI density.

Excited State 2: Singlet-A 3.8120 eV **325.25 nm** f=0.0125 <S**2>=0.000

69 -> 71 0.36218

70 -> 72 0.59886

Excited State 3: Singlet-A 3.9786 eV **311.63 nm** f=0.5341 <S**2>=0.000

69 -> 71 0.12609

70 -> 73 0.68561

Excited State 4: Singlet-A 4.3590 eV **284.43 nm** f=0.0146 <S**2>=0.000

67 -> 71 -0.16206

68 -> 71 0.57476

70 -> 74 -0.34561

A1.9.4 Compound 2.9a

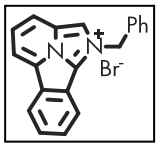

*N-Benzyl replaced by N-Methyl

Gaussian input file for ground state optimization

%chk=C:\Program Files2\Gaussian\G09W\Scratch\MethylatedMinimOrb631Gdp.chk

%mem=7GB

%nprocshared=1

# opt b3lyp/6-31g(d,p) scrf=(solvent=methanol) guess=(always,local,save)
pop=(nbo,savemixed,full) geom=connectivity

MethylatedMinimOrb631Gdp

1 1

N	-0.17202753	-0.00147707	-0.86296243
C	0.05604119	-0.00223147	-2.09930300
C	0.87253503	-0.00213459	-0.16216924
C	-1.00549787	-0.00142089	-2.91536421
C	1.39873142	-0.00312171	-2.15505671
C	-1.26697890	0.00057909	-0.24038326
N	1.91489027	-0.00038177	-0.94414161
C	0.44977192	-0.00242472	1.10766540
C	-2.22562252	0.00066972	-2.33010845
H	-0.88291423	-0.00190062	-4.00921412
H	2.00313791	-0.00149977	-3.07096542
C	-2.38061452	0.00186126	-0.98559093
C	-0.90172588	0.00072924	1.05252190
C	3.36830912	0.00749196	-0.55723524
C	1.09943255	-0.00561344	2.27663836
H	-3.12404572	0.00173057	-2.97067035
H	-3.37750839	0.00365058	-0.51852091
C	-1.63317178	0.00331681	2.17334465
H	3.56689525	-0.81319987	0.09997742

H	3.97181585	-0.08512153	-1.43592880
H	3.60019241	0.92639871	-0.06050541
C	0.36262433	-0.00206137	3.40106881
H	2.19865869	-0.01287627	2.31840613
C	-0.98229104	0.00256916	3.34993421
H	-2.73387770	0.00614275	2.13224336
H	0.87031648	-0.00436958	4.38051356
H	-1.56196801	0.00480250	4.28861897

1 6 1.0 2 1.0 3 1.0

2 4 1.0 5 2.0

3 7 2.0 8 1.0

4 9 2.0 10 1.0

5 7 1.0 11 1.0

6 12 2.0 13 1.0

7 14 1.0

8 13 2.0 15 1.0

9 12 1.0 16 1.0

10

11

12 17 1.0

13 18 1.0

14 19 1.0 20 1.0 21 1.0

15 22 2.0 23 1.0

16

17

18 24 2.0 25 1.0

19

20

21

22 24 1.0 26 1.0

23

24 27 1.0

25

26

27

Frontier molecular orbitals from checkpoint file

HOMO: 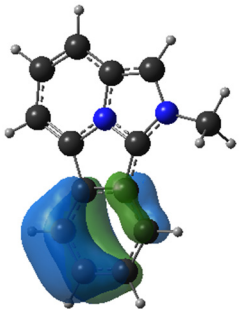 LUMO: 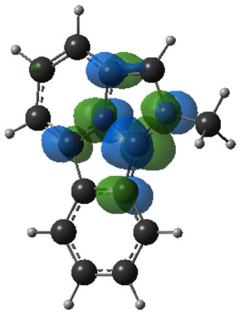

Gaussian input file for TD-DFT with optimized atomic coordinates

%chk=C:\Program Files2\Gaussian\G09W\Scratch\MethylatedTD631Gdp.chk

%mem=7GB

%nprocshared=1

td=(nstates=4) b3lyp/6-31g(d,p) scrf=(solvent=methanol) geom=connectivity

MethylatedTD631Gdp

1 1

C	-2.42018119	-2.34220941	0.00003499
C	-0.99633897	-2.49304881	0.00002557
C	-0.20953420	-1.36622025	-0.00003256
N	-0.91900458	-0.18403167	-0.00016138
C	-2.27239266	0.05525262	0.00003097
C	-3.06775924	-1.11781098	0.00005584
C	-0.17563880	0.93346033	-0.00021753

N	-1.06899709	1.95734525	-0.00018560
C	-2.35350080	1.45122353	0.00007062
C	1.18235838	-0.92500056	-0.00006472
C	1.21034626	0.51698952	-0.00017789
C	2.37694220	-1.64701655	0.00010083
C	3.58100365	-0.94554039	0.00015538
C	3.60397702	0.45892366	0.00002319
C	2.42678324	1.20431388	-0.00014842
C	-0.73276556	3.38635258	0.00028525
H	-3.02112014	-3.24453548	0.00005181
H	-0.55765955	-3.48314262	0.00011293
H	-4.14832467	-1.05265964	0.00014771
H	-3.21108870	2.10346393	-0.00015346
H	2.36814890	-2.73176857	0.00017996
H	4.51730808	-1.49346219	0.00031109
H	4.55793346	0.97570100	0.00007131
H	2.46069158	2.28797029	-0.00028318
H	-0.15477004	3.62494356	-0.89347925
H	-1.65850291	3.95754845	-0.00054205
H	-0.15640025	3.62473104	0.89516285

1 2 1.0 6 2.0 17 1.0

2 3 2.0 18 1.0

3 4 1.0 10 1.0

4 5 1.0 7 1.0

5 6 1.0 9 2.0

6 19 1.0

7 8 2.0 11 1.0

8 9 1.0 16 1.0

9 20 1.0

10 11 2.0 12 1.0

11 15 1.0

12 13 2.0 21 1.0

13 14 1.0 22 1.0

14 15 2.0 23 1.0

15 24 1.0

16 25 1.0 26 1.0 27 1.0

17

18

19

20

21

22

23

24

25

26

27

TD-DFT predicted excitation energies and oscillator strengths

Excited State 1: Singlet-A 3.2509 eV **381.39 nm** f=0.2193 <S**2>=0.000

53 -> 55 0.11048

53 -> 56 -0.11532

54 -> 55 0.68491

This state for optimization and/or second-order correction.

Total Energy, E(TD-HF/TD-KS) = -649.369342090

Copying the excited state density for this state as the 1-particle RhoCI density.

Excited State 2: Singlet-A 3.8646 eV **320.82 nm** f=0.0815 <S**2>=0.000

53 -> 55 0.64998

54 -> 56 0.22920

Excited State 3: Singlet-A 4.5476 eV **272.64 nm** f=0.2092 <S**2>=0.000

51 -> 55 -0.13904

53 -> 55 -0.19462

54 -> 56 0.64422

Excited State 4: Singlet-A 4.7006 eV **263.76 nm** f=0.0057 <S**2>=0.000

52 -> 55 0.66122

53 -> 56 0.11388

53 -> 57 -0.13302

54 -> 57 0.10875

Annexe 2 : Informations supplémentaires associées à l'article «Improved Zinc-Catalyzed Simmons-Smith Reaction: Access to Various 1,2,3-Trisubstituted Cyclopropanes»

A2.1.General Information

Unless otherwise stated, reactions were run under an argon atmosphere with rigid exclusion of moisture from reagents and glassware using standard techniques for manipulating air-sensitive compounds.[149] All glassware was flame-dried or oven-dried prior to use. THF, DCM, Toluene, and Et_2O were obtained by filtration through drying columns on a filtration system. MeOH was distilled from CaH_2 and stored under argon. Analytical thin-layer chromatography (TLC) was performed on precoated, glass-backed silica gel (Silicycle Glass Backed TLC Extra Hard Layer, 60 Å). Visualization of the developed chromatogram was performed by UV or aqueous potassium permanganate ($KMnO_4$). Flash column chromatography was performed on an automatic purification system (Teledyne Isco Combiflash® Companion). Pre-packed normal phase silica gel columns were used for separation of products using Teledyne Isco RediSep® Rf High Performance Gold or Grace Reveleris® High Performance columns. Melting points were obtained on a Buchi melting point apparatus and are uncorrected. Nuclear magnetic resonance spectra (^1H, ^{13}C, ^{19}F, DEPT-135, NOE) were recorded on an Avance AV500 MHz, Avance AV400 MHz, Avance AV 300 MHZ, or Avance DRX400 MHz spectrometer. Chemical shifts for ^1H NMR spectra are recorded in parts per million from tetramethylsilane with the solvent resonance as the internal standard (chloroform, δ = 7.26 ppm). Data are reported as follows: chemical shift, multiplicity (s = singlet, d = doublet, t = triplet, q = quartet, qn = quintet, sx = sextet, h = heptet, o = octet, n = nonet, m = multiplet, br = broad and app = apparent), coupling constant in Hz and integration. Chemical shifts for ^{13}C NMR spectra are recorded in parts per million from tetramethylsilane using the central peak of deuterated chloroform (δ = 77.16 ppm) as the internal standard. All ^{13}C NMR spectra were obtained with complete proton decoupling. Infrared spectra were taken on a Bruker Alpha Vertex Series ATR (neat) and are reported in reciprocal centimetres (cm^{-1}). High resolution

mass spectra were performed by the Centre régional de spectroscopie de masse de l'Université de Montréal.

A2.2. Reagents

Unless otherwise stated, commercial reagents were used without purification. I_2 was commercially available and used as received. Et_2Zn was purchased neat from Akzo Nobel and used as received. 2,6-di-*tert*-butylphenol was purified by precipitation from dry hexanes at -78 °C, followed by filtration and drying under vacuum. It was then stored in a desiccator. Starting alkenes were either commercially available or synthesized according to previously reported procedures.

A2.3. Experimental Procedures and Characterization Data

A2.3.1. Diazo reagent

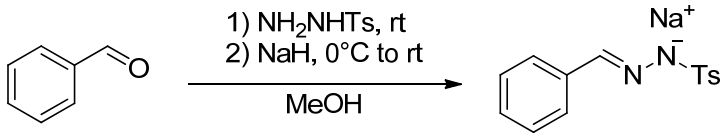

Sodium (E)-2-benzylidene-1-tosylhydrazin-1-ide:[157] To an oven-dried 50 mL glass beaker equipped with a magnetic stirring bar were added *p*-toluenesulfonyl hydrazide (10.0 g, 53.8 mmol, 1.10 equiv) and methanol (13.0 mL). To the resulting suspension was added benzaldehyde (5.19 g, 4.94 mL, 48.9 mmol, 1.00 equiv). Mixture becomes quickly homogenous. 4-5 minutes later, a white precipitate appears (slight exotherm). The solid is recovered using a fritted glass filter and washed with dry MeOH.

The solid is then transferred into an oven-dried 100mL round bottom flask and suspended in dry MeOH (35.0 mL). Under strong agitation, the slurry is cooled to 0 □ C and NaH (60% in mineral oil, 2.15 g, 53.8 mmol, 1.10 equiv) was added portion-wise (strong gas evolution). The milky mixture was warmed to rt and stirred for 15 minutes before concentrating under vacuum, crushing the solid periodically with a metal spatula. This solid can be used directly in the next step. Washing with hexanes and concentrating under vacuum again yielded a white solid (12.1 g, 40.8 mmol, 84% yield). **^{1}H NMR** (D_2O, 300 MHz): 7.96 (s, 1H), 7.75 (d, J = 8.1 Hz, 2H), 7.55-7.52 (m, 2H), 7.41-7.34 (m, 5H), 2.38 (s, 3H). Product corresponds to literature characterization data.[2]

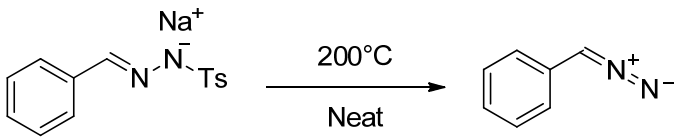

Phenyldiazomethane:[115,158] To the 100 mL round bottom flask containing sodium (E)-2-benzylidene-1-tosylhydrazin-1-ide (14.5 g, 48.9 mmol) was fitted a simple distillation head-condenser and a 100 mL dry round bottom flask for distillate recovery. Whole setup was torched under vacuum, purged with argon and put under vacuum. Then the recovery flask was cooled to -50 °C (acetone/dry ice bath) and the reaction flask heated to 100 °C in an oil bath. When a small amount of red liquid appears in recovery flask, mixture is heated to 200 °C in increments. After about 1 h, no more product is collecting in the recovery flask. Setup is purged with Ar and 20.0 mL of CH_2Cl_2 is added through the thermometer opening. The resulting red solution is dried using Na_2SO_4. It is then transferred under a positive argon pressure (using a needle with a filter paper taped around the female Luer Lok® end), rinsing with 15.0 mL of CH_2Cl_2, into a dry 50 mL round bottom flask containing a dozen KOH pellets. Approximately 40 mL of a 0.76 M phenyldiazomethane solution are recovered (30.0 mmol, 3.50 g, 61% yield from benzaldehyde).

The solution was titrated using a solution of I_2 in toluene. It can be kept in the freezer (-20 °C) under argon for a month without significant variation of concentration or reactivity. A 1:1 mixture of acetic acid and acetone was used to neutralize any trace of diazo reagent on lab ware.

The diazo reagent could be concentrated under vacuum at 0 °C to yield a red oil. **^{1}H NMR** ($CDCl_3$, 400 MHz): 7.30 (t, J = 8.0 Hz, 2H), 7.04 (t, *J* = 7.6 Hz, 1H), 6.92 (d, *J* = 8.4 Hz, 2H), 4.94 (s, 1H). Product corresponds to literature characterization data.[113]

A2.3.2.General Cyclopropanation Procedures

Procedure A: To a flame-dried 5 mL microwave tube, iodine (16.5 mg, 0.0650 mmol, 0.130 equiv) was added, followed by 1.0 mL of CH_2Cl_2. Once the iodine was completely dissolved, mixture was cooled to 0°C and Et_2Zn (8.03 mg, 6.66 µL, 0.0650 mmol, 0.130 equiv) was added dropwise (mixture changes from a violet solution to a white suspension). 2,6-Di-*t*-butylphenol (13.4 mg, 0.0650 mmol, 0.130 equiv) was transferred into mixture using 1.0 mL of CH_2Cl_2. Reaction vessel was warmed to rt and **alkene (0.500 mmol, 1.00 equiv)** was transferred into it using 1.0 mL of CH_2Cl_2. Phenyldiazomethane (1.32 mL of a 0.76 M solution in CH_2Cl_2, 1.00 mmol, 2.00 equiv) was

added over 1h30 using a syringe pump (instant gas evolution). Once the red color of the diazo has faded away (usually less than 1 h after complete addition), mixture was quenched with saturated $NaHCO_3$. Phases were separated and aqueous phase was extracted with CH_2Cl_2 (3 × 10.0 mL). The organic phases were combined, dried with $MgSO_4$, filtered and concentrated under reduced pressure.

Procedure B: To a flame-dried 5 mL microwave tube, iodine (25.3 mg, 0.100 mmol, 0.200 equiv) was added, followed by 2.0 mL of CH_2Cl_2. Once the iodine was completely dissolved, mixture was cooled to 0°C and Et_2Zn (6.18 mg, 5.13 µL, 0.0500 mmol, 0.100 equiv) was added dropwise (mixture changes from a violet solution to a white suspension). Reaction vessel was warmed to rt and **alkene (0.500 mmol, 1.00 equiv)** was transferred into it using 1.0 mL of CH_2Cl_2. Phenyldiazomethane (1.32 mL of a 0.76 M solution in CH_2Cl_2, 1.00 mmol, 2.00 equiv) was added over 1h30 using a syringe pump (instant gas evolution). Once the red color of the diazo has faded away (usually less than 1 h after complete addition), mixture was quenched with saturated $NaHCO_3$. Phases were separated and aqueous phase was extracted with CH_2Cl_2 (3 × 10.0 mL). Organic phases were combined, dried with $MgSO_4$, filtered and concentrated under reduced pressure.

Procedure C: Same as **procedure B**, but using 0.300 equiv of iodine (38.0 mg, 0.150 mmol), 0.150 equiv of Et_2Zn (9.27 mg, 7.69 µL, 0.0750 mmol) and 2.50 equiv of phenyldiazomethane (1.65 mL of a 0.76 M solution in CH_2Cl_2, 1.25 mmol).

General procedure for the removal of remaining starting alkene by dihydroxylation:
To a 20 mL vial was added the purified cyclopropane contaminated with the starting alkene (0.5 mmol), acetone (1.0 mL), water (1.0 mL), acetonitrile (1.0 mL), K_2OsO_4 (2.0 mg, 5.4 µmol, 0.075 equiv) and NMO (0.15 mL of a 50% solution in H_2O, 0.72 mmol, 1,4 equiv). The reaction mixture was stirred 40 h at room temperature. Water and Et_2O are then added and the mixture was extracted with Et_2O (3 × 10 mL). The organic phases were combined, dried with $MgSO_4$, filtered and concentrated under reduced pressure. The pure cyclopropane was obtained after purification by flash chromatography.

A2.3.3.Cyclopropylmethyl Ethers and Ester (products 3.3a to 3.3g)

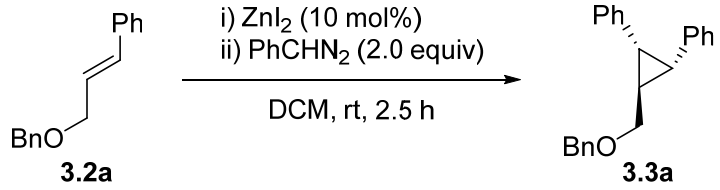

3.2a **3.3a**

((1*R*,2*S*,3*r*)-3-((benzyloxy)methyl)cyclopropane-1,2-diyl)dibenzene (3.3a): The starting alkene was synthesized according to a previously known procedure.[159] The reaction was performed using **procedure B**. Yield (99%) and diastereomeric ratio (>95:5) were determined by ^{1}H-NMR analysis of the crude mixture using triphenylmethane as internal standard. The crude product was purified by flash chromatography (0%-10% ethyl acetate / hexanes) to yield a white solid (131 mg, 0.42 mmol, 83% yield). **mp:** 57-59 °C; **^{1}H-NMR** ($CDCl_3$, 500 MHz): δ 7.40-7.35 (m, 4H), 7.32-7.29 (m, 1H), 7.12-7.05 (m, 6H), 6.96-6.94 (m, 4H), 4.67 (s, 2H), 3.73 (d, *J* = 6.5 Hz, 2H), 2.42 (d, *J* = 5.5 Hz, 2H), 2.10 (qn, *J* = 6.0 Hz, 1H); **^{13}C-NMR** ($CDCl_3$, 75 MHz): δ 138.6 (C), 137.7 (C), 129.1 (CH), 128.6 (CH), 127.9 (CH), 127.8 (CH), 127.7 (CH), 125.9 (CH), 73.2 (CH_2), 72.7 (CH_2), 29.9 (CH), 25.2 (CH); **FTIR** (cm^{-1}) (neat): 3026 (w), 2854 (w), 1603 (w), 1496 (m), 1454 (w), 1087 (m), 1074 (m), 749 (m), 696 (s); **HRMS** (ESI, Pos): calcd for $C_{23}H_{26}NO$ $[M+NH_4]^+$: 332.2009 *m/z*, found: 332.2010 *m/z*. Relative configuration determined by analogy with **3.5a**.

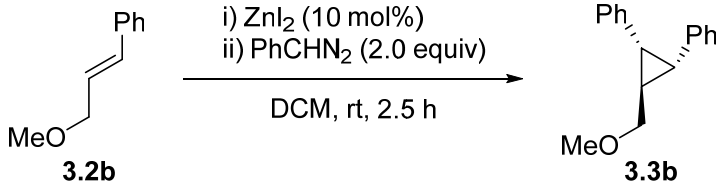

3.2b **3.3b**

((1*R*,2*S*,3*r*)-3-(methoxymethyl)cyclopropane-1,2-diyl)dibenzene (3.3b): The starting alkene was synthesized according to a previously known procedure.[160] The reaction was performed using **procedure B**. Yield (95%) and diastereomeric ratio (>95:5) were determined by ^{1}H-NMR analysis of the crude mixture using triphenylmethane as internal standard. The crude product was purified by flash chromatography (0%-15% ethyl acetate / hexanes) to yield a clear oil (100 mg, 0.42 mmol, 84% yield). **^{1}H-NMR** ($CDCl_3$, 300 MHz): δ 7.15-7.04 (m, 6H), 6.97-6.94 (m, 4H), 3.65 (d, *J* = 8.4 Hz, 2H), 3.47 (s, 3H), 2.43 (d, *J* = 5.7 Hz, 2H), 2.07 (qn, *J* = 6.0 Hz, 1H); **^{13}C-NMR** ($CDCl_3$, 75 MHz): δ 137.6 (C), 129.1 (CH), 127.9 (CH), 125.9 (CH), 75.8 (CH_2), 58.6 (CH_3), 29.9 (CH), 25.0 (CH); **FTIR** (cm^{-1}) (neat): 3025 (w), 2923 (w), 2856 (w), 2822 (w), 1603 (w), 1496 (m), 1446 (w),

1378 (w), 1196 (w), 1098 (s), 750 (m), 695 (s), 523 (w); **HRMS** (ESI, Pos): calcd for $C_{17}H_{22}NO$ $[M+NH_4]^+$: 256.1696 *m/z*, found: 256.1700 *m/z*. Relative configuration determined by analogy with **3.5a**.

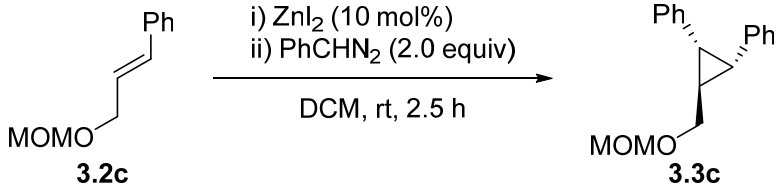

3.2c **3.3c**

((1*R*,2*S*,3*r*)-3-((methoxymethoxy)methyl)cyclopropane-1,2-diyl)dibenzene (3.3c): The starting alkene was synthesized according to a previously known procedure.[161] The reaction was performed using **procedure B**. Yield (99%) and diastereomeric ratio (>95:5) were determined by ^{1}H-NMR analysis of the crude mixture using triphenylmethane as internal standard. The crude product was purified by flash chromatography (0%-5% ethyl acetate / hexanes) to yield a clear oil (119 mg, 0.44 mmol, 89% yield). **^{1}H-NMR** ($CDCl_3$, 400 MHz) : δ 7.12-7.03 (m, 6H), 6.95-6.93 (m, 4H), 4.73 (s, 2H), 3.77 (d, *J* = 6.4 Hz, 2H), 3.39 (s, 3H), 2.43 (d, *J* = 5.6 Hz, 2H), 2.08 (qn, *J* = 6.0 Hz, 1H); **^{13}C-NMR** ($CDCl_3$, 75 MHz) : δ 137.6 (C), 129.1 (CH), 127.9 (CH), 125.9 (CH), 96.3 (CH_2), 70.9 (CH_2), 55.4 (CH_3), 30.0 (CH), 25.1 (CH); **FTIR** (cm^{-1}) (neat): 3026 (w), 2930 (w), 2881 (w), 1602 (w), 1497 (w), 1148 (m), 1104 (m), 1037 (s), 917 (m), 751 (m), 696 (s), 524 (w); **HRMS** (ESI, Pos): calcd for $C_{18}H_{24}NO_2$ $[M+NH_4]^+$: 286.1802 *m/z*, found: 286.1805 *m/z*. Relative configuration determined by analogy with **3.5a**.

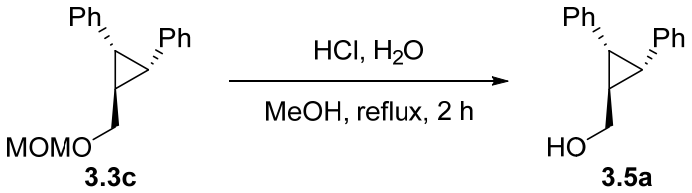

3.3c **3.5a**

((1*r*,2*R*,3*S*)-2,3-diphenylcyclopropyl)methanol (3.5a): In a 5mL microwave tube, **3.3c** (25.0 mg, 0.090 mmol, 1.0 equiv) was dissolved in 1.0 mL of methanol. 25% HCl (0.05 mL, 0.35 mmol, 3.9 equiv) was added dropwise and mixture was heated to reflux for 2h. Mixture was cooled down to rt and saturated $NaHCO_3$ was added dropwise until gas evolution ceased. 3 mL of Et_2O was added, phases were separated and aqueous phase was extracted with Et_2O (2 × 5 mL). The organic phases were combined, dried with $MgSO_4$, filtered and concentrated under reduced pressure to yield a

white crystalline product (18 mg, 0.080 mmol, 90% yield). Product corresponds to the characterization data of **3.5a** (vide infra).

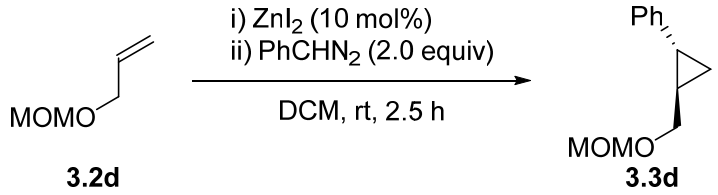

3.2d **3.3d**

***rac*-((1*R*,2*R*)-2-((methoxymethoxy)methyl)cyclopropyl)benzene (3.3d):** The starting alkene was synthesized according to a previously known procedure.[162] The reaction was performed using **procedure B**. Yield (53%) and diastereomeric ratio (85:15) were determined by ^{1}H-NMR analysis of the crude mixture using triphenylmethane as internal standard. The crude product was purified by flash chromatography (4% diethyl ether/hexanes) to yield both diastereomers as a clear oil (36 mg, 0.24 mmol, 49% yield). **^{1}H-NMR** ($CDCl_3$, 400 MHz): δ 7.28-7.24 (m, 2H), 7.17-7.14 (m, 1H), 7.09-7.07 (m, 2H), 4.67 (s, 2H), 3.58 (dd, *J* = 6.8, 10.8 Hz, 1H), 3.52 (dd, *J* = 6.8, 10.4 Hz, 1H), 3.38 (s, 3H), 1.84 (dt, *J* = 4.8, 8.8 Hz, 1H), 1.49-1.41 (m, 1H), 1.02-0.92 (m, 2H); Product corresponds to literature characterization data.[62]

3.2e **3.3e**

***rac*-((1*S*,2*R*,3*R*)-2-ethyl-3-((methoxymethoxy)methyl)cyclopropyl)benzene (3.3e):** The starting alkene was synthesized according to a previously known procedure.[16] The reaction was performed using **procedure B**. Yield (64%) and diastereomeric ratio (57:43) were determined by ^{1}H-NMR analysis of the crude mixture using triphenylmethane as internal standard. The crude product was purified by flash chromatography (4% ethyl acetate/hexanes) to yield major diastereomer (pictured) as a clear oil (43 mg, 0.19 mmol, 39% yield) and minor diastereomer as a clear oil (33.0 mg, 0.150 mmol, 30% yield). **^{1}H-NMR** ($CDCl_3$, 400 MHz): δ 7.32-7.24 (m, 4H), 7.22-7.16 (m, 1H), 4.65 (s, 2H), 3.64 (dd, *J* = 7.2, 10.4 Hz, 1H), 3.46 (dd, *J* = 7.6, 10.4 Hz, 1H), 3.37 (s, 3H), 2.30 (t, *J* = 8.8 Hz, 1H), 1.57-1.46 (m, 2H), 1.27-1.18 (m, 1H), 1.17-1.09 (m, 1H), 1.06 (t, *J* = 6.8 Hz, 3H); **^{13}C-NMR** ($CDCl_3$, 75 MHz): δ 137.1 (C), 130.9 (CH), 128.3 (CH), 126.2 (CH), 96.9 (CH_2), 65.8 (CH_2), 55.5 (CH_3), 23.8 (CH), 21.8 (CH), 19.1 (CH), 18.6 (CH_2), 14.6 (CH_3); **FTIR** (cm^-

[1]) (neat): 2959 (w), 2930 (w), 2875 (w), 1497 (w), 1445 (w), 1147 (m), 1104 (s), 1039 (s), 916 (m), 780 (m), 721 (m), 700 (s), 458 (w); **HRMS** (ESI, Pos): calcd for $C_{14}H_{20}AgO_2$ [M + Ag]$^+$: 327.0509 *m*/*z*, found: 327.0497 *m*/*z*. Relative configuration determined by analogy with **3.5n**.

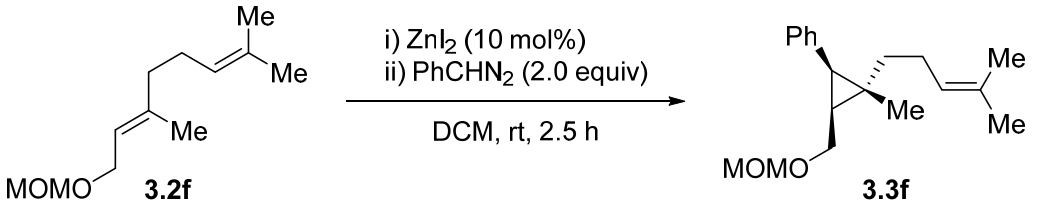

***rac*-((1*R*,2*S*,3S)-3-((methoxymethoxy)methyl)-2-methyl-2-(4-methylpent-3-en-1-yl)cyclopropyl)benzene (3.3f):** The starting alkene was synthesized according to a previously known procedure.[167] The reaction was performed using **procedure B**. Yield (69%) and diastereomeric ratio (65:35) were determined by ^{1}H-NMR analysis of the crude mixture using triphenylmethane as internal standard. The crude product was purified by flash chromatography (0%-5% diethyl ether/hexanes) to yield major diastereomer as a clear oil (105 mg, 0.36 mmol, 73% yield). **^{1}H-NMR** ($CDCl_3$, 300 MHz): δ 7.30-7.17 (m, 5H), 5.18 (t, *J* = 6.9 Hz, 1H), 4.64 (s, 2H), 3.63 (dd, *J* = 7.2, 10.5 Hz, 1H), 3.40 (dd, *J* = 7.8, 10.5 Hz, 1H), 3.37 (s, 3H), 2.20 (q, *J* = 7.2 Hz, 2H), 2.05 (d, *J* = 9.0 Hz, 1H), 1.70 (s, 3H), 1.65 (s, 3H), 1.61-1.51 (m, 1H), 1.29-1.21 (m, 2H), 0.95 (s, 3H); **^{13}C-NMR** ($CDCl_3$, 75 MHz): δ 137.5 (C), 131.5 (C), 131.0 (CH), 128.3 (CH), 126.2 (CH), 124.6 (CH), 96.7 (CH_2), 66.3 (CH_2), 55.4 (CH_3), 43.0 (CH_2), 31.4 (CH), 27.2 (CH), 25.9 (CH_3), 25.6 (CH_2), 23.7 (C), 17.8 (CH_3), 14.2 (CH_3); **FTIR** (cm^{-1}) (neat): 2922 (m), 2880 (w), 1445 (m), 1378 (w), 1149 (m), 1104 (s), 1039 (s), 917 (m), 731 (m), 700 (s); **HRMS** (ESI, Pos): calcd for $C_{19}H_{28}NaO_2$ [M + Na]$^+$: 311.1982 *m*/*z*, found: 311.1988 *m*/*z*. Relative configuration determined by analogy with **3.5m**.

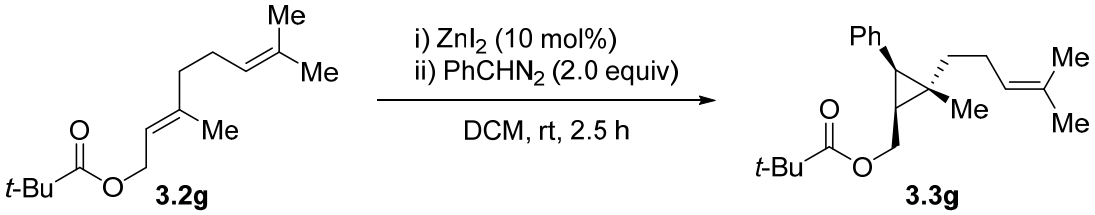

***rac*-((1*S*,2*S*,3*R*)-2-methyl-2-(4-methylpent-3-en-1-yl)-3-phenylcyclopropyl)methyl pivalate (3.3g):** The starting alkene was synthesized according to a previously known procedure.[163] The reaction was performed using **procedure B**. Yield (43%) and diastereomeric ratio (65:35) were determined by ^{1}H-NMR analysis of the crude mixture using triphenylmethane as internal standard.

The crude product was purified by flash chromatography (0.4% diethyl ether/hexanes) to yield both diastereomers as a clear oil (80 mg, 0.24 mmol, 49% yield). Major diastereomer (pictured): **^{1}H-NMR** ($CDCl_3$, 400 MHz): δ 7.28-7.23 (m, 2H), 7.18-7.12 (m, 3H), 5.32 (t, *J* = 6.4 Hz, 1H), 4.55 (d, *J* = 7.2 Hz, 2H), 2.11 (q, *J* = 7.6 Hz, 2H), 1.83 (d, *J* = 8.8 Hz, 1H), 1.67 (s, 3H), 1.58-1.52 (m, 2H), 1.30-1.15 (m, 1H), 1.26 (s, 3H), 1.19 (s, 9H), 0.95 (s, 3H); **^{13}C-NMR** ($CDCl_3$, 75 MHz): δ 178.8 (C), 142.0 (C), 138.8 (C), 131.0 (CH), 128.1 (CH), 125.8 (CH), 119.0 (CH), 61.5 (CH_2), 40.2 (CH_2), 38.9 (C), 31.3 (CH), 28.2 (CH) 27.4 (CH_3), 25.0 (CH_2), 21.7 (CH_3) 19.4 (C), 17.1 (CH_3), 16,6 (CH_3); **FTIR** (cm^{-1}) (neat): 2972 (m), 2934 (m), 2865 (w), 1726 (s), 1458 (m), 1281 (m), 1148 (s), 953 (w), 727 (w), 700 (m); **HRMS** (ESI, Pos): calcd for $C_{22}H_{36}NO_2$ $[M+NH_4]^+$: 346.2741 *m*/*z*, found: 346.2733 *m*/*z*. Relative configuration determined by analogy with **5m**.

A2.3.4.Arylcyclopropanes from Unactivated Alkenes (products 3.3h to 3.3n)

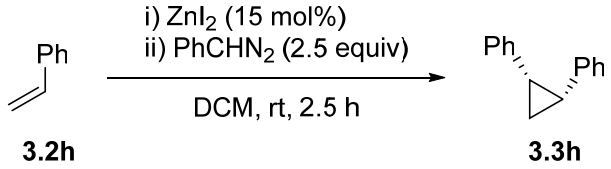

(1*R*,2*S*)-1,2-diphenylcyclopropane (3.3h): The starting alkene was obtained from a commercial source and purified by distillation under argon. The reaction was performed using **procedure C**. Diastereomeric ratio (92:8) was determined by ^{1}H-NMR analysis of the crude mixture using 4-dimethylaminopyridine as internal standard. Dihydroxylation was used to remove the remaining starting alkene and stilbenes. The crude product was purified by flash chromatography (100% hexanes) to yield both diastereomers as a clear oil (69 mg, 0.36 mmol, 71% yield). **^{1}H-NMR** ($CDCl_3$, 400 MHz): δ 7.19-7.04 (m, 6H), 6.99-6.97 (m, 4H), 2.52 (dd, *J* = 8.8, 11.2 Hz, 2H), 1.54-1.46 (m, 1H), 1.44-1.38 (m, 1H); Product corresponds to literature characterization data.[79]

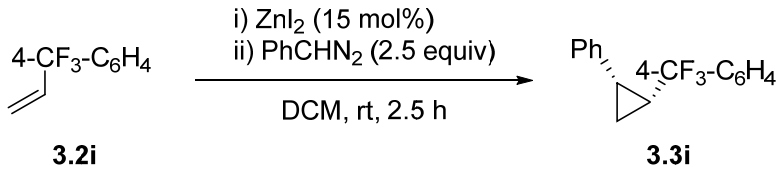

***rac*-1-((1*R*,2*S*)-2-phenylcyclopropyl)-4-(trifluoromethyl)benzene (3.3i):** The starting alkene was synthesized according to a previously known procedure.[164] The reaction was performed using

procedure C. Yield (64%) and diastereomeric ratio (>95:5) were determined by ^{1}H-NMR analysis of the crude mixture using 4-dimethylaminopyridine as internal standard. Dihydroxylation was used to remove the remaining starting alkene and stilbenes. The crude product was purified by flash chromatography (100% hexanes) to yield both diastereomers as a clear oil (70 mg, 0.27 mmol, 53% yield). **^{1}H-NMR** ($CDCl_3$, 400 MHz): δ 7.54 (d, J = 11.2 Hz, 2H), 7.15-7.04 (m, 3H), 7.01-6.95 (m, 4H), 2.63-2.46 (m, 2H), 1.58-1.50 (m, 1H), 1.45-1.39 (m, 1H); **^{13}C-NMR** ($CDCl_3$, 75 MHz): δ 143.2 (C, q, *J* = 1,3 Hz), 137.6 (C), 129.3 (CH), 129.0 (CH), 128.0 (CH), 127.8 (C, q, *J* = 32.0 Hz), 126.2 (CH), 124.7 (CH, q, J = 3.8 Hz), 124.5 (C, q, J = 270.2 Hz) 25.2 (CH), 24.0 (CH), 11.9 (CH_2); **^{19}F-NMR** (C_6F_6/$CDCl_3$, 282 MHz) : δ 65.4 (s, 3F); **FTIR** (cm^{-1}) (neat): 3028 (w), 1619 (w), 1322 (s), 1161 (m), 1110 (s), 1065 (s), 1015 (s), 835 (m), 696 (s); **HRMS** (ESI, Pos): calcd for $C_{16}H_{14}F_3$ $[M+H]^+$: 263.1048 *m*/*z*, found: 263.1035 *m*/*z*. Relative configuration determined by analogy with **3.3h**.

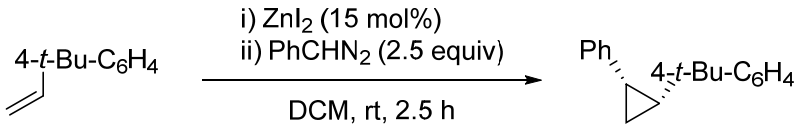

3.2j **3.3j**

***rac*-1-(*tert*-butyl)-4-((1*R*,2*S*)-2-phenylcyclopropyl)benzene (3.3j):** The starting alkene was obtained from a commercial source and purified by flash chromatography. The reaction was performed using **procedure C**. Yield (76%) and diastereomeric ratio (92:8) were determined by ^{1}H-NMR analysis of the crude mixture using 4-dimethylaminopyridine as internal standard. Dihydroxylation was used to remove the remaining starting alkene and stilbenes. The crude product was purified by flash chromatography (100% hexanes) to yield both diastereomers as a clear oil (83 mg, 0.33 mmol, 66% yield). **^{1}H-NMR** ($CDCl_3$, 400 MHz): δ 7.15-7.06 (m, 5H), 6.98-6.95 (m, 2H), 6.87 (d, *J* = 8.4 Hz. 2H), 2.45 (dd, *J* = 6.4, 8.4 Hz, 2H), 1.51-1.42 (m, 1H), 1.34-1.30 (m, 1H), 1.24 (s, 9H); **^{13}C-NMR** ($CDCl_3$, 75 MHz): δ 148.5 (C), 138.8 (C), 135.5 (C), 129.1 (CH), 128.7 (CH), 127.7 (CH), 125.6 (CH), 124.7 (CH), 34.4 (C), 31.5 (CH_3), 24.4 (CH), 24.1 (CH), 12.0 (CH_2); **FTIR** (cm^{-1}) (neat): 3026 (w), 2961 (m), 2867 (w), 1518 (w), 1498 (w), 1458 (w), 1362 (w), 828 (m), 769 (m), 696 (s), 555 (m); **HRMS** (ESI, Pos): calcd for $C_{19}H_{22}Ag$ $[M + Ag]^+$: 357.0767 *m*/*z*, found: 357.0751 *m*/*z*. Relative configuration determined by analogy with **3h**.

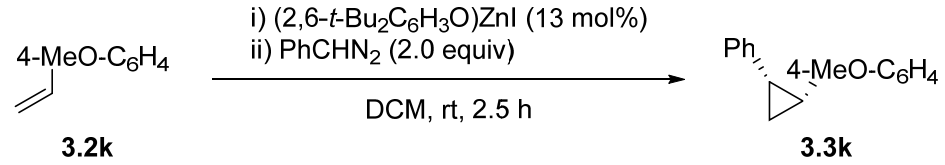

***rac*-1-methoxy-4-((1*R*,2*S*)-2-phenylcyclopropyl)benzene (3.3k):** The starting alkene was synthesized according to a previously known procedure.[165] The reaction was performed using **procedure A**. Yield (54%) and diastereomeric ratio (81:19) were determined by ^{1}H-NMR analysis of the crude mixture using triphenylmethane as internal standard. Dihydroxylation was used to remove the remaining starting alkene. The crude product was purified by flash chromatography (100% hexanes) to yield both diastereomers as a clear oil (60 mg, 0.27 mmol, 53% yield). **^{1}H-NMR** ($CDCl_3$, 400 MHz): δ 7.21-7.02 (m, 3H), 6.95-6.88 (m, 4H), 6.66 (d, *J* = 11.6 Hz), 3.72 (s, 3H), 2.46-2.41 (m, 2H), 1.49-1.41 (m, 1H), 1.33-1.27 (m, 1H); Product corresponds to literature characterization data.[168]

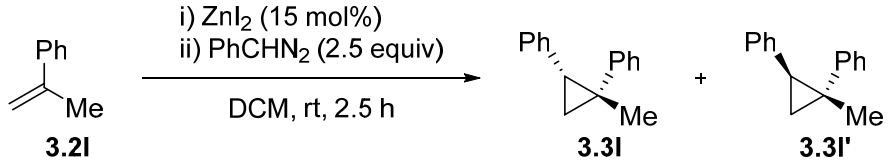

***rac*-((1*R*,2*R*)-1-methylcyclopropane-1,2-diyl)dibenzene (3.3l):** The starting alkene was obtained from a commercial source and purified by flash chromatography. The reaction was performed using **procedure C**. Yield (74%) and diastereomeric ratio (69:31) were determined by ^{1}H-NMR analysis of the crude mixture using 4-dimethylaminopyridine as internal standard. Dihydroxylation was used to remove the remaining starting alkene and stilbenes. The crude product was purified by flash chromatography (100% hexanes) to yield major diastereomer as a clear oil (52 mg, 0.25 mmol, 50% yield) and minor diastereomer as a clear oil (30 mg, 0.14 mmol, 29% yield). Major diastereomer (**3l**): **^{1}H-NMR** ($CDCl_3$, 400 MHz): δ 7.18-6.95 (m, 8H), 6.75-6.72 (m, 2H), 2.22 (dd, *J* = 8.0, 11.6 Hz, 1H), 1.54 (s, 3H), 1.53-1.48 (m, 1H), 1.28-1.22 (m, 1H); Product corresponds to literature characterization data.[157] Minor diastereomer (**3l'**) : **^{1}H-NMR** ($CDCl_3$, 400 MHz): δ 7.40-7.18 (m, 10H), 2.41 (dd, *J* = 8.8, 11.6 Hz, 1H), 1.45 (dd, *J* = 6.8, 11.6 Hz, 1H), 1.24 (dd, *J* = 6.8, 8.8 Hz, 1H); Product corresponds to literature characterization data.[157]

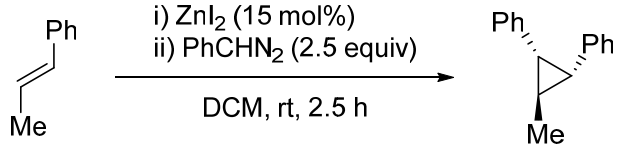

3.2m **3.3m**

((1*R*,2*S*,3*s*)-3-methylcyclopropane-1,2-diyl)dibenzene (3.3m): The starting alkene was obtained from a commercial source and purified by flash chromatography. The reaction was performed using **procedure C**. Yield (52%) and diastereomeric ratio (75:25) were determined by ^{1}H-NMR analysis of the crude mixture using 4-dimethylaminopyridine as internal standard. Dihydroxylation was used to remove stilbenes. The crude product was purified by flash chromatography (100% hexanes) to yield both diastereomers as a clear oil (48 mg, 0.23 mmol, 46% yield). **^{1}H-NMR** ($CDCl_3$, 400 MHz): δ 7.10-7.01 (m, 6H), 6.92-6.90 (m, 4H), 2.20 (d, *J* = 6.0 Hz, 2H), 1.71 (sx, *J* = 6.0 Hz, 1H), 1.39 (d, J = 6.0 Hz, 3H); Product corresponds to literature characterization data.[166]

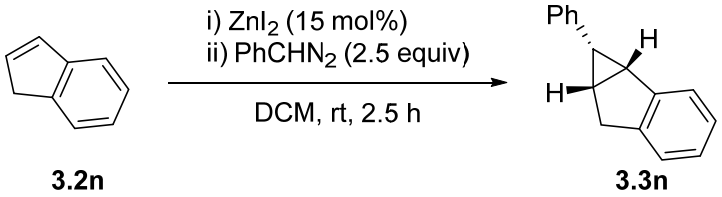

3.2n **3.3n**

***rac*-(1*S*,1a*R*,6a*R*)-1-phenyl-1,1a,6,6a-tetrahydrocyclopropa[α]indene (3.3n):** The starting alkene was obtained from a commercial source and purified by flash chromatography. The reaction was performed using **procedure C**. Yield (85%) and diastereomeric ratio (>95:5) were determined by ^{1}H-NMR analysis of the crude mixture using 4-dimethylaminopyridine as internal standard. Dihydroxylation was used to remove stilbenes. The crude product was purified by flash chromatography (100% hexanes) to yield a clear oil (67 mg, 0.32 mmol, 65% yield). **^{1}H-NMR** ($CDCl_3$, 400 MHz): δ 7.39 (d, *J* = 7.6 Hz, 1H), 7.17-6.95 (m, 6H), 6.91 (t, *J* = 7.6 Hz 1H), 6.77 (d, *J* = 7.2 Hz, 1H), 3.13 (dd, *J* = 7.2, 17.2 Hz, 1H), 2.93 (t, *J* = 7.2 Hz, 1H), 2.70 (d, *J* = 17.2 Hz, 1H), 2.46 (t, *J* = 8.0 Hz, 1H), 2.29-2.24 (m, 1H); Product corresponds to literature characterization data.[167]

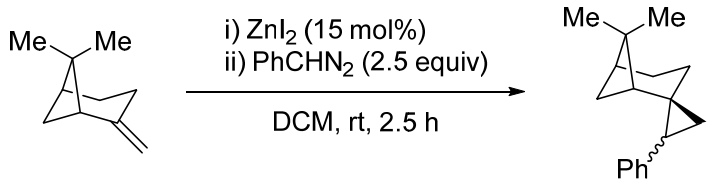

3.2o **3.3o**

(1*R*,1'*R*,5*S*)-6,6-dimethyl-2'-phenylspiro[bicyclo[3.1.1]heptane-2,1'-cyclopropane] (3.3o): The starting alkene was obtained from a commercial source and purified by flash chromatography. The reaction was performed using **procedure C**. Yield (45%) and diastereomeric ratio (50:50) were determined by ^{1}H-NMR analysis of the crude mixture using 4-dimethylaminopyridine as internal standard. Dihydroxylation was used to remove stilbenes. The crude product was purified by flash chromatography (100% hexanes) to yield both diastereomers as a clear oil (32 mg, 0.14 mmol, 28% yield). Characterization data of the diastereomer mixture (1:1) : $[\alpha]_D^{20}$: + 25.9 (c 0.85, $CHCl_3$); **^{1}H-NMR** ($CDCl_3$, 400 MHz) : δ 7.30-7.21 (m, 4H), 7.15-7.10 (m, 6H), 2.36-2.20 (m, 2H), 2.05-1.78 (m, 7H), 1.72-1.65 (m, 2H), 1.57-1.39 (m, 4H), 1.36-1.26 (m, 2H), 1.21 (s, 3H), 1.09 (s, 3H), 1.06-0.96 (m, 2H), 1,03 (s, 3H), 0.99 (s, 3H), 0.94-0.86 (m, 3H); **^{13}C-NMR** ($CDCl_3$, 75 MHz) : δ 140.4 (C), 140.2 (C), 129.1 (CH), 126.6 (CH), 128.0 (CH), 127.1 (CH), 125.5 (CH), 125.4 (CH), 53.2 (CH), 45.0 (CH), 41.0 (C), 40.7 (CH), 40.5 (C), 40.4 (CH), 28.8 (CH_2), 28.5 (CH), 28.3 (CH), 27.8 (C), 27.5 (C), 27.3 (CH_2), 26.8 (CH_2), 26.72 (CH_3), 26.68 (CH_3), 24.6 (CH_2), 24.0 (CH_2), 22.1 (CH_2), 22.0 (CH_3), 21.9 (CH_3), 21.5 (CH_2), 20.4 (CH_2); **FTIR** (cm^{-1}) (neat): 2984 (w), 2921 (m), 2866 (w), 1062 (w), 1497 (w), 1456 (m), 1028 (w), 773 (w), 739 (m), 696 (s); **HRMS** (ESI, Pos): calcd for $C_{17}H_{23}$ $[M+H]^+$: 227.1794 *m/z*, found: 227.1791 *m/z*.

A2.3.5.Cyclopropylmethanols (products 3.5a to 3.5n)

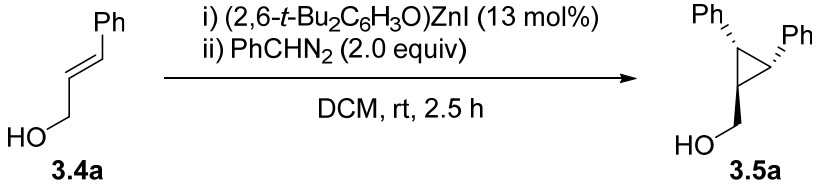

3.4a **3.5a**

((1*r*,2*R*,3*S*)-2,3-diphenylcyclopropyl)methanol (3.5a): The starting alkene was obtained from a commercial source and purified by distillation under reduced pressure. The reaction was performed using **procedure A**. Yield (81%) and diastereomeric ratio (90:10) were determined by ^{1}H-NMR

analysis of the crude mixture using triphenylmethane as internal standard. The crude product was purified by flash chromatography (5%-25% ethyl acetate/hexanes) to yield the major diastereomer as a white solid (84 mg, 0.37 mmol, 75% yield). **mp:** 88-90 °C, lit:[73] 95 °C; **^{1}H-NMR** ($CDCl_3$, 400 MHz): δ 7.13-7.04 (m, 6H), 6.95-6.93 (m, 4H), 3.86 (d, *J* = 6.4 Hz, 2H), 2.42 (d, *J* = 5.6 Hz, 2H), 2.10 (qn, *J* = 6.0 Hz, 1H), 1.54 (br, 1H). Product corresponds to literature characterization data.[73]

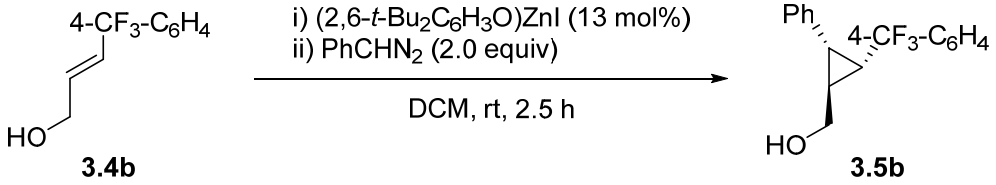

***rac*-((1*S*,2*R*,3*S*)-2-phenyl-3-(4-(trifluoromethyl)phenyl)cyclopropyl)methanol (3.5b):** The starting alkene was synthesized according to a previously known procedure.[73] The reaction was performed using **procedure A**. Yield (73%) and diastereomeric ratio (94:6) were determined by ^{1}H-NMR analysis of the crude mixture using triphenylmethane as internal standard. The crude product was purified by flash chromatography (12%-20% ethyl acetate / hexanes) to yield both diastereomers as a white solid (108 mg, 0.37 mmol, 74% yield). **mp:** 46-49 °C, lit:[73] <25 °C (oil) (enantioenriched product); **^{1}H-NMR** ($CDCl_3$, 400 MHz) : δ 7.34 (d, *J* = 11.2 Hz, 2H), 7.14-7.11 (m, 3H), 7.01-6.94 (m, 4H), 3.88 (dd, *J* = 3.6, 8.4 Hz, 2H), 2.53 (dd, J = 7.6, 12.8 Hz, 1H), 2.44 (dd, J = 7.6, 12.8 Hz, 1H), 2.12 (qn, *J* = 8.0 Hz, 1H), 1.64 (br, 1H). Product corresponds to literature characterization data.[73]

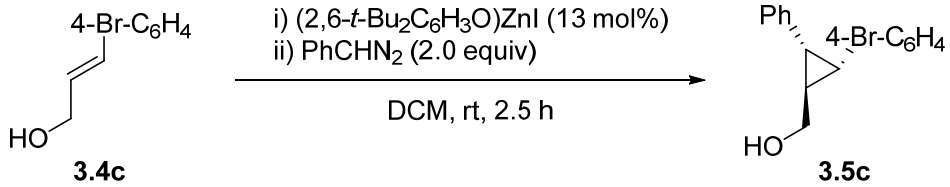

***rac*-((1*S*,2*S*,3*R*)-2-(4-bromophenyl)-3-phenylcyclopropyl)methanol (3.5c):** The starting alkene was synthesized according to a previously known procedure.[73] The reaction was performed using **procedure A**, but using only 1.60 equiv of phenyldiazomethane (1.05 mL of a 0.76 M solution in DCM, 0.800 mmol). Yield (76%) and diastereomeric ratio (91:9) were determined by ^{1}H-NMR analysis of the crude mixture using triphenylmethane as internal standard. The crude product was purified by flash chromatography (12%-20% ethyl acetate / hexanes) to yield the major diastereomer as a white solid (102 mg, 0.34 mmol, 67% yield). **mp:** 89-92 °C, lit:[73] 98 °C (enantioenriched product); **^{1}H-NMR** ($CDCl_3$, 400 MHz) : δ 7.21 (d, *J* = 8.8 Hz, 2H), 7.15-7.09 (m,

3H), 6.93 (d, *J* = 6.8 Hz, 2H), 6.79 (d, *J* = 8.4 Hz, 2H), 3.85 (dd, *J* = 3.6, 6.4 Hz, 2H), 2.44 (dd, *J* = 6.0, 9.6 Hz, 1H), 2.35 (dd, *J* = 6.0, 10.0 Hz, 1H), 2.05 (qn, *J* = 6.0 Hz, 1H), 1.57 (br, 1H); Product corresponds to literature characterization data.[73]

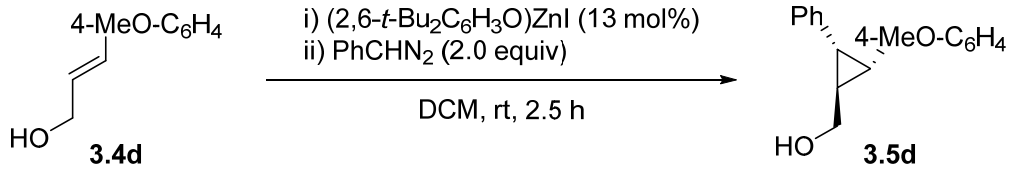

***rac*-((1*S*,2*S*,3*R*)-2-(4-methoxyphenyl)-3-phenylcyclopropyl)methanol (3.5d):** The starting alkene was synthesized according to a previously known procedure.[86b] The reaction was performed using **procedure A**, but using only 1.60 equiv of phenyldiazomethane (1.05 mL of a 0.76 M solution in DCM, 0.800 mmol). Yield (85%) and diastereomeric ratio (88:12) were determined by ^{1}H-NMR analysis of the crude mixture using triphenylmethane as internal standard. The crude product was purified by flash chromatography (12%-20% ethyl acetate / hexanes) to yield the major diastereomer as a white solid (82 mg, 0.32 mmol, 65% yield). **mp:** 85-86 °C; **^{1}H-NMR** ($CDCl_3$, 400 MHz): δ 7.14-7.04 (m, 3H), 6.93-6.85 (m, 4H), 6.68-6.65 (m, 2H), 3.83 (d, *J* = 6.8 Hz, 2H), 3.71 (s, 3H), 2.36 (ddd, *J* = 5.6, 9.6, 13.2 Hz, 2H), 2.02 (qn, *J* = 6.0 Hz, 1H), 1.72 (br, 1H); **^{13}C-NMR** ($CDCl_3$, 75 MHz): δ 157.9 (C), 137.7 (C), 130.2 (CH), 129.3 (C), 128.9 (CH), 127.9 (CH), 125.9 (CH), 113.4 (CH), 66.5 (CH_2), 55.2 (CH_3), 29.3 (CH), 29.1 (CH), 28.0 (CH); **FTIR** (cm^{-1}) (neat): 3349 (br), 3025 (w), 2935 (w), 2835 (w), 1611 (w), 1514 (s), 1463 (w), 1246 (s), 1179 (w), 1032 (s), 744 (w), 699 (m); **HRMS** (ESI, Pos): calcd for $C_{17}H_{22}NO_2$ $[M + NH_4]^+$: 272.1645 *m/z*, found: 272.1650 *m/z*.

Relative configuration determined through 1D-nOe spectra (irradiated protons in bold):

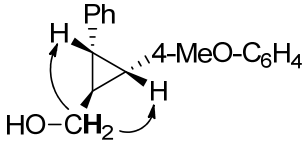

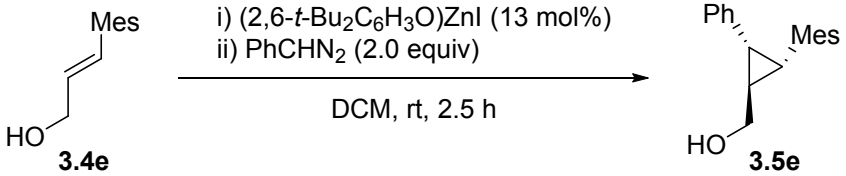

***rac*-((1*S*,2*S*,3*R*)-2-mesityl-3-phenylcyclopropyl)methanol (3.5e):** The starting alkene was synthesized according to a previously known procedure.[168] The reaction was performed using **procedure A**. Yield (65%) and diastereomeric ratio (85:15) were determined by ^{1}H-NMR analysis of the crude mixture using triphenylmethane as internal standard. Dihydroxylation was used to remove the remaining starting alkene. The crude product was purified by flash chromatography (12%-20% ethyl acetate / hexanes) to yield the major diastereomer as a white solid (60 mg, 0.23 mmol, 45% yield). **mp:** 89-90 °C; **^{1}H-NMR** ($CDCl_3$, 400 MHz): δ 7.05-7.01 (m, 3H); 6.72 (s, 2H), 6.65-6.63 (m, 2H), 4.10-4.06 (m, 1H), 3.75 (dd, *J* = 7.6, 11.2 Hz, 1H), 2.30 (dd, *J* = 5.2, 8.8 Hz, 1H), 2.26-2.16 (m, 10H), 1.87 (qn, *J* = 6.2 Hz, 1H), 1.59 (br, 1H). **^{13}C-NMR** ($CDCl_3$, 75 MHz): δ 140.0 (C), 138.8 (C), 135.9 (C), 129.9 (C), 129.0 (CH), 127.6 (CH), 126.6 (CH), 125.4 (CH), 66.6 (CH_2) 32.5 (CH), 29.2 (CH), 27.7 (CH), 21.0 (CH_3), 20.9 (CH_3); **FTIR** (cm^{-1}) (neat): 3336 (br), 3026 (w), 2949 (w), 2918 (m), 2862 (w), 1603 (w), 1497 (m), 1455 (m), 1201 (w), 1030 (s), 851 (m), 754 (m), 697 (s); **HRMS** (ESI, Pos): calcd for $C_{19}H_{26}NO$ $[M + NH_4]^+$: 284.2009 *m*/*z*, found: 284.2002 *m*/*z*. Relative configuration determined by analogy with **3.5d**.

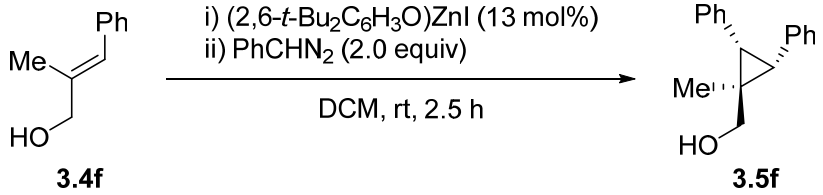

3.4f **3.5f**

((1*s*,2*R*,3*S*)-1-methyl-2,3-diphenylcyclopropyl)methanol (3.5f): The starting alkene was synthesized according to a previously known procedure.[Erreur ! Signet non défini.] The reaction was performed using **procedure A**. Yield (80%) and diastereomeric ratio (90:10) were determined by ^{1}H-NMR analysis of the crude mixture using triphenylmethane as internal standard. The crude product was purified by flash chromatography (5%-25% ethyl acetate / hexanes) to yield the major diastereomer as a white solid (91 mg, 0.38 mmol, 76% yield). **mp:** 81-82 °C; **^{1}H-NMR** ($CDCl_3$, 400 MHz): δ 7.23-7.15 (m, 6H), 6.98-6.96 (m, 4H), 3.70 (d, *J* = 6.0 Hz, 2H), 2.44 (s, 2H), 1.56 (t, *J* = 6.0 Hz, 1H), 1.20 (s, 3H); **^{13}C-NMR** ($CDCl_3$, 75 MHz): δ 136.7 (C), 130.8 (CH), 127.9 (CH), 125.9 (CH), 73.6 (CH_2), 31.2 (CH), 29.8 (C), 12.7 (CH_3); **FTIR** (cm^{-1}) (neat): 3353 (br), 3027 (w), 2926 (w), 2869 (w), 1602 (w), 1496 (m), 1445 (s), 1030 (m), 1020 (m), 727 (m), 700 (s); **HRMS** (ESI, Pos): calcd for $C_{17}H_{18}AgO$ $[M + Ag]^+$: 345.0403 *m*/*z*, found: 345.03988 *m*/*z*.

Relative configuration determined through 1D-nOe spectra (irradiated protons in bold):

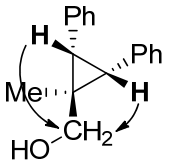

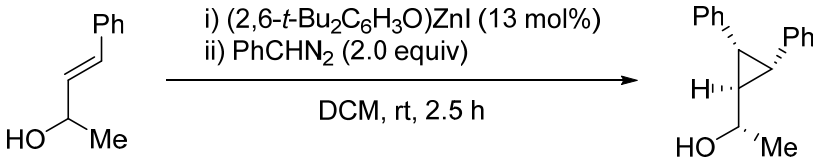

3.4g **3.5g**

***rac*-(*S*)-1-((1*r*,2*R*,3*S*)-2,3-diphenylcyclopropyl)ethanol (3.5g):** The starting alkene was synthesized according to a previously known procedure.[169] The reaction was performed using **procedure A**. Yield (79%) and diastereomeric ratio (>95:5) were determined by ^{1}H-NMR analysis of the crude mixture using triphenylmethane as internal standard. The crude product was purified by flash chromatography (5%-25% ethyl acetate / hexanes) to yield the major diastereomer as a white solid (90 mg, 0.38 mmol, 76% yield). **mp:** 112-113 °C; **^{1}H-NMR** ($CDCl_3$, 400 MHz): δ 7.15-7.04 (m, 6H), 6.95-6.93 (m, 4H), 3.68 (qn, *J* = 8.4Hz, 1H), 2.50 (dd, *J* = 7.6, 12.8 Hz, 1H), 2.41 (dd, *J* = 7.6, 12.8 Hz, 1H), 1.95-1.89 (m, 1H), 1.78 (br, 1H), 1.47 (d, *J* = 8.4 Hz, 3H); **^{13}C-NMR** ($CDCl_3$, 75 MHz): δ 137.7 (C), 137.4 (C), 129.1 (CH), 129.0 (CH), 127.93 (CH), 127.90 (CH), 126.0 (CH), 125.9 (CH), 71.5 (CH), 33.4 (CH), 29.7 (CH), 29.1 (CH), 22.7 (CH_3); **FTIR** (cm^{-1}) (neat): 3294 (br), 3015 (w), 2928 (w), 1602 (w), 1497 (m), 1092 (m), 1074 (m), 757 (m), 697 (s), 532 (w); **HRMS** (ESI, Pos): calcd for $C_{17}H_{18}AgO$ $[M + Ag]^+$: 345.0403 *m*/*z*, found: 345.0409 *m*/*z*. Relative configuration determined by analogy with (1*S*)-1-[(1*S*,2*S*,3*R*)-2-(4-methylphenyl)-3-phenylcyclopropyl]ethanol.[Erreur ! Signet non défini.]

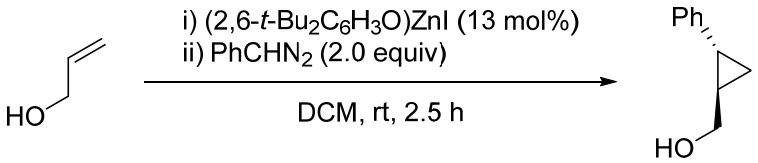

3.4h **3.5h**

***rac*-((1*R*,2*S*)-2-phenylcyclopropyl)methanol (3.5h):** The starting alkene was obtained from a commercial source and purified by distillation under argon. The reaction was performed using **procedure A**. Yield (60%) and diastereomeric ratio (82:18) were determined by ^{1}H-NMR analysis of the crude mixture using triphenylmethane as internal standard. The crude product was purified

by flash chromatography (4%-15% ethyl acetate / hexanes) to yield the major diastereomer as a clear oil (36 mg, 0.24 mmol, 49% yield). **^{1}H-NMR** ($CDCl_3$, 400 MHz): δ 7.29-7.24 (m, 2H), 7.18-7.14 (m, 1H), 7.09-7.07 (m, 2H), 3.67-3.58 (m, 2H), 1.86-1.81 (m, 1H), 1.51-1.43 (m, 2H), 1.00-0.91 (m, 1H); Product corresponds to literature characterization data.[170]

3.4i **3.5i**

***rac*-((1*R*,2*R*)-1-methyl-2-phenylcyclopropyl)methanol (3.5i):** The starting alkene was obtained from a commercial source and purified by distillation under argon. The reaction was performed using **procedure A**. Yield (77%) and diastereomeric ratio (>95:5) were determined by ^{1}H-NMR analysis of the crude mixture using triphenylmethane as internal standard. The crude product was purified by flash chromatography (4%-15% ethyl acetate / hexanes) to yield a clear oil (53 mg, 0.33 mmol, 65% yield). **^{1}H-NMR** ($CDCl_3$, 400 MHz): δ 7.30-7.27 (m, 2H), 7.21-7.17 (m, 3H), 3.55 (s, 2H), 2.05 (dd, *J* = 11.2, 12.8 Hz, 1H), 1.44 (br, 1H), 0.94 (dd, *J* = 5.2, 9.2 Hz, 1H), 0.89 (s, 3H), 0.89-0.86 (m, 1H); Product corresponds to literature characterization data.[162]

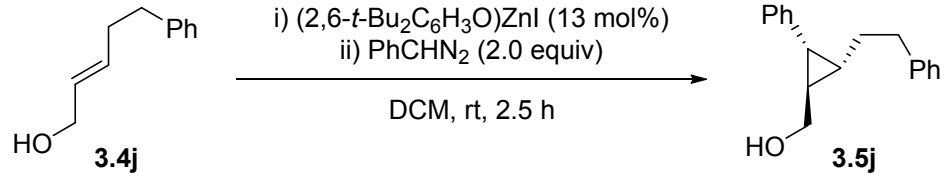

3.4j **3.5j**

***rac*-((1*R*,2*S*,3*R*)-2-phenethyl-3-phenylcyclopropyl)methanol (3.5j):** The starting alkene was synthesized according to a previously known procedure.[159] The reaction was performed using **procedure A**. Yield (54%) and diastereomeric ratio (87:13) were determined by ^{1}H-NMR analysis of the crude mixture using triphenylmethane as internal standard. The crude product was purified by flash chromatography (5%-25% ethyl acetate / hexanes) to yield the major diastereomer as a yellowish oil (69 mg, 0.28 mmol, 55% yield). **^{1}H-NMR** ($CDCl_3$, 400 MHz): δ 7.30-7.13 (m, 8H), 7.04-7.02 (m, 2H), 3.64 (dd, *J* = 6.8, 11.2 Hz, 1H), 3.54 (dd, *J* = 7.2, 11.2 Hz, 1H), 2.57 (t, *J* = 8.4 Hz, 2H), 2.04 (dd, *J* = 5.6, 9.2 Hz, 1H), 1.57-1.48 (m, 1H), 1.42 (qn, J = 6.0 Hz, 1H), 1.39-1.29 (m, 1H), 1.26 (br, 1H), 1.05 (qn, *J* = 6.8 Hz, 1H). Product corresponds to literature characterization data.[159]

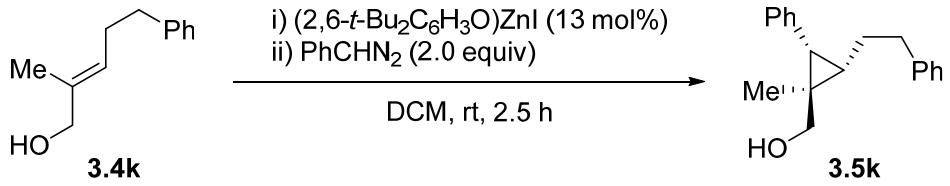

***rac*-((1*R*,2*S*,3*S*)-1-methyl-2-phenethyl-3-phenylcyclopropyl)methanol (3.5k):** The starting alkene was synthesized according to a previously known procedure.[171] The reaction was performed using **procedure A**. Yield (85%) and diastereomeric ratio (85:15) were determined by ^{1}H-NMR analysis of the crude mixture using triphenylmethane as internal standard. The crude product was purified by flash chromatography (5%-30% ethyl acetate / hexanes) to yield the major diastereomer as a yellowish oil (96 mg, 0.36 mmol, 72% yield). **^{1}H-NMR** ($CDCl_3$, 400 MHz): δ 7.30-7.26 (m, 4H), 7.21-7.17 (m, 6H), 3.51 (s, 2H), 2.78-2.65 (m, 2H), 1.99 (d, J = 9.2 Hz, 1H), 1.96-1.89 (m, 1H), 1.39-1.30 (m, 1H), 1.37 (br, 1H), 1.09-1.04 (m, 1H), 1.00 (s, 3H); **^{13}C-NMR** ($CDCl_3$, 75 MHz): δ 142.3 (C), 137.3 (C), 131.0 (CH), 128.6 (CH), 128.5 (CH), 128.3 (CH), 126.1 (CH), 126.0 (CH), 73.6 (CH_2), 36.5 (CH_2), 28.4 (CH), 28.0 (CH_2), 26.4 (C), 25.2 (CH), 12.6 (CH_3); **FTIR** (cm^{-1}) (neat): 3359 (br), 3024 (w), 2923 (m), 2861 (m), 1062 (w), 1496 (m), 1454 (w), 1032 (m), 747 (m), 699 (s); **HRMS** (ESI, Pos): calcd for $C_{19}H_{26}NO$ $[M+NH_4]^+$: 284.2009 *m/z*, found: 284.2008 *m/z*.

Relative configuration determined through 1D-nOe spectra (irradiated protons in bold):

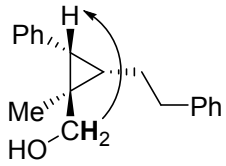

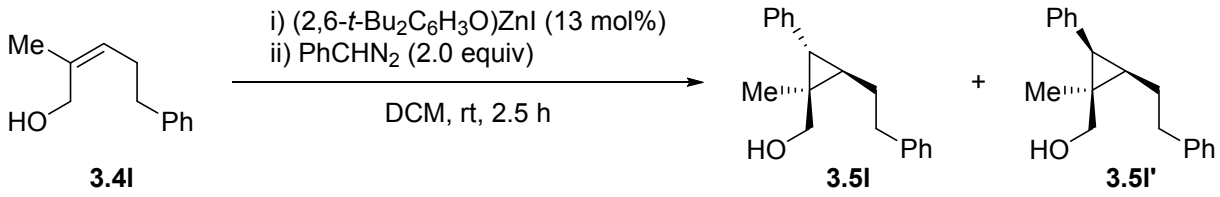

***rac*-((1*R*,2*R*,3*S*)-1-methyl-2-phenethyl-3-phenylcyclopropyl)methanol (3.5l):** The starting alkene was synthesized according to a previously known procedure.[172] Yield (93%) and diastereomeric ratio (61:39) were determined by ^{1}H-NMR analysis of the crude mixture using triphenylmethane as internal standard. The reaction was performed using **procedure A**. The crude

product was purified by flash chromatography (5%-30% ethyl acetate / hexanes) to yield major diastereomer (**3.5l**) as a yellowish oil (74 mg, 0.28 mmol, 56% yield) and minor diastereomer (**3.5l'**) (51.0 mg, 0.190 mmol, 38% yield). Major diastereomer (**3.5l**) : **^{1}H-NMR** ($CDCl_3$, 400 MHz): □ 7.32-7.17 (m, 8H), 7.14-7.12 (m, 2H), 3.69 (d, *J* = 11.2 Hz, 1H), 3.54 (d, *J* = 11.2 Hz, 1H), 2.89-2.75 (m, 2H), 1.97 (sx, *J* = 7.2 Hz, 1H), 1.82 (sx, *J* = 7.2 Hz, 1H), 1.76 (d, *J* = 5.6 Hz, 1H), 1.20 (q, *J* = 7.2 Hz, 1H), 1.12 (br, 1H), 0.86 (s, 3H); **^{13}C-NMR** ($CDCl_3$, 75 MHz): δ 142.3 (C), 139.0 (C), 129.2 (CH), 128.7 (CH), 128.6 (CH), 128.1 (CH), 126.1 (CH), 126.0 (CH), 68.1 (CH_2), 36.5 (CH_2), 33.6 (CH), 31.3 (CH_2), 29.7 (C), 29.2 (CH), 17.8 (CH_3); **FTIR** (cm^{-1}) (neat): 3375 (br), 3025 (w), 2926 (m), 2862 (m), 1602 (w), 1497 (m), 1453 (m), 1028 (m), 746 (m), 699 (s); **HRMS** (ESI, Pos): calcd for $C_{19}H_{22}AgO$ $[M + Ag]^+$: 373.0716 *m/z*, found: 373.0710 *m/z*. Minor diastereomer (**5l'**): **^{1}H-NMR** ($CDCl_3$, 400 MHz) : δ 7.32-7.24 (m, 6H), 7.22-7.17 (m, 4H), 3.65 (d, *J* = 15.2 Hz, 1H), 3.42 (d, *J* = 15.2 Hz, 1H), 2.88-2.71 (m, 2H), 2.07 (d, *J* = 12 Hz, 1H), 1.96-1.84 (m, 1H), 1.55-1.45 (m, 1H), 1.34 (s, 3H), 1.17 (br, 1H), 1.10-1.03 (m, 1H); **^{13}C-NMR** ($CDCl_3$, 75 MHz): □ 142.5 (C), 137.6 (C), 130.5 (CH), 128.7 (CH), 128.5 (CH), 128.4 (CH), 126.2 (CH), 126.0 (CH), 64.4 (CH_2), 36.9 (CH_2), 32.2 (CH), 28.9 (CH), 28.5 (CH_2), 25.1 (C), 24.5 (CH_3); **FTIR** (cm^{-1}) (neat): 3411 (br), 3025 (w), 2949 (m), 2925 (m), 2862 (w), 1602 (w), 1496 (m), 1454 (w), 1014 (m), 749 (w), 699 (s); **HRMS** (ESI, Pos): calcd for $C_{19}H_{22}NaO$ $[M + Na]^+$: 289.1563 *m/z*, found: 289.1564 *m/z*.

Relative configuration of minor diastereomer determined through 1D-nOe spectra (irradiated proton in bold):

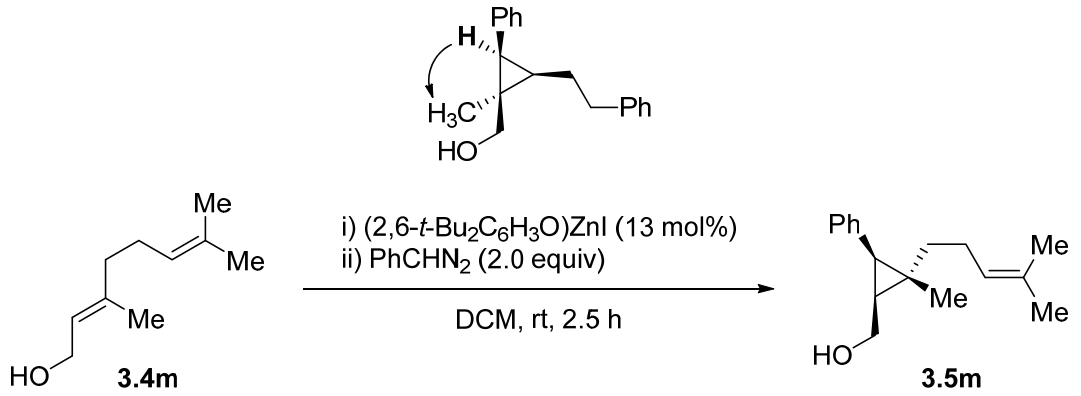

***rac*-((1*S*,2*S*,3*S*)-2-methyl-2-(4-methylpent-3-en-1-yl)-3-phenylcyclopropyl)methanol (3.5m):** The starting alkene was obtained from a commercial source and purified by flash chromatography. The reaction was performed using **procedure A**. Yield (96%) and diastereomeric ratio (73:27) were determined by ^{1}H-NMR analysis of the crude mixture using triphenylmethane as internal standard.

The crude product was purified by flash chromatography (5%-25% ethyl acetate / hexanes) to yield major diastereomer (pictured) as a clear oil (79 mg, 0.32 mmol, 65% yield) and minor diastereomer as a yellowish oil (25 mg, 0.10 mmol, 21% yield). **^{1}H-NMR** ($CDCl_3$, 400 MHz): δ 7.30-7.26 (m, 2H), 7.21-7.17 (m, 3H), 5.18 (tt, *J* = 1.2, 7.2 Hz, 1H), 3.83 (dd, *J* = 6.8, 11.2 Hz, 1H), 3.48 (dd, *J* = 8.4, 11.2 Hz, 1H), 2.21 (n, *J* = 7.6 Hz, 2H), 2.05 (d, *J* = 9.2 Hz, 1H), 1.71 (s, 3H), 1.66 (s, 3H), 1.46 (t, *J* = 8.0 Hz, 2H), 1.33 (br, 1H), 1.25 (td, J = 6.8, 8.8 Hz, 1H), 0.97 (s, 3H); Product corresponds to literature characterization data.[173]

Relative configuration confirmed through 1D-nOe spectra (irradiated protons in bold):

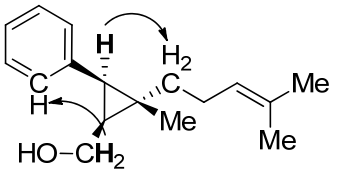

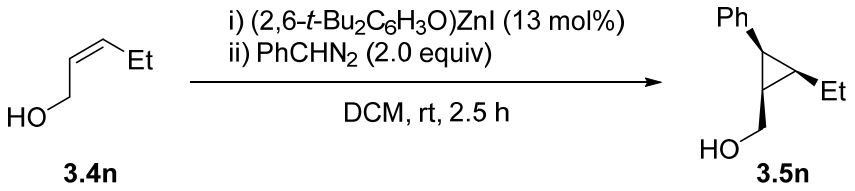

3.4n **3.5n**

***rac*-((1*R*,2*R*,3*S*)-2-ethyl-3-phenylcyclopropyl)methanol (3.5n):** The starting alkene was obtained from a commercial source and purified by flash chromatography. The reaction was performed using **procedure A**. Yield (78%) and diastereomeric ratio (40:60) were determined by ^{1}H-NMR analysis of the crude mixture using triphenylmethane as internal standard. The crude product was purified by flash chromatography (12%-20% ethyl acetate / hexanes) to yield major diastereomer (pictured) as a clear oil (42 mg, 0.24 mmol, 48% yield) and minor diastereomer as a yellowish oil (27 mg, 0.15 mmol, 31% yield). **^{1}H-NMR** ($CDCl_3$, 400 MHz) : δ 7.28-7.22 (m, 4H), 7.18-7.15 (m, 1H), 3.75 (dd, *J* = 7.6, 11.2 Hz, 1H), 3.59 (dd, *J* = 7.6, 11.2 Hz, 1H), 2.26 (t, *J* = 8.8 Hz, 1H), 1.55-1.39 (m, 2H), 1.34 (br, 1H), 1.23-1.07 (m, 2H), 1.03 (t, *J* = 7.2 Hz, 3H) ; **^{13}C-NMR** ($CDCl_3$, 75 MHz) : δ 137.3 (C), 130.8 (CH), 128.3 (CH), 126.2 (CH), 60.4 (CH_2), 24.0 (CH), 22.0 (CH), 21.9 (CH), 18.5 (CH_2) 14.7 (CH_3); **FTIR** (cm^{-1}) (neat): 3335 (br), 2961 (m), 2931 (w), 2872 (w), 1602 (w), 1497 (w), 1017 (s), 780 (m), 721 (m), 700 (s), 458 (w); **HRMS** (ESI, Pos): calcd for $C_{12}H_{20}NO$ $[M+NH_4]^+$: 194.1539 *m/z*, found: 194.1535 *m/z*.

Relative configuration determined through 1D-nOe spectra (irradiated protons in bold):

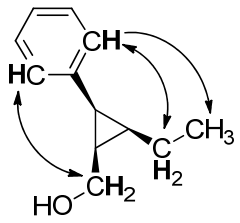
CH
HC
CH3
C
H2
CH2
HO

Annexe 3 : Informations supplémentaires associées à l'article «Continuous flow synthesis and purification of aryldiazomethanes via hydrazone fragmentation»

A3.1.General Information

Unless otherwise stated, reactions were run under air in air-exposed glassware. EtOH, CH_2Cl_2 and 1,4-dioxane were used directly from the bottle. Dry CH_2Cl_2 was obtained by filtration under Argon through an alumina drying column on a filtration system. Analytical thin-layer chromatography (TLC) was performed on precoated, glass-backed silica gel (Silicycle Glass Backed TLC Extra Hard Layer, 60 Å). Visualization of the developed chromatogram was performed by 254nm UV light or aqueous cerium ammonium molybdate (CAM). Flash column chromatography was performed on an automatic purification system (Teledyne Isco Combiflash® Companion). Pre-packed normal phase silica gel columns were used for separation of products using Teledyne Isco RediSep® Rf High Performance Gold or Grace Reveleris® High Performance columns. Melting points were obtained on a Buchi melting point apparatus and are uncorrected. Nuclear magnetic resonance spectra (^1H, ^{13}C, ^{19}F, DEPT-135, NOE) were recorded on an Avance AV500 MHz, Avance AV400 MHz, Avance AV 300 MHZ, or Avance DRX400 MHz spectrometer. Chemical shifts for NMR spectra are recorded in parts per million from tetramethylsilane with the following resonances as internal standard. ^1H NMR : $CHCl_3$, δ = 7.26 ppm. ^{13}C NMR : $CDCl_3$, δ = 77.16 ppm or DMSO-d6, δ = 39.52 ppm. ^{19}F NMR : $PhCF_3$, δ = -63.72 ppm Data are reported as follows: chemical shift, multiplicity (s = singlet, d = doublet, t = triplet, q = quartet, qn = quintet, sx = sextet, h = heptet, o = octet, n = nonet, m = multiplet, br = broad and app = apparent), coupling constant in Hz and integration. All ^{13}C NMR spectra were obtained with complete proton decoupling. Infrared spectra were taken on a Bruker Alpha Vertex Series ATR (neat) and are reported in reciprocal centimetres (cm^{-1}). High resolution mass spectra were performed by the Centre régional de spectroscopie de masse de l'Université de Montréal. DSC-TGA analysis performed on a TA instruments SDT Q600 V20.9 Build 20, using alumina cups with alumina caps and heating from 50°C to 300°C on a 2°C/min linear temperature ramp. The

flow chemistry apparatus uses PFA tubing of 0.75mm or 1.00mm internal diameter, connected to the various parts using PFA or PEEK ferrules

A3.2.Reagents

Unless otherwise stated, commercial reagents were used without purification. Tetramethylguanidine (TMG) was purified by distillation from dry Barium oxide. TMG and mesitylsulfonylhydrazone solutions in CH_2Cl_2 were kept at -20°C for up to 6 weeks. The drying column for the diazo solutions was filled with an approximately 1:1 mix of powdered 4Å molecular sieves and powdered diatomaceous earth (Celite®). The solid mixture was dried under vacuum at 180°C for 2h before use.

A3.3.Continuous Flow Apparatus

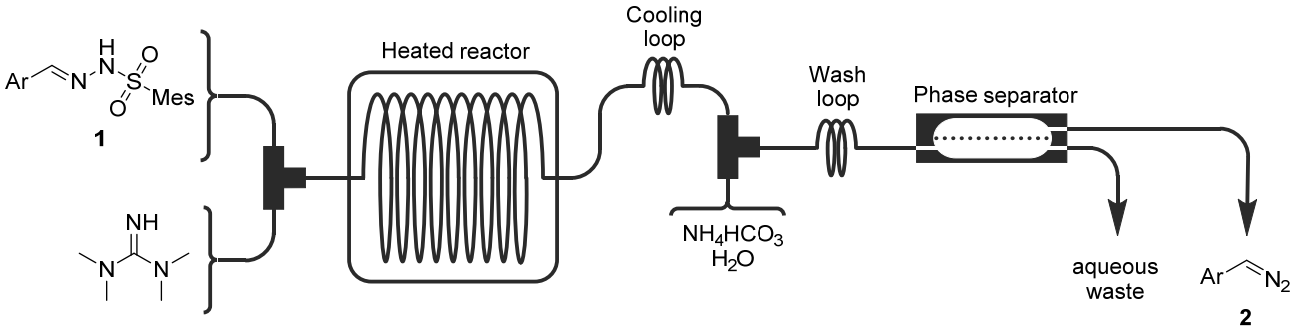

Figure S1: Simplified continuous flow setup

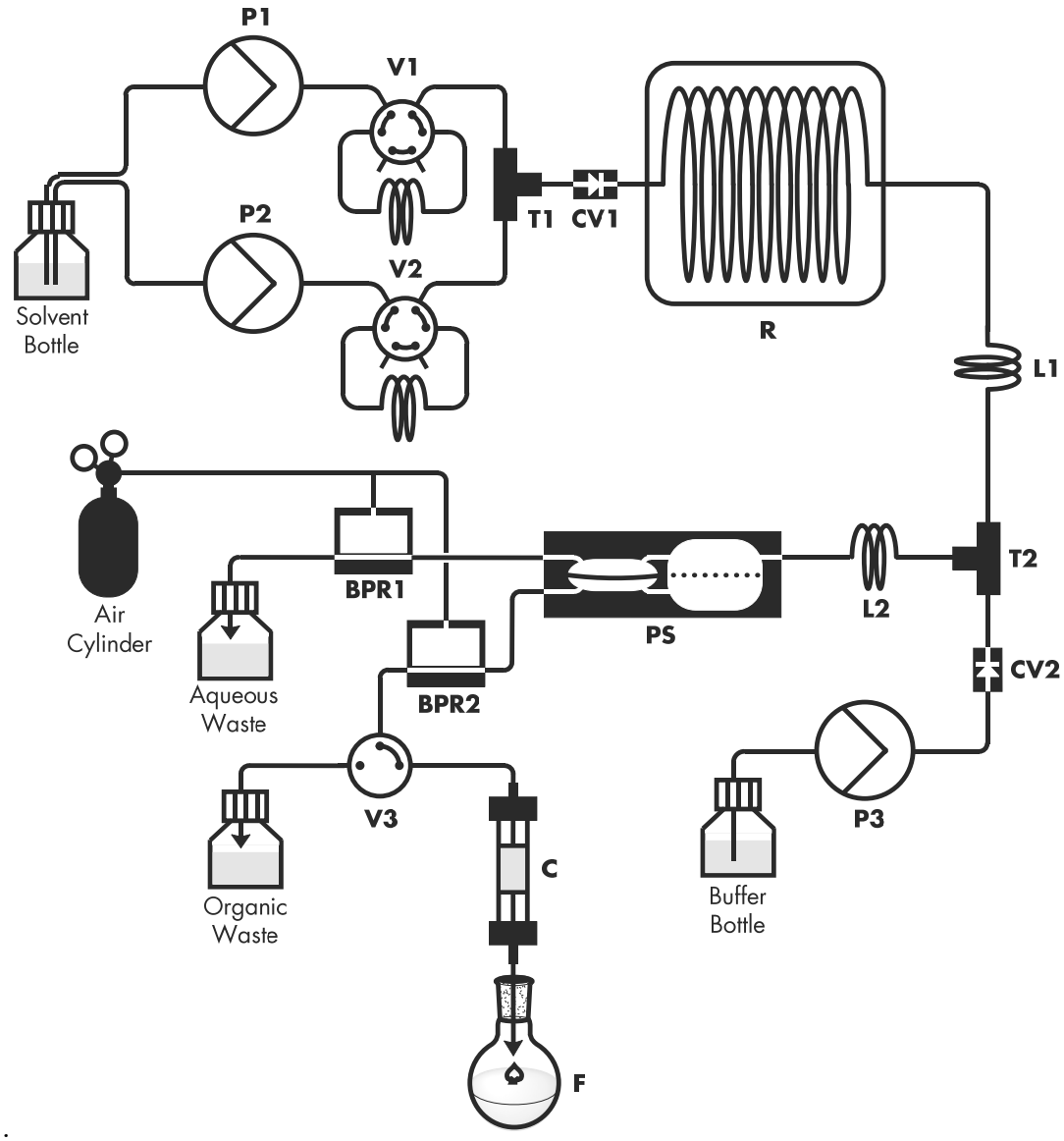

Figure S2: Detailed continuous flow setup.

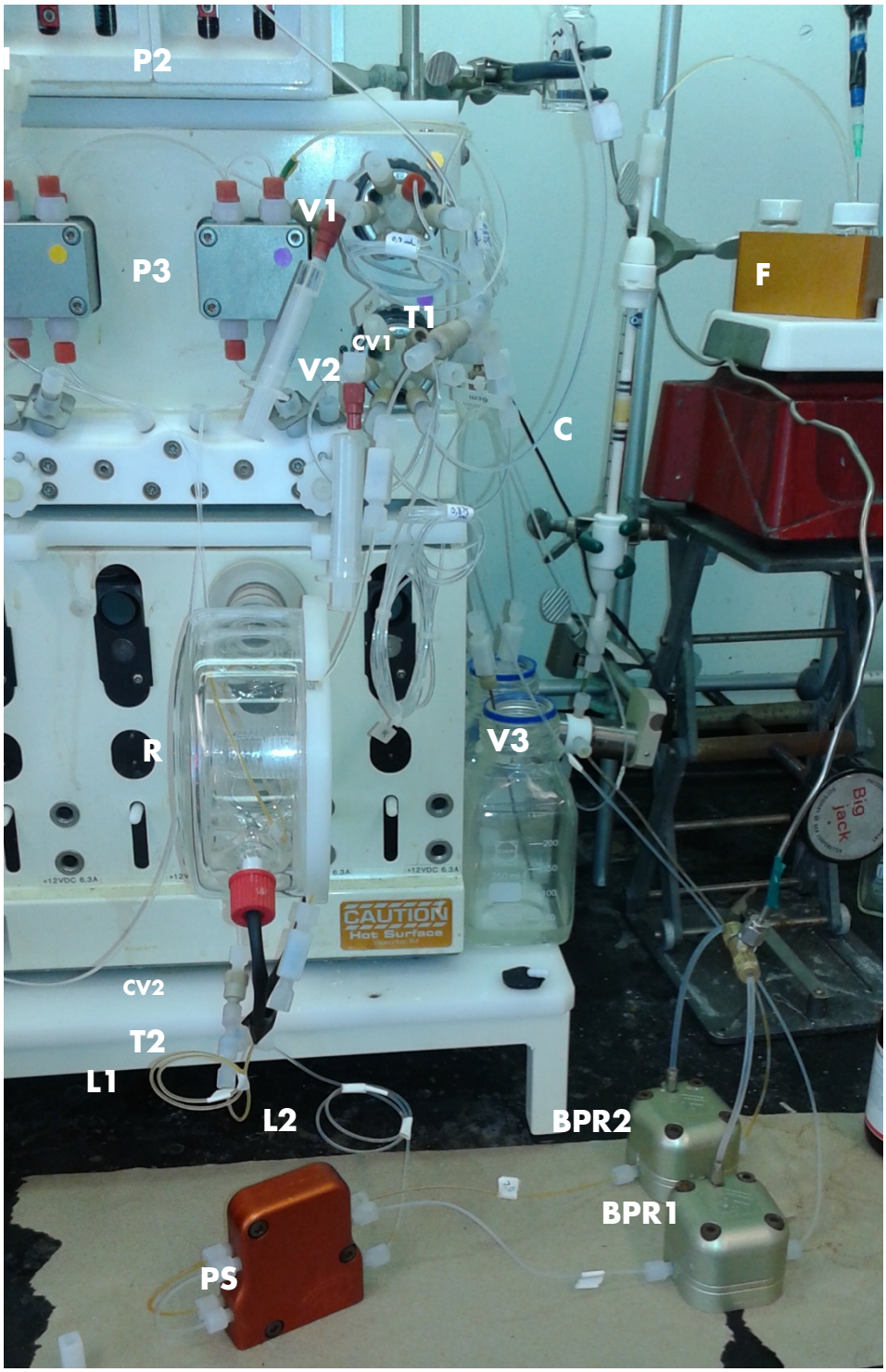

Figure S3: Picture of continuous flow setup

A3.4.Continuous Flow Procedures

Solvent Bottle : CH_2Cl_2, exposed to air.

Buffer Bottle : Aqueous NH_4HCO_3

P1 and **P2** : Syrris Asia syringe pump. **P1** uses 50 μL and 100 μL syringes (yellow), **P2** uses 250 μL and 500 μL syringes (green).

P3 : Pump from Vapourtech R2 pumps module

V1 and **V2** : 6-way valves with injection loops from a Vapourtech R2 pumps module.

T1 : PFA mixing "T" connector.

CV1 : One-way check valve.

R : Heated reactor. PFA tubing of predetermined volume coiled in a Vapourtech coil reactor heater on a Vapourtech R4 module.

L1 : 0.25 mL PFA cooling loop.

CV2 : One-way check valve

T2 : PFA mixing "T" connector.

L2 : 0.25 mL PFA mixing loop.

PS : Zaiput phase separator. 1.0 μm pores membrane for CH_2Cl_2 flow rates between 100 and 400 μm/minute. 0.5 μm pores membrane for slower rates.

BPR1 and **BPR2** : Zaiput back-pressure regulators. Set with the pressure from an N_2 cylinder. BPR1 (aqueous stream) set to 3.2 atm. BPR2 (organic stream) set to 3.0 atm.

V3 : 3-way diverter valve from a Vapourtech R2 pumps module.

C : Optional drying column filled with a dry 1:1 mixture of 4 Å molecular sieves and powdered diatoms. Needed if follow-up reaction is water-sensitive.

F: Reaction flask in which diazo reagent is added to be consumed.

"**TC**" = Target Concentration (if diazo yield = 100%). Either 0.50 M or 0.25 M

"**DAR**" = Desired diazo Addition Rate

On small scales, 5-20% extra volume can be added on the TMG injection loops to ensure the entire sulfonylhydrazone solution plug is exposed to TMG. Pump 2 started slightly earlier. This problem is avoided on larger scales by discarding the beginning and the end of the reagent plug.

Procedure A:

Injection loops 1 and 2 are the same volume and are pumped at the same flow rate. Sulfonylhydrazone solution is (TC*2) M in CH_2Cl_2 and contains between 1 and 5 equiv of formamide to avoid precipitation. Tetramethylguanidine (TMG) solution is (TC*4) M in CH_2Cl_2. Reactor volume is adjusted for a 6 min reaction time. Aqueous buffer ((2*TC) M) is pumped at 3*DAR.

Procedure B:

n = nb of moles ($n_{TMG} = 2n_1$)

V = volume

Injection loop 1 contains sulfonylhydrazone (**1**) solution in CH_2Cl_2 ($V_1 = n_1/TC - v_{TMG}$, pump flow rate = $DAR*TC*V_1/n_1$) and injection loop 2 contains pure Tetramethylguanidine (TMG) ($V_{TMG} = \rho_{TMG*}n_{TMG}$, pump flow rate = $DAR(1-TC*V_1/n_1)$. Hydrazone contains between 1 and 5 equiv of formamide to avoid precipitation. Reactor volume is adjusted for a 6 min reaction time. Aqueous buffer ((2*TC) M) is pumped at 3*DAR.

Procedure C:

Single injection loop is loaded with a premixed solution of hydrazone ((MOC) M) and Tetramethylguanidine (TMG) ((MOC*2) M) in CH_2Cl_2. Reactor volume is adjusted for a 6 min reaction time. Aqueous buffer ((MOC*2) M) is pumped at thrice the total organic phase rate.

Parameters examples :

Proc.	Scale (mmol)	TC (mol/L)	DAR (µL/min)	Pump 1 rate (µL/min)	Pump 2 rate (µL/min)	Loop 1 volume (mL)	Loop 2 volume (mL)	Sulfonyl-hydrazone conc. (mol/L in CH_2Cl_2)	TMG conc. (mol/L in CH_2Cl_2)	Reactor volume (mL)	Pump 3 rate (mL/min)	NH_4HCO_3 conc. (mol/L in H_2O)
A	0.24	0.50	333	167	167	0.24	0.24	1.00	2.0	2.00	1.00	1.0
A	0.12	0.25	333	167	167	0.24	0.24	0.50	1.0	2.00	1.00	0.5
A	1.00	0.25	67	33	33	2.00	2.00	0.50	1.0	0.40	0.20	0.5

B	0.50	0.50	333	291	42	0.88	0.12	0.58	8.0[a]	2.00	1.00	1.0
B	0.50	0.50	167	146	21	0.88	0.12	0.58	8.0[a]	1.00	0.50	1.0
B	1.00	0.50	333	291	42	1.75	0.25	0.58	8.0[a]	2.00	1.00	1.0
B	0.50	0.25	333	312	21	1.88	0.12	0.27	8.0[a]	2.00	1.00	0.5
B	1.00	0.25	67	63	4	3.75	0.25	0.27	8.0[a]	0.40	0.20	0.5
B	10.0	0.50	333	291	42	17.6	2.4	0.58	8.0[a]	2.00	1.00	1.0
C	0.25	0.25	333	333	-	0.50	-	0.25[b]	0.50[b]	2.00	1.00	1.0

[a] Pure tetramethylguanidine. [b] Together in the same solution

Typical by-products:

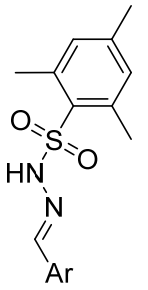

1 - 9 %

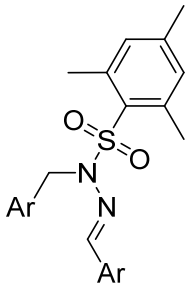

0 - 7 %

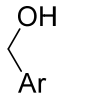

0 - 6 %

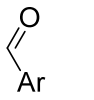

0 - 3 %

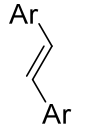

0 - 5 %

A3.5.Experimental Procedures and Characterization Data

A3.5.1.Sulfonylhydrazide synthesis

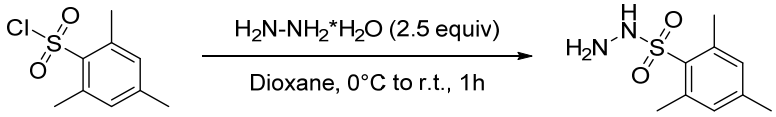

Mesitylsulfonylhydrazide: Hydrazine hydrate (7.12 mL, 114 mmol, 2.50 equiv) was added to a 500 mL round-bottom flask equipped with a magnetic stirring bar and cooled to 0°C. A solution of mesitylsulfonylchloride (10.0 g, 45.7 mmol, 1.00 equiv) in 240 mL of 1,4-dioxane was added by syringe. The resulting suspension was warmed to r.t. and stirred for 1h. 250 mL of EtOAc were added and solution was washed with brine (250 mL, 3X). Organic phase was dried over $MgSO_4$, filtrated and concentrated under vacuum until volume is down to about 20 mL. 100 mL of cold hexanes were added. The resulting white solid (8.50g, 39.7 mmol, 87%) is recovered using a fritted glass filter and washed with cold hexanes. **mp:** 109-111 °C, lit. 114-116 °C[174]; **^{1}H NMR** ($CDCl_3$,

300 MHz): □ ppm 7.00 (s, 1 H), 2.66 (s, 3 H), 2.32 (s, 2 H). Product corresponds to literature characterization data.[174]

A3.5.2.Methoxymethyl (MOM) protection of alcohol

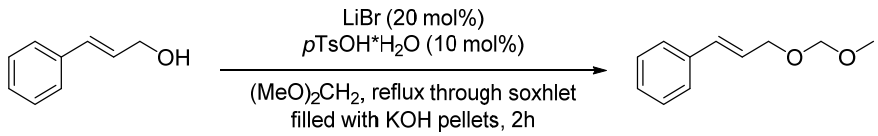

(*E*)-(3-(Methoxymethoxy)prop-1-en-1-yl)benzene: To a 50 mL round bottom flask containing (E)-3-phenylprop-2-en-1-ol (1.50 g, 11.2 mmol, 1.00 equiv), LiBr (195 mg, 2.24 mmol, 0.20 equiv), *p*-toluenesulfonic acid monohydrate (193 mg, 1.12 mmol, 0.10 equiv) and dimethoxymethane (24.7 mL, 278 mmol, 25.0 equiv) was fitted a soxhlet and condenser setup containing uncrushed KOH pellets. Mixture was refluxed for 2h. Saturated $NaHCO_3$ was added. Mixture was extracted with Et_2O (3X). Organic phases were combined, dried with MgSO4, filtrated and concentrated under vacuum to yield a yellowish oil. Mixture was purified by flash chromatography (0-5% Et_2O/Hexanes) to yield a clear oil (1.74 g, 9.76 mmol, 87%). **^{1}H NMR** ($CDCl_3$, 300 MHz): □ ppm 7.36 - 7.44 (m, 2 H), 7.28 - 7.36 (m, 2 H), 7.20 - 7.34 (m, 1 H), 6.64 (d, *J*=16.0 Hz, 1 H), 6.30 (dt, *J*=15.9, 6.1 Hz, 1 H), 4.70 (s, 2 H), 4.24 (dd, *J*=6.1, 1.4 Hz, 2 H), 3.41 (s, 3 H). Product corresponds to literature characterization data.[175]

A3.5.3.Hydrazone synthesis (products 4.1a to 4.1w)

General procedure for aldehyde condensation: To a 20 mL glass vial containing a suspension of mesitylsulfonylhydrazide (1.00 equiv) in EtOH (0.67M) was added at once aldehyde (1.01 or 1.05 equiv) and acetic acid (0.05 equiv). Heterogenous mixture was vigourously stirred for 2h. Mixture was concentrated under vacuum until about 1/10th of original volume and excess hexanes was added. The resulting solid is recovered using a fritted glass filter and washed with cold hexanes. If aldehyde still remains, trituration in hexanes or 10% EtOAc/hexanes mixture can remove it.

General procedure for ketone condensation: To a 20 mL glass vial containing a suspension of mesitylsulfonylhydrazide (1.00 equiv) in EtOH (0.67M) was added at once ketone (1.01 equiv) and 12N aqueous hydrochloric acid (0.25 equiv). Heterogenous mixture was vigourously stirred for 24h. Mixture was concentrated under vacuum and purified by flash chromatography (5-15% EtOAc/Hexanes) to yield a white solid.

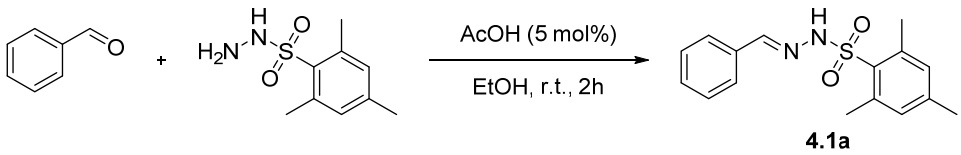

(*E*)-*N'*-Benzylidene-2,4,6-trimethylbenzenesulfonohydrazide (4.1a): Synthesized from benzaldehyde (0.495 mL, 4.90 mmol, 1.05 equiv), acetic acid (13 µL, 0.23 mmol, 0.05 equiv) and mesitylsulfonylhydrazide (1.00 g, 4.67 mmol, 1.00 equiv) using the **general procedure for aldehyde condensation**. Product obtained as a white solid (1.32g, 4.37 mmol, 94%). **mp**: 145-147 °C, lit. 147 °C[176]; **^{1}H-NMR** ($CDCl_3$, 500 MHz): δ ppm 7.94 (br s, 1 H), 7.72 (s, 1 H), 7.48 - 7.54 (m, 2 H), 7.30 - 7.39 (m, 3 H), 6.97 (s, 2 H), 2.73 (s, 6 H), 2.29 (s, 3 H). Product corresponds to literature characterization data.[176] **DSC analysis:** Endothermic event (melting, interrupted by next event) at 140° C (6.6 J/g), exothermic event (degradation/gas evolution) at 145°C (-274.1 J/g, 18% mass decrease (predicted for SO_2 loss: 21%)).

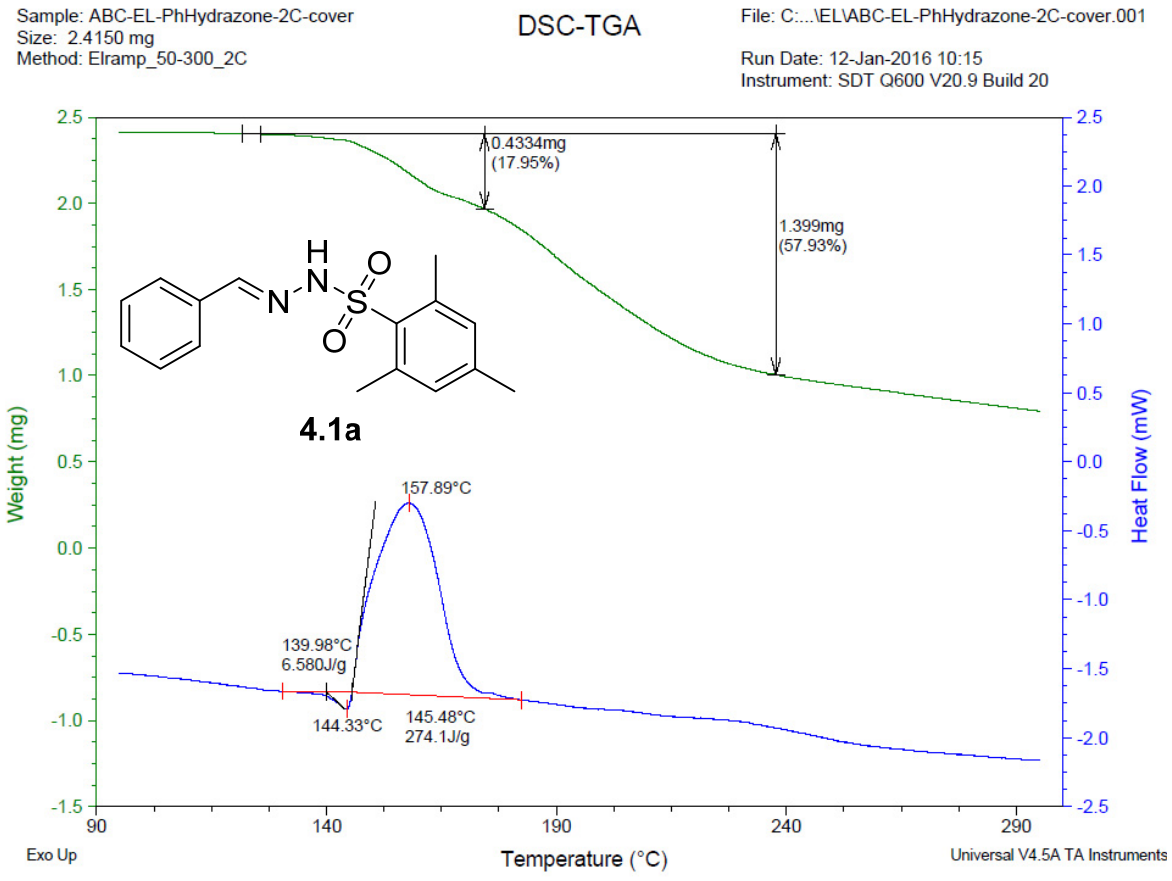

Comparison with known compound. *p*-Acetamidobenzylsulfonyl azide (*p*-ABSA) is generally considered a safe azide for large scale handling. Its DSC-TGA analysis yielded the following results: Endothermic event (melting) at 109°C (62.9 J/g), exothermic event (degradation/gas evolution) at 146°C (-724.0 J/g, 13% mass decrease (predicted for N_2 loss : 12%)). These results agree with previously reported literature data: Endothermic event (-720 J/g, starts at 120°C).[109b] **4.1a** releases little more than a third of the energy released by pABSA when degrading at the same temperature.

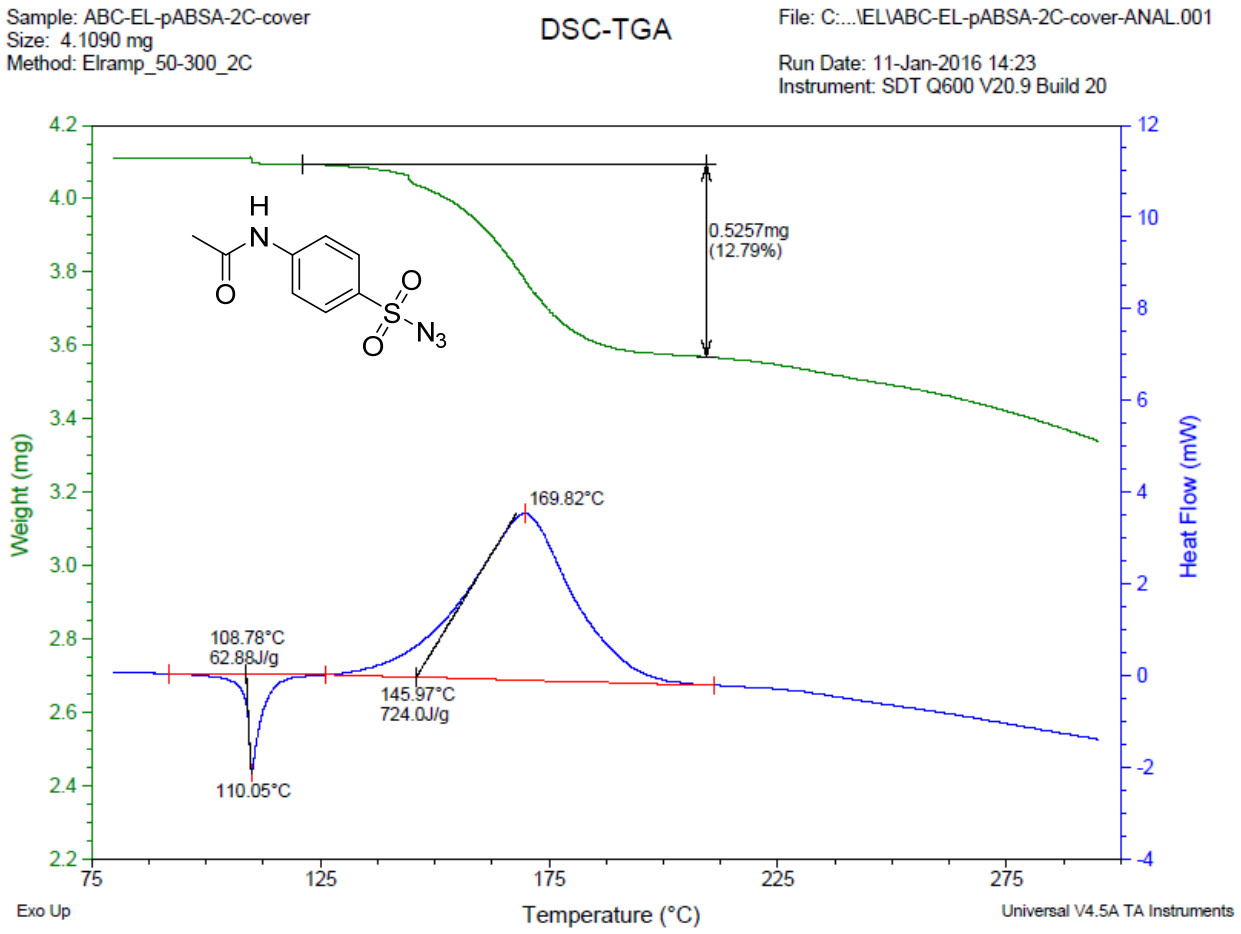

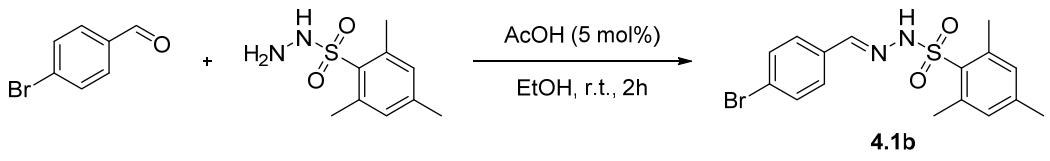

4.1b

(*E*)-*N'*-(4-Bromobenzylidene)-2,4,6-trimethylbenzenesulfonohydrazide (4.1b): Synthesized from 4-bromobenzaldehyde (0.994 g, 5.37 mmol, 1.01 equiv), acetic acid (15 μL, 0.27 mmol, 0.05 equiv) and mesitylsulfonylhydrazide (1.14 g, 5.33 mmol, 1.00 equiv) using the **general procedure for aldehyde condensation**. Product obtained as an off-white solid (1.89 g, 4.96 mmol, 93%). **mp**: 156-158 °C; **^{1}H-NMR** ($CDCl_3$, 300 MHz): δ ppm 7.98 (br s, 1 H), 7.66 (s, 1 H), 7.43 - 7.50 (m, 2 H), 7.33 - 7.41 (m, 2 H), 6.98 (s, 2 H), 2.72 (s, 6 H), 2.31 (s, 3 H); **^{13}C-NMR** ($CDCl_3$, 125 MHz): δ ppm 145.21 (CH), 143.41 (C), 140.40 (2 C), 132.36 (C), 132.30 (C), 132.16 (2 CH), 132.05 (2 CH), 128.68 (2 CH), 124.68 (C), 23.42 (2 CH_3), 21.17 (CH_3); **FTIR** (cm^{-1}) (neat): 3198 (br), 2939 (w), 1368 (m), 1167 (s), 939 (m), 819 (m), 664 (s), 508 (m); **HRMS** (ESI, Pos): calcd for $C_{16}H_{18}BrN_2O_2S$ $[M+H]^+$: 381.02669 m/z, found: 381.02847 m/z.

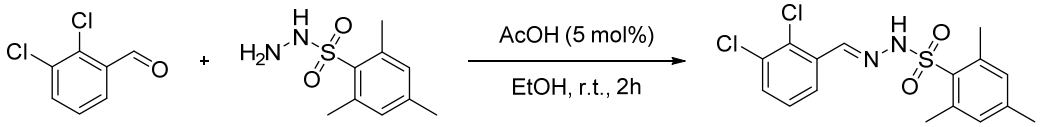

4.1c

(*E*)-*N'*-(2,3-Dichlorobenzylidene)-2,4,6-trimethylbenzenesulfonohydrazide (4.1c): Synthesized from 2,3-dichlorobenzaldehyde (220 mg, 1.26 mmol, 1.01 equiv), acetic acid (4 μL, 0.06 mmol, 0.05 equiv) and mesitylsulfonylhydrazide (268 mg, 1.25 mmol, 1.00 equiv) using the **general procedure for aldehyde condensation**. Product obtained as a white solid (397 mg, 1.07 mmol, 86 %). **mp**: 176-178 °C; **^{1}H-NMR** ($CDCl_3$, 400 MHz): δ ppm 8.25 (s, 1 H), 8.15 (s, 1 H), 7.69 (dd, *J*=8.0, 1.6 Hz, 1 H), 7.43 (dd, *J*=8.0, 1.6 Hz, 1 H), 7.16 (t, *J*=8.0 Hz, 1 H), 6.98 (s, 2 H), 2.73 (s, 6 H), 2.30 (s, 3 H); **^{13}C-NMR** ($CDCl_3$, 75 MHz): δ ppm 143.50 (C), 142.24 (CH), 140.41 (2 C), 133.61 (C), 133.08 (C), 132.27 (C), 132.25 (C), 132.19 (2 CH), 131.68 (CH), 127.50 (CH), 125.52 (CH), 23.41 (2 CH_3), 21.18 (CH_3); **FTIR** (cm^{-1}) (neat): 3182 (br), 2938 (br w), 1432 (m) 1402 (m), 1380 (m), 1164 (s), 652 (m), 596 (m), 508 (s); **HRMS** (ESI, Pos): calcd for $C_{16}H_{17}Cl_2N_2O_2S$ $[M+H]^+$: 371.03823 m/z, found: 371.04004 m/z.

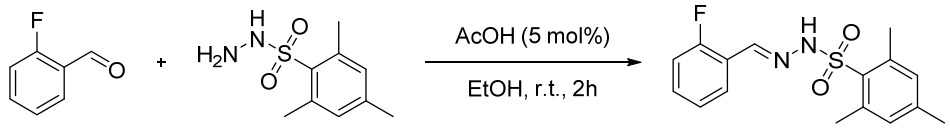

4.1d

(*E*)-*N'*-(2-Fluorobenzylidene)-2,4,6-trimethylbenzenesulfonohydrazide (4.1d): Synthesized from 2-fluorobenzaldehyde (163 mg, 1.31 mmol, 1.05 equiv), acetic acid (4 μL, 0.06 mmol, 0.05 equiv) and mesitylsulfonylhydrazide (268 mg, 1.25 mmol, 1.00 equiv) using the **general procedure for aldehyde condensation**. Product obtained as a white solid (333 mg, 1.04 mmol, 83 %). **mp**: 160-163 °C; **^{1}H-NMR** ($CDCl_3$, 300 MHz): δ ppm 8.04 (br s, 1 H), 7.98 (s, 1 H), 7.73 (td, *J*=7.6, 1.8 Hz, 1 H), 7.27 - 7.36 (m, 1 H), 7.10 (t, *J*=7.5 Hz, 1 H), 7.02 (ddd, *J*=10.5, 8.0, 1.0 Hz, 1 H), 6.98 (s, 2 H), 2.73 (s, 6 H), 2.30 (s, 3 H); **^{13}C-NMR** ($CDCl_3$, 75 MHz): δ ppm 161.31 (d, *J*=252.1 Hz, C), 143.34 (s, C), 140.43 (2 C), 139.54 (d, *J*=5.2 Hz, CH), 132.37 (C), 132.13 (2 CH), 131.87 (d, *J*=8.4 Hz, CH), 126.83 (d, *J*=2.6 Hz, CH), 124.50 (d, *J*=3.6 Hz, CH), 121.31 (d, *J*=9.9 Hz, C), 115.84 (d, *J*=20.9 Hz, CH), 23.40 (2 CH_3), 21.15 (CH_3); **^{19}F-NMR** ($PhCF_3$/$CDCl_3$, 471 MHz): δ ppm -121.02 (ddd, *J*=12.0, 6.0, 4.5 Hz, 1 F); **FTIR** (cm^{-1}) (neat): 3198 (br), 2942 (w), 1316 (m), 1160 (s), 1050 (m), 942 (m), 839 (m) 759 (s), 656 (m), 596 (m), 533 (m); **HRMS** (ESI, Pos): calcd for $C_{16}H_{18}FN_2O_2S$ $[M+H]^+$: 321.10675 m/z, found: 321.10742 m/z.

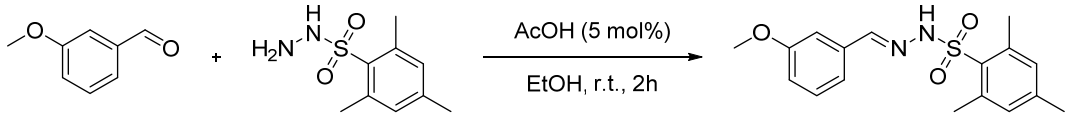

4.1e

(*E*)-*N'*-(3-Methoxybenzylidene)-2,4,6-trimethylbenzenesulfonohydrazide (4.1e): Synthesized from 3-methoxybenzaldehyde (220 mg, 1.62 mmol, 1.01 equiv), acetic acid (5 μL, 0.08 mmol, 0.05 equiv) and mesitylsulfonylhydrazide (343 mg, 1.60 mmol, 1.00 equiv) using the **general procedure for aldehyde condensation**. Product obtained as a white solid (452 mg, 1.36 mmol, 85 %). **mp**: 107-109 °C; **^{1}H-NMR** ($CDCl_3$, 300 MHz): δ ppm 7.91 (br s, 1 H), 7.68 (s, 1 H), 7.24 (t, *J*=7.9 Hz, 1 H), 7.11 (dd, *J*=2.4, 1.3 Hz, 1 H), 7.05 (dt, *J*=7.6, 1.0 Hz, 1 H), 6.97 (s, 2 H), 6.90 (ddd, *J*=8.3, 2.6, 1.0 Hz, 1 H), 3.79 (s, 3 H), 2.73 (s, 6 H), 2.29 (s, 3 H); **^{13}C-NMR** ($CDCl_3$, 75 MHz): δ ppm 159.85 (C), 146.37 (CH), 143.25 (C), 140.39 (2 C), 134.82 (C), 132.44 (C), 132.10 (2 CH), 129.75 (CH), 120.51 (CH), 116.83 (CH), 111.19 (CH), 55.34 (CH_3), 23.41 (2 CH_3), 21.14 (CH_3); **FTIR** (cm^{-1}) (neat): 3205 (m), 1597 (w), 1267 (m), 1168 (s), 1032 (m), 889 (m), 659 (s); **HRMS** (ESI, Pos): calcd for $C_{17}H_{21}N_2O_3S$ $[M+H]^+$: 333.12674 m/z, found: 333.12744 m/z.

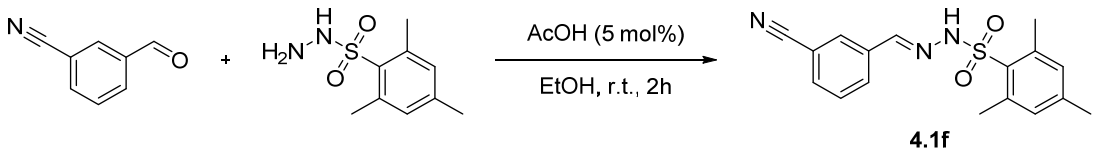

4.1f

(*E*)-*N'*-(3-Cyanobenzylidene)-2,4,6-trimethylbenzenesulfonohydrazide (4.1f): Synthesized from 3-cyanobenzaldehyde (166 mg, 1.26 mmol, 1.01 equiv), acetic acid (4 μL, 0.06 mmol, 0.05 equiv) and mesitylsulfonylhydrazide (268 mg, 1.25 mmol, 1.00 equiv) using the **general procedure for aldehyde condensation**. Product obtained as a white solid (338 mg, 1.03 mmol, 83 %). **mp**: 144-146 °C; **^{1}H-NMR** ($CDCl_3$, 300 MHz): δ ppm 8.15 (br s, 1 H), 7.74 (tt, *J*=7.5, 1.5 Hz, 2 H), 7.70 (s, 1 H), 7.62 (dt, *J*=7.8, 1.4 Hz, 1 H), 7.46 (t, *J*=7.8 Hz, 1 H), 7.00 (s, 2 H), 2.73 (s, 6 H), 2.31 (s, 3 H); **^{13}C-NMR** ($CDCl_3$, 75 MHz): δ ppm 143.66 (C), 143.32 (CH), 140.44 (2 C), 134.75 (C), 133.37 (CH), 132.26 (2 CH), 132.08 (C), 131.16 (CH), 130.57 (CH), 129.71 (CH), 118.29 (C), 113.25 (C), 23.40 (2 CH_3), 21.20 (CH_3); **FTIR** (cm^{-1}) (neat): 3156 (br), 2227 (m), 1600 (w), 1314 (m), 1155 (s), 883 (m), 659 (s), 578 (m), 528 (m), 477 (m); **HRMS** (ESI, Pos): calcd for $C_{17}H_{17}N_3O_2S$ $[M+H]^+$: 328.11142 m/z, found: 328.11151 m/z.

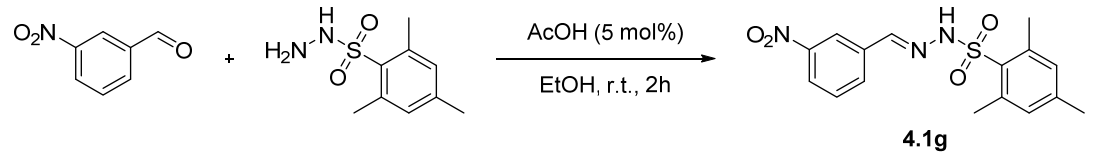

4.1g

(*E*)-*N'*-(3-Nitrobenzylidene)-2,4,6-trimethylbenzenesulfonohydrazide (4.1g): Synthesized from 3-nitrobenzaldehyde (712 mg, 4.71 mmol, 1.01 equiv), acetic acid (13 μL, 0.23 mmol, 0.05 equiv) and mesitylsulfonylhydrazide (1.00 g, 4.67 mmol, 1.00 equiv) using the **general procedure for aldehyde condensation**. Product obtained as a white solid (1.45 g, 4.17 mmol, 89 %). **mp**: 160-162 °C; **^{1}H-NMR** ($CDCl_3$, 300 MHz): δ ppm 8.74 (br s, 1 H), 8.36 (s, 1 H), 8.32 (t, *J*=1.9 Hz, 1 H), 8.18 (ddd, *J*=8.2, 2.3, 1.1 Hz, 1 H), 7.84 (dt, *J*=7.8, 1.3 Hz, 1 H), 7.79 (s, 1 H), 7.52 (t, *J*=8.0 Hz, 1 H), 7.00 (s, 2 H), 2.75 (s, 6 H), 2.31 (s, 3 H); **^{13}C-NMR** ($CDCl_3$, 125 MHz): δ ppm 148.66 (C), 143.69 (C), 143.17 (CH), 140.49 (2 C), 135.29 (C), 132.51 (CH), 132.26 (2 CH), 132.10 (C), 129.86 (CH), 124.66 (CH), 122.05 (CH), 23.40 (2 CH_3), 21.20 (CH_3); **FTIR** (cm^{-1}) (neat): 3194 (br), 1544 (m), 1347 (s), 1162 (s), 1053 (m), 816 (s), 660 (s), 595 (s), 525 (s); **HRMS** (ESI, Pos): calcd for $C_{16}H_{18}N_3O_4S$ $[M+H]^+$: 348.10125 m/z, found: 348.10274 m/z.

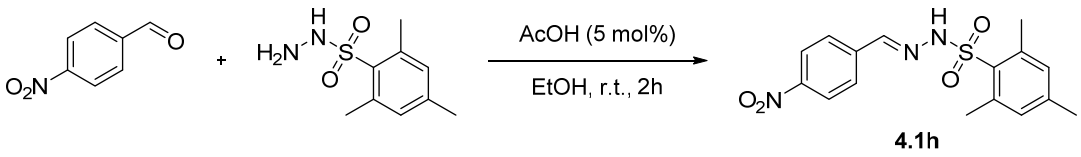

4.1h

(*E*)-*N'*-(4-Nitrobenzylidene)-2,4,6-trimethylbenzenesulfonohydrazide (4.1h): Synthesized from 4-nitrobenzaldehyde (244 mg, 1.62 mmol, 1.00 equiv), acetic acid (5 μL, 0.08 mmol, 0.05 equiv) and mesitylsulfonylhydrazide (343 mg, 1.60 mmol, 1.00 equiv) using the **general procedure for aldehyde condensation**. Product obtained as an off-white solid (482 mg, 1.39 mmol, 87 %). **mp**: 152-154 °C; **^{1}H-NMR** ($CDCl_3$, 300 MHz): δ ppm 8.25 (br s, 2 H), 8.20 (d, *J*=8.8 Hz, 2 H), 7.76 (s, 1 H), 7.66 (d, *J*=8.8 Hz, 2 H), 7.00 (s, 2 H), 2.73 (s, 6 H), 2.31 (s, 3 H); **^{13}C-NMR** ($CDCl_3$, 75 MHz): δ ppm 148.64 (C), 143.76 (C), 142.98 (CH), 140.47 (2 C), 139.33 (C), 132.27 (2 CH), 132.06 (C), 127.81 (2 CH), 124.16 (2 CH), 23.42 (2 CH_3), 21.21 (CH_3); **FTIR** (cm^{-1}) (neat): 3211 (br w), 2942 (br w), 1599 (w), 1515 (m), 1342 (s), 1162 (s), 856 (m); **HRMS** (ESI, Pos): calcd for $C_{16}H_{17}N_3O_4SLi$ (Li salt of **1h**) $[M+H]^+$: 354.10943 m/z, found: 354.10952 m/z.

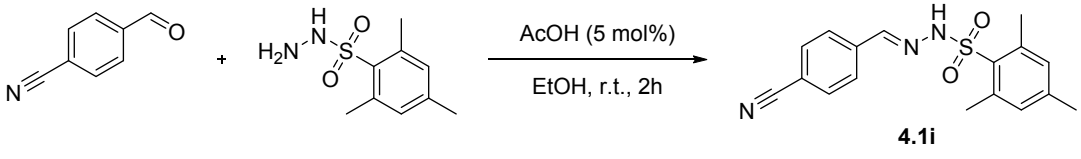

4.1i

(*E*)-*N'*-(4-Cyanobenzylidene)-2,4,6-trimethylbenzenesulfonohydrazide (4.1i): Synthesized from 4-cyanobenzaldehyde (0.62 g, 4.71 mmol, 1.01 equiv), acetic acid (13 μL, 0.23 mmol, 0.05 equiv) and mesitylsulfonylhydrazide (1.00 g, 4.67 mmol, 1.00 equiv) using the **general procedure for aldehyde condensation**. Product obtained as a white solid (1.47 g, 4,49 mmol, 96 %). **mp**: 188-190 °C (degradation); **^{1}H-NMR** ($CDCl_3$, 300 MHz): δ ppm 8.25 (br s, 1 H), 7.72 (s, 1 H), 7.57 - 7.65 (m, 4 H), 2.00 (s, 2 H), 2.72 (s, 6 H), 2.31 (s, 3 H); **^{13}C-NMR** ($CDCl_3$, 75 MHz): δ ppm 143.68 (C), 143.55 (CH), 140.45 (2 C), 137.61 (C), 132.60 (2 CH), 132.24 (2 CH), 132.09 (C), 127.59 (2 CH), 118.51 (C), 113.48 (C), 23.40 (2 CH_3), 21.20 (CH_3); **FTIR** (cm^{-1}) (neat): 3173 (br), 2973 (br w), 2233 (w), 1603 (w), 1448 (w), 1330 (m), 1166 (s), 1052 (m), 933 (s), 830 (s), 530 (s); **HRMS** (ESI, Pos): calcd for $C_{17}H_{18}N_3O_2S$ $[M+H]^+$: 328.11142 m/z, found: 328.11222 m/z.

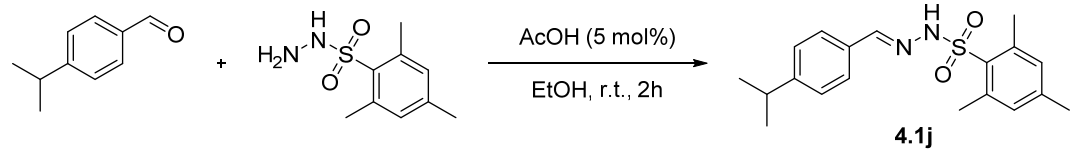

4.1j

(*E*)-*N'*-(4-Isopropylbenzylidene)-2,4,6-trimethylbenzenesulfonohydrazide (4.1j): Synthesized from 4-isopropylbenzaldehyde (311 mg, 2.10 mmol, 1.05 equiv), acetic acid (6 μL, 0.10 mmol, 0.05 equiv) and mesitylsulfonylhydrazide (429 mg, 2.00 mmol, 1.00 equiv) using the **general procedure for aldehyde condensation**. Product obtained as a white solid (634 mg, 1.84 mmol, 92 %). **mp**: 138-141 °C; **^{1}H-NMR** ($CDCl_3$, 400 MHz): δ ppm 8.01 (br s, 1 H), 7.71 (s, 1 H), 7.44 (d, *J*=8.1 Hz, 2 H), 7.19 (d, *J*=8.1 Hz, 2 H), 6.96 (s, 2 H), 2.89 (spt, *J*=6.9 Hz, 1 H), 2.73 (s, 6 H), 2.29 (s, 3 H), 1.22 (d, *J*=7.0 Hz, 6 H); **^{13}C-NMR** ($CDCl_3$,75 MHz): δ ppm 151.72 (C), 147.05 (CH), 143.16 (C), 140.35 (2 C), 132.48 (C), 132.09 (2 CH), 131.03 (C), 127.49 (2 CH), 126.90 (2 CH), 34.21 (CH), 23.88 (2 CH_3), 23.43 (2 CH_3), 21.13 (CH_3); **FTIR** (cm^{-1}) (neat): 3202 (br), 2960 (br), 1604 (w), 1362 (m), 1319 (m), 1164 (s), 1032 (m), 937 (m), 828 (m), 659 (s), 534 (s); **HRMS** (ESI, Pos): calcd for $C_{19}H_{24}N_2O_2S$ $[M+H]^+$: 345.16313 m/z, found: 345.16376 m/z.

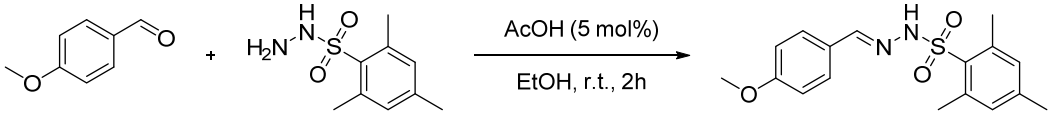

4.1k

(*E*)-*N'*-(4-Methoxybenzylidene)-2,4,6-trimethylbenzenesulfonohydrazide (4.1k): Synthesized from 4-methoxybenzaldehyde (286 mg, 2.10 mmol, 1.05 equiv), acetic acid (6 μL, 0.10 mmol, 0.05 equiv) and mesitylsulfonylhydrazide (429 mg, 2.00 mmol, 1.00 equiv) using the **general procedure for aldehyde condensation**. Product obtained as a white solid (614 mg, 1.85 mmol, 92 %). **mp**: 156-158 °C; **^{1}H-NMR** ($CDCl_3$, 400 MHz): δ ppm 7.74 (br s, 1 H), 7.68 (s, 1 H), 7.46 (d, *J*=8.9 Hz, 2 H), 6.97 (s, 2 H), 6.85 (d, *J*=8.9 Hz, 1 H), 3.81 (s, 3 H), 2.72 (s, 6 H), 2.29 (s, 3 H); **^{13}C-NMR** ($CDCl_3$, 75 MHz): δ ppm 161.57 (C), 147.16 (CH), 143.15 (C), 140.37 (2 C), 132.49 (C), 132.09 (2 CH), 129.03 (2 CH), 126.04 (C), 114.27 (2 CH), 55.49 (CH_3), 23.43 (2 CH_3), 21.15 (CH_3); **FTIR** (cm^{-1}) (neat): 3224 (br), 2938 (br w), 1604 (m), 1511 (m), 1249 (s), 1159 (s), 1025 (s), 830 (s), 659 (s), 536 (s); **HRMS** (ESI, Pos): calcd for $C_{17}H_{21}N_2O_3S$ $[M+H]^+$: 333.12674 m/z, found: 333.12789 m/z.

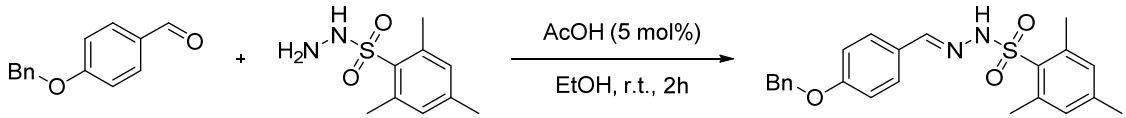

4.1l

(*E*)-*N'*-(4-Benzyloxybenzylidene)-2,4,6-trimethylbenzenesulfonohydrazide (4.1l): Synthesized from 4-benzyloxybenzaldehyde (1.14 g, 5.37 mmol, 1.01 equiv), acetic acid (15 µL, 0.27 mmol, 0.05 equiv) and mesitylsulfonylhydrazide (1.14 g, 5.32 mmol, 1.00 equiv) using the **general procedure for aldehyde condensation**. Product obtained as a white solid (1.88 g, 4.60 mmol, 87 %). **mp**: 134-136 °C; **^{1}H-NMR** ($CDCl_3$, 300 MHz): δ ppm 7.80 (s, 1 H), 7.67 (s, 1 H), 7.45 (dt, *J*=9.0, 2.5 Hz, 2 H), 7.28 - 7.42 (m, 5 H), 6.97 (s, 2 H), 6.92 (dt, *J*=9.0, 2.5 Hz, 2 H), 5.06 (s, 2 H), 2.72 (s, 6 H), 2.29 (s, 3 H); **^{13}C-NMR** ($CDCl_3$, 125 MHz): δ ppm 160.64 (C), 146.84 (CH), 143.13 (C), 140.36 (2 C), 136.58 (C), 132.50 (C), 132.08 (2 CH), 128.96 (2 CH), 128.79 (2 CH), 128.27 (CH), 127.57 (2 CH), 126.37 (C), 115.15 (2 CH), 70.18 (CH_3), 23.43 (2 CH_3), 21.14 (CH_3); **FTIR** (cm^{-1}) (neat): 3226 (w), 2940 (br w), 1605 (m), 1359 (m), 1253 (m), 1165 (s), 1026 (m), 664 (s), 532 (s); **HRMS** (ESI, Pos): calcd for $C_{23}H_{25}N_2O_3S$ $[M+H]^+$: 409.15804 m/z, found: 409.15988 m/z.

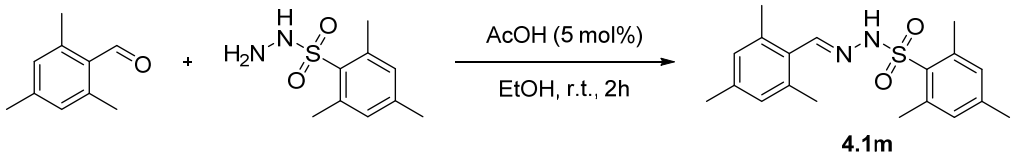

4.1m

(*E*)-2,4,6-Trimethyl-N'-(2,4,6-trimethylbenzylidene)benzenesulfonohydrazide (4.1m): Synthesized from mesitaldehyde (358 mg, 2.42 mmol, 1.51 equiv), acetic acid (5 µL, 0.08 mmol, 0.05 equiv) and mesitylsulfonylhydrazide (343 mg, 1.60 mmol, 1.00 equiv) using the **general procedure for aldehyde condensation**. Product obtained as a yellow solid (461 mg, 1.34 mmol, 84 %). **mp**: 146-149 °C; **^{1}H-NMR** ($CDCl_3$, 400 MHz) Major atropoisomer: δ ppm 8.04 (s, 1 H), 7.89 (br s, 1 H), 6.96 (s, 2 H), 6.80 (s, 2 H), 2.69 (s, 6 H), 2.29 (s, 3 H), 2.24 (s, 3 H), 2.20 (s, 6 H); Minor atropoisomer: δ ppm 7.68 (br s, 1 H), 7.54 (s, 1 H), 6.97 (s, 2 H), 6.91 (s, 2 H), 2.59 (s, 6 H), 2.31 (s, 3 H), 2.31 (s, 3 H), 2.07 (s, 6 H); **^{13}C-NMR** ($CDCl_3$, 125 MHz) Major atropoisomer: δ ppm 146.69 (CH), 143.16 (C), 140.22 (2 C), 139.45 (C), 136.06 (2 C), 132.47 (C), 132.06 (2 CH), 129.06 (2 CH), 125.83 (C), 23.17 (2 CH_3), 21.26 (CH_3), 21.17 (CH_3), 19.38 (2 CH_3); Minor atropoisomer: δ ppm 146.41 (CH), 143.14 (C), 140.24 (2 C), 140.16 (C), 137.97 (2 C), 132.39 (C), 132.03 (2 CH), 129.73 (2 CH), 127.20 (C) 23.24 (2 CH_3), 21.23 (CH_3), 21.23 (2 CH_3), 21.13 (CH_3); **FTIR** (cm^{-1}) (neat): 3193 (br), 2923 (br w), 1604 (w), 1322 (m), 1158 (s), 942 (m), 659 (s), 589 (s), 536 (s); **HRMS** (ESI, Pos): calcd for $C_{19}H_{25}N_2O_2S$ $[M+H]^+$: 345.16313 m/z, found: 345.16411 m/z.

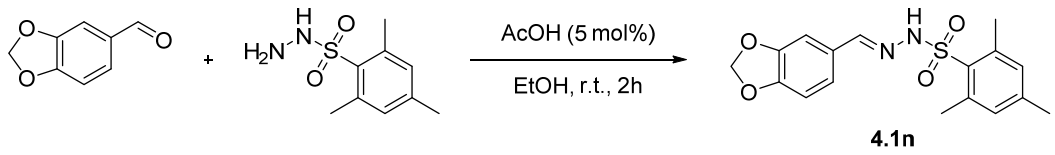

4.1n

(*E*)-*N'*-(Benzo[d][1,3]dioxol-5-ylmethylene)-2,4,6-trimethylbenzenesulfonohydrazide (4.1n): Synthesized from piperonal (368 mg, 2.45 mmol, 1.05 equiv), acetic acid (7 μL, 0.12 mmol, 0.05 equiv) and mesitylsulfonylhydrazide (500 mg, 2.33 mmol, 1.00 equiv) using the **general procedure for aldehyde condensation**. Product obtained as a white solid (800 mg, 2.31 mmol, 99 %). **mp**: 136-138 °C; **^{1}H-NMR** ($CDCl_3$, 300 MHz): δ ppm 7.79 (br s, 1 H), 7.64 (s, 1 H), 7.10 (d, *J*=1.5 Hz, 1 H), 6.97 (s, 2 H), 6.89 (dd, *J*=8.0, 1.5 Hz, 1 H), 6.75 (d, *J*=7.9 Hz, 1 H), 5.97 (s, 2 H), 2.72 (s, 6 H), 2.29 (s, 3 H); **^{13}C-NMR** ($CDCl_3$, 75 MHz): δ ppm 149.89 (C), 148.40 (C), 147.00 (CH), 143.24 (C), 140.39 (2 C), 132.40 (C), 132.13 (2 CH), 127.84 (C), 123.88 (CH), 108.29 (CH), 105.81 (CH), 101.65 (CH_2), 23.44 (2 CH_3), 21.17 (CH_3); **FTIR** (cm^{-1}) (neat): 3239 (br), 2912 (br w), 1597 (w), 1453 (m), 1257 (s), 1164 (s), 1034 (s), 658 (s), 535 (s); **HRMS** (ESI, Pos): calcd for $C_{17}H_{19}N_2O_4S$ $[M+H]^+$: 347.10600 m/z, found: 347.10735 m/z.

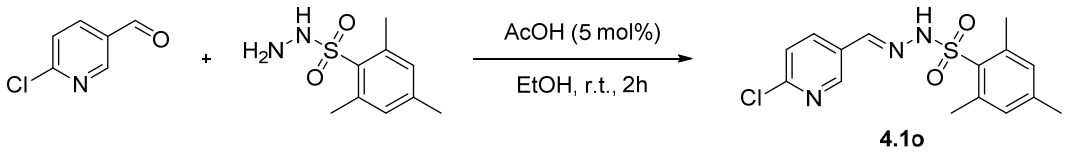

4.1o

(*E*)-*N'*-((6-Chloropyridin-3-yl)methylene)-2,4,6-trimethylbenzenesulfonohydrazide (4.1o): Synthesized from 6-chloronicotinaldehyde (0.67 g, 4.71 mmol, 1.01 equiv), acetic acid (13 μL, 0.23 mmol, 0.05 equiv) and mesitylsulfonylhydrazide (1.00 g, 4.67 mmol, 1.00 equiv) using the **general procedure for aldehyde condensation**. Product obtained as a pale yellow solid (1.52 g, 4.5 mmol, 96 %). **mp**: 178-182 °C (degradation); **^{1}H-NMR** ($CDCl_3$, 300 MHz): δ ppm 8.43 (d, *J*=2.3 Hz, 1 H), 8.16 (s, 1 H), 7.85 (dd, *J*=8.3, 2.5 Hz, 1 H), 7.71 (s, 1 H), 7.31 (d, *J*=7.8 Hz, 1 H), 6.99 (s, 2 H), 2.71 (s, 6 H), 2.30 (s, 3 H); **^{13}C-NMR** ($CDCl_3$, 125 MHz): δ ppm 151.07 (C), 148.60 (CH), 142.77 (C), 141.33 (2 C), 139.46 (CH), 136.34 (CH), 133.35 (C), 131.93 (2 CH), 129.56 (C), 124.92 (CH), 22.93 (2 CH_3), 20.64 (CH_3); **FTIR** (cm^{-1}) (neat): 2887 (br w), 1465 (w), 1329 (m), 1165 (s), 1082 (m), 951 (m), 835 (w), 592 (s), 524 (s); **HRMS** (ESI, Pos): calcd for $C_{15}H_{17}ClN_3O_2S$ $[M+H]^+$: 338.07245 m/z, found: 338.07342 m/z.

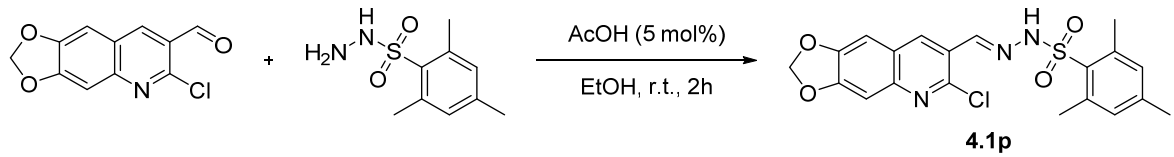

4.1p

(*E*)-*N'*-((6-Chloro-[1,3]dioxolo[4,5-*g*]quinolin-7-yl)methylene)-2,4,6-trimethylbenzenesulfonohydrazide (4.1p): Synthesized from 6-chloro-[1,3]dioxolo[4,5-g]quinoline-7-carbaldehyde (381 mg, 1.62 mmol, 1.01 equiv), acetic acid (5 µL, 0.08 mmol, 0.05 equiv) and mesitylsulfonylhydrazide (343 mg, 1.60 mmol, 1.00 equiv) using the **general procedure for aldehyde condensation**. Product obtained as a beige solid (638 mg, 1.48 mmol, 92 %). **mp**: 180-183 °C (degradation); **^{1}H-NMR** ($CDCl_3$, 300 MHz): δ ppm 8.33 (s, 1 H), 8.25 (s, 1 H), 8.15 (s, 1 H), 7.23 (s, 1 H), 7.02 (s, 1 H), 7.00 (s, 2 H), 6.13 (s, 2 H), 2.76 (s, 6 H), 2.30 (s, 3 H); **^{13}C-NMR** ($CDCl_3$, 75 MHz): δ ppm 152.72 (C), 148.88 (C), 146.96 (C), 146.91 (C), 143.53 (CH), 141.72 (s, 1 C), 140.32 (2C), 134.49 (C), 132.40 (C), 132.25 (2 CH), 124.29 (C), 123.30 (C), 105.17 (CH), 103.20 (CH), 102.43 (CH_2), 23.43 (2 CH_3), 21.18 (CH_3); **FTIR** (cm^{-1}) (neat): 3218 (br w), 1589 (w), 1452 (s), 1366 (m), 1238 (s), 1158 (s), 1031 (s), 925 (m), 658 (s), 598 (s), 529 (m); **HRMS** (ESI, Pos): calcd for $C_{20}H_{19}ClN_3O_4S$ $[M+H]^+$: 432.07793 m/z, found: 432.08007 m/z.

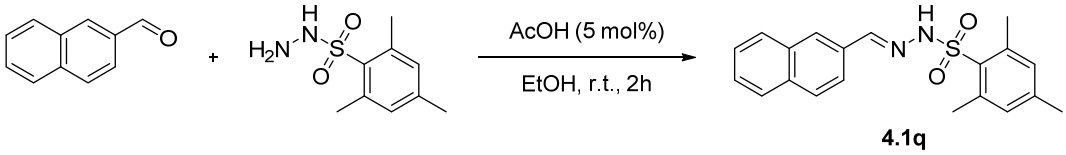

4.1q

(*E*)-2,4,6-Trimethyl-N'-(naphthalen-2-ylmethylene)benzenesulfonohydrazide (4.1q): Synthesized from 2-naphtaldehyde (197 mg, 1.26 mmol, 1.01 equiv), acetic acid (4 µL, 0.06 mmol, 0.05 equiv) and mesitylsulfonylhydrazide (268 mg, 1.25 mmol, 1.00 equiv) using the **general procedure for aldehyde condensation**. Product obtained as a white solid (382 mg, 1.08 mmol, 87 %). **mp**: 159-161 °C (degradation); **^{1}H-NMR** ($CDCl_3$, 400 MHz): δ ppm 8.48 - 8.54 (m, 1 H), 8.32 (s, 1 H), 8.19 (br s, 1 H), 7.81 - 7.88 (m, 2 H), 7.64 (d, *J*=7.1 Hz, 1 H), 7.40 - 7.54 (m, 3 H), 6.99 (s, 2 H), 2.78 (s, 6 H), 2.29 (s, 3 H); **^{13}C-NMR** ($CDCl_3$, 75 MHz): δ ppm 146.72 (CH), 143.33 (C), 140.47 (2 C), 133.90 (C), 132.37 (C), 132.15 (2 CH), 131.09 (CH), 130.49 (C), 128.93 (C), 128.80 (CH), 128.58 (CH), 127.21 (CH), 126.31 (CH), 125.22 (CH), 124.63 (CH), 23.42 (2 CH_3), 21.15 (CH_3); **FTIR** (cm^{-1}) (neat): 3213 (br), 133 (w), 1322 (m), 1167 (s), 1044 (m), 773 (s), 659 (s), 597 (s), 534 (s); **HRMS** (ESI, Pos): calcd for $C_{20}H_{21}N_2O_2S$ $[M+H]^+$: 353.13183 m/z, found: 353.13342 m/z.

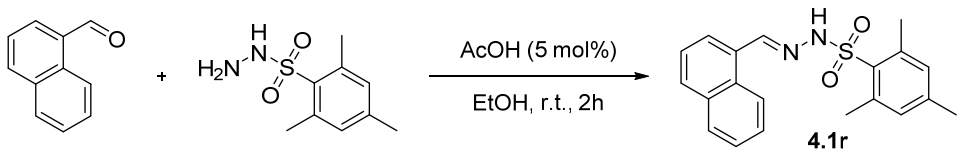

(*E*)-2,4,6-Trimethyl-N'-(naphthalen-1-ylmethylene)benzenesulfonohydrazide (4.1r): Synthesized from 1-naphtaldehyde (383 mg, 2.45 mmol, 1.05 equiv), acetic acid (7 µL, 0.12 mmol, 0.05 equiv) and mesitylsulfonylhydrazide (500 mg, 2.33 mmol, 1.05 equiv) using the **general procedure for aldehyde condensation**. Product obtained as a white solid (750 mg, 2.13 mmol, 91 %). **mp**: 166-168 °C (degradation) ; **^{1}H-NMR** ($CDCl_3$, 400 MHz): δ ppm 7.96 (s, 1 H), 7.87 (s, 1 H), 7.78 - 7.83 (m, 3 H), 7.77 (s, 2 H), 7.44 - 7.53 (m, 2 H), 6.99 (s, 2 H), 2.77 (s, 6 H), 2.29 (s, 3 H); **^{13}C-NMR** ($CDCl_3$, 75 MHz): δ ppm 146.79 (CH), 143.29 (C), 140.42 (2 C), 134.43 (C), 133.08 (C), 132.45 (C), 132.15 (2 CH), 131.14 (C), 129.18 (CH), 128.73 (CH), 128.47 (CH), 128.01 (CH), 127.32 (CH), 126.78 (CH), 122.84 (CH), 23.47 (2 CH_3), 21.16 (CH_3); **FTIR** (cm^{-1}) (neat): 3190 (br), 1447 (w), 1318 (m), 1165 (s), 1049 (m), 657 (s), 581 (s), 533 (s); HRMS (ESI, Pos): calcd for $C_{20}H_{21}N_2O_2S$ $[M+H]^+$: 353.13183 m/z, found: 353.13355 m/z.

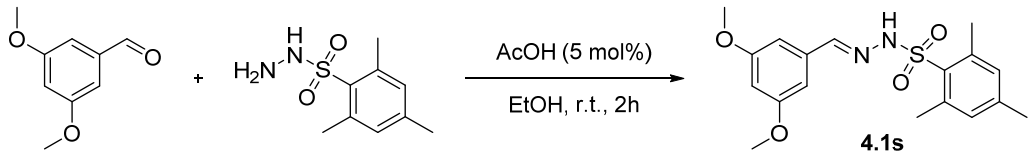

(*E*)-*N'*-(3,5-Dimethoxybenzylidene)-2,4,6-trimethylbenzenesulfonohydrazide (4.1s): Synthesized from 3,5-dimethoxybenzaldehyde (349 mg, 2.10 mmol, 1.05 equiv), acetic acid (6 µL, 0.10 mmol, 0.05 equiv) and mesitylsulfonylhydrazide (429 mg, 2.00 mmol, 1.00 equiv) using the **general procedure for aldehyde condensation**. Product obtained as a white solid (680 mg, 1.88 mmol, 94 %). **mp**: 168-170 °C; **^{1}H-NMR** ($CDCl_3$, 400 MHz): δ ppm 7.90 (s, 1 H), 7.62 (s, 1 H), 6.97 (s, 2 H), 6.67 (d, *J*=2.3 Hz, 2 H), 6.44 (t, *J*=2.3 Hz, 1 H), 3.77 (s, 6 H), 2.73 (s, 6 H), 2.29 (s, 3 H); **^{13}C-NMR** ($CDCl_3$, 75 MHz): δ ppm 160.98 (2 C), 146.30 (CH), 143.31 (C), 140.38 (2 C), 135.28 (C), 132.41 (C), 132.11 (2 CH), 105.17 (2 CH), 102.89 (CH), 55.50 (2 CH_3), 23.41 (2 CH_3), 21.15 (CH_3); **FTIR** (cm^{-1}) (neat): 3209 (w), 2932 (br w), 1593 (m), 1418 (w), 1319 (m), 1151 (s), 898 (m), 669 (s), 577 (m); **HRMS** (ESI, Pos): calcd for $C_{18}H_{23}N_2O_4S$ $[M+H]^+$: 363.1373 m/z, found: 363.13901 m/z.

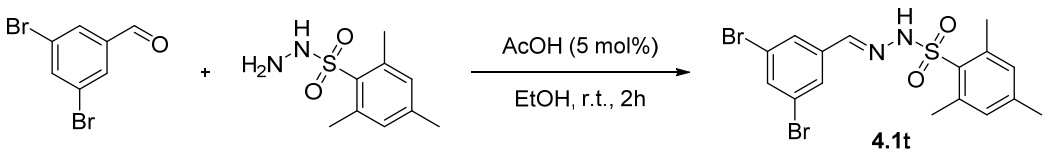

(*E*)-*N'*-(3,5-Dibromobenzylidene)-2,4,6-trimethylbenzenesulfonohydrazide (4.1t): Synthesized from 3,5-dibromobenzaldehyde (333 mg, 1.26 mmol, 1.01 equiv), acetic acid (4 µL, 0.06 mmol, 0.05 equiv) and mesitylsulfonylhydrazide (268 mg, 1.25 mmol, 1.00 equiv) using the **general procedure for aldehyde condensation**. Product obtained as a white solid (510 mg, 1.11 mmol, 89 %). **mp**: 174-176 °C; **^{1}H-NMR** ($CDCl_3$, 300 MHz): δ ppm 8.18 (br s, 1 H), 7.63 (t, *J*=1.2 Hz, 1 H), 7.58 (s, 1 H), 7.57 (d, *J*=1.2 Hz, 2 H), 7.01 (s, 2 H), 2.73 (s, 6 H), 2.32 (s, 3 H); **^{13}C-NMR** ($CDCl_3$, 125 MHz): δ ppm 143.74 (C), 142.87 (CH), 140.50 (2 C), 136.97 (C), 135.53 (CH), 132.37 (2 CH), 132.23 (C), 128.86 (2 CH), 123.45 (2 C), 23.47 (2 CH_3), 21.30 (CH_3); **FTIR** (cm^{-1}) (neat): 3175 (br), 2933 (br w), 1551 (m), 1312 (m), 1158 (s), 856 (s), 746 (m), 526 (m); **HRMS** (ESI, Pos): calcd for $C_{16}H_{17}Br_2N_2O_2S$ $[M+H]^+$: 458.9372 m/z, found: 458.93897 m/z.

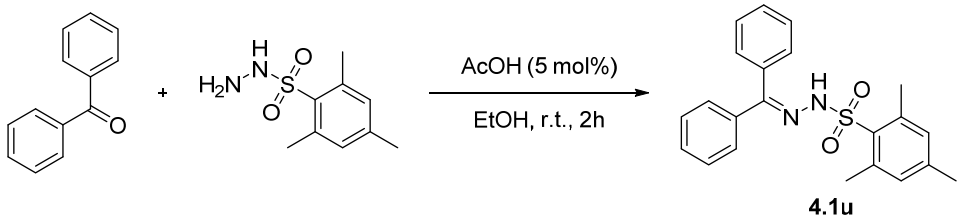

***N'*-(Diphenylmethylene)-2,4,6-trimethylbenzenesulfonohydrazide (4.1u):** Synthesized from benzophenone (429 mg, 2.36 mmol, 1.01 equiv), acetic acid (7 µL, 0.12 mmol, 0.05 equiv) and mesitylsulfonylhydrazide (500 mg, 2.33 mmol, 1.00 equiv) using the **general procedure for ketone condensation**. Product obtained as a white solid (724 mg, 1.91 mmol, 82 %). **mp**: 116-118 °C; **^{1}H-NMR** ($CDCl_3$, 300 MHz): δ ppm 7.67 (br s, 1 H), 7.48 - 7.62 (m, 3 H), 7.35 - 7.41 (m, 2 H), 7.21 - 7.33 (m, 3 H), 7.14 - 7.20 (m, 2 H), 6.98 (s, 2 H), 2.66 (s, 6 H), 2.31 (s, 3 H); **^{13}C-NMR** ($CDCl_3$, 100 MHz): δ ppm 153.57 (C), 143.12 (C), 140.27 (2 C), 136.60 (C), 132.63 (C), 132.08 (2 CH), 131.29 (C), 130.23 (CH), 129.97 (2 CH), 129.86 (CH), 128.46 (2 CH), 128.34 (2 CH), 127.56 (2 CH), 23.29 (2 CH_3), 21.18 (CH_3); **FTIR** (cm^{-1}) (neat): 3220 (w), 1600 (w), 1376 (m), 1346 (m), 1162 (s), 771 (m), 663 (s), 528 (s); **HRMS** (APCI, Pos): calcd for $C_{22}H_{23}N_2O_2S$ $[M+H]^+$: 379.14748 m/z, found: 379.14920 m/z.

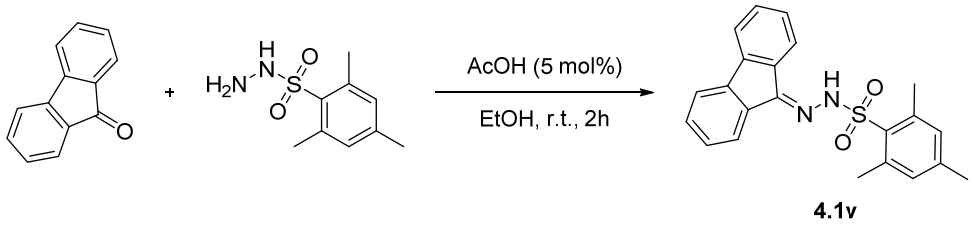

4.1v

***N'*-(9*H*-Fluoren-9-ylidene)-2,4,6-trimethylbenzenesulfonohydrazide (4.1v):** Synthesized from fluorenone 425 mg, 2.36 mmol, 1.01 equiv), acetic acid (7 μL, 0.12 mmol, 0.05 equiv) and mesitylsulfonylhydrazide (500 mg, 2.33 mmol, 1.00 equiv) using the **general procedure for ketone condensation**. Product obtained as a white solid (600 mg, 1.59 mmol, 68 %). **mp**: 182-184 °C (degradation); **^{1}H-NMR** ($CDCl_3$, 500 MHz): δ ppm 8.56 (s, 1 H), 7.85 (d, *J*=7.6 Hz, 1 H), 7.68 (d, *J*=7.5 Hz, 1 H), 7.59 (d, *J*=7.5 Hz, 1 H), 7.55 (d, *J*=7.5 Hz, 1 H), 7.47 (t, *J*=7.5 Hz, 1 H), 7.35 (q, *J*=7.6 Hz, 2 H), 7.23 (t, *J*=7.5 Hz, 1 H), 6.98 (s, 2 H), 2.80 (s, 6 H), 2.29 (s, 3 H); **^{13}C-NMR** ($CDCl_3$, 125 MHz): δ ppm 149.37 (C), 143.51 (C), 142.66 (C), 140.70 (2 C), 139.70 (C), 136.57 (C), 132.13 (2 CH), 132.07 (C), 131.72 (CH), 130.41 (CH), 129.84 (C), 128.39 (CH), 128.37 (CH), 125.95 (CH), 122.20 (CH), 121.10 (CH), 119.85 (CH), 23.57 (2 CH_3), 21.17 (CH_3); **FTIR** (cm^{-1}) (neat): 3217 (w), 2935 (br w), 1599 (w), 1451 (m), 1329 (m), 1310 (m), 1164 (s), 1031 (m), 855 (m), 730 (s), 676 (s), 504 (s); **HRMS** (ESI, Pos): calcd for $C_{22}H_{21}N_2O_2S$ $[M+H]^+$: 377.13183 m/z, found: 377.13349 m/z.

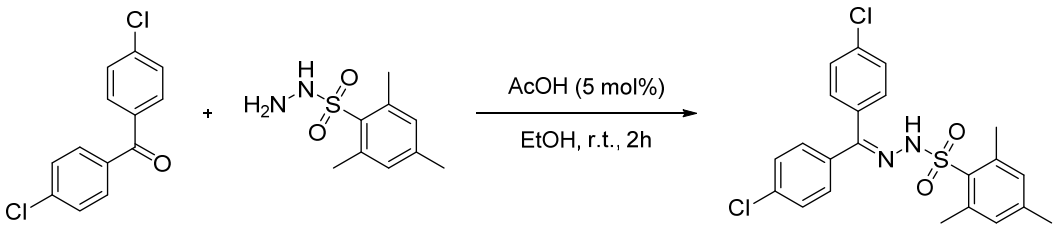

4.1w

***N'*-(Bis(4-chlorophenyl)methylene)-2,4,6-trimethylbenzenesulfonohydrazide (4.1w):** Synthesized from 4,4'-dichlorobenzophenone (296 mg, 1.18 mmol, 1.01 equiv), acetic acid (3 μL, 0.06 mmol, 0.05 equiv) and mesitylsulfonylhydrazide (250 mg, 1.17 mmol, 1.00 equiv) using the **general procedure for ketone condensation**. Product obtained as a white solid (170 mg, 0.38 mmol, 33 %). **mp**: 178-180 °C; **^{1}H-NMR** ($CDCl_3$, 400 MHz): δ ppm 7.61 (s, 1 H), 7.55 (dt, *J*=8.6, 2.3 Hz, 2 H), 7.25 - 7.30 (m, 2 H), 7.22 - 7.25 (m, 2 H), 7.12 (dt, *J*=8.6, 2.3 Hz, 2 H), 6.99 (s, 2 H), 2.65 (s, 6 H), 2.32 (s, 3 H); **^{13}C-NMR** ($CDCl_3$, 75 MHz): δ ppm 151.08 (C), 143.39 (C), 140.30 (2 C), 136.80 (C), 136.18 (C), 134.82 (C), 132.37 (C), 132.14 (2 CH), 130.50 (2 CH), 129.94 (2 CH),

129.08 (C), 128.72 (2 CH), 128.66 (2 CH), 23.31 (2 CH_3), 21.20 (CH_3); **FTIR** (cm^{-1}) (neat): 3154 (br), 2937 (br w), 1597 (w), 1490 (w), 1332 (m), 1313 (m), 1157 (s), 1088 (m), 981 (m), 823 (s), 653 (s), 573 (s), 531 (s); **HRMS** (ESI, Pos): calcd for $C_{22}H_{21}Cl_2N_2O_2S$ $[M+H]^+$: 447.06953 m/z, found: 447.06884 m/z.

A3.5.4.Continuous flow arydiazomethane synthesis (products 4.2a to 4.2w)

Caution! Diazo compounds are presumed to be highly toxic and potentially explosive. All manipulations should be carried out in a hood. Acetic acid (neat or diluted in alcohol or acetone) should be used to neutralize any spilled material.

See page 195 for procedures **A**, **B** and **C**

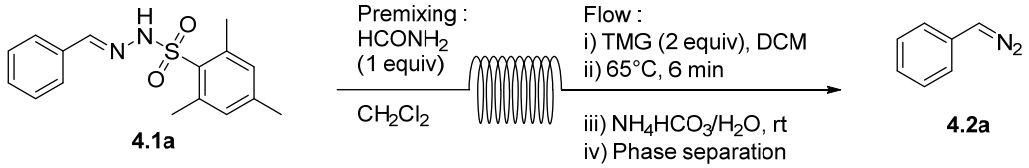

4.1a **4.2a**

(Diazomethyl)benzene (2a): Synthesised from **4.1a** (36 mg, 0.12 mmol, 1.0 equiv) and TMG (28 mg, 0.24 mmol, 2.0 equiv) using procedure **A** at MOC = 0.25 M with flow rate (**DAR**) = 333 µL/min and reactor temperature = 65 °C. Red liquid (79 % from isolation of the corresponding benzoate **4.3a**).

Synthesised from **4.1a** (36 mg, 0.12 mmol, 1.0 equiv) and TMG (28 mg, 0.24 mmol, 2.0 equiv) using procedure **A** at MOC = 0.25 M with flow rate (**DAR**) = 66 µL/min and reactor temperature = 65 °C. Red liquid (72 % from isolation of the corresponding benzoate **4.3a**).

Synthesised from **4.1a** (72 mg, 0.24 mmol, 1.0 equiv) and TMG (56 mg, 0.48 mmol, 2.0 equiv) using procedure **A** at MOC = 0.50 M with flow rate (**DAR**) = 333 µL/min and reactor temperature = 65 °C. Red liquid (75 % from isolation of the corresponding benzoate **4.3a**).

Synthesised from **4.1a** (151 mg, 0.5 mmol, 1.0 equiv) and TMG (0.12 mL, 115 mg, 1.0 mmol, 2.0 equiv) using procedure **B** at MOC = 0.25 M with flow rate (**DAR**) = 333 µL/min and reactor temperature = 65 °C. Red liquid (78 % from isolation of the corresponding benzoate **4.3a**).

Synthesised from **4.1a** (151 mg, 0.5 mmol, 1.0 equiv) and TMG (0.12 mL, 115 mg, 1.0 mmol, 2.0 equiv) using procedure **B** at MOC = 0.25 M with flow rate (**DAR**) = 333 µL/min and reactor

temperature = 65 °C. Stream passed through a 2.0*0.5 cm column packed with a dried 1:1 mixture of Celite® and 4Å molecular sieves. Red liquid (78 % from isolation of the corresponding benzoate **4.3a**).

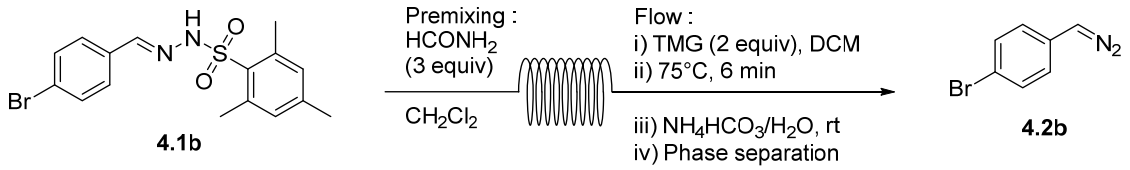

1-Bromo-4-(diazomethyl)benzene (4.2b): Synthesised from **4.1b** (46 mg, 0.12 mmol, 1.0 equiv) and TMG (28 mg, 0.24 mmol, 2.0 equiv) using procedure **A or B** at MOC = 0.25 M with flow rate (**DAR**) = 333 μL/min and reactor temperature = 75 °C. Orange-red liquid (80 % from isolation of the corresponding benzoate **4.3b**).

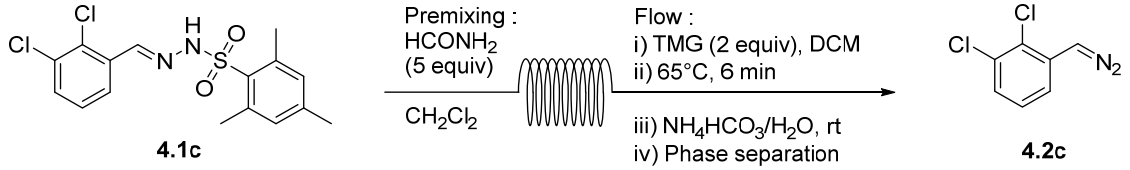

1,2-Dichloro-3-(diazomethyl)benzene (4.2c): Synthesised from **4.1c** (186 mg, 0.5 mmol, 1.0 equiv) and TMG (0.12 mL, 115 mg, 1.0 mmol, 2.0 equiv) using procedure **B** at MOC = 0.25 M with flow rate (**DAR**) = 333 μL/min and reactor temperature = 65 °C. Orange liquid (95 % from isolation of the corresponding benzoate **4.3c**).

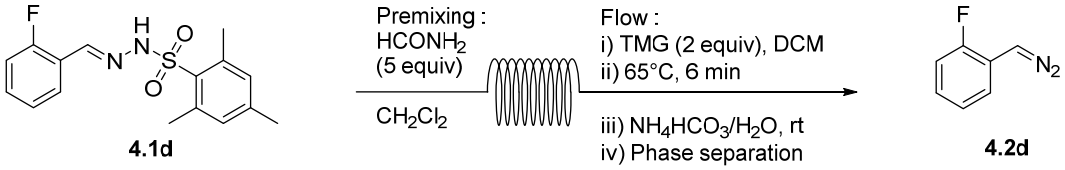

1-(Diazomethyl)-2-fluorobenzene (4.2d): Synthesised from **4.1d** (38 mg, 0.12 mmol, 1.0 equiv) and TMG (28 mg, 0.24 mmol, 2.0 equiv) using procedure **A** at MOC = 0.25 M with flow rate (**DAR**) = 333 □L/min and reactor temperature = 65 °C. Orange liquid (87 % from isolation of the corresponding benzoate **4.3d**).

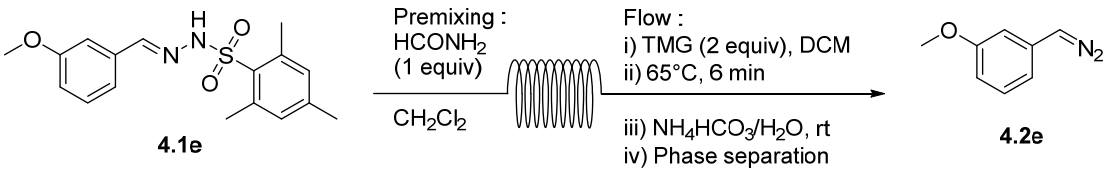

1-(Diazomethyl)-3-methoxybenzene (2e): Synthesised from **4.1e** (80 mg, 0.24 mmol, 1.0 equiv) and TMG (56 mg, 0.48 mmol, 2.0 equiv) using procedure **A or B** at MOC = 0.50 M with flow rate (**DAR**) = 333 µL/min and reactor temperature = 65 °C. Red liquid (71 % from isolation of the corresponding benzoate **4.3e**).

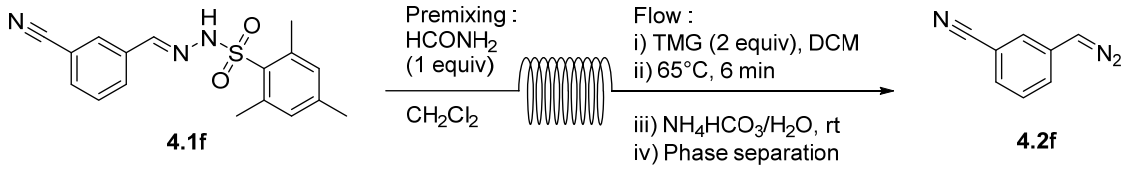

3-(Diazomethyl)benzonitrile (2f): Synthesised from **4.1f** (39 mg, 0.12 mmol, 1.0 equiv) and TMG (28 mg, 0.24 mmol, 2.0 equiv) using procedure **A** at at MOC = 0.25 M with flow rate (**DAR**) = 333 µL/min and reactor temperature = 65 °C. Red liquid (84 % from isolation of the corresponding benzoate **4.3f**).

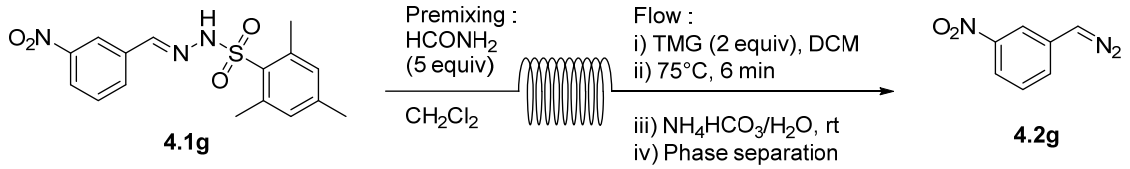

1-(Diazomethyl)-3-nitrobenzene (2g): Synthesised from **4.1g** (42 mg, 0.12 mmol, 1.0 equiv) and TMG (28 mg, 0.24 mmol, 2.0 equiv) using procedure **A or B** at MOC = 0.25 M with flow rate (**DAR**) = 333 µL/min and reactor temperature = 75 °C. Dark orange liquid (94 % from isolation of the corresponding benzoate **4.3g**).

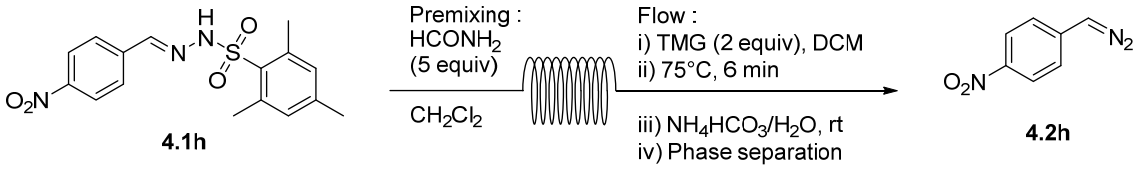

1-(Diazomethyl)-4-nitrobenzene (4.2h): Synthesised from **4.1h** (42 mg, 0.12 mmol, 1.0 equiv) and TMG (28 mg, 0.24 mmol, 2.0 equiv) using procedure **A** at MOC = 0.25 M with flow rate (**DAR**) = 333 µL/min and reactor temperature = 75 °C. Dark orange liquid (86 % from isolation of the corresponding benzoate **4.3h**).

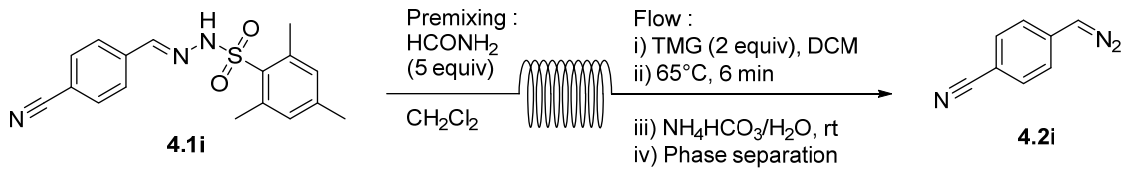

4-(Diazomethyl)benzonitrile (4.2i): Synthesised from **4.1i** (39 mg, 0.12 mmol, 1.0 equiv) and TMG (28 mg, 0.24 mmol, 2.0 equiv) using procedure **A or B** at MOC = 0.25 M with flow rate (**DAR**) = 333 µL/min and reactor temperature = 65 °C. Orange liquid (74 % from isolation of the corresponding benzoate **4.3i**).

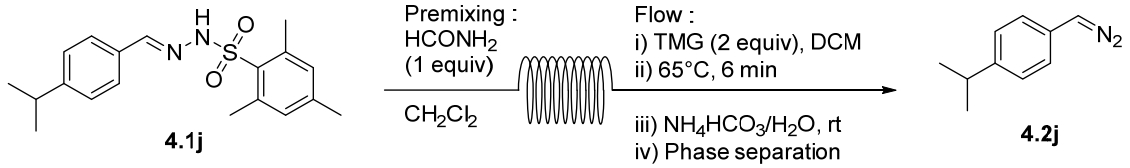

-(Diazomethyl)-4-isopropylbenzene (4.2j): Synthesised from **4.1j** (83 mg, 0.24 mmol, 1.0 equiv) and TMG (56 mg, 0.48 mmol, 2.0 equiv) using procedure **A** at MOC = 0.50 M with flow rate (**DAR**) = 333 µL/min and reactor temperature = 65 °C. Red liquid (57 % from isolation of the corresponding benzoate **4.3j**).

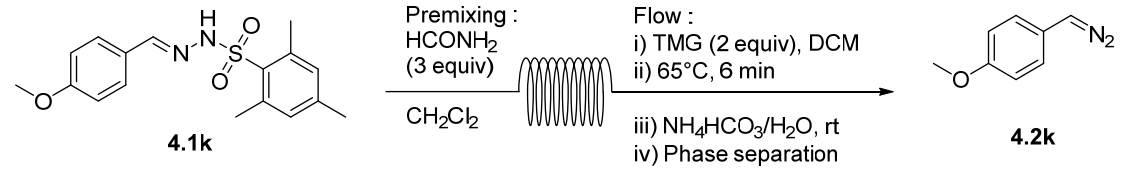

1-(Diazomethyl)-4-methoxybenzene (4.2k): Synthesised from **4.1k** (40 mg, 0.12 mmol, 1.0 equiv) and TMG (28 mg, 0.24 mmol, 2.0 equiv) using procedure **A** at MOC = 0.25 M with flow rate (**DAR**) = 333 µL/min and reactor temperature = 75 °C. Pink liquid (52 % from isolation of the corresponding benzoate **4.3k**).

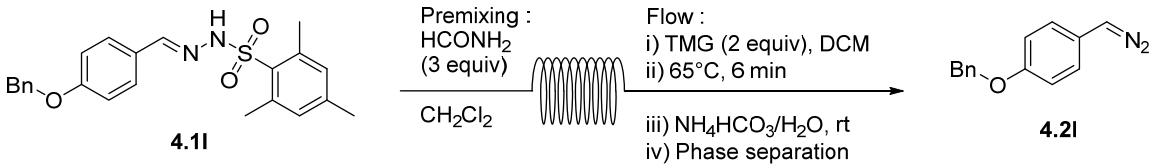

1-(Benzyloxy)-4-(diazomethyl)benzene (2l): Synthesised from **4.1l** (49 mg, 0.12 mmol, 1.0 equiv) and TMG (28 mg, 0.24 mmol, 2.0 equiv) using procedure **A or B** at MOC = 0.25 M with

flow rate (**DAR**) = 333 μL/min and reactor temperature = 65 °C. Burgundy liquid (72 % from isolation of the corresponding benzoate **4.3l**).

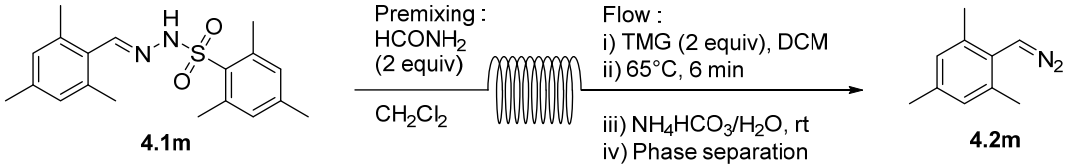

2-(Diazomethyl)-1,3,5-trimethylbenzene (4.2m): Synthesised from **4.1m** (41 mg, 0.12 mmol, 1.0 equiv) and TMG (28 mg, 0.24 mmol, 2.0 equiv) using procedure **A** at MOC = 0.25 M with flow rate (**DAR**) = 333 μL/min and reactor temperature = 65 °C. Red liquid (52 % from isolation of the corresponding benzoate **4.3m**).

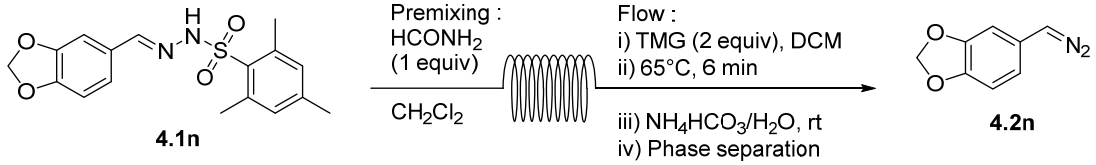

5-(Diazomethyl)benzo[d][1,3]dioxole (4.2n): Synthesised from **4.1n** (83 mg, 0.24 mmol, 1.0 equiv) and TMG (56 mg, 0.48 mmol, 2.0 equiv) using procedure **A** at MOC = 0.50 M with flow rate (**DAR**) = 333 μL/min and reactor temperature = 65 °C. Dark pink liquid (57 % from isolation of the corresponding benzoate **4.3n**).

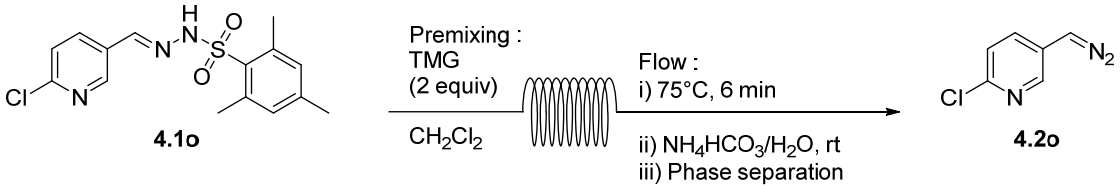

2-Chloro-5-(diazomethyl)pyridine (4.2o): Synthesised from **4.1o** (42 mg, 0.12 mmol, 1.0 equiv) and TMG (29 mg, 0.25 mmol, 2.0 equiv) using procedure **C** at MOC = 0.25 M with flow rate (**DAR**) = 333 μL/min and reactor temperature = 75 °C. orange liquid (71 % from isolation of the corresponding benzoate **4.3o**).

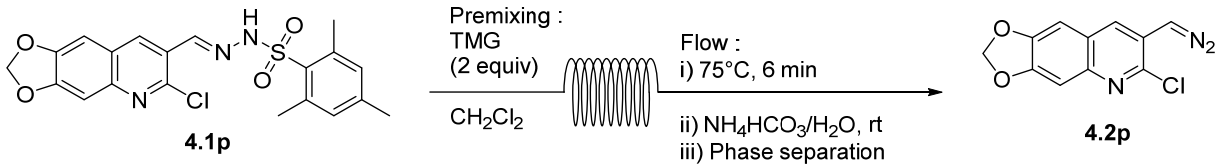

6-Chloro-7-(diazomethyl)-[1,3]dioxolo[4,5-*g*]quinoline (4.2p): Synthesised from **4.1p** (54 mg, 0.12 mmol, 1.0 equiv) and TMG (29 mg, 0.25 mmol, 2.0 equiv) using procedure **C** at MOC = 0.25 M with flow rate (**DAR**) = 333 µL/min and reactor temperature = 75 °C. orange-brown liquid (68 % from isolation of the corresponding benzoate **4.3p**).

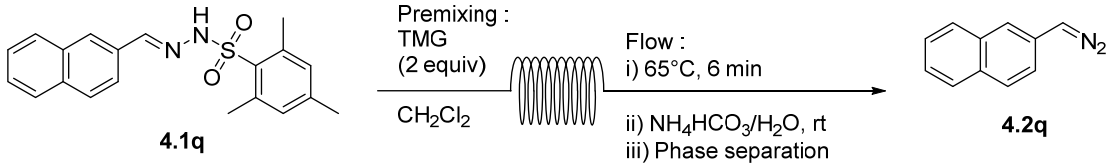

2-(Diazomethyl)naphthalene (4.2q): Synthesised from **4.1q** (44 mg, 0.12 mmol, 1.0 equiv) and TMG (29 mg, 0.25 mmol, 2.0 equiv) using procedure **C** at MOC = 0.25 M with flow rate (**DAR**) = 333 µL/min and reactor temperature = 65 °C. Red liquid (73% from isolation of the corresponding benzoate **4.3q**).

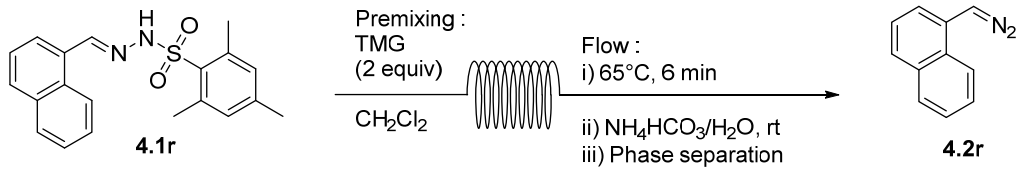

1-(Diazomethyl)naphthalene (4.2r): Synthesised from **4.1r** (44 mg, 0.12 mmol, 1.0 equiv) and TMG (29 mg, 0.25 mmol, 2.0 equiv) using procedure **C** at MOC = 0.25 M with flow rate (**DAR**) = 333 µL/min and reactor temperature = 65 °C. Red liquid (79 % from isolation of the corresponding benzoate **4.3r**).

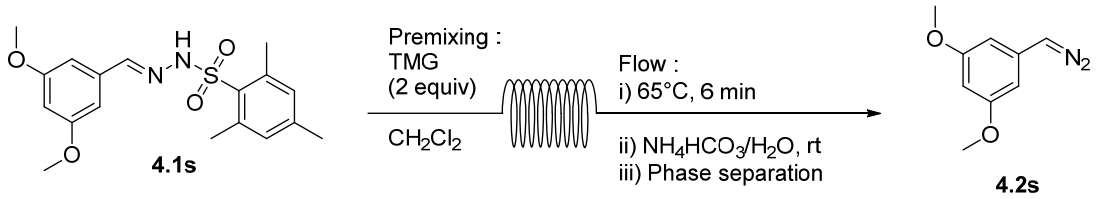

1-(Diazomethyl)-3,5-dimethoxybenzene (4.2s): Synthesised from **4.1s** (45 mg, 0.12 mmol, 1.0 equiv) and TMG (29 mg, 0.25 mmol, 2.0 equiv) using procedure **C** at MOC = 0.25 M with flow rate (**DAR**) = 333 µL/min and reactor temperature = 65 °C. Red liquid (85 % from isolation of the corresponding benzoate **4.3s**).

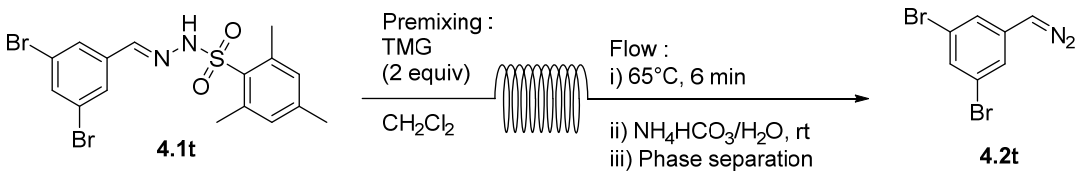

1,3-Dibromo-5-(diazomethyl)benzene (2t): Synthesised from **4.1t** (72 mg, 0.12 mmol, 1.0 equiv) and TMG (29 mg, 0.25 mmol, 2.0 equiv) using procedure **C** at MOC = 0.25 M with flow rate (**DAR**) = 333 μL/min and reactor temperature = 65 °C. Red liquid (67 % from isolation of the corresponding benzoate **4.3t**).

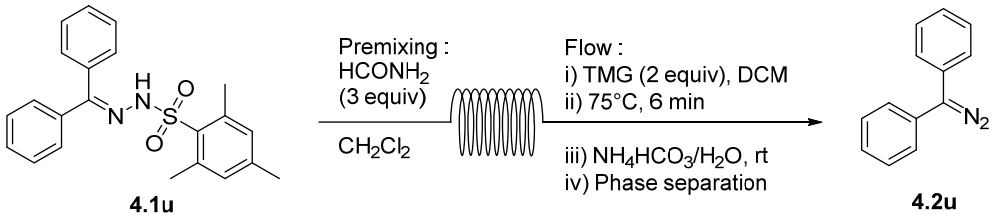

(Diazomethylene)dibenzene (4.2u): Synthesised from **4.1u** (45 mg, 0.12 mmol, 1.0 equiv) and TMG (28 mg, 0.24 mmol, 2.0 equiv) using procedure **A** at MOC = 0.25 M with flow rate (**DAR**) = 333 μL/min and reactor temperature = 75°C. Violet liquid (81 % from isolation of the corresponding benzoate **4.3u**).

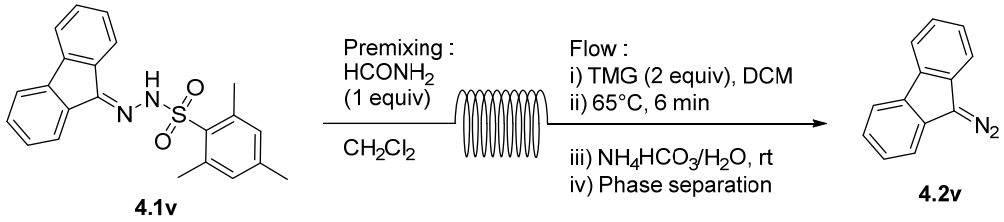

9-Diazo-9*H*-fluorene (4.2v): Synthesised from **4.1v** (94 mg, 0.25 mmol, 1.0 equiv) and TMG (58 mg, 0.50 mmol, 2.0 equiv) using procedure **C** at MOC = 0.25 M with flow rate (**DAR**) = 333 μL/min and reactor temperature = 75°C. Burgundy liquid (100 % from isolation of the corresponding benzoate **4.3v**).

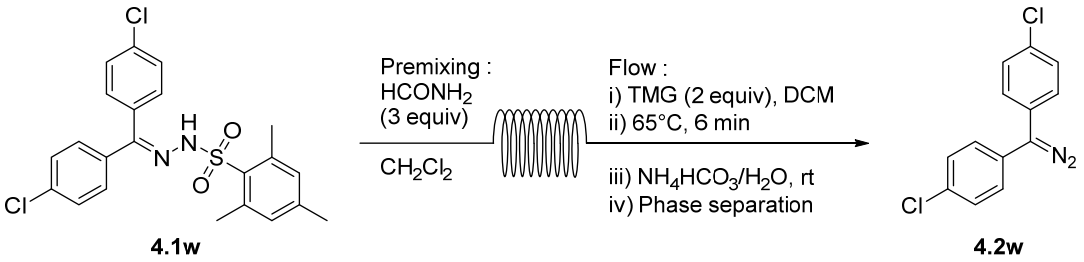

4,4'-(Diazomethylene)bis(chlorobenzene) (4.2w): Synthesised from **4.1w** (54 mg, 0.12 mmol, 1.0 equiv) and TMG (28 mg, 0.24 mmol, 2.0 equiv) using procedure **A** at MOC = 0.25 M with flow rate (**DAR**) = 333 μL/min and reactor temperature = 75 °C. Burgundy liquid (93 % from isolation of the corresponding benzoate **4.3w**.

A3.5.5.Ester synthesis (products 4.3a to 4.3w)

General procedure for diazo titration with benzoic acid: The diazo solution stream was dropped directly in a 20 mL vial containing a 1.0 M solution of benzoic acid (2 equiv in relation to hydrazine precursor) in CH_2Cl_2. Mixture was concentrated under vacuum and purified by flash chromatography.

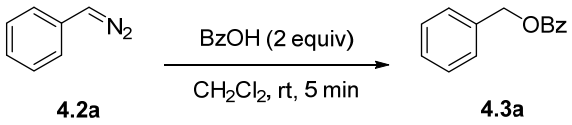

Benzyl benzoate (4.3a): Synthesised from **4.2a** (11 mg, 0.095 mmol, 1.0 equiv) and benzoic acid (29 mg, 0.24 mmol, 2.5 equiv) using **general procedure for diazo titration with benzoic acid**. Flash chromatography (20-70% CH_2Cl_2/Hexanes) yielded a clear oil (20 mg, 0.095 mmol, supposed 100%). ^{1}H-NMR ($CDCl_3$, 300 MHz): δ ppm 8.05 - 8.13 (m, 2 H), 7.57 (s, 1 H), 7.33 - 7.49 (m, 7 H), 5.37 (s, 2 H). Product corresponds to literature characterization data.[177]

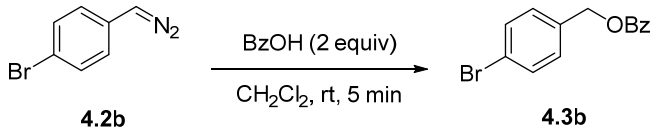

4-Bromobenzyl benzoate (4.3b): Synthesised from **4.2b** (19 mg, 0.096 mmol, 1.0 equiv) and benzoic acid (29 mg, 0.24 mmol, 2.5 equiv) using **general procedure for diazo titration with benzoic acid**. Flash chromatography (20-70% CH_2Cl_2/Hexanes) yielded a clear oil (28 mg, 0.096

mmol, supposed 100%). **^{1}H-NMR** ($CDCl_3$, 300 MHz): δ ppm 8.03 - 8.10 (m, 2 H), 7.54 - 7.60 (m, 1 H), 7.51 (dt, *J*=8.3, 2.0 Hz, 2 H), 7.40 - 7.48 (m, 2 H), 7.29 - 7.37 (m, 2 H), 5.31 (s, 1 H). Product corresponds to literature characterization data.[120 a]

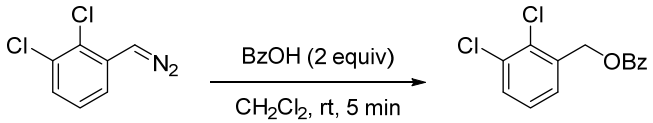

4.2c **4.3c**

2,3-Dichlorobenzyl benzoate (4.3c): Synthesised from **4.2c** (187 mg, 0.48 mmol, 1.0 equiv) and benzoic acid (122 mg, 1.0 mmol, 2.1 equiv) using **general procedure for diazo titration with benzoic acid**. Flash chromatography (20-70% CH_2Cl_2/Hexanes) yielded a clear oil (134 mg, 0.48 mmol, supposed 100%). **^{1}H-NMR** ($CDCl_3$, 300 MHz): δ ppm 8.06 - 8.13 (m, 2 H), 7.53 - 7.62 (m, 1 H), 7.39 - 7.51 (m, 3 H), 7.24 (t, *J*=7.8 Hz, 1 H), 5.48 (s, 2 H). Product corresponds to literature characterization data.[178]

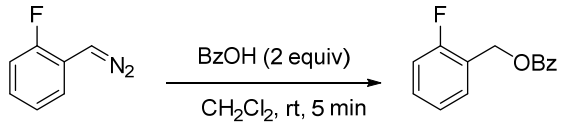

4.2d **4.3d**

2-Fluorobenzyl benzoate (4.3d): Synthesised from **4.2d** (14 mg, 0.10 mmol, 1.0 equiv) and benzoic acid (29 mg, 0.24 mmol, 2.4 equiv) using **general procedure for diazo titration with benzoic acid**. Flash chromatography (20-70% CH_2Cl_2/Hexanes) yielded a clear oil (24 mg, 0.10 mmol, supposed 100%). **^{1}H-NMR** ($CDCl_3$, 300 MHz): δ ppm 8.03 - 8.12 (m, 2 H), 7.57 (s, 1 H), 7.40 - 7.52 (m, 3 H), 7.34 (tdd, *J*=8.0, 8.0, 5.5, 2.0 Hz, 1 H), 7.16 (td, *J*=7.5, 1.0 Hz, 1 H), 7.10 (ddd, *J*=10.0, 8.5, 1.0 Hz, 1 H), 5.44 (s, 2 H). Product corresponds to literature characterization data.[179]

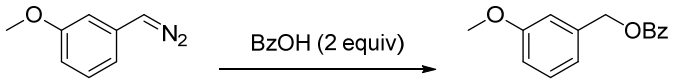

4.2e **4.3e**

3-Methoxybenzyl benzoate (4.3e): Synthesised from **4.2e** (25 mg, 0.17 mmol, 1.0 equiv) and benzoic acid (58 mg, 0.48 mmol, 2.8 equiv) using **general procedure for diazo titration with benzoic acid**. Flash chromatography (20-70% CH_2Cl_2/Hexanes) yielded a clear oil (41 mg, 0.17 mmol, supposed 100%). **^{1}H-NMR** ($CDCl_3$, 300 MHz): δ ppm 8.04 - 8.14 (m, 2 H), 7.51 - 7.60 (m,

1 H), 7.40 - 7.51 (m, 2 H), 7.31 (t, *J*=7.9 Hz, 1 H), 6.95 - 7.08 (m, 2 H), 6.89 (dd, *J*=8.4, 2.0 Hz, 1 H), 5.35 (s, 2 H), 3.83 (s, 3 H). Product corresponds to literature characterization data.[180]

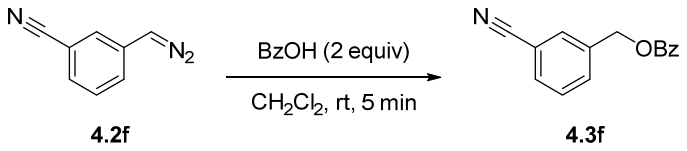

4.2f **4.3f**

3-Cyanobenzyl benzoate (4.3f): Synthesised from **4.2f** (14 mg, 0.10 mmol, 1.0 equiv) and benzoic acid (29 mg, 0.24 mmol, 2.4 equiv) using **general procedure for diazo titration with benzoic acid**. Flash chromatography (20-70% CH_2Cl_2/Hexanes) yielded a white solid (24 mg, 0.10 mmol, supposed 100%). **mp**: 39-41 °C, lit. 45 °C[181]; **^{1}H-NMR** ($CDCl_3$, 300 MHz): δ ppm 8.05 - 8.11 (m, 2 H), 7.76 (s, 1 H), 7.56 - 7.71 (m, 3 H), 7.44 - 7.55 (m, 3 H), 5.39 (s, 2 H). Product corresponds to literature characterization data.[181]

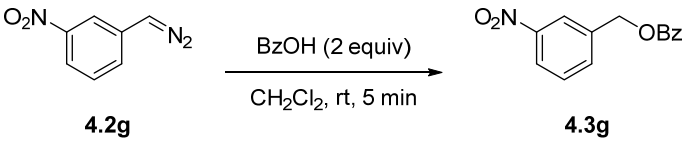

4.2g **4.3g**

3-Nitrobenzyl benzoate (4.3g): Synthesised from **4.2g** (18 mg, 0.11 mmol, 1.0 equiv) and benzoic acid (29 mg, 0.24 mmol, 2.2 equiv) using **general procedure for diazo titration with benzoic acid**. Flash chromatography (20-70% CH_2Cl_2/Hexanes) yielded a white solid (28 mg, 0.11 mmol, supposed 100%). **mp**: 63-65 °C, lit. 71 °C[181]; **^{1}H-NMR** ($CDCl_3$, 300 MHz): δ ppm 8.33 (t, *J*=1.7 Hz, 1 H), 8.16 - 8.26 (m, 1 H), 8.06 - 8.12 (m, 2 H), 7.79 (d, *J*=7.6 Hz, 1 H), 7.52 - 7.69 (m, 2 H), 7.43 - 7.52 (m, 2 H), 5.46 (s, 2 H). Product corresponds to literature characterization data.[179]

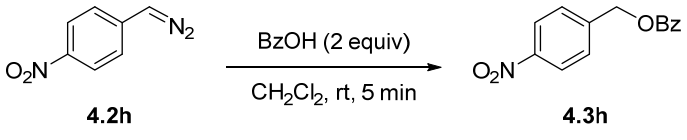

4.2h **4.3h**

4-Nitrobenzyl benzoate (4.3h): Synthesised from **4.2h** (17 mg, 0.10 mmol, 1.0 equiv) and benzoic acid (29 mg, 0.24 mmol, 2.4 equiv) using **general procedure for diazo titration with benzoic acid**. Flash chromatography (20-70% CH_2Cl_2/Hexanes) yielded a white solid (26 mg, 0.10 mmol, supposed 100%). **mp:** 84-85 °C, lit. 88-89 °C[182]; **^{1}H-NMR** ($CDCl_3$, 300 MHz): δ ppm 8.26 (ddd, *J*=9.0, 2.3, 1.8 Hz, 2 H), 8.06 - 8.13 (m, 2 H), 7.55 - 7.67 (m, 3 H), 7.42 - 7.52 (m, 2 H), 5.47 (s, 2 H). Product corresponds to literature characterization data.[182]

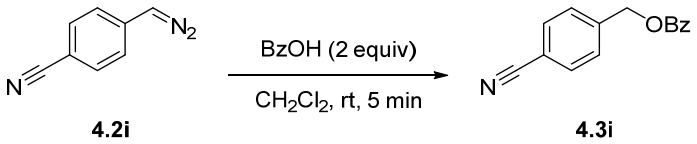

4.2i **4.3i**

4-Cyanobenzyl benzoate (4.3i): Synthesised from **4.2i** (13 mg, 0.089 mmol, 1.0 equiv) and benzoic acid (29 mg, 0.24 mmol, 2.7 equiv) using **general procedure for diazo titration with benzoic acid**. Flash chromatography (20-70% CH_2Cl_2/Hexanes) yielded a white solid (21 mg, 0.089 mmol, supposed 100%). **mp**: 47-49 °C, lit. 64-65 °C[181]; **^{1}H-NMR** ($CDCl_3$, 300 MHz): δ ppm 8.04 - 8.12 (m, 2 H), 7.64 - 7.72 (m, 2 H), 7.51 - 7.64 (m, 3 H), 7.43 - 7.51 (m, 2 H), 5.41 (s, 2 H). Product corresponds to literature characterization data.[181]

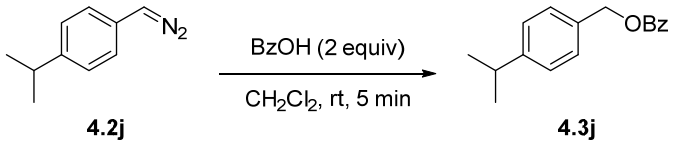

4.2j **4.3j**

4-Isopropylbenzyl benzoate (4.3j): Synthesised from **4.2j** (22 mg, 0.14 mmol, 1.0 equiv) and benzoic acid (58 mg, 0.48 mmol, 3.4 equiv) using **general procedure for diazo titration with benzoic acid**. Flash chromatography (20-70% CH_2Cl_2/Hexanes) yielded a clear oil (35 mg, 0.14 mmol, supposed 100%). ^{1}H-NMR ($CDCl_3$, 300 MHz): δ ppm 8.04 - 8.12 (m, 2 H), 7.49 - 7.61 (m, 1 H), 7.36 - 7.47 (m, 4 H), 7.22 - 7.28 (m, 2 H), 5.34 (s, 2 H), 2.93 (spt, *J*=6.9 Hz, 1 H), 1.26 (d, *J*=6.9 Hz, 6 H). Product corresponds to literature characterization data.[179]

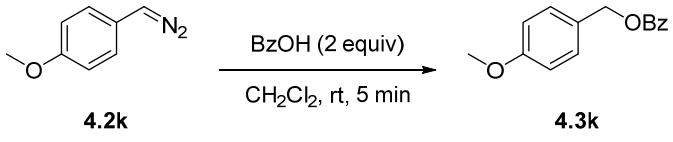

4.2k **4.3k**

4-Methoxybenzyl benzoate (4.3k): Synthesised from **4.2k** (9.2 mg, 0.062 mmol, 1.0 equiv) and benzoic acid (29 mg, 0.24 mmol, 3.9 equiv) using **general procedure for diazo titration with benzoic acid**. Flash chromatography (20-70% CH_2Cl_2/Hexanes) yielded a clear oil (15 mg, 0.062 mmol, supposed 100%). **^{1}H-NMR** ($CDCl_3$, 300 MHz): δ ppm 8.03 - 8.09 (m, 2 H), 7.51 - 7.58 (m, 1 H), 7.36 - 7.47 (m, 4 H), 6.92 (ddd, *J*=9.0, 2.7, 2.2 Hz, 2 H), 5.30 (s, 2 H), 3.82 (s, 3 H). Product corresponds to literature characterization data.[183]

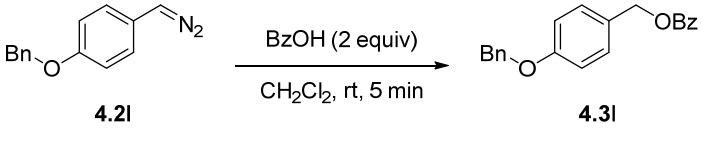

4.2l **4.3l**

4-(Benzyloxy)benzyl benzoate (4.3l): Synthesised from **4.2l** (19 mg, 0.086 mmol, 1.0 equiv) and benzoic acid (29 mg, 0.24 mmol, 2.8 equiv) using **general procedure for diazo titration with benzoic acid**. Flash chromatography (20-70% CH_2Cl_2/Hexanes) yielded a clear oil (27 mg, 0.086 mmol, supposed 100%). **mp**: 69-70 °C; **^{1}H-NMR** ($CDCl_3$, 400 MHz): δ ppm 8.06 (d, *J*=8.1 Hz, 2 H), 7.55 (t, *J*=7.6 Hz, 1 H), 7.43 (t, *J*=7.6 Hz, 4 H), 7.36 - 7.41 (m, 4 H), 7.31 - 7.36 (m, 1 H), 6.99 (d, *J*=8.5 Hz, 2 H), 5.30 (s, 2 H), 5.08 (s, 2 H). **^{13}C-NMR** ($CDCl_3$, 75 MHz): □ ppm 166.64 (C), 158.99 (C), 136.99 (C), 133.08 (CH), 130.39 (C), 130.19 (2 CH), 129.81 (2 CH), 128.75 (2 CH), 128.60 (C), 128.47 (2 CH), 128.15 (CH), 127.59 (2 CH), 115.05 (2 CH), 70.18 (CH_2), 66.64 (CH_2); **FTIR** (cm^{-1}) (neat): 2960 (w), 1711 (s), 1610 (w), 1513 (m), 1452 (w), 1270 (s), 1242 (s), 1098 (m), 1013 (m), 713 (m); **HRMS** (ESI, Pos): calcd for $C_{21}H_{18}O_3Na$ $[M+Na]^+$: m/z, 341.11482 found: 341.11622 m/z.

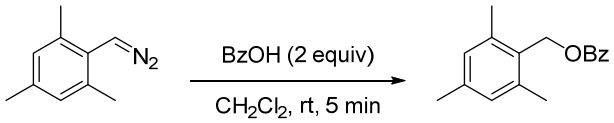

4.2m **4.3m**

2,4,6-Trimethylbenzyl benzoate (4.3m): Synthesised from **4.2m** (10 mg, 0.062 mmol, 1.0 equiv) and benzoic acid (29 mg, 0.24 mmol, 3.9 equiv) using **general procedure for diazo titration with benzoic acid**. Flash chromatography (20-70% CH_2Cl_2/Hexanes) yielded a clear oil (16 mg, 0.062 mmol, supposed 100%). **^{1}H-NMR** ($CDCl_3$, 300 MHz): δ ppm 7.94 - 8.10 (m, 2 H), 7.47 - 7.61 (m, 1 H), 7.34 - 7.45 (m, 2 H), 6.91 (s, 2 H), 5.41 (s, 2 H), 2.41 (s, 6 H), 2.30 (s, 3 H). Product corresponds to literature characterization data.[184]

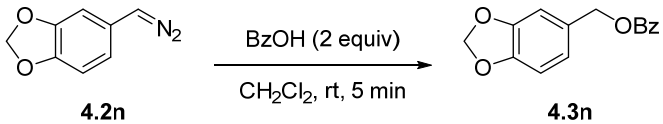

4.2n **4.3n**

Benzo[*d*][1,3]dioxol-5-ylmethyl benzoate (4.3n): Synthesised from **4.2n** (22 mg, 0.14 mmol, 1.0 equiv) and benzoic acid (29 mg, 0.24 mmol, 3.4 equiv) using **general procedure for diazo titration with benzoic acid**. Flash chromatography (20-70% CH_2Cl_2/Hexanes) yielded a white solid (36 mg, 0.14 mmol, supposed 100%). **mp**: 61-63 °C, lit. 63-64 °C[185] **^{1}H-NMR** ($CDCl_3$, 300 MHz): δ ppm 8.01 - 8.12 (m, 2 H), 7.56 (t, *J*=7.4 Hz, 1 H), 7.43 (t, *J*=7.5 Hz, 2 H), 6.88 - 6.99 (m, 2 H), 6.81 (d, *J*=7.4 Hz, 1 H), 5.97 (s, 2 H), 5.26 (s, 2 H). Product corresponds to literature characterization data.[185]

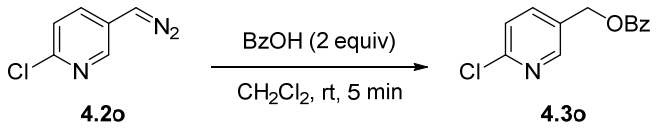

4.2o **4.3o**

(6-Chloropyridin-3-yl)methyl benzoate (4.3o): Synthesised from **4.2o** (14 mg, 0.089 mmol, 1.0 equiv) and benzoic acid (31 mg, 0.25 mmol, 2.8 equiv) using **general procedure for diazo titration with benzoic acid**. Flash chromatography (20-100% CH_2Cl_2/Hexanes) yielded a clear oil (22 mg, 0.089 mmol, supposed 100%). **mp:** 57-59 °C; **^{1}H-NMR** ($CDCl_3$, 300 MHz): δ ppm 8.50 (d, *J*=2.0 Hz, 1 H), 8.00 - 8.08 (m, 2 H), 7.76 (dd, *J*=8.2, 2.5 Hz, 1 H), 7.53 - 7.61 (m, 1 H), 7.39 - 7.49 (m, 2 H), 7.35 (d, *J*=8.2 Hz, 1 H), 5.35 (s, 2 H); **^{13}C-NMR** ($CDCl_3$, 125 MHz): δ ppm 166.32 (C), 151.68 (C), 149.77 (CH), 139.04 (CH), 133.56 (CH), 130.82 (C), 129.86 (2 CH), 129.64 (C), 128.67 (2 CH), 124.46 (CH), 63.41 (CH_2); **FTIR** (cm^{-1}) (neat): 1710 (s), 1460 (m), 1296 (m), 1100 (w), 710 (m); **HRMS** (APCI, Pos): calcd for $C_{13}H_{11}ClNO_2$ $[M+H]^+$: 248.04728 m/z, found: 248.04682 m/z.

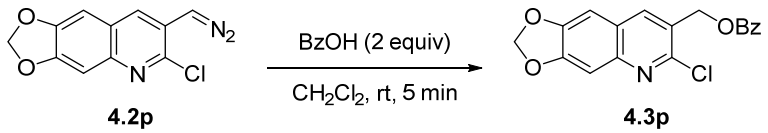

4.2p **4.3p**

(6-Chloro-[1,3]dioxolo[4,5-*g*]quinolin-7-yl)methyl benzoate (4.3p): Synthesised from **4.2p** (21 mg, 0.085 mmol, 1.0 equiv) and benzoic acid (31 mg, 0.25 mmol, 2.9 equiv) using **general procedure for diazo titration with benzoic acid**. Flash chromatography (20-100% CH_2Cl_2/Hexanes) yielded a white solid (29 mg, 0.085 mmol, supposed 100%). **mp**: 161-162 °C; **^{1}H-NMR** ($CDCl_3$, 300 MHz): δ ppm 8.07 - 8.14 (m, 3 H), 7.53 - 7.63 (m, 1 H), 7.44 - 7.51 (m, 2 H), 7.32 (s, 1 H), 7.07 (s, 1 H), 6.13 (s, 2 H), 5.55 (d, *J*=0.8 Hz, 2 H); **^{13}C-NMR** ($CDCl_3$, 75 MHz): δ ppm 166.34 (C), 151.92 (C), 148.65 (C), 147.91 (C), 145.94 (C), 137.36 (CH), 133.48 (CH), 129.94 (2 CH), 129.85 (C), 128.65 (2 CH), 125.95 (CH), 124.23 (CH), 105.26 (C), 102.87 (CH_2), 102.26 (C), 63.72 (CH_2); **FTIR** (cm^{-1}) (neat): 1711 (s), 1479 (m), 1289 (s), 1229 (s), 1117 (m), 1028 (m), 925 (m), 706 (s); **HRMS** (ESI, Pos): calcd for $C_{18}H_{12}ClNO_4$ $[M+H]^+$: 342.05276 m/z, found: 342.05412 m/z.

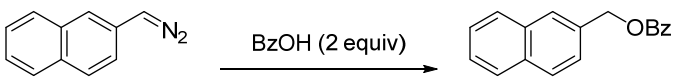

4.2q **4.3q**

Naphthalen-2-ylmethyl benzoate (4.3q): Synthesised from **4.2q** (15 mg, 0.091 mmol, 1.0 equiv) and benzoic acid (31 mg, 0.25 mmol, 2.7 equiv) using **general procedure for diazo titration with benzoic acid**. Flash chromatography (20-70% CH_2Cl_2/Hexanes) yielded a clear oil (24 mg, 0.091 mmol, supposed 100%). **^{1}H-NMR** ($CDCl_3$, 300 MHz): δ ppm 8.05 - 8.16 (m, 2 H), 7.92 (s, 1 H), 7.81 - 7.91 (m, 3 H), 7.41 - 7.60 (m, 6 H), 5.53 (s, 2 H). Product corresponds to literature characterization data.[186]

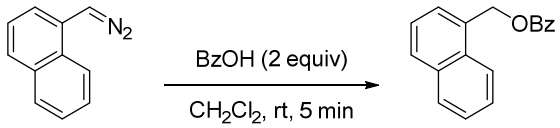

4.2r **4.3r**

Naphthalen-1-ylmethyl benzoate (4.3r): Synthesised from **4.2r** (17 mg, 0.099 mmol, 1.0 equiv) and benzoic acid (31 mg, 0.25 mmol, 2.5 equiv) using **general procedure for diazo titration with benzoic acid**. Flash chromatography (20-70% CH_2Cl_2/Hexanes) yielded a clear oil (26 mg, 0.099 mmol, supposed 100%). **^{1}H-NMR** ($CDCl_3$, 300 MHz): δ ppm 8.10 - 8.15 (m, 1 H), 8.03 - 8.10 (m, 2 H), 7.83 - 7.96 (m, 2 H), 7.65 (d, *J*=6.1 Hz, 1 H), 7.47 - 7.62 (m, 4 H), 7.38 - 7.47 (m, 2 H), 5.83 (s, 2 H). Product corresponds to literature characterization data.[187]

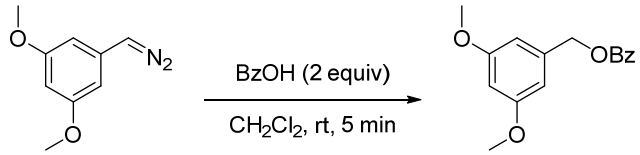

4.2s **4.3s**

3,5-Dimethoxybenzyl benzoate (4.3s): Synthesised from **4.2s** (19 mg, 0.11 mmol, 1.0 equiv) and benzoic acid (31 mg, 0.25 mmol, 2.3 equiv) using **general procedure for diazo titration with benzoic acid**. Flash chromatography (20-70% CH_2Cl_2/Hexanes) yielded a clear oil (30 mg, 0.11 mmol, supposed 100%). **^{1}H-NMR** ($CDCl_3$, 300 MHz): δ ppm 8.04 - 8.13 (m, 2 H), 7.50 - 7.62 (m, 1 H), 7.44 (t, *J*=7.5 Hz, 2 H), 6.59 (d, *J*=2.3 Hz, 2 H), 6.44 (t, *J*=2.2 Hz, 1 H), 5.30 (s, 2 H), 3.81 (s, 6 H). Product corresponds to literature characterization data.[183]

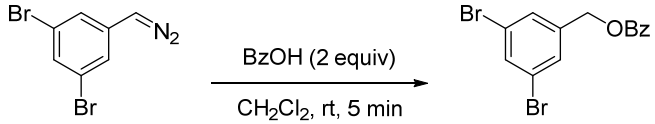

4.2t **4.3t**

3,5-Dibromobenzyl benzoate (4.3t): Synthesised from **4.2t** (23 mg, 0.084 mmol, 1.0 equiv) and benzoic acid (31 mg, 0.25 mmol, 3.0 equiv) using **general procedure for diazo titration with benzoic acid**. Flash chromatography (20-70% CH_2Cl_2/Hexanes) yielded a clear oil (31 mg, 0.084 mmol, supposed 100%). **mp**: 58-60 °C. **^{1}H-NMR** ($CDCl_3$, 300 MHz): δ ppm 8.04 - 8.11 (m, 2 H), 7.64 (t, *J*=1.7 Hz, 1 H), 7.55 - 7.63 (m, 1 H), 7.51 - 7.55 (m, 2 H), 7.41 - 7.51 (m, 2 H), 5.29 (s, 2 H); **^{13}C NMR** ($CDCl_3$, 75 MHz) δ ppm 166.24 (C), 140.04 (C), 134.03 (CH), 133.52 (CH), 129.91 (2 CH), 129.87 (2 CH), 129.69 (C), 128.66 (2 CH), 123.27 (2 C), 65.01 (CH_2); **FTIR** (cm^{-1}) (neat): 3069 (w), 1715 (s), 1557 (w), 1277 (s), 1117 (s), 848 (m), 706 (s); **HRMS** (ESI, Pos): calcd for $C_{14}H_{11}Br_2O_2$ $[M+H]^+$: 368.91203 m/z, found: 368.91186 m/z.

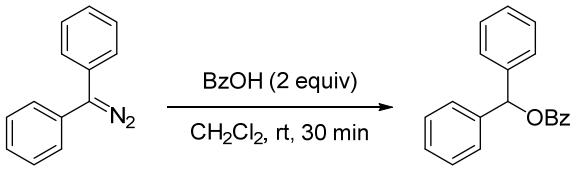

4.2u **4.3u**

Benzhydryl benzoate (4.3u): Synthesised from **4.2u** (19 mg, 0.097 mmol, 1.0 equiv) and benzoic acid (29 mg, 0.24 mmol, 2.5 equiv) using **general procedure for diazo titration with benzoic acid**. Flash chromatography (20-70% CH_2Cl_2/Hexanes) yielded a clear oil (29 mg, 0.097 mmol, supposed 100%). **mp**: 83-84 °C, lit. 85-86 °C[188] **^{1}H-NMR** ($CDCl_3$, 300 MHz): δ ppm 8.12 - 8.18 (m, 2 H), 7.54 - 7.62 (m, 1 H), 7.40 - 7.49 (m, 6 H), 7.28 - 7.40 (m, 6 H), 7.10 - 7.15 (m, 1 H). Product corresponds to literature characterization data.[188]

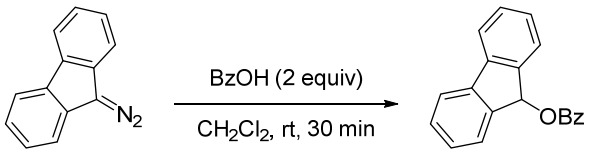

4.2v **4.3v**

9*H*-Fluoren-9-yl benzoate (4.3v): Synthesised from **4.2v** (48 mg, 0.25 mmol, 1.0 equiv) and benzoic acid (62 mg, 0.50 mmol, 2.0 equiv) using **general procedure for diazo titration with benzoic acid**. Flash chromatography (20-70% CH_2Cl_2/Hexanes) yielded a white solid (72 mg, 0.25 mmol, supposed 100%). **mp**: 90-92 °C; **^{1}H-NMR** ($CDCl_3$, 300 MHz): δ ppm 8.12 - 8.20 (m, 2 H), 7.76 (d, *J*=7.6 Hz, 2 H), 7.70 (d, *J*=7.5 Hz, 2 H), 7.57 - 7.65 (m, 1 H), 7.44 - 7.54 (m, 4 H), 7.32 - 7.41 (m, 2 H), 7.11 (s, 1 H); **^{13}C-NMR** ($CDCl_3$, 100 MHz): δ 167.44 (C), 142.29 (2 C), 141.23 (2 C),

133.32 (CH), 130.11 (C), 130.05 (2 CH), 129.63 (2 CH), 128.51 (2 CH), 128.00 (2 CH), 126.18 (2 CH), 120.18 (2 CH), 75.73 (CH); **FTIR** (cm^{-1}) (neat): 3067 (w), 1713 (s), 1449 (m), 1257 (s), 1092 (s), 740 (m), 704 (s); **HRMS** (ESI, Pos): calcd for $C_{20}H_{14}O_2Na$ $[M+Na]^+$: 309.0886 m/z, found: 309.08873 m/z.

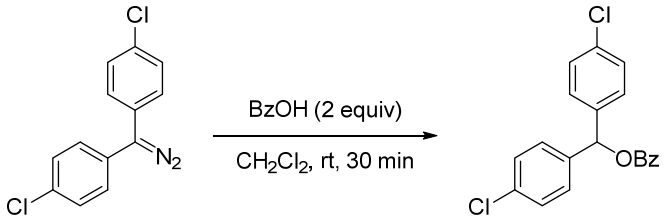

4.2w **4.3w**

Bis(4-chlorophenyl)methyl benzoate (4.3w): Synthesised from **4.2w** (29 mg, 0.11 mmol, 1.0 equiv) and benzoic acid (29 mg, 0.24 mmol, 2.2 equiv) using **general procedure for diazo titration with benzoic acid**. Flash chromatography (20-70% CH_2Cl_2/Hexanes) yielded a clear oil (39 mg, 0.11 mmol, supposed 100%). **^{1}H-NMR** ($CDCl_3$, 300 MHz): δ ppm 8.08 - 8.14 (m, 2 H), 7.55 - 7.64 (m, 1 H), 7.43 - 7.51 (m, 2 H), 7.34 (s, 8 H), 7.04 (s, 1 H); **^{13}C-NMR** ($CDCl_3$, 125 MHz): δ ppm 165.49 (C), 138.45 (2 C), 134.24 (CH), 133.55 (2 C), 131.45 (C), 129.89 (2 CH), 129.01 (4 CH), 128.68 (2 CH), 128.62 (4 CH), 76.16 (CH); **FTIR** (cm^{-1}) (neat): 3063 (br w), 1718 (s), 1490 (m), 1261 (s), 1087 (s), 1014 (m), 790 (m), 707 (s), 523 (m); **HRMS** (ESI, Pos): calcd for $C_{20}H_{14}Cl_2O_2Na$ $[M+Na]^+$: 379.02631 m/z, found: 379.02635 m/z.

A3.5.6.Cyclooctenone synthesis (products 4.4a to 4.4d)

General procedure for cyclic ketone ring expansion (modified literature procedure[137]): The diazo solution (1.0 mL, 0.35 M, 1.5 equiv, 333 µL/min) stream was run through a drying column and dropped directly under N_2 in a dry 4mL vial containing cycloheptanone (1.0 equiv) and $Sc(OTf)_3$ (0.10 equiv) at 0°C. Mixture was agitated at 0°C until diazo color has vanished. Saturated $NaHCO_3$ was added and phases were separated. Aqueous phase was extracted with CH_2Cl_2 (2x). Combined organic phases were dried over $MgSO_4$ and concentrated under vacuum. Mixture was purified by flash chromatography.

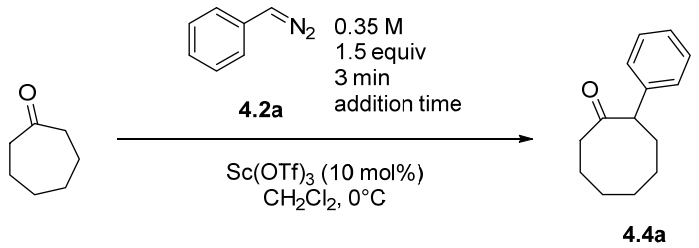

2-Phenylcyclooctan-1-one (4.4a): Synthesised from **4.2a** (41 mg, 0.35 mmol, 1.5 equiv (1.0 mL at MOC = 0.50 M, 70% expected yield)), cycloheptanone (26 mg, 0.23 mmol, 1.0 equiv) and $Sc(OTf)_3$ (9 mg, 0.018 mmol, 0.10 equiv) using **general procedure for cyclic ketone ring expansion**. Flash chromatography (0-20% Et_2O/Hexanes) yielded a clear oil (41 mg, 0.20 mmol. 87%). **^{1}H-NMR** ($CDCl_3$, 300 MHz): δ ppm 7.17 - 7.40 (m, 5 H), 3.79 (dd, *J*=12.3, 3.6 Hz, 1 H), 2.62 (ddd, *J*=13.0, 11.5, 5.0 Hz, 1 H), 2.36 (tdd, *J*=13.3, 11.5, 3.6 Hz, 1 H), 2.26 (ddd, *J*=13.0, 6.0, 3.9 Hz, 1 H), 1.84 - 2.03 (m, 3 H), 1.69 - 1.84 (m, 2 H), 1.37 - 1.65 (m, 4 H). Product corresponds to literature characterization data.[137]

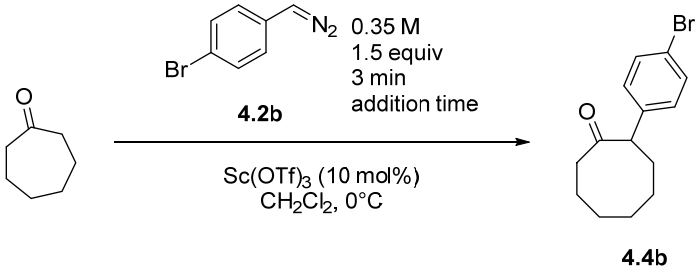

2-(4-Bromophenyl)cyclooctan-1-one (4.4b): Synthesised from **4.2b** (69 mg, 0.35 mmol, 1.5 equiv (1.0 mL at MOC = 0.50 M, 70% expected yield)), cycloheptanone (26 mg, 0.23 mmol, 1.0 equiv) and $Sc(OTf)_3$ (9 mg, 0.018 mmol, 0.10 equiv) using **general procedure for cyclic ketone ring expansion**. Flash chromatography (0-15% Et_2O/Hexanes) yielded a white solid (56 mg, 0.20 mmol, 85%). **mp**: 53-55 °C; **^{1}H-NMR** ($CDCl_3$, 400 MHz): δ ppm 7.43 (ddd, *J*=8.6, 2.2, 1.8 Hz, 2 H), 7.21 (ddd, *J*=8.6, 2.2, 1.9 Hz, 2 H), 3.78 (dd, *J*=12.2, 2.9 Hz, 1 H), 2.55 (td, *J*=12.5, 4.4 Hz, 1 H), 2.29 (ddd, *J*=13.0, 6.5, 2.9 Hz, 1 H), 2.25 (ddd, *J*=13.8, 12.2, 4.4 Hz, 1 H), 1.85 - 2.04 (m, 3 H), 1.69 - 1.81 (m, 2 H), 1.41 - 1.62 (m, 4 H); **^{13}C-NMR** ($CDCl_3$, 75 MHz): δ ppm 216.06 (C), 138.59 (C), 131.70 (2 CH), 129.72 (2 CH), 121.15 (C), 56.54 (CH), 40.90 (CH_2), 32.41 (CH_2), 27.07 (CH_2), 26.56 (CH_2), 26.50 (CH_2), 24.73 (CH_2); **FTIR** (cm^{-1}) (neat): 2927 (s br), 2855 (w), 1698 (s), 1487 (m), 1073 (w), 1010 (m), 821 (m), 523 (m); **HRMS** (ESI, Pos): calcd for $C_{14}H_{18}BrO$ $[M+H]^+$: 281.05355 m/z, found: 281.05254 m/z.

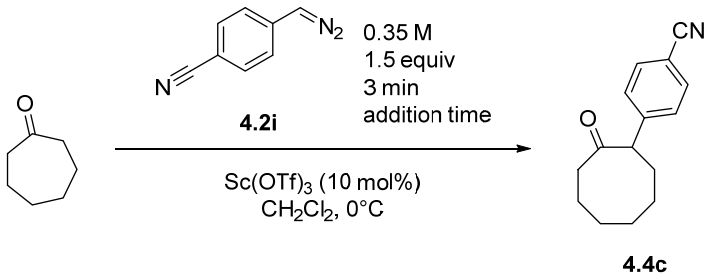

4.4c

4-(2-Oxocyclooctyl)benzonitrile (4.4c): Synthesised from **4.2i** (50 mg, 0.35 mmol, 1.5 equiv (1.0 mL at MOC = 0.50 M, 70% expected yield)), cycloheptanone (26 mg, 0.23 mmol, 1.0 equiv) and $Sc(OTf)_3$ (9 mg, 0.018 mmol, 0.10 equiv) using **general procedure for cyclic ketone ring expansion**. Flash chromatography (0-20% Et_2O/Hexanes) yielded a clear oil (50 mg, 0.22 mmol, 94%). **^{1}H-NMR** ($CDCl_3$, 400 MHz): δ ppm 7.59 (d, *J*=8.3 Hz, 2 H), 7.45 (d, *J*=8.2 Hz, 2 H), 3.93 (dd, *J*=12.0, 2.9 Hz, 1 H), 2.52 (td, *J*=12.8, 3.5 Hz, 1 H), 2.36 (ddd, *J*=13.4, 6.3, 3.5 Hz, 1 H), 2.23 (dddd, *J*=13.8, 12.0, 11.5, 4.0 Hz, 1 H), 1.87 - 2.10 (m, 3 H), 1.68 - 1.84 (m, 2 H), 1.42 - 1.62 (m, 4 H); **^{13}C-NMR** ($CDCl_3$, 125 MHz): δ ppm 215.26 (C), 145.10 (C), 132.34 (2 CH), 128.96 (2 CH), 118.93 (C), 111.02 (C), 56.65 (CH), 41.81 (CH_2), 33.43 (CH_2), 27.33 (CH_2), 26.23 (CH_2), 25.82 (CH_2), 24.70 (CH_2); **FTIR** (cm^{-1}) (neat): 2929 (s br), 2857 (w), 2227 (m), 1701 (s), 837 (m), 558 (m); **HRMS** (ESI, Pos): calcd for $C_{15}H_{21}N_2O$ $[M+NH_4]^+$: 245.16484 m/z, found: 245.16489 m/z.

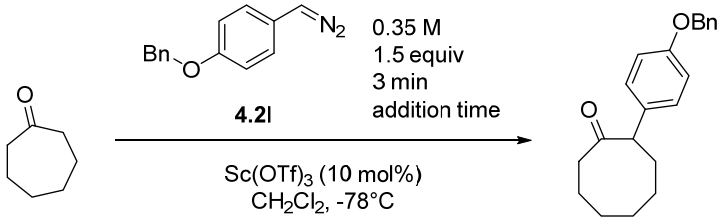

4.4d

2-(4-(Benzyloxy)phenyl)cyclooctan-1-one (4.4d): Synthesised from **4.2l** (78 mg, 0.35 mmol, 1.5 equiv (1.0 mL at MOC = 0.58 M, 60% expected yield)), cycloheptanone (26 mg, 0.23 mmol, 1.0 equiv) and $Sc(OTf)_3$ (9 mg, 0.018 mmol, 0.10 equiv) using **general procedure for cyclic ketone ring expansion, but at -78°C**. Flash chromatography (0-50% CH_2Cl_2/Hexanes) yielded a clear oil (49 mg, 0.16 mmol, 68 %). **^{1}H-NMR** ($CDCl_3$, 400 MHz): δ ppm 7.25 - 7.50 (m, 7 H), 6.93 - 7.02 (m, *2* H), 5.07 (s, 2 H), 3.75 (dd, *J*=12.4, 2.8 Hz, 1 H), 2.63 (td, *J*=12.0, 4.4 Hz, 1 H), 2.35 (dddd, *J*=14.0, 12.4, 11.5, 4.4 Hz, 1 H), 2.26 (ddd, *J*=12.3, 5.5, 4.4 Hz, 1 H), 1.84 - 2.03 (m, 3 H), 1.73 - 1.84 (m, 2 H), 1.56 - 1.66 (m, 2 H), 1.39 - 1.56 (m, 2 H); **^{13}C-NMR** ($CDCl_3$, 125 MHz): δ ppm

216.85 (C), 158.05 (C), 137.17 (C), 131.80 (C), 128.93 (2 CH), 128.73 (2 CH), 128.10 (CH), 127.61 (2 CH), 115.03 (2 CH), 70.17 (CH_2), 56.77 (CH), 40.11 (CH_2), 31.55 (CH_2), 27.14 (CH_2), 26.90 (CH_2), 26.83 (CH_2), 24.77 (CH_2); **FTIR** (cm^{-1}) (neat): 2925 (br m), 2856 (w), 1694 (m), 1607 (w), 1508 (s), 1240 (s), 1017 (m), 829 (m), 737 (m), 696 (m); **HRMS** (ESI, Pos): calcd for $C_{21}H_{25}O_2$ $[M+H]^+$: 309.18491 m/z, found: 309.18432 m/z.

A3.5.7.Epoxide synthesis (products 4.5a to 4.5d)

General procedure for aldehyde epoxidation (modified literature procedure[123a]): The diazo solution stream (4.0 mL, 0.18 M, 2.5 equiv, 66 µL/min) was run through a drying column and dropped directly under N_2 in a dry 20mL vial containing 4-nitrobenzaldehyde (1.0 equiv), dimethyl sulfide (2.0 equiv) and $Cu(acac)_2$ (0.10 equiv). Mixture was agitated at room temperature for 16h. Saturated $NaHCO_3$ was added and phases were separated. Aqueous phase was extracted with CH_2Cl_2 (2x). Combined organic phases were dried over $MgSO_4$ and concentrated under vacuum. Mixture was purified by flash chromatography or recrystallization from CH_2Cl_2/petroleum ether.

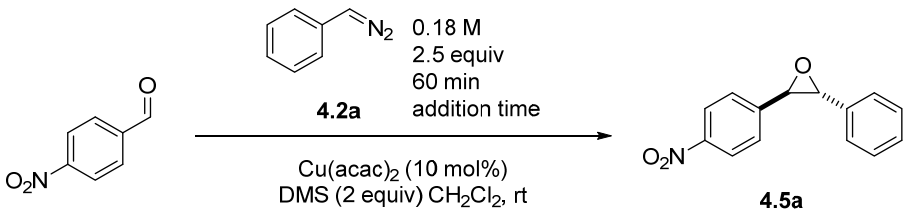

***rac*-(2*R*,3*R*)-2-(4-Nitrophenyl)-3-phenyloxirane (4.5a):** Synthesised from **4.2a** (83 mg, 0.70 mmol, 2.5 equiv (4.0 mL at MOC = 0.25 M, 70% expected yield)), 4-nitrobenzaldehyde (42 mg, 0.28 mmol, 1.0 equiv), dimethyl sulfide (41 µL, 35 mg, 0.56 mmol, 2.0 equiv) and $Cu(acac)_2$ (7 mg, 0.028 mmol, 0.10 equiv) using **general procedure for aldehyde epoxidation**. Flash chromatography (0-10% EtOAc/Hexanes then 20-70% CH_2Cl_2/Hexanes) yielded a white solid (54 mg, 0.22 mmol, 80%, dr: >95:5). **mp:** 123-125 °C, lit. 126-128 °C[123a]; **^{1}H-NMR** ($CDCl_3$, 300 MHz): δ ppm 8.26 (ddd, *J*=8.8, 2.2, 1.8 Hz, 2 H), 7.53 (ddd, *J*=8.8, 2.2, 1.8 Hz, 2 H), 7.33 - 7.47 (m, 5 H), 3.99 (d, *J*=1.5 Hz, 1 H), 3.87 (d, *J*=1.7 Hz, 1 H). Product corresponds to literature characterization data. [123a]

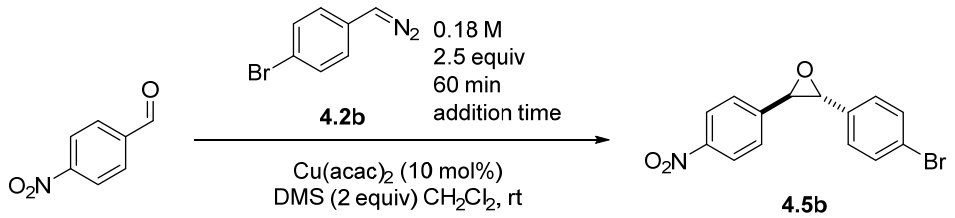

***rac*-(2*R*,3*R*)-2-(4-Bromophenyl)-3-(4-nitrophenyl)oxirane (4.5b):** Synthesised from **4.2b** (138 mg, 0.70 mmol, 2.5 equiv (4.0 mL at MOC = 0.25 M, 70% expected yield)), 4-nitrobenzaldehyde (42 mg, 0.28 mmol, 1.0 equiv), dimethyl sulfide (41 μL, 35 mg, 0.56 mmol, 2.0 equiv) and $Cu(acac)_2$ (7 mg, 0.028 mmol, 0.10 equiv) using **general procedure for aldehyde epoxidation**. Flash chromatography (20-70% CH_2Cl_2/Hexanes then recrystallization from boiling CH_2Cl_2/petroleum ether) yielded a white solid (66 mg, 0.21 mmol. 74%, dr: >95:5). **mp**: 123-125 °C; **^{1}H-NMR** ($CDCl_3$, 400 MHz): δ ppm 8.25 (d, *J*=8.2 Hz, 2 H), 7.54 (d, *J*=8.2 Hz, 2 H), 7.51 (d, *J*=8.2 Hz, 2 H), 7.23 (d, *J*=8.2 Hz, 2 H), 3.93 (s, 1 H), 3.82 (s, 1 H); **^{13}C-NMR** ($CDCl_3$, 100 MHz): δ ppm 148.15 (C), 144.12 (C), 135.27 (C), 132.08 (2 CH), 127.33 (2 CH), 126.42 (2 CH), 124.12 (2 CH), 122.96 (C), 62.87 (CH), 61.82 (CH); **FTIR** (cm^{-1}) (neat): 2920 (br w), 1601 (w), 1515 (s), 1486 (m), 1342 (s), 1068 (m), 1009 (m), 847 (s), 814 (s),, 744 (s), 693 (m), 523 (s); **HRMS** (ESI, Pos): calcd for $C_{14}H_{10}Br_2O_2$ $[M+H]^+$: 319.99186 m/z, found: 319.99135 m/z.

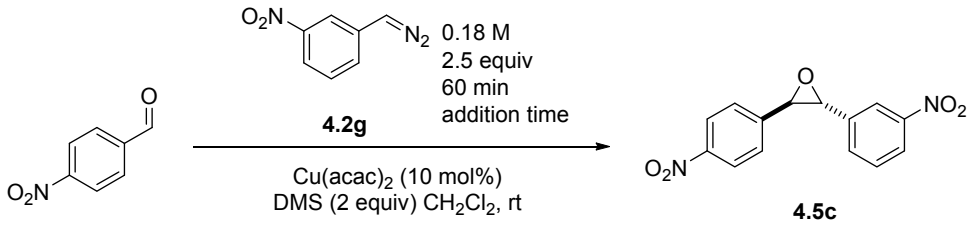

***rac*-(2*R*,3*R*)-2-(3-Nitrophenyl)-3-(4-nitrophenyl)oxirane (4.5c):** Synthesised from **4.2g** (114 mg, 0.70 mmol, 2.5 equiv (4.0 mL at MOC = 0.20 M, 88% expected yield)), 4-nitrobenzaldehyde (42 mg, 0.28 mmol, 1.0 equiv), dimethyl sulfide (41 μL, 35 mg, 0.56 mmol, 2.0 equiv) and $Cu(acac)_2$ (7 mg, 0.028 mmol, 0.10 equiv) using **general procedure for aldehyde epoxidation**. Flash chromatography (20-70% CH_2Cl_2/Hexanes then recrystallization from boiling CH_2Cl_2/petroleum ether) yielded a white solid (63 mg, 0.22 mmol, 78%, dr: 92:8). **mp**: 143-144 °C; **^{1}H-NMR** ($CDCl_3$, 500 MHz): δ ppm 8.31 (ddd, *J*=8.8, 2.3, 1.8 Hz, 2 H), 8.25 - 8.28 (m, 2 H), 7.73 (dt, *J*=7.7, 1.2 Hz, 1 H), 7.63 (dd, *J*=8.8, 7.7 Hz, 1 H), 7.56 (ddd, *J*=8.8, 2.3, 1.8 Hz, 2 H), 4.02 (dd, *J*=8.8, 1.7 Hz, 2 H); **^{13}C-NMR** ($CDCl_3$, 125 MHz): δ ppm 148.82 (C), 148.32 (C), 143.40 (C), 138.52 (C), 131.63

(CH), 130.02 (CH), 126.52 (2 CH), 124.20 (2 CH), 123.85 (CH), 120.81 (CH), 62.11 (CH), 62.00 (CH); **FTIR** (cm^{-1}) (neat): 2922 (br w), 1603 (w), 1515 (s), 1345 (s), 845 (m), 826 (m), 806 (m), 738 (m); **HRMS** (ESI, Pos): calcd for $C_{14}H_{11}N_2O_5$ $[M+H]^+$: 287.06625 m/z, found: 287.06574 m/z.

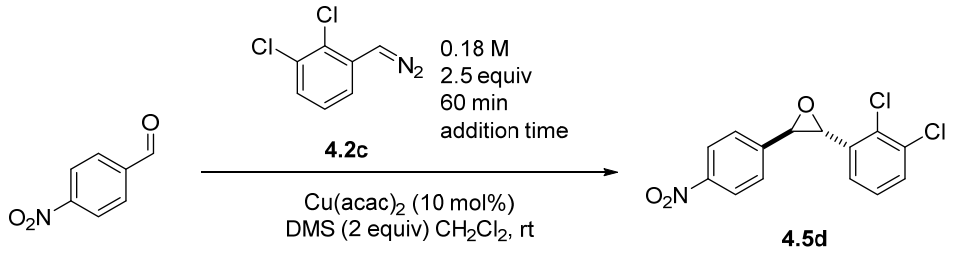

***rac*-(2*R*,3*R*)-2-(2,3-Dichlorophenyl)-3-(4-nitrophenyl)oxirane (4.5d):** Synthesised from **2c** (131 mg, 0.70 mmol, 2.5 equiv (4.0 mL at MOC = 0.20 M, 88% expected yield)), 4-nitrobenzaldehyde (42 mg, 0.28 mmol, 1.0 equiv), dimethyl sulfide (41 μL, 35 mg, 0.56 mmol, 2.0 equiv) and $Cu(acac)_2$ (7 mg, 0.028 mmol, 0.10 equiv) using **general procedure for aldehyde epoxidation**. Flash chromatography (0-10% Et_2O/Hexanes) yielded a white solid (79 mg, 0.25 mmol. 91%, dr: >95:5). mp: 153-155°C; **^{1}H-NMR** ($CDCl_3$, 400 MHz): δ ppm 8.28 (ddd, *J*=8.8, 2.3, 1.8 Hz, 2 H), 7.56 (ddd, *J*=8.8, 2.3, 1.8 Hz, 2 H), 7.47 (dd, *J*=7.6, 1.9 Hz, 1 H), 7.32 (dd, *J*=7.6, 1.9 Hz, 1 H), 7.29 (d, *J*=7.6 Hz, 1 H), 4.18 (d, *J*=1.7 Hz, 1 H), 3.84 (d, *J*=1.7 Hz, 1 H); **^{13}C-NMR** ($CDCl_3$, 125 MHz): δ ppm 148.25 (C), 143.78 (C), 136.77 (C), 133.28 (C), 131.48 (C), 130.40 (CH), 127.97 (CH), 126.54 (2 CH), 124.17 (CH), 124.16 (2 CH), 61.03 (CH), 60.98 (CH); **FTIR** (cm^{-1}) (neat): 2927 (br w), 1603 (w), 1512 (s), 1342 (s), 1106 (w), 846 (m), 787 (m), 696 (s), 461 (m); **HRMS** (ESI, Pos): calcd for $C_{14}H_{10}Cl_2NO_3$ $[M+H]^+$: 310.00323 m/z, found: 310.00356 m/z.

A3.5.8.Cyclopropane synthesis (products 4.6a to 4.6d)

General procedure for alkene cyclopropanation:[189] The diazo solution (1.0 mL, 0.35 M, 2.5 equiv, 166 μL/min) stream was run through a drying column and dropped directly under N_2 in a dry 4mL vial containing (E)-(3-(methoxymethoxy)prop-1-en-1-yl)benzene (1.0 equiv) and ZnI_2 (0.20 equiv). Mixture was agitated at room temperature until diazo color has vanished. Saturated $NaHCO_3$ was added and phases were separated. Aqueous phase was extracted with CH_2Cl_2 (2X). Combined organic phases were dried over $MgSO_4$ and concentrated under vacuum. Mixture was purified by flash chromatography.

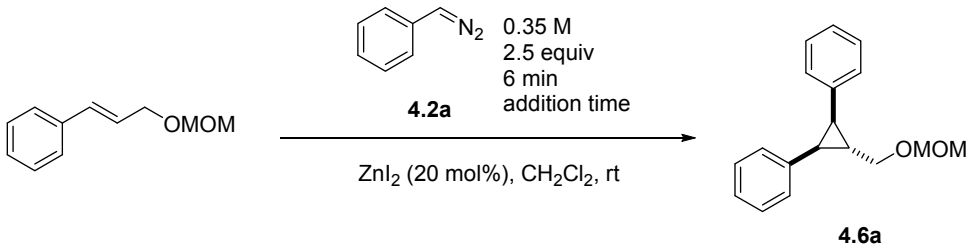

***rac*-((1*R*,2*S*,3*r*)-3-((Methoxymethoxy)methyl)cyclopropane-1,2-diyl)dibenzene (4.6a):** Synthesised from **4.2a** (41 mg, 0.35 mmol, 2.5 equiv (1.0 mL at MOC = 0.50 M, 70% expected yield)), (E)-(3-(methoxymethoxy)prop-1-en-1-yl)benzene (25 mg, 0.14 mmol, 1.0 equiv) and ZnI_2 (9 mg, 0.028 mmol, 0.20 equiv) using **general procedure for alkene cyclopropanation**. Flash chromatography (0-5% Et_2O/Hexanes) yielded a clear oil (32 mg, 0.12 mmol. 85%, dr: >95:5). **^{1}H-NMR** ($CDCl_3$, 300 MHz): δ ppm 7.02 - 7.14 (m, 6 H), 6.91 - 6.98 (m, 4 H), 4.73 (s, 2 H), 3.77 (d, *J*=6.5 Hz, 2 H), 3.39 (d, *J*=0.6 Hz, 3 H), 2.43 (d, *J*=5.6 Hz, 2 H), 2.08 (quin, *J*=6.1 Hz, 1 H). Product corresponds to literature characterization data.[189]

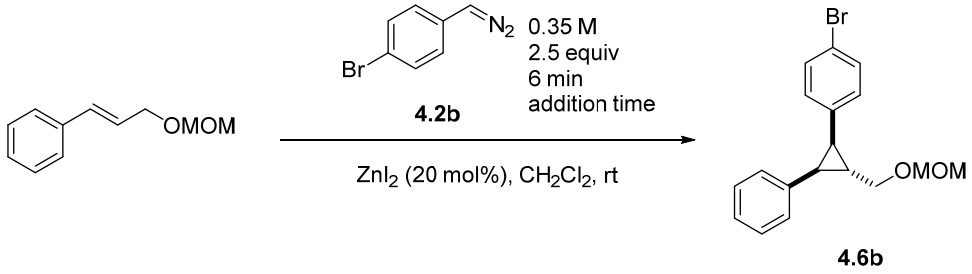

***rac*-1-Bromo-4-((1*R*,2*R*,3*S*)-2-((methoxymethoxy)methyl)-3-phenylcyclopropyl)benzene (4.6b):** Synthesised from **4.2b** (69 mg, 0.35 mmol, 2.5 equiv (1.0 mL at MOC = 0.50 M, 70% expected yield)), (E)-(3-(methoxymethoxy)prop-1-en-1-yl)benzene (25 mg, 0.14 mmol, 1.0 equiv) and ZnI_2 (9 mg, 0.028 mmol, 0.20 equiv) using **general procedure for alkene cyclopropanation**. Flash chromatography (0-5% Et_2O/Hexanes) yielded a clear oil (44 mg, 0.13 mmol. 91%, dr: >95:5). **^{1}H-NMR** ($CDCl_3$, 300 MHz): δ ppm 7.21 (ddd, *J*=8.5, 2.2, 1.9 Hz, 2 H), 7.05 - 7.17 (m, 3 H), 6.89 - 6.99 (m, 2 H), 6.79 (ddd, *J*=8.5, 2.0, 1.7 Hz, 2 H), 4.72 (s, 2 H), 3.75 (qd, *J*=10.4, 6.6 Hz, 2 H), 3.38 (s, 3 H), 2.44 (dd, *J*=9.0, 5.8 Hz, 1 H), 2.35 (dd, *J*=9.0, 5.8 Hz, 1 H), 2.03 (quin, *J*=6.1 Hz, 1 H); Product corresponds to literature characterization data.[189]

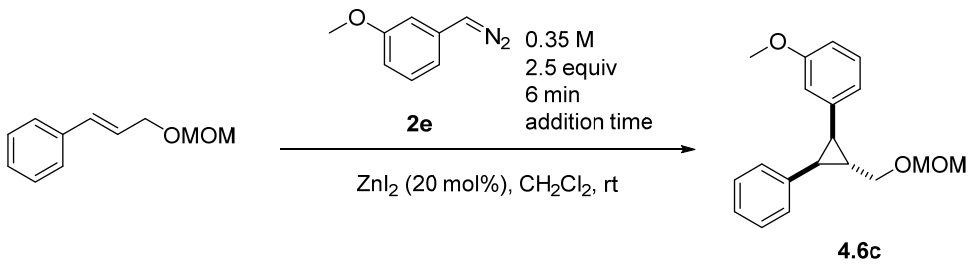

4.6c

***rac*-1-Methoxy-3-((1*R*,2*R*,3*S*)-2-((methoxymethoxy)methyl)-3-phenylcyclopropyl)benzene (4.6c):** Synthesised from **4.2e** (52 mg, 0.35 mmol, 2.5 equiv (1.0 mL at MOC = 0.50 M, 70% expected yield)), (E)-(3-(methoxymethoxy)prop-1-en-1-yl)benzene (25 mg, 0.14 mmol, 1.0 equiv) and ZnI_2 (9 mg, 0.028 mmol, 0.20 equiv) using **general procedure for alkene cyclopropanation**. Flash chromatography (0-8% Et_2O/Hexanes) yielded a clear oil (29 mg, 0.097 mmol. 69%, dr: >95:5). **^{1}H-NMR** ($CDCl_3$, 300 MHz): δ ppm 6.97 - 7.18 (m, 6 H), 6.56 - 6.64 (m, 2 H), 6.40 - 6.44 (m, 1 H), 4.74 (s, 2 H), 3.77 (d, *J*=6.5 Hz, 2 H), 3.61 (s, 3 H), 3.40 (s, 3 H), 2.45 (br dd, *J*=10.0, 6.1 Hz, 1 H), 2.40 (dd, *J*=10.0, 6.1 Hz, 1 H), 2.07 (quin, *J*=6.1 Hz, 1 H); **^{13}C-NMR** ($CDCl_3$, 75 MHz): δ ppm 159.21 (C), 139.40 (C), 137.58 (C), 129.19 (2 CH), 128.78 (CH), 127.96 (2 CH), 126.00 (CH), 121.63 (CH), 114.31 (CH), 111.74 (CH), 96.28 (CH_2), 70.82 (CH_2), 55.42 (CH_3), 55.13 (CH_3), 30.07 (CH), 29.85 (CH), 25.37 (CH); **FTIR** (cm^{-1}) (neat): 2942 (br), 1602 (m), 1493 (w), 1151 (m), 1105 (m), 1039 (s), 697 (m); **HRMS** (ESI, Pos): calcd for $C_{19}H_{22}O_3Na$ $[M+Na]^+$: 321.14612 m/z, found: 321.14512 m/z.

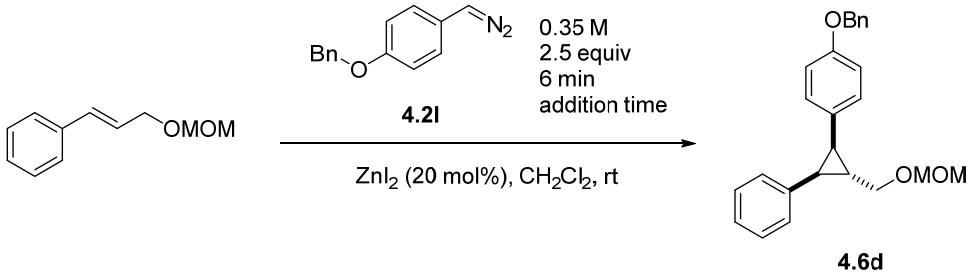

4.6d

***rac*-1-(Benzyloxy)-4-((1*R*,2*R*,3*S*)-2-((methoxymethoxy)methyl)-3-phenylcyclopropyl)benzene (4.6d):** Synthesised from **4.2l** (78 mg, 0.35 mmol, 2.5 equiv (1.0 mL at MOC = 0.58 M, 60% expected yield)), (E)-(3-(methoxymethoxy)prop-1-en-1-yl)benzene (25 mg, 0.14 mmol, 1.0 equiv) and ZnI_2 (9 mg, 0.028 mmol, 0.20 equiv) using **general procedure for alkene cyclopropanation**. Flash chromatography (0-5% Et_2O/Hexanes) yielded a white solid (16 mg, 0.043 mmol. 31%, dr: >95:5). **mp**: 51-52 °C **^{1}H-NMR** ($CDCl_3$, 400 MHz): δ ppm 7.27 - 7.42

(m, 5 H), 7.00 - 7.15 (m, 3 H), 6.90 - 6.95 (m, 2 H), 6.87 (ddd, *J*=8.8, 2.3, 1.8 Hz, 2 H), 6.73 (ddd, *J*=8.8, 2.3, 1.8 Hz, 2 H), 4.96 (s, 2 H), 4.72 (s, 2 H), 3.75 (d, *J*=6.5 Hz, 2 H), 3.38 (s, 3 H), 2.38 (dd, *J*=9.6, 5.8 Hz, 1 H), 2.35 (dd, *J*=9.6, 5.8 Hz, 1 H), 2.00 (quin, *J*=6.1 Hz, 1 H); **^{13}C-NMR** ($CDCl_3$, 100 MHz): δ ppm 156.99 (C), 137.75 (C), 137.13 (C), 130.08 (2 CH), 129.74 (C), 128.83 (2 CH), 128.51 (2 CH), 127.87 (CH), 127.75 (2 CH), 127.48 (2 CH), 125.67 (CH), 114.28 (2 CH), 96.14 (CH_2), 70.85 (CH_2), 69.94 (CH_2), 55.27 (CH_3), 29.45 (CH), 29.28 (CH), 25.15 (CH); **FTIR** (cm^{-1}) (neat): 2927 (br), 1609 (w), 1512 (m), 1239 (m), 1104 (m), 1036 (s), 737 (m), 695 (s); **HRMS** (ESI, Pos): calcd for $C_{25}H_{26}O_3Na$ $[M+Na]^+$: 397.17742 m/z, found: 397.17720 m/z.

Bibliographie

(1)Gillespie, R. J. *Coord. Chem. Rev.* **2008**, *252*, 1315.

(2) Lakowicz, J. R. *Principles of fluorescence spectroscopy*, 3rd ed.; Springer: New York, **2006**.

(3) Image originale : https://commons.wikimedia.org/wiki/File:Franck-Condon-diagram.png (Page consultée le 2016/10/03)

(4) Terai, T.; Nagano, T. *Pfluegers Arch.* **2013**, *465*, 347.

(5) Itoh, T. *Chem. Rev.* **2012**, *112*, 4541.

(6) Williams, A. T. R.; Winfield, S. A.; Miller, J. N. *The Analyst* **1983**, *108* (1290), 1067.

(7) Panchuk-Voloshina, N. *et al J. Histochem. Cytochem.* **1999**, *47*, 1179.

(8) Sun, W.; Gee, K. R.; Klaubert, D. H.; Haugland, R. P. *J. Org. Chem.* **1997**, *62*, 6469.

(9) Youziel, J.; Akhbar, A. R.; Aziz, Q.; Smith, M. E. B.; Caddick, S.; Tinker, A.; Baker, J. R. *Org. Biomol. Chem.* **2014**, 12, 557.

(10) Mujumdar, R. B.; Ernst, L. a. *et al Bioconjugate Chem.* **1993**, *4*, 105.

(11) (a) Kim, E.; Koh, M.; Ryu, J.; Park, S. B. *J. Am. Chem. Soc.* **2008**, *130*, 12206. (b) Kim, E.; Koh, M.; Lim, B. J.; Park, S. B. *J. Am. Chem. Soc.* **2011**, *133*, 6642. (c) Choi, E. J.; Kim, E.; Lee, Y.; Jo, A.; Park, S. B. *Angew Chem Int Ed Engl* **2014**, *53*, 1346.

(12) Sezukuri, K.; Suzuki, M.; Hayashi, H.; Kuzuhara, D.; Aratani, N.; Yamada, H. *Chem. Commun.* **2016**, *52*, 4872.

(13) Miyaura, N.; Suzuki, A. *Chemical Reviews* **1995**, *95*, 2457.

(14) Carey, F. A.; Sundberg, R. J. *Advanced Organic Chemistry*; Springer US: Boston, MA, **2007**.

(15) Bechara, W. S.; Pelletier, G.; Charette, A. B. *Nature Chemistry* **2012**, *4*, 228.

(16) Pelletier, G.; Charette, A. B. *Org. Lett.* **2013**, *15*, 2290.

(17) Aginagalde, M.; Vara, Y.; Arrieta, A.; Zangi, R.; Cebolla, V. L.; Delgado-Camón, A.; Cossío, F. P. *J. Org. Chem.* **2010**, *75*, 2776.

(18) (a) Firmansyah, D.; Banasiewicz, M.; Gryko, D. T. Org. Biomol. Chem. **2015**, *13,* 1367. (b) Stasyuk, A. J.; Banasiewicz, M.; Ventura, B.; Cyrański, M. K.; Gryko, D. T. *New J. Chem.* **2014**, *38*, 189. (c) Sadowski, B.; Klajn, J.; Gryko, D. T. *Org. Biomol. Chem.* **2016**, *14*, 7804.

(19) Firmansyah, D.; Banasiewicz, M.; Deperasińska, I.; Makarewicz, A.; Kozankiewicz, B.; Gryko, D. T. *Chem. Asian J.* **2014**, *9* (9), 2483.

([20]) (a) Lane, T. J.; Quinlan, K. P. *J. Am. Chem. Soc.* **1960**, *82* (12), 2994. (b) Armarego, W. L. F. *J. Chem Soc. (Resumed)* **1964**, 4226. (c) Lerner, D. A.; Evleth, E. M. *Chem. Phys. Lett.* **1972**, *15* (2), 260.

(21) Shibahara, F.; Yamaguchi, E.; Kitagawa, A.; Imai, A.; Murai, T. *Tetrahedron* **2009**, *65*, 5062.

(22) (a) Kim, H. M.; Cho, B. R. *Chem. Rev.* **2015**, *115*, 5014. (b) Williams, F. J.; Fiedler, D. *ACS Chem. Biol.* **2015**, *10*, 1958. (c) Dean, K. M.; Palmer, A. E. *Nat. Chem. Biol.* **2014**, *10*, 512. (d) Lukinavicius, G.; Umezawa, K.; Olivier, N.; Honigmann, A.; Yang, G.; Plass, T.; Mueller, V.; Reymond, L.; Correa, I. R.; Luo, Z.-G.; Schultz, C.; Lemke, E. A.;

Heppenstall, P.; Eggeling, C.; Manley, S.; Johnsson, K. *Nat. Chem.* **2013**, *5*, 132. (e) Jameson, D. M.; Ross, J. A. *Chem. Rev.* **2010**, *110*, 2685.

(23) (a) Westphal, V.; Rizzoli, S. O.; Lauterbach, M. A.; Kamin, D.; Jahn, R.; Hell, S. W. *Science* **2008**, *320*, 246. (b) Klar, T. A.; Hell, S. W. *Opt. Lett.* **1999**, *24*, 954. (c) Hell, S. W.; Wichman, J. *Opt. Lett.* **1994**, *19*, 780. For comprehensive reviews, see: (d) Müller, T.; Schumann, C.; Kraegeloh, A. *ChemPhysChem* **2012**, *13*, 1986. (e) Eggeling, C.; Willig, K. I.; Barrantes, F. J. *J. Neurochem.* **2013**, *123*, 203. (f) Schermelleh, L.; Heintzmann, R.; Leonhardt, H. *J. Cell. Biol.* **2010**, *190*, 165.

(24) (a) Betzig, Sougrat, R.; Lindwasser, O. W.; Olenych, S.; Bonifacino, J. S.; Davidson, M. W.; Lippincott-Schwartz, J.; Hess, H. F. *Science* **2006**, *313*, 1642. (b) Moerner, W. E.; Fromm, D. P. *Rev. Sci. Instrum.* **2003**, *74*, 3597. (c) Manley, S.; Gillette, J. M.; Patterson, G. H.; Shroff, H.; Hess, H. F.; Betzig, E.; Lippincott-Schwartz, J. *Nat. Methods* **2008**, *5*, 155. (d) Hess, H. F.; Betzig, E.; Harris, T. D.; Pfeiffer, L. N.; West, K. W. *Science* **1994**, *264*, 1740. (d) Ambrose, W. P.; Moerner, W. E. *Nature* **1991**, *349*, 225. (e) Moerner, W. E.; Kador, L. *Phys. Rev. Lett.* **1989**, *62*, 2535. For a comprehensive review, see: (f) Peterman, E. J. G.; Sosa, H.; Moerner, W. E. *Annu. Rev. Phys. Chem.* **2004**, *55*, 79.

(25) The Nobel prize in chemistry was awarded to Betzig, Hell, and Moerner in 2014 for this technology. For recent applications, see: (a) Eggeling, C.; Willig, K. I.; Sahl, S. J.; Hell, S. W. *Q. Rev. Biophys.* **2015**, *48*, 178. (b) Wang, C.; Fukazawa, A.; Taki, M.; Sato, Y.; Higashiyama, T.; Yamaguchi, S. *Angew. Chem., Int. Ed.* **2015**, *54*, 15213. (c) Kolmakov, K.; Wurm, C. A.; Meineke, D. N. H.; Göttfert, F.; Boyarskiy, V. P.; Belov, V. N.; Hell, S. W. *Chem.–Eur. J.* **2014**, *20*, 146. (d) Chozinski, T. J.; Gagnon, L. A.; Vaughan, J. C. *FEBS Lett.* **2014**, *588*, 3603. (e) Trouillon, R.; Passarelli, M. K.; Wang, J.; Kurczy, M. E.; Ewing, A. G. *Anal. Chem.* **2013**, *85*, 522.

(26) For examples of fluorescent organic small-molecules, see: (a) Wuerthner, F.; Saha-Moeller, C. R.; Fimmel, B.; Ogi, S.; Leowanawat, P.; Schmidt, D. *Chem. Rev.* **2016**, *116*, 962. (b) Wirth, R.; White, J. D.; Moghaddam, A. D.; Ginzburg, A. L.; Zakharov, L. N.; Haley, M. M.; DeRose, V. J. *J. Am. Chem. Soc.* **2015**, *137*, 15169. (c) Lian, Y.; Bergman, R. G.; Lavis, L. D.; Ellman, J. A. *J. Am. Chem. Soc.* **2013**, *135*, 7122. (d) Branigan, E.; Pliotas, C.; Hagelueken, G.; Naismith, J. H. *Nat. Protoc.* **2013**, *8*, 2090. (e) Loudet, A.; Burgess, K. *Chem. Rev.* **2007**, *107*, 4891.

(27) For examples of fluorescent metal complexes, see: (a) Chia, Y. Y.; Tay, M. G. *Dalton Trans.* **2014**, *43*, 13159. (b) Geisser, B.; Ponce, A.; Alsfasser, R. *Inorg. Chem.* **1999**, *38*, 2030.

(28) For example of GFPs and other fluorescent proteins, see: (a) Nienhaus, K.; Nienhaus, G. U. *Chem. Soc. Rev.* **2014**, 4*3*, 1088. (b) Day, R. N.; Davidson, M. W. *Chem. Soc. Rev.* **2009**, *38*, 2887. (c) Shaner, N. C.; Steinbach, P. A.; Tsien, R. Y. *Nature Methods* **2005**, *2*, 905.

(29) Hu, J.-Y.; Pu, Y.-J.; Nakata, G.; Kawata, S.; Sasabe, H.; Kido, J. *Chem. Commun.* **2012**, *48*, 8434.

(30) (a) T. Miura, Y. Urano, K. Tanaka, T. Nagano, K. Ohkubo, S. Fukuzumi, *J. Am. Chem. Soc.* **2003**, *125*, 8666. (b) T. Ueno, Y. Urano, K. Setsukinai, H. Takakusa, H. Kojima, K. Kikuchi, K. Ohkubo, S. Fukuzumi, T. Nagano, *J. Am. Chem. Soc.* **2004***, 126*, 14079. (c) Y. Urano, M. Kamiya, K. Kanda, T. Ueno, K. Hirose, T. Nagano*, J. Am. Chem. Soc.* **2005**, *127*, 4888. (d) T. Ueno, Y. Urano, H. Kojima, T. Nagano, *J. Am. Chem. Soc.* **2006**, *128*, 10640.

(31) Brightness is a measure of a fluorophore's light output. It is the product of the molar absorptivity with the quantum yield and is expressed in (kL/mol*cm).

(32) (a) Lavis, L. D.; Raines, R. T. *ACS Chem. Biol.* **2008**, *3*, 142–155. (b) Yang, T.; Goddard, J. D. *J. Phys. Chem. A* **2007**, *111*, 4489.

(33)Yang, D.-T.; Radtke, J.; Mellerup, S. K.; Yuan, K.; Wang, X.; Wagner, M.; Wang, S. *Org. Lett.* **2015**, *17*, 2486.

(34) To ease large-scale reactions, the chromatographic purification reported in Puglisi, A.; Benaglia, M.; Roncan, G. *Eur. J. Org. Chem.* **2003**, 1552. was replaced by a recrystallization.

(35) (a) Yamashita, M.; Hartwig, J. F. *J. Am. Chem. Soc.* **2004**, *126*, 5344. (b) Fleckenstein, C. A.; Plenio, H. *Chem. Soc. Rev.* **2010**, *39*, 694.

(36) Many reactions involving a CMD require the presence of a proton shuttle such as a carboxylate or a carbonate. See (a) Liégault, B.; Lapointe, D.; Caron, L.; Vlassova, A.; Fagnou, K. *J. Org. Chem.* **2009**, *74*, 1826. (b) Roman, D. S.; Charette, A. B. *Org. Lett.* **2013**, *15* (17), 4394.

(37) Simmons, E. M.; Hartwig, J. F. *Angew. Chem., Int. Ed.* **2012**, *51*, 3066.

(38) (a) Shibahara, F.; Yamaguchi, E.; Murai, T. *J. Org. Chem.* **2011**, *76*, 2680. (b) Shibahara, F.; Yamaguchi, E.; Murai, T. *Chem. Commun.* **2010**, *46*, 2471. (c) Yamaguchi, E.; Shibahara, F.; Murai, T. *Chem. Lett.* **2011**, *40*, 939. (d) Preparation of the catalyst : Milani, B.; Anzilutti, A.; Vicentini, L.; Sessanta o Santi, A.; Zangrando, E.; Geremia, S.; Mestroni, G. *Organometallics* **1997**, *16*, 5064.

(39) Allen, F. H.; Kennard, O.; Watson, D. G.; Brammer, L.; Orpen, A. G.; Taylor, R. *J. Chem. Soc., Perkin Trans. 2* **1987**, No. 12, S1.

(40) For other examples of high Stokes Shift fluorophores and their applications, see (a) Araneda, J. F.; Piers, W. E.; Heyne, B.; Parvez, M.; McDonald, R. *Angew. Chem., Int. Ed.* **2011**, *50*, 12214. (b) Sanguineti, A.; Sassi, M.; Turrisi, R.; Ruffo, R.; Vaccaro, G.; Meinardi, F.; Beverina, L. *Chem. Commun.* **2013**, *49*, 1618. (c) Horvath, P.; Sebej, P.; Solomek, T.; Klan, P. *J. Org. Chem.* **2015**, *80*, 1299.

(41) Kruse, H.; Goerigk, L.; Grimme, S. *J. Org. Chem.* **2012**, *77*, 10824.

(42) B3LYP 6-31G (d,p) basis set was used for DFT calculations. Please see supplementary information for more details.

(43) (a) Jacquemin, D.; Preat, J.; Wathelet, V.; Perpète, E. A. *J. Chem. Phys.* **2006**, *124*, 74104. (b) Bauschlicher, C. W.; Partridge, H. *Chem. Phys. Lett.* **1995**, *240*, 533.

(44) Tanaka, H.; Shizu, K.; Nakanotani, H.; Adachi, C. *J. Phys. Chem. C* **2014**, *118*, 15985.

(45) (a) Hansch, C.; Leo, A.; Taft, R. W. *Chem. Rev.* **1991**, *91*, 165–195. (b) McDaniel, D. H.; Brown, H. C. *J. Org. Chem.* **1958**, *23*, 420.

(46) Aqueous solutions of **10a**'s sodium salt or **10e** can be repeatedly washed with DCM without significant loss of yield.

(47) (a) Reetz, M.T. *J. Am. Chem. Soc.* **2013**, *135*, 12480. (b) Rashidian, M., Dozier, J.K., Distefano, M.D. *Bioconjugate Chem.*, **2013**, *25*, 1483.

(48) (a) Rachel, N. M.; Pelletier, J. N. *Biomolecules* **2013**, *3*, 870–888. (b) Ando, H.; Adachi, M.; Umeda, K.; Matsuura, A.; Nonaka, M.; Uchio, R.; Tanaka, H.; Motoki, M. *Agr. Biol. Chem. Tokyo* **1989**, *53,* 2613. (c) Yokoyama, K.; Nio, N.; Kikuchi, Y. *Appl. Microbiol. Biot.* **2004**, *64*, 447

(49) Gundersen, M. T.; Keillor, J. W.; Pelletier, J. N. *Appl. Microbiol. and Biotech.* **2014**, *98*, 219.

(50) (a) Rachel, N. M.; Pelletier, J. N. *Chem. Commun.* **2016**, *52*, 2541. (b) Nieuwenhuizen, W.F., Dekker, H.L., de Koning, L.J., Gröneveld, T., de Koster, C.G., de Jong, G.A. *J. Agric. Food. Chem.*, **2003**, *51*, 7132. (c) Spolaore, B.; Raboni, S.; Molina, A. R.; Satwekar, A.; Damiano, N.; Fontana, A. *Biochemistry-Us* **2012***, 51*, 8679.

(51) Le Bras, J.; Muzart, J. *Chem, Rev.* **2011**, *111*, 1170.

(52) Simmons, H. E.; Smith, R. D. *J. Am. Chem. Soc.* **1958**, 5323.

(53) Winstein, S.; Sonnenberg, J.; DeVries, L. *J. Am. Chem. Soc.* **1959**, 6523.

(54) Lebel, H.; Marcoux, J.-F.; Molinaro, C.; Charette, A. B. *Chem. Rev.* **2003**, *103*, 977.

(55) (a) Boche, G.; Lohrenz, J. C. W. Chem. Rev. **2001**, 101 (3), 697–756. (b) Pasco, M.; Gilboa, N.; Mejuch, T.; Marek, I. Organometallics **2013**, 32, 942.

(56) (a) Boersma, J. Zn-compounds in *Comprehensive Organometallic Chemistry*; Wilkinson, G., Ed.; Pergamon Press: Oxford, **1982**; Vol. 2, p 823. (b) Knochel, P. Zn-compounds in *Comprehensive Organometallic Chemistry II*; Abel, E. W., Stone, F. G. A., Wilkinson, G., Eds.; Pergamon Press: New York, **1995**; Vol. 11, p 159

(57) Charette, A. B.; Marcoux, J.-F. Synlett **1995**, 1995 (12), 1197.

(58) (a) Denmark, S. E.; Edwards, J. P.; Wilson, *S. R. J. Am. Chem. Soc.* **1992**, *114,* 2592. (b) Denmark, S. E.; Christenson, B. L.; Coe, D. M.; O'Connor, S. P. *Tet. Lett.* **1995**, *36* (13), 2215.

(59) Charette, A. B.; Marcoux, J.-F. *J. Am. Chem. Soc.* **1996**, *118* (19), 4539.

(60) Charette, A. B.; Marcoux, J.-F.; Bélanger-Gariépy, F. *J. Am. Chem. Soc.* **1996**, *118* (28), 6792.

(61) Charette, A. B.; Beauchemin, A.; Francoeur, S. *J. Am. Chem. Soc.* **2001**, *123* (33), 8139–8140.

(62) Lacasse, M.-C.; Poulard, C.; Charette, A. B. *J. Am. Chem. Soc.* **2005**, *127* (36), 12440.

(63) Long, J.; Xu, L.; Du, H.; Li, K.; Shi, Y. *Org. Lett.* **2009**, *11* (22), 5226.

(64) Nakamura, M.; Hirai, A.; Nakamura, E. J. Am. Chem. Soc. **2003**, 125, 2341.

(65) Charette, A. B.; Marcoux, J.-F.; Molinaro, C.; Beauchemin, A.; Brochu, C.; Isabel, É. *J. Am. Chem. Soc.* **2000**, *122* (18), 4508

(66)

Alkyl : (a) Charette, A. B.; Lemay, J. *Angew. Chem. Int. Ed.* **1997**, *36* (10), 1090. (b) Bull, J. A.; Charette, A. B. *J. Am. Chem. Soc.* **2010**, *132* (6), 1895.

Aryl : *Refs 72 et 74*.

Zinc :(c) A. B. Charette, A. Gagnon, J.-F. Fournier, *J. Am. Chem. Soc.* **2002**, *124*, 386. (d) Fournier, J.-F.; Charette, A. B. *Eur. J. Org. Chem.* **2004**, 1401. (e) Fournier, J.-F.; Mathieu, S.; Charette, A. B. *J. Am. Chem. Soc.* **2005**, *127* (38), 13140. (f) Zimmer, L. E.; Charette, A. B. *J. Am. Chem. Soc.* **2009**, *131* (43), 15624.

Iodide : (g) Beaulieu, L.-P. B.; Zimmer, L. E.; Charette, A. B. *Chem. Eur. J.* **2009**, *15* (44), 11829.

Bromide : (h) Taillemaud, S.; Diercxsens, N.; Gagnon, A.; Charette, A. B. *Angew. Chem. Int. Ed.* **2015**, *54* (47), 14108.

Chloride : (i) Beaulieu, L.-P. B.; Zimmer, L. E.; Gagnon, A.; Charette, A. B. *Chem. Eur. J.* **2012**, *18* (46), 14784.

Fluoride : (j) Beaulieu, L.-P. B.; Schneider, J. F.; Charette, A. B. *J. Am. Chem. Soc.* **2013**, *135* (21), 7819–7822.

(67) Denmark, S. E.; Edwards, J. P. *J Org. Chem.* **1991**, *56* (25), 6974.

(68) Furukawa, J.; Kawabata, N.; Nishimura, J., *Tet. Lett.* **1966**, 3353.

(69) Wittig, G.; Schwarzenbach, K. *Angew.Chem.* **1959**, *71*, 652.

(70) (a) Chai, Z.-Y.; Zhang, C.; Wang, Z.-X. *Organometallics* **2008**, *27* (7), 1626. (b) Hoppe, H.-R.; Andrä, K. *Zeitschrift für Chemie* **1986**, *26* (2), 75.

(71) Furukawa, J.; Kawabata, N.; Nishimura, J. *Tet. Lett.* **1968**, 3495 (b) Durandelli, S.; Sibille, S.; Périchon, J. *J. Org. Chem.* **1991**, *14*, 3255.

(72) (a) Goh, S. H.; Closs, L. E.; Closs, G. L. *J. Org. Chem.* **1969**, *34*, 25. (b) Crumrine, D. S.; Haberkamp, T. J.; Sutherl, D. J. *J. Org. Chem.* **1975**, *40*, 2274. (c) Marvell, E. N.; Lin, C. *J. Am. Chem. Soc.* **1978**, *100*, 877. (d) Altman, L. J.; Kowerski, R. C.; Laungani, D. R. *J. Am. Chem. Soc.* **1978**, *100*, 6174.

(73) Goudreau, S. R.; Charette, A. B. *J. Am. Chem. Soc.* **2009**, *131*, 15633.

(74) Lévesque, É.; Goudreau, S. R.; Charette, A. B. *Org. Lett.* **2014**, *16*, 1490.

(75) Wong, H. N. C.; Hon, M. Y.; Tse, C. W.; Yip, Y. C.; Tanko, J.; Hudlicky, T. *Chem. Rev.* **1989**, *89*, 165.

(76) (a) Charette, A. B.; Beauchemin, A. *Org. React.* **2001**, *58*, 1. (b) Furukawa, J.; Kawabata, N. *Adv. Organomet. Chem.* **1974**, *12*, 83. (c) Charette, A. B.; Juteau, H. *J. Am. Chem. Soc.* **1994**, *116*, 2651.

(77) Wilb, N.; Charette, A. B. *Synlett* **2002**, *1*, 176.

(78) Emschwiller, G. *Compt. Rend.* **1929**, *188*, 1555.

(79) A similar, metal-free transformation has already been reported, but it requires high temperatures and long reaction times : Barluenga, J.; Quiñones, N.; Tomás-Gamasa, M.; Cabal, M.-P. *Eur. J. Org. Chem.* **2012**, 2312.

(80) ZnI_2 was generated in-situ from Et_2Zn and I_2 to ensure reproductibility. Commercial ZnI_2, which is hygroscopic, can also be used, but results are dependent on batch quality and storage conditions.

(81) After the cyclopropanation, the MOM group could be cleaved using aqueous HCl in refluxing MeOH for 2h. The yield of isolated alcohol was 90%. This reaction was carried out on a 0.10 mmol scale.

(82) Verdecchia, M.; Tubaro, C.; Biffis, A. *Tet. Lett.* **2011**, *52*, 1136.

(83) Hamaker, C. G.; Mirafzal, G. A.; Woo, L. K. *Organometallics* **2001**, *20*, 5171.

(84) Maas, G.; Seitz, J. *Tet. Lett.* **2001**, *42*, 6137.

(85) Hamaker, C. G.; Djukic, J.; Smith, D. A.; Woo, L. K. *Organometallics* **2001**, *20*, 5189.

(86) (a) Charette, A. B.; Brochu, C. *J. Am. Chem. Soc.* **1995**, *117*, 11367. (b) Charette, A. B.; Molinaro, C.; Brochu, C. *J. Am. Chem. Soc.* **2001**, *123*, 12160.

(87) The previously reported preforming of the substrate's sodium alkoxide with NaH should also be a suitable way to avoid benzylation. However, this procedure suffers from solubility and reproducibility problems when a calatytic amount of zinc is used.

(88) (a) Charette, A. B.; Francoeur, S.; Martel, J.; Wilb, N. *Angew. Chem. Int. Ed.* **2000**, *39*, 4539.

(89) The anion of butylated hydroxytoluene (BHT) is also a suitable ligand, giving 80% yield in the conditions depicted in Table 1, entry 7.

(90) Nishimura, J.; Kawabata, N.; Furukawa, J. *Tetrahedron* **1969**, *25*, 2647.

(91) P. A. Bray, R. K. Sokas, *J. Occup. Environ. Med.* **2015**, *57*, e15.

(92) Doyle, M. P.; McKervey, M. A.; Ye, T. *Modern catalytic methods for organic synthesis with diazo compounds: from cyclopropanes to ylides*; Wiley: New York, **1998**.

(93) Black, T.H. *Aldrichimica Acta* **1983**, 16, 3.

(94) (a) Bamford, W. R.; Stevens, T. S. *J. Chem. Soc.* **1952**, 4735; (b) Bartlett, R. K.; Stevens, T. S. *J. Chem. Soc. C* **1967**, 1964.

(95) (a) Wommack, A. J.; Moebius, D. C.; Travis, A. L.; Kingsbury, J. S. *Org. Lett.* **2009**, *11* (15), 3202. (b) Rendina, V.; Kaplan, H.; Kingsbury, J. *Synthesis* **2012**, *44* (5), 686. (c) Mahmood, S. J.; Saha, A. K.; Hossain, M. M. *Tetrahedron* **1998**, *54* (3–4), 349. (d) Loeschorn, C. A.; Nakajima, M.; McCloskey, P. J.; Anselme, J. P. *J. Org. Chem.* **1983**, *48* (23), 4407.

(96) Wong, F. M.; Wang, J.; Hengge, A. C.; Wu, W. *Org. Lett.* **2007**, *9* (9), 1663.

(97) Prato, M.; Bianco, A.; Maggini, M.; Scorrano, G.; Toniolo, C.; Wudl, F. *J. Org. Chem.* **1993**, *58* (21), 5578.

(98) Lindsay, V. N. G.; Viart, H. M.-F.; Sarpong, R. *J. Am. Chem. Soc.* **2015**, *137* (26), 8368.

(99) Lévesque, É.; Campeau, L.-C.; Gauvreau, D. *Synlett* **2010**, *2010* (20), 3086.

(100) Lindsay, V. N. G.; Nicolas, C.; Charette, A. B. *J. Am. Chem. Soc.* **2011**, *133* (23), 8972.

(101) Lebel, H.; Davi, M. *Adv. Synth. Catal.* **2008**, *350* (14–15), 2352.

(102) Pereira, A.; Martín, C.; Maya, C.; Belderrain, T. R.; Pérez, P. J. *Adv. Synth. Catal.* **2013**, *355* (14–15), 2942.

(103) Aggarwal, V. K.; Thompson, A.; Jones, R. V. H.; Standen, M. C. H. *Phosphorus, Sulfur, and Silicon and the Related Elements* **1997**, *120* (1), 361.

(104) Sivaguru, J.; Sunoj, R. B.; Wada, T.; Origane, Y.; Inoue, Y.; Ramamurthy, V. *J Org. Chem.* **2004**, *69* (20), 6533.

(105) Oku, A.; Numata, M. *J. Org. Chem.* **2000**, *65* (7), 1899.

(106) Padwa, A. *Helvetica Chimica Acta* **2005**, *88* (6), 1357.

(107) (a) Jin, T.; Yamamoto, Y. *Angew. Chem. Int. Ed.* **2007**, *46* (18), 3323. (b) Creary, X. *J. Org. Chem.* **1980**, *45* (23), 4653.(c) Santos, B. S.; Gomes, C. S. B.; Pinho e Melo, T. M. V. D. *Tetrahedron* **2014**, *70* (24), 3812.

(108) Holton, T. L.; Schechter, H. *J. Org. Chem.* **1995**, *60*, 4725.

(109) (a) Wurz, R. P.; Lin, W.; Charette, A. B. *Tet. Lett.* **2003**, *44* (49), 8845. (b) Baum, J. S.; Shook, D. A.; Davies, H. M. L.; Smith, H. D. *Synth. Commun.* **1987**, *17* (14), 1709.

(110) de Boer, Th. J.; Backer, H. J. *Org. Synth.* **1956**, *36*, 16.

(111) La première synthèse de la fonction diazo rapportée a été effectuée par cette voie. Curtius, T. *Berichte der deutschen chemischen Gesellschaft* **1884**, *17* (1), 953.

(112) (a) Staudinger, H.; Gaule, A. *Chem Ber.* **1916**, *4*, 1897. (b) Mohrbacher, R. J.; Cromwell, N. H. *J. Am. Chem. Soc.* **1957**, *79*, 401.

(113) Javed, M. I.; Brewer, M. *Org. Lett.* **2007**, *9*, 1789.

(114) Overberger, C. G.; Anselme, J.-P. *J. Org. Chem.* **1963**, *28* (2), 592.

(115) Creary, X. *Org. Synth.* **1986**, *64*, 207.

(116) (a) Gutmann, B.; Cantillo, D.; Kappe, C. O. *Angew. Chem.* **2015**, *127*, 6788; *Angew. Chem. Int. Ed.* **2015**, *54*, 6688 (b) Deadman, B. J.; Collins, S. G.; Maguire, A. R. *Chem. Eur. J.* **2015**, *21* (6), 2298. (c) Müller, S. T. R.; Wirth, T. *ChemSusChem* **2015**, *8* (2), 245.

(117) a) Mastronardi, F.; Gutmann, B.; Kappe, C. O. *Org. Lett.* **2013**, *15*, 5590; b) Pieber, B.; Kappe, C. O. *Org. Lett.* **2016**, *18*, 1076.

(118) Pechmann, H. V. *Berichte der deutschen chemischen Gesellschaft* **1894**, *27* (2), 1888

(119) (a) Bartrum, H. E.; Blakemore, D. C.; Moody, C. J.; Hayes, C. J. *Chem. Eur. J.* **2011**, *17*, 9586; (b) Bartrum, H. E.; Blakemore, D. C.; Moody, C. J.; Hayes, C. J. *Tetrahedron* **2013**, *69*, 2276.

(120) (a) Tran, D. N.; Battilocchio, C.; Lou, S.-B.; Hawkins, J. M.; Ley, S. V. *Chem. Sci.* **2015**, *6*, 1120; (b) N. M. Roda, D. N. Tran, C. Battilocchio, R. Labes, R. J. Ingham, J. M. Hawkins, S. V. Ley, *Org. Biomol. Chem.* **2015**, *13*, 2550; (c) Battilocchio, C.; Feist, F.; Hafner, A.; Simon, M.; Tran, D. N.; Allwood, D. M.; Blakemore, D. C.; Ley, S. V. *Nature Chem.* **2016**, *8* (4), 360.

(121) Kralj, J. G.; Sahoo, H. R.; Jensen, K. F. *Lab Chip* **2007**, *7* (2), 256.

(122) (a) Maurya, R. A.; Min, K.-I.; Kim, D.-P. *Green Chem.* **2014**, *16* (1), 116. (b) Un exemple siilaire avec diazomethane: Maurya, R. A.; Park, C. P.; Lee, J. H.; Kim, D.-P. *Angew. Chem.* **2011**, *123*, 5894; *Angew. Chem. Int Ed.* **2011**, *50*, 5952.

(123) a) Aggarwal, V. K.; Abdel-Rahman, H.; Fan, L.; Jones, R. V. H.; Standen, M. C. H. *Chem. Eur. J.* **1996**, *2*, 1024; b) Creary, X.; Hinckley, J.; Kraft, C.; Genereux, M. *J. Org. Chem.* **2011**, *76*, 2062.

(124) Metobo, S. E.; Jin, H.; Tsiang, M.; Kim, C. U. *Bioorg. Med. Chem. Lett.* **2006**, *16*, 3985.

(125) Candeias, N. R.; Paterna, R.; Gois, P. M. P. *Chem. Rev.* **2016**, *116*, 2937.

(126) Bug, T.; Hartnagel, M.; Schlierf, C.; Mayr, H. *Chem. Eur. J.* **2003**, *9*, 4068.

(127) Furrow, M. E.; Myers, A. G. *J. Am. Chem. Soc.* **2004**, *126*, 5436.

(128) See Supporting Information (**Annexe 3**) for DSC-TGA analysis.

(129) Samples were kept at room temperature under air for months with no observable chemical change. The sulfonylhydrazone formation was even used as a mean of aldehyde purification/storage: Jiricny, J.; Orere, D. M.; Reese, C. B. *Synthesis* **1978**, 919.

(130) a) Zhu, S.-F.; Cai, Y.; Mao, H.-X.; Xie, J.-H.; Zhou, Q.-L. *Nature Chem.* **2010**, *2*, 546; b) Doyle, M. P.; Bagheri, V.; Harn, N. K. *Tetrahedron Lett.* **1988**, *29*, 5119.

(131) Dudman, C. C.; Reese, C. B.; *Synthesis* **1982**, 419.

(132) Rodima, T.; Kaljurand, I.; Pihl, A.; Mäemets, V.; Leito, I.; Koppel, I. A. *J. Org. Chem.* **2002**, *67*, 1873.

(133) Higher or lower rates graze the operating limits of the Zaiput® phase separator but could probably be attained by more adapted setups.

(134) Numbers suppose a 100% diazo yield. Multiply by the yield in **Figure 68** to obtain the rates and concentration for a specific substrate. Lower concentrations are also possible.

(135) For comparison, the free hydrazone oxidation method reported in *Ref. 120* yields 70% of **4.2a**, 74% of **4.2b**, 48% of **4.2e**, 87% of **4.2g** and 43% of **4.2l**.

(136) See Supporting Information (**Annexe 3**).

(137) See Supporting Information from Moebius, D. C.; Kingsbury, J. S. *J. Am. Chem. Soc.* **2009**, *131*, 878.

(138) Gutow, J. H. *Journal of Chemical Education* **2005**, *82* (2), 302.

(139) Sreenath, K.; Clark, R. J.; Zhu, L. *J. Org. Chem.* **2012**, *77* (18), 8268.

(140) Suzuki, T.; Fujikura, K.; Higashiyama, T.; Takata, K. *J. Histochem. Cytochem.* **1997**, *45* (1), 49.

(141) Ranallo, S.; Rossetti, M.; Plaxco, K. W.; Vallée-Bélisle, A.; Ricci, F. *Angew. Chem. Int Ed.* **2015**, *54* (45), 13214.

(142) Clegg, R. M. In *Laboratory Techniques in Biochemistry and Molecular Biology*; Elsevier, **2009**; Vol. 33, pp 1–57.

(143) Amblard, F.; Cho, J. H.; Schinazi, R. F. *Chem. Rev.* **2009**, *109*, 4207.

(144) Satsangi, A.; Roy, S. S.; Satsangi, R. K.; Vadlamudi, R. K.; Ong, J. L. *Mol. Pharma.* **2014**, *11*, 1906.

(145) Fomich, M. A.; Kvach, M. V.; Navakouski, M. J.; Weise, C.; Baranovsky, A. V.; Korshun, V. A.; Shmanai, V. V. *Org. Lett.* **2014**, *16* (17), 4590.

(146) Yamaguchi, A.; Matsuda, T.; Ohtake, K.; Yanagisawa, T.; Yokoyama, S.; Fujiwara, Y.; Watanabe, T.; Hohsaka, T.; Sakamoto, K. *Bioconjugate Chem.* **2016**, *27*, 198.

(147) Grätzel, M. *J. Photochem. Photobiol. C: Photochem. Rev.* **2003**, *4*, 145.

(148) (a) Wu, C.-G.; Chung, M.-F.; Tsai, H.-H. G.; Tan, C.-J.; Chen, S.-C.; Chang, C.-H.; Shih, T.-W. *ChemPlusChem* **2012**, *77*, 832. (b) Singh, P.; Baheti, A.; Thomas, K. R. J.; Lee, C.-P.; Ho, K.-C. *Dyes and Pigments* **2012**, *95*, 523. (c) Hara,

K.; Kurashige, M.; Dan-oh, Y.; Kasada, C.; Shinpo, A.; Suga, S.; Sayama, K.; Arakawa, H. *New J. Chem.* **2003**, *27*, 783. (d) Kim, S.-M.; Balanay, M. P.; Lee, S. H.; Kim, D. H. *Bull. Korean Chem. Soc.* **2013**, *34*, 1329.

(149) Shriver, D. F. & Drezdzon, M. A. *The Manipulation of Air-Sensitive Compounds*; 2nd Edition; Wiley: New York, 1986.

(150) Hicks, R. G.; Koivisto, B. D.; Lemaire, M. T. *Org. Lett.* **2004**, *6*, 1887.

(151) Nakanishi, S.; Ueda, M. *Chem. Lett.* **2007**, *36*, 452.

(152) Sajiki, H.; Kurita, T.; Esaki, H.; Aoki, F.; Maegawa, T.; Hirota, K. *Org. Lett.* **2004**, *6*, 3521.

(153) Milani, B.; Anzilutti, A.; Vicentini, L.; Sessanta o Santi, A.; Zangrando, E.; Geremia, S.; Mestroni, G. *Organometallics* **1997**, *16*, 5064.

(154) (a) Pitts, W. J.; Kempson, J.; Guo, J.; Das, J.; Langevine, C. M.; Spergel, S. H.; Watterson, S. H. U.S. 7737279, **2010**. (b) Liang, J.; Zhang, J.; Zhu, L.; Durandin, A.; Young, V. G., Jr.; Geacintov, N.; Canary, J. W. *Inorg. Chem.* **2009**, *23*, 11196.

(155) Firmansyah, D.; Ciuciu, A. I.; Hugues, V.; Blanchard-Desce, M.; Flamigni, L.; Gryko, D. T. *Chem. Asian J.* **2013**, *8* (6), 1279.

(156) Irvin, J. L.; Irvin, E. M. *J. Biol. Chem.* **1948** *174*: 589.

(157) Aggarwal, V. K.; de Vicente, J.; Bonnert, R. V *Org. Lett.* **2001**, *3*, 2785.

(158) Caution! Diazo compounds are presumed to be highly toxic and potentially explosive. All manipulations should be carried out in a hood. Although in numerous preparations we have never observed an explosion, all pyrolyses and distillations should be carried out behind a safety shield. Acetic acid should be used to neutralize any spilled material.

(159) Denmark, S. E.; Edwards, J. P. *J. Org. Chem.* **1991**, *56*, 6974.

(160) Zhao, H.; Wang, Y.; Sha, J.; Sheng, S.; Cai, M. *Tetrahedron* **2008**, *64*, 7517.

(161) Gras, J.-L.; Chang, Y.-Y. K. W.; Guerin, A. *Synthesis* **1985**, 74.

(162) Goff, D. A.; Harris, R. N.; Bottaro, J. C.; Bedford, C. D. *J. Org. Chem.* **1986**, *51*, 504.

(163) Barriault, L.; Ouellet, S. G.; Deslongchamps, P. *Tetrahedron*, **1997**, *53*, 14937.

(164) Lindsay, V. N. G.; Fiset, D.; Gritsch, P. J.; Azzi, S.; Charette, A. B. *J. Am. Chem. Soc.* **2013**, *135*, 1463.

(165) Marcoux, D.; Goudreau, S. R.; Charette, A. B. *J. Org. Chem.* **2009**, *74*, 8939.

(166) Fleming, I.; Urch, C. J. *J. Organomet. Chem.* **1985**, *285*, 173.

(167) Lamberts, J. J. M.; Laarhoven, W. H. *J. Org. Chem.* **1983**, *48*, 2202.

(168) Beaulieu, L.-P. B.; Schneider, J. F.; Charette, A. B. *J. Am. Chem. Soc.* **2013**, *135*, 7819.

(169) Charette, A. B.; Lebel, H. *J. Org. Chem.* **1995**, *60*, 2966.

(170) Charette, B.; Molinaro, C. *J. Am. Chem. Soc.* **1998**, 11943.

(171) Gras, J.-L.; Chang, Y.-Y. K. W.; Guerin, A. *Synthesis* **1985**, 74.

(172) Lifchits, O.; Reisinger, C. M.; List, B. *J. Am. Chem. Soc.* **2010**, *132*, 10227.

(173) Zimmer, L. E.; Charette, A. B. *J. Am. Chem. Soc.* **2009**, *131*, 15624.

(174) Reid, J. R.; Dufresne, R. F.; Chapman, J. J. *Org. Synth.* **1997**, *74*, 217.

(175) Gras, J.-L.; Chang, Y.-Y. K. W.; Guerin, A. *Synthesis* **1985**, *1985* (01), 74.

(176) Jiricny, J.; Orere, D. M.; Reese, C. B. *Synthesis* **1978**, *1978* (12), 919.

(177) Losch, P.; Felten, A.-S.; Pale, P. *Adv. Synth. Catal.* **2015**, *357*, 2931.

(178) García-Muñoz, A.-H.; Tomás-Gamasa, M.; Pérez-Aguilar, M. C.; Cuevas-Yañez, E.; Valdés, C. *Eur. J. Org. Chem.* **2012**, 3925.

(179) Ohno, O.; Ye, M.; Koyama, T.; Yazawa, K.; Mura, E.; Matsumoto, H.; Ichino, T.; Yamada, K.; Nakamura, K.; Ohno, T.; Yamaguchi, K.; Ishida, J.; Fukamizu, A.; Uemura, D. *Bioorg. Med. Chem.* **2008**, *16*, 7843.

(180) Ma, R.; He, L.-N.; Liu, A.-H.; Song, Q.-W. *Chem. Commun.* **2016**, *52*, 2145.

(181) Yukawa, Y.; Tsuno, Y.; Sawada, M. *Bull. Chem. Soc. Japan* **1972**, *45*, 1198.

(182) Gaspa, S.; Porcheddu, A.; De Luca, L. *Adv. Synth. Catal.* **2016**, *358*, 154.

(183) Lim, S.; Ji, M.; Wang, X.; Lee, C.; Jang, H.-Y. *Eur. J. Org. Chem.* **2015**, 591.

(184) Gok, Y.; Alici, B.; Çetinkaya, E.; Özdemir, I.; Özero□lu, Ö. *Turk. J. Chem.* **2010**, *34*, 187.

(185) Damião, M. C. F. C. B.; Pasqualoto, K. F. M.; Ferreira, A. K.; Teixeira, S. F.; Azevedo, R. A.; Barbuto, J. A. M.; Palace-Berl, F.; Franchi-Junior, G. C.; Nowill, A. E.; Tavares, M. T.; Parise-Filho, R. *Archiv der Pharmazie* **2014**, *347* 885.

(186) Karmel, I. S. R.; Fridman, N.; Tamm, M.; Eisen, M. S. *Organometallics* **2015**, *34*, 2933.

(187) Rendina, V. L.; Kingsbury, J. S. *J. Org. Chem.* **2012**, *77*, 1181.

(188) White, E. H.; Ribi, M.; Cho, L. K.; Egger, N.; Dzadzic, P. M.; Todd, M. J. *J. Org. Chem.* **1984**, *49*, 4866.